DESIGN AND OPERATION OF A FUTURE HYDROGEN SUPPLY CHAIN

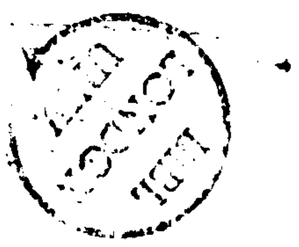
By

Ali Almansoori

April 2006

A thesis submitted for the degree of Doctor of Philosophy of the University of London and for the Diploma of Membership of the Imperial College London

Centre for Process Systems Engineering
Department of Chemical Engineering and Chemical Technology
Imperial College London
London SW7 2AZ
United Kingdom



ABSTRACT

Most of the work in the area of hydrogen supply chain design examines individual components of the hydrogen network, such as production plants, storage facilities, distribution modes, or fuelling technologies. A simulation-based approach is commonly used to mimic and test the behaviour of these components in order to compare alternatives and choose accordingly. The selection is determined based on some performance objectives, such as cost or environmental impact. Up to date, little attention has been directed towards using quantitative tools in designing and operating the future hydrogen supply chain. Adopting a mathematical programming-based approach would aid in finding the optimal hydrogen supply chain configuration among a large number of different hydrogen pathways. It would also help in revealing the layout of the network prior to building it in real-life. This may be of vital importance in forming national and international policy as well as strategic decisions in industry.

The aims of this thesis are to: (1) develop a mathematical model that can support strategic decisions in hydrogen supply chain design and operation, (2) identify the main data requirements for such an activity, and (3) assess the capability of supply chain design models to address such problems. Five different hydrogen supply chain models are development for vehicle refuelling in Great Britain. The first model considers the design of a steady-state, "snapshot" hydrogen supply chain network. The second model is an extension of the first one and includes the availability of primary energy sources and different sizes of hydrogen production and storage facilities. In the third model, we address the design of multi-period hydrogen supply chain over a long-term planning horizon. The third model is then extended to incorporate fuelling stations and secondary distribution of hydrogen. The last model represents a stochastic design of a hydrogen supply chain under demand uncertainty. In all models, the demand of hydrogen is assumed to be known beforehand, except for the last one where demand is subject to variations.

The proposed hydrogen networks comprise two echelons, namely production plants, transportation modes, and storage facilities. In two cases, the network is expanded to include another echelon: fuelling stations. The system is modelled as a mixed-integer linear programming (MILP) optimisation problem. The decisions to be determined include: (1) the number, location, size, and capacity of hydrogen production and storage facilities, (2) the transportation links necessary for establishing the network, (3) the flow rates of hydrogen and energy sources, and (4) the production rates and the average inventory of materials. The objective of the formulation is the minimisation of the total daily cost of the network, taking into consideration both capital and operating costs. A case study is provided to illustrate the applicability of the models.

This thesis reveals that, based on our assumptions, the optimal future hydrogen supply chain would entail the production of hydrogen from natural gas in small-to-large reforming plants. Together with these plants, uncommitted hydrogen from existing production facilities, such as petroleum refineries, should be utilised to establish the hydrogen market. The hydrogen is then distributed as a liquid via trucks and rail, and stored in different sizes of storage facilities in order to replenish customers with their demand.

Acknowledgements

First and foremost, I would like to thank my supervisor Professor Nilay Shah for giving me the opportunity to pursue my studies at Imperial College London, and for his continuous support and excellent supervision throughout my PhD degree. A similar thank you goes to my sponsor, Abu Dhabi National Oil Company (ADNOC), for their financial support and aid.

During my PhD course, I had the opportunity to make some new friends inside and outside the college. I would like acknowledge them for sharing ideas and providing assistance and inspiration.

Finally and most importantly, I would like to express my sincere gratitude to my parents for their love, help, and encouragement during all these years of studies, both undergraduate and postgraduate.

Contents

Figures viii

Tables x

1 Introduction 1
- 1.1 Aim of this Project 3
- 1.2 Structure of this Thesis 4

2 Literature Review 6
- 2.1 Hydrogen Energy 6
  - 2.1.1 Energy Transition 6
  - 2.1.2 Hydrogen Discovery and History 8
  - 2.1.3 Why Hydrogen? 11
  - 2.1.4 Hydrogen Uses 17
  - 2.1.5 Hydrogen Economy 18
  - 2.1.6 Hydrogen Safety 20
  - 2.1.7 Hydrogen Projects 22
- 2.2 Hydrogen Supply Chain 26
  - 2.2.1 Overview 26
  - 2.2.2 Components of the Hydrogen Supply Chain 27
  - 2.2.3 Design of Hydrogen Supply Chain 35
  - 2.2.4 Uncertainty in Hydrogen Supply Chain 43

3 Steady-State Design of Hydrogen Supply Chain 48
- 3.1 Problem Description 48
- 3.2 Model Structure and Components 49
  - 3.2.1 Grid Squares 49
  - 3.2.2 Production Facilities 51
  - 3.2.3 Product Physical Forms 51
  - 3.2.4 Transportation Modes 52
  - 3.2.5 Storage Facilities 52
- 3.3 Model Formulation 53
  - 3.3.1 Nomenclature 53
  - 3.3.2 Constraints 55
  - 3.3.3 Objective Function 59
  - 3.3.4 Model Summary 63
- 3.4 Great Britain-Based Case Study 63
  - 3.4.1 Input Data 65
  - 3.4.2 Results and Discussion 68
  - 3.4.3 Concluding Remarks 76

4 Design of an Extended Hydrogen Supply Chain **78**
4.1 Problem Description 78
4.2 Model Structure and Components 79
4.2.1 Primary Energy Sources 79
4.2.2 Production and Storage Sizes 81
4.3 Model Formulation 81
4.3.1 Nomenclature 81
4.3.2 Constraints 85
4.3.3 Objective Function 90
4.3.4 Model Summary 96
4.4 Case Study Revisited 97
4.4.1 Input Data 98
4.4.2 Results and Discussion 104
4.4.3 Sensitivity Analysis 110
4.4.4 Concluding Remarks 114

5 Multi-Period Design of Hydrogen Supply Chain **116**
5.1 Problem Description 116
5.2 Model Structure and Components 117
5.2.1 Demand Evolution 119
5.3 Model Formulation 119
5.3.1 Nomenclature 119
5.3.2 Constraints 122
5.3.3 Objective Function 128
5.3.4 Model Summary 131
5.4 Case Study Revisited 131
5.4.1 Input Data 132
5.4.2 Results and Discussion 135
5.4.3 Concluding Remarks 153

6 Extension to the Multi-Echelon Case **155**
6.1 Problem Description 155
6.2 Model Structure and Components 156
6.2.1 Fuelling Stations 157
6.2.2 Secondary Transportation Modes 157
6.3 Model Formulation 157
6.3.1 Nomenclature 158
6.3.2 Constraints 158
6.3.3 Objective Function 159
6.3.4 Model Summary 164
6.4 Case Study Revisited 164
6.4.1 Input Data 165
6.4.2 Results and Discussion 165
6.4.3 Concluding Remarks 170

7 Design of Stochastic Hydrogen Supply Chain under Demand Uncertainty **171**
7.1 Problem Description 171
7.2 Model Structure and Components 173
7.2.1 Demand Uncertainty 173

7.3 Model Formulation 174
7.3.1 Nomenclature 174
7.3.2 Constraints 176
7.3.3 Objective Function 183
7.3.4 Model Summary 185
7.4 Extension to Stochastic Multi-Echelon Case 186
7.4.1 Constraints 186
7.4.2 Objective Function 186
7.4.3 Model Summary 188
7.5 Case Study Revisited 188
7.5.1 Input Data 189
7.5.2 Results and Discussion 192
7.5.3 Risk Analysis 213
7.5.4 Concluding Remarks 216

8 Conclusions and Further Work **218**
8.1 Contribution of this Thesis 218
8.2 Potential Future Work 223
8.2.1 Hydrogen Supply Chain Modelling 223
8.2.2 Solution Algorithm 225

References **226**

Appendices **237**
A Hydrogen Demand **237**
A.1 Introduction 237
A.2 Total Demand 237
A.3 Demand Distribution 238
A.4 Grid Demand 240

B Delivery Distances **242**
B.1 Introduction 242
B.2 Local Distances 242
B.3 Regional Distances 243

C Hydrogen Supply Chain Cost Analysis **245**
C.1 Introduction 245
C.2 Hydrogen Production Technologies 246
C.3 Hydrogen Storage Technologies 263
C.4 Hydrogen Distribution Technologies 266
C.4.1 Capital Cost 266
C.4.2 Operating Cost 267
C.5 Hydrogen Dispensing Technologies 268

D Availability of Primary Energy Sources **270**
D.1 Introduction 270
D.2 Natural Gas 270
D.2.1 Resource Availability 270
D.2.2 Resource Allocation 271
D.3 Coal 273

D.3.1 Resource Availability 273
D.3.2 Resource Allocation 274
D.4 Biomass 275
D.4.1 Resource Availability 275
D.4.2 Resource Allocation 276
D.5 Electricity 276
D.5.1 Resource Availability 276
D.5.2 Resource Allocation 277

E Detailed Results **278**
E.1 Introduction 278
E.2 Steady-State Model 278
E.3 Extended Model 281
E.4 Multi-Period Model 283
E.5 Multi-Echelon Model 293
E.6 Stochastic Model 293

Figures

2.1 Transition of global energy systems from 1850 to 2150 7
2.2 Hydrogen demand scenarios for vehicles considered by the US DOE 36
3.1 Superstructure of the steady-state model 50
3.2 Multi-mode network structure of liquid hydrogen for the steady-state model 70
3.3 Multi-mode network structure of compressed-gaseous hydrogen for the steady-state model 71
3.4 Single-mode network structure of liquid hydrogen for the steady-state model 72
4.1 Superstructure of the extended model 80
4.2 Unit cost versus size 94
4.3 Single-mode network structure of liquid hydrogen for the extended model 105
4.4 Multi-mode network structure of liquid hydrogen for the extended model 106
5.1 Hydrogen demand profile to be examined 117
5.2 Superstructure of the multi-period model 118
5.3 Single-mode network structure of liquid hydrogen during the first time period and 5% penetration in the transport market 137
5.4 Single-mode network structure of liquid hydrogen during the second time period and 20% penetration in the transport market 138
5.5 Single-mode network structure of liquid hydrogen during the third time period and 50% penetration in the transport market 139
5.6 Single-mode network structure of liquid hydrogen during the fourth time period and 85% penetration in the transport market 140
5.7 Single-mode network structure of liquid hydrogen during the fifth time period and 100% penetration in the transport market 141
5.8 Multi-mode network structure of liquid hydrogen during the first time period and 5% penetration in the transport market 146
5.9 Multi-mode network structure of liquid hydrogen during the second time period and 20% penetration in the transport market 147
5.10 Multi-mode network structure of liquid hydrogen during the third time period and 50% penetration in the transport market 148
5.11 Multi-mode network structure of liquid hydrogen during the fourth time period and 85% penetration in the transport market 149
5.12 Multi-mode network structure of liquid hydrogen during the fifth time period and 100% penetration in the transport market 150
7.1 Demand scenario tree of interest 172
7.2 Single-mode network structure of liquid hydrogen during time period 1 and scenario 1 193
7.3 Single-mode network structure of liquid hydrogen during time period 2 and scenario 1 194

7.4 Single-mode network structure of liquid hydrogen during time period 2 and scenario 5 195
7.5 Single-mode network structure of liquid hydrogen during time period 2 and scenario 9 196
7.6 Single-mode network structure of liquid hydrogen during time period 3 and scenario 1 197
7.7 Single-mode network structure of liquid hydrogen during time period 3 and scenario 5 198
7.8 Single-mode network structure of liquid hydrogen during time period 3 and scenario 9 199
7.9 Multi-mode network structure of liquid hydrogen during time period 1 and scenario 1 203
7.10 Multi-mode network structure of liquid hydrogen during time period 2 and scenario 1 204
7.11 Multi-mode network structure of liquid hydrogen during time period 2 and scenario 5 205
7.12 Multi-mode network structure of liquid hydrogen during time period 2 and scenario 9 206
7.13 Multi-mode network structure of liquid hydrogen during time period 3 and scenario 1 207
7.14 Multi-mode network structure of liquid hydrogen during time period 3 and scenario 5 208
7.15 Multi-mode network structure of liquid hydrogen during time period 3 and scenario 9 209
7.16 Cost profile of the base case 213
7.17 Probability versus the cost of hydrogen network per kilometre 215
A.1 Demand of hydrogen in Great Britain 241
B.1 Illustration of local distance calculation 242
B.2 Example of regional distance calculations 243
C.1 Components of a generic hydrogen production 246

Tables

2.1 Ten elements leading to a hydrogen economy 19

3.1 Production, storage, and distribution technologies of the steady-state model 64
3.2 Hydrogen demand in each grid square for the steady-state model 66
3.3 Capital and unit production costs of hydrogen production technologies 67
3.4 Capital cost and capacity of transportation modes 67
3.5 Characteristics of transportation modes 68
3.6 Capital and unit storage costs of hydrogen storage technologies 68
3.7 Breakdown of total network costs for the steady-state model 74
3.8 Summary of computational results for the steady-state model 75
4.1 Network configurations to be studied for the extended model 98
4.2 Hydrogen demand in each grid square for the extended model 98
4.3 Availability of primary energy sources for the extended model 99
4.4 Costs associated with primary energy sources 100
4.5 Production capacities and costs of hydrogen plants 102
4.6 Costs and characteristics of transportation modes 103
4.7 Storage capacities and costs of liquid hydrogen storage facilities 104
4.8 Breakdown of total network cost for the extended model 109
4.9 Summary of computational results for the extended model 109
4.10 Scenarios testing the sensitivity of the extended model 110
4.11 Sensitivity of the first network configuration 111
4.12 Sensitivity of the second network configuration 112
5.1 Hydrogen demand of each grid and period for the multi-period model 132
5.2 Initial availability of energy sources for the multi-period model 133
5.3 Number of existing hydrogen plants in each grid 134
5.4 Number of existing storage facilities in each grid 135
5.5 Overall percentage of demand met by local production plants 152
5.6 Itemisation of cost for the first configuration of the multi-period model 152
5.7 Itemisation of cost for the second configuration of the multi-period model 152
5.8 Summary of computational results for the multi-period model 153
6.1 Number of fuelling stations for network configurations 1 and 2 166
6.2 Number of new distributed plants for network configurations 1 and 2 167
6.3 Breakdown of total cost for configuration 1 of the multi-echelon model 168
6.4 Breakdown of total cost for configuration 2 of the multi-echelon model 168
6.5 Comparison between hydrogen- and petrol-based supply chains 169
6.6 Summary of computational results for the multi-echelon model 170
7.1 Network configurations to be examined under demand uncertainty 189
7.2 Scenario penetration factor during each time period 190
7.3 Hydrogen demand for each time period and scenario 190
7.4 Probability of demand scenarios 190
7.5 Grid hydrogen demand for all scenarios over first and second periods 191

7.6	Grid hydrogen demand for all scenarios over third period	191
7.7	Number of fuelling stations during the first time period	210
7.8	Number of fuelling stations during the second and third time periods	211
7.9	Summary of cost for the studied network configurations	212
7.10	Summary of computational results for the stochastic model	212
7.11	Average daily demand of hydrogen for each scenario and time period	214
7.12	Average total cost of hydrogen network per tonne delivered	214
7.13	Average total cost of hydrogen network per kilometre	214
7.14	Assumptions used to estimate the cost of the current petrol network	215
A.1	Parameters used in total hydrogen demand calculations	237
A.2	Population of Great Britain	239
A.3	Grid population in London and the South East region	239
A.4	Population density of the studied example	239
A.5	Hydrogen demand of the studied example	240
B.1	Local and regional delivery distances	244
C.1	Hydrogen production pathways examined	248
C.2	Data used for calculating the total cost of SMR-LRG-LH_2	248
C.3	Cost analysis of SMR-LRG-LH_2	248
C.4	Summary of results for SMR-MED-LH_2	249
C.5	Summary of results for SMR-SML-LH_2	250
C.6	Summary of results for SMR-LRG-CH_2	251
C.7	Summary of results for CG-LRG-LH_2	252
C.8	Summary of results for CG-MED-LH_2	253
C.9	Summary of results for CG-LRG-CH_2	255
C.10	Summary of results for BG-LRG-LH_2	256
C.11	Summary of results for BG-MED-LH_2	258
C.12	Summary of results for BG-LRG-CH_2	259
C.13	Summary of results for WE-MED-LH_2	261
C.14	Summary of results for WE-SML-LH_2	262
C.15	Summary of results for large-scale liquid hydrogen storage	264
C.16	Summary of results for medium-scale liquid hydrogen storage	264
C.17	Summary of results for small-scale liquid hydrogen storage	265
C.18	Summary of results for large-scale compressed hydrogen storage	266
C.19	Data used for LH_2-based fuelling station	269
D.1	Location of gas terminals in the UK	272
D.2	Location of gas terminals with respect to grid number	272
D.3	Availability of natural gas for the steady-state model	272
D.4	Average availability of natural gas for the multi-period model	273
D.5	Location of coalfields with respect to grid number	274
D.6	Availability of coal in each grid for the steady-state model	274
D.7	Average availability of coal in each grid for the multi-period model	275
E.1	Flow rate of liquid hydrogen by transport modes for the steady-state model	278
E.2	Flow rate of hydrogen gas via transport modes for the steady-state model	279
E.3	Summary of results of configurations 1 and 3 for the steady-state model	279
E.4	Summary of results of configuration 2 for the steady-state model	280
E.5	Flow rate of liquid hydrogen via transport modes for the extended model	281
E.6	Surplus of natural gas in each grid for the extended model	282
E.7	Summary of results for the extended model	282
E.8	Flow rate of liquid hydrogen via transport modes during the first period	283

E.9 Flow rate of liquid hydrogen via transport modes during the second period 283
E.10 Flow rate of liquid hydrogen via transport modes during the third period 284
E.11 Flow rate of liquid hydrogen via transport modes during the fourth period 285
E.12 Flow rate of liquid hydrogen via transport modes during the fifth period 285
E.13 Flow rate of natural gas between grids during the first time period 286
E.14 Flow rate of natural gas between grids during the second time period 286
E.15 Flow rate of natural gas between grids during the third time period 287
E.16 Flow rate of natural gas between grids during the fourth time period 287
E.17 Flow rate of natural gas between grids during the fifth time period 287
E.18 Availability of primary energy source during the first time period 288
E.19 Availability of primary energy source during the second time period 288
E.20 Availability of primary energy source during the third time period 289
E.21 Availability of primary energy source during the fourth time period 289
E.22 Availability of primary energy source during the fifth time period 289
E.23 Summary of results for the first time period 289
E.24 Summary of results for the second period 290
E.25 Summary of results for the third time period 291
E.26 Summary of results for the fourth time period 292
E.27 Summary of results for the fifth time period 292
E.28 Flow rate of liquid hydrogen during time period 1 and scenario 1 293
E.29 Flow rate of liquid hydrogen during time period 2 and scenario 1 294
E.30 Flow rate of liquid hydrogen during time period 2 and scenario 5 294
E.31 Flow rate of liquid hydrogen during time period 2 and scenario 9 295
E.32 Flow rate of liquid hydrogen during time period 3 and scenario 1 296
E.33 Flow rate of liquid hydrogen during time period 3 and scenario 5 296
E.34 Flow rate of liquid hydrogen during time period 3 and scenario 9 297
E.35 Flow rate of primary energy source during time period 1 and scenario 1 298
E.36 Flow rate of primary energy source during time period 2 and scenario 1 298
E.37 Flow rate of primary energy source during time period 2 and scenario 5 298
E.38 Flow rate of primary energy source during time period 2 and scenario 9 299
E.39 Flow rate of primary energy source during time period 3 and scenario 1 299
E.40 Flow rate of primary energy source during time period 3 and scenario 5 299
E.41 Flow rate of primary energy source during time period 3 and scenario 9 300
E.42 Availability of primary energy source at time period 1 and scenario 1 300
E.43 Availability of primary energy source at time period 2 and scenario 1 300
E.44 Availability of primary energy source at time period 2 and scenario 5 301
E.45 Availability of primary energy source at time period 2 and scenario 9 301
E.46 Availability of primary energy source at time period 3 and scenario 1 301
E.47 Availability of primary energy source at time period 3 and scenario 5 301
E.48 Availability of primary energy source at time period 3 and scenario 9 302
E.49 Summary of results during time period 1 and scenario 1 302
E.50 Summary of results during time period 2 and scenario 1 303
E.51 Summary of results during time period 2 and scenario 5 303
E.52 Summary of results during time period 2 and scenario 9 304
E.53 Summary of results during time period 3 and scenario 1 305
E.54 Summary of results during time period 3 and scenario 5 305
E.55 Summary of results during time period 3 and scenario 9 306

Chapter 1

Introduction

Thirty years from now there will be a huge amount of oil—and no buyers. Oil will be left in the ground. The Stone Age came to an end, not because we had a lack of stones, and the oil age will come to an end not because we have a lack of oil.... [Hydrogen] is coming before the end of the decade and will cut gasoline consumption by almost 100 percent.
—Sheikh Ahmad Zaki Yamani, Oil Minister of Saudi Arabia (1962–1986) and head of OPEC* for 25 years [1].

The statement of Sheikh Yamani indicates that the world would eventually win the oil endgame by finding a better fuel. Oil and its derivative products will no longer be the prime mover of our modern industrial civilisation. The main impetus behind this energy transition is the concern over urban air quality, the build-up of greenhouse gases that threaten to trigger sever climate change, and the dependence on depleting foreign oil. The advances in fuel cell technology and its usefulness in a wide range of applications, particularly for transport purposes, is another factor behind the transition to an alternative fuel.

For many decades, environmentalists and energy specialists have been calling for the use of fuels derived from renewable sources as a substitute to the existing non-renewable petroleum-based fuels. A variety of alternative fuels have been suggested, including methanol, ethanol, methane, liquefied petroleum gas, and hydrogen. Among these fuels, hydrogen may offer the greatest potential benefits in terms of reducing greenhouse gases and harmful pollutant emissions. Hydrogen is also a means of improving security of energy supplies since it can be produced from diverse primary energy sources. Despite these advantages, hydrogen presents a number of technical and economical hurdles that need to be overcome in the near future.

*Organisation of petroleum exporting countries.

Hydrogen is the most abundant element in the universe. Every cubic centimetre of the interstellar space contains a few atoms of hydrogen. Every cubic centimetre of the interior of plant Jupiter contains more than 10 million billion billion hydrogen atoms [2]. According to The Columbia Encyclopedia [3], hydrogen is believed to make up about 75% of the mass of the universe and to account for more than 90% of its molecules. Hydrogen is the simplest and the lightest of molecules. It is also the fuel of stars and galaxies and essential in innumerable chemical and biological processes. Overall, "Hydrogen is the mother of all atoms and molecules," as Physicist John S. Rigden pointed out in the prologue to his 2002 book *Hydrogen: The Essential Element* [2].

Even though hydrogen is everywhere, it is not an energy source that can be harnessed and used immediately. It has to be extracted from sources such as water or natural gas. However, hydrogen is a versatile energy carrier since it can be produced from almost any energy source and used in a wide range of energy services, including internal combustion engines (ICEs), fuel cells, and combustion turbines. Unlike electricity, hydrogen can be stored in large amounts and converted readily to electricity when needed with zero harmful emissions.

The utilisation of hydrogen in the transport sector has been looked at by many researchers as the most attractive candidate for solving the current energy-related issues. This is because transportation is a leader in energy consumption and responsible for a large part of the greenhouse gas emissions as well as the deterioration of urban air quality around the Globe. For instance, about two-thirds of the United States (US) oil consumption is in the transport sector—which is the only sector of the US economy totally dependent on oil [4]. This sector also accounts for one-third of the US carbon dioxide (CO_2) emissions in 2004 [5]. Likewise, in the United Kingdom (UK), the transport sector has been the fastest growing and the biggest energy user in the UK economy for the past 18 years [6]. It accounted for 36% of the final energy consumption in 2004 and contributed to nearly one-fourth of the total UK's carbon emissions [7]. This continued reliance on petroleum-based fuels in road transport poses a great threat to the environment and human health.

The widespread use of hydrogen as the future transport fuel necessitates the development of an appropriate vehicular refuelling supply chain. As with the existing petroleum supply system, the future hydrogen infrastructure ought to include production sites, storage facilities, delivery options, as well as conversion and end-use applications. The hydrogen infrastructure should be as ubiquitous as the one present now with refuelling points supporting daily and seasonal demand fluctuations. The infrastructure should also be safe, cost-effective, and environmentally friendly.

The design of the future hydrogen supply chain will be different from those of the past. The supply network will be driven by different environmental pressures and economics. In addition, a mix of various hydrogen supply options will emerge. This is because hydrogen can be produced from a variety of primary energy feedstocks in a wide range of production technologies and sizes. The scale of hydrogen production varies from dedicated, centralised sites producing large quantities to household scale producing small quantities at the point of use. Following its production, hydrogen can be distributed in different forms using various technologies. Gaseous hydrogen, for example, can be transported in a dedicated pipeline network over long distances while liquid hydrogen can be delivered in tankers via rail, ship, or truck. Also, there are a number of storage options for storing hydrogen ranging from large-scale stationary level to small-scale mobile applications. The diversity in production, distribution, and storage dimensions inevitably leads to many possible hydrogen supply pathways. Therefore, a mathematical programming-based approach is essential to determine which supply option is the best among all of these alternatives.

1.1 Aim of this Project

Most of the reviews in the area of hydrogen supply chain design emphasise evaluating the performance of a pre-determined hydrogen supply pathway using a steady-state simulation approach. Others focus on studying individual components of the supply chain, such as production, transportation, storage, or utilisation technologies. Very little effort has been invested in realising the capability of mathematical programming technique to assist in identifying the optimum configuration of the future hydrogen

supply chain. The aim of this work is, therefore, to develop an optimisation framework that can support strategic decisions in hydrogen supply chain design and operation for vehicular use in Great Britain. The work also aims to map out the data points required for such an activity as well as to study the feasibility of supply chain design models in addressing such problems.

1.2 Structure of this Thesis

The structure of this thesis is as follows. A brief background on hydrogen energy and an overview of hydrogen supply chain are presented in Chapter 2. Later in the chapter, the design aspects and approaches of the hydrogen supply chain are described, along with the effect of uncertainty on hydrogen network design. Chapter 3 introduces a steady-state hydrogen supply chain network formulated as a mixed-integer linear programming (MILP) model. Chapter 4 extends the model presented in Chapter 3 to take into account the availability of primary energy sources and the establishment of different sizes of production and storage facilities. The extended model also addresses the logistics concerning the distribution of energy sources as well as the local distribution of hydrogen within a particular region. The sensitivity of the model, to several input parameters, is tested through a number of benchmarks.

In Chapter 5, the two aforementioned snapshot models are modified to consider the evolution of the hydrogen network over a long-term planning horizon. Unlike the earlier models, which had a static demand level, the hydrogen demand for the multi-period model is assumed to vary from one time period to the next. The multi-period model is then expanded by adding an extra echelon: fuelling stations. This change is presented in Chapter 6 together with the secondary distribution of hydrogen. Chapter 7 revisits the formulation of Chapters 5 and 6 but within a stochastic context. In this case, the demand is not known exactly due to the presence of some uncertainty. A risk analysis is also included in Chapter 7 to study the effect of demand uncertainty on the cost and structure of the hydrogen supply chain network. All of models given in Chapters 3–7 were accompanied with a case study to illustrate their applicability. These case studies were based on Great Britain and were used to determine the

optimal configuration of a hydrogen supply chain for the transport sector. Finally, Chapter 8 concludes this thesis by summarising the work that has been done and outlining some possible future research directions.

Chapter 2

Literature Review

2.1 Hydrogen Energy

2.1.1 Energy Transition

Energy, without doubt, is one of the most fundamental components of our universe. It plays a very important role in all aspects of modern society, especially in industry and transportation. This is why man has devoted so much of his time and effort to finding an economical, sustainable, efficient, and clean source of energy. Such a source would greatly influence the present way of life.

In an effort to achieve the above criteria, the global energy system has been evolving from using one form of energy to another. In less than one and a half centuries, our energy system has moved gradually from solid fuels to liquid fuels then to gas fuels. Basically, wood gave way to coal, coal was superseded by oil, and currently oil is being challenged by natural gas and hydrogen. It is evident that each type of fuel contains more hydrogen and less carbon from the one it replaced. As stated by Jesse Ausubel [8], "The trend toward "decarbonisation" is the heart of understanding the evolution of the energy system." In fact, the decarbonisation of energy would inevitably lead to hydrogen as the future chief fuel.

The transition trend of the global energy system over time is illustrated in Figure 2.1. The figure shows that until the mid-19th century wood and hay were the common source of energy in most parts of the world. They were excessively used for many domestic purposes, including heating, cooking, and lighting. However, wood progressively began to lose out to coal because of its bulkiness, inefficiency, and

difficulty to transport. Another reason behind the phase out of wood and the rise of an alternative fuel like coal was the sudden increase in demand for energy caused by the rapid growth in population, particularly in dense cities [8, 9].

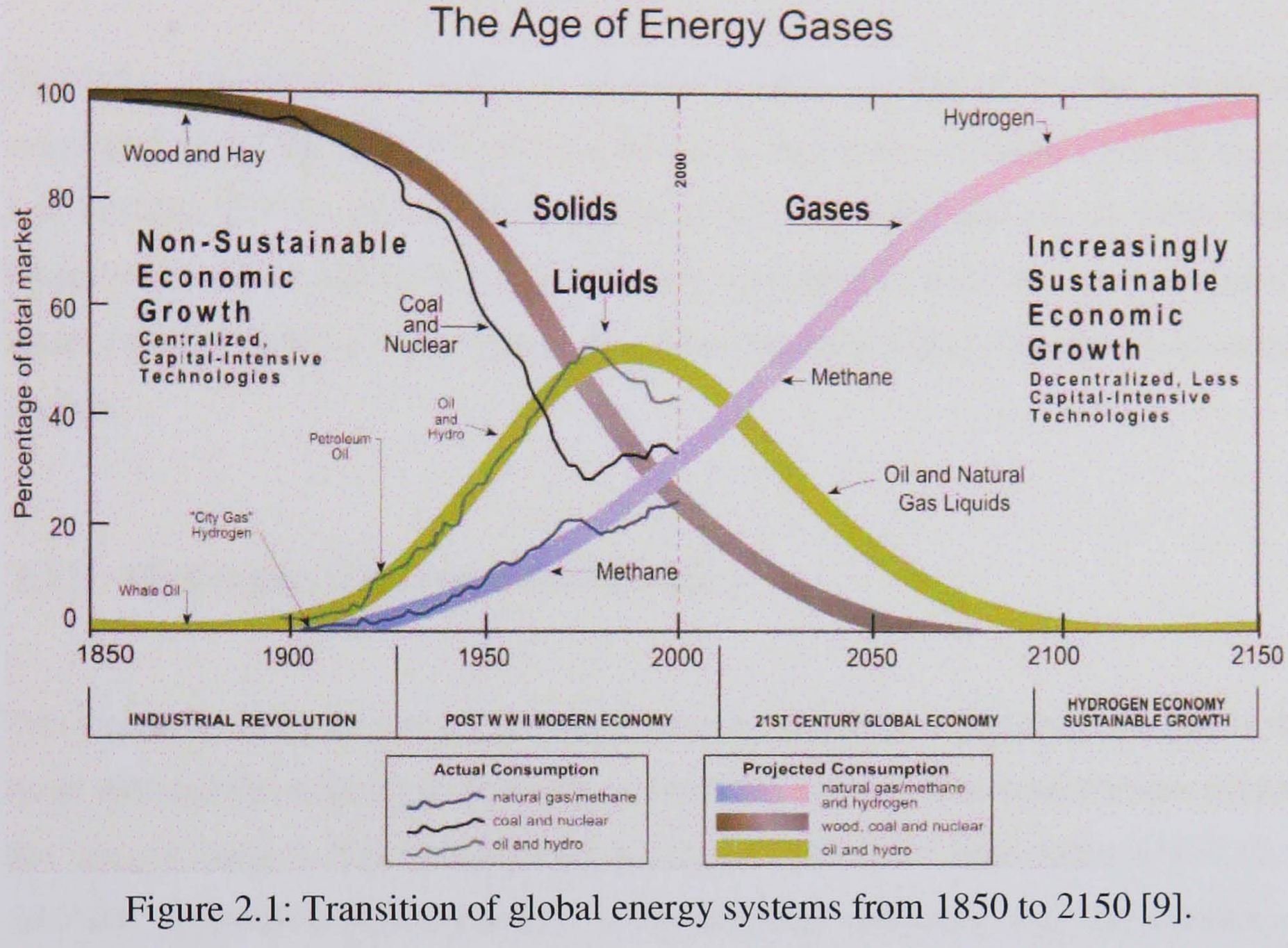


Figure 2.1: Transition of global energy systems from 1850 to 2150 [9].

Stimulated by the industrial revolution, the use of coal started to boom steadily. This was due to the fact that coal was as abundant as wood but more concentrated and not as bulky to transport. Nevertheless, by 1900 great potential was shifted towards using fluid fuels, especially in transport systems. Oil began to displace solid fuels since it has, compared to its predecessors, a higher energy density, a lower carbon-to-hydrogen ratio, and the ability to flow through pipelines and into tanks. In addition, oil can easily be used to power a wide range of automobiles because it occupies less volume and has less weight. By the middle of the 20th century, oil turned out to be the world's leading energy source [8, 9].

After the oil crisis in 1973, oil slowly started becoming less dominant and the market for natural gas kicked off. More recently, there has been great interest in natural gas and its uses have grown, particularly in electricity generation and heating. This is because natural gas is a very clean, light, and efficient fuel. It can also be easily

distributed through a network of pipes with a minimal cost compared to oil. Additionally, natural gas only has one carbon atom to four hydrogen atoms. This virtue makes natural gas emit much less CO_2 per unit of energy than its predecessors, ultimately leading to a cleaner environment [8, 9].

Hydrogen completes the trend of decarbonisation. Compared to the previously mentioned fuels, the ratio of hydrogen to carbon has increased from 1–10 for wood, 1–2 for coal, 2–1 for oil, and 4–1 for natural gas [8]. Hydrogen, on the other hand, contains no carbon atoms, which means zero emissions of CO_2. Its utilisation as the future primary energy source signals the end of the long reign of hydrocarbon energy sources.

2.1.2 Hydrogen Discovery and History

The discovery of hydrogen gas emerged from the doubts of scientists that water is the basic element from which everything evolved. This idea is dated back to the time of the ancient Greeks. Thales, a Greek philosopher who lived from about 624 B.C. to 545 B.C, explained that water was a fundamental substance and the essence of everything in the world. However, it was not until the end of the fifteenth century when the renaissance physician and alchemist Paracelsus (1493–1541) unwittingly discovered hydrogen. He found out that dissolving metal in acids yields a flammable gas, which was recognised about 200 years later as hydrogen gas [10].

Even though hydrogen was first discovered by Paracelsus, the English scientist Henry Cavendish (1731–1810) is usually credited for discovering hydrogen. Cavendish demonstrated that hydrogen is much lighter than air and was the first to produce water by combing oxygen and hydrogen molecules with the aid of an electrical spark. He named oxygen "life-sustaining air" and hydrogen "inflammable air". The French chemist Antoine Laurent Lavoisier (1743–1794) went further by taking a reverse route: splitting water molecules into its constituents. Lavoisier, who went to the guillotine, was the first to give hydrogen its name from the Greek words *hydro* for water and *genes* which means forming [11]. He also labelled the "life-sustaining air" oxygen [10].

In 1783, the French physicist Jacques César Charles (1746–1823) flew a balloon filled with hydrogen gas to an altitude of almost two miles. The first practical use of hydrogen took place ten years later, in 1793, not surprisingly, during warfare. The well-known French chemist Guyton de Norveau suggested the use of hydrogen-filled balloons as observation platforms for army exploration. As a result, the first hydrogen generation unit was built in an army camp close to Paris [10].

The potential uses of hydrogen as a chemical fuel were discussed for the first time during the nineteenth century by scientists and writers of science fiction. Perhaps the most famous example is Jules Verne's description in his book, *The Mysterious Island*, of how hydrogen would become the world's chief fuel [12]. In a passage, an engineer informs his colleagues, "Yes, my friends, I believe that water will one day be employed as fuel, that hydrogen and oxygen which constitute it, used singly or together, will furnish an inexhaustible source of heat and light, of an intensity of which coal is not capable.... Water will be the coal of the future."

Soon after the First World War, the world witnessed a flourished interest in hydrogen as a new source of energy, especially in Europe and North America. In England, the young Scottish scientist J.B.S. Haldane was the first to envision the full potential of hydrogen as an all-purpose fuel of the future. In a lecture delivered at Cambridge University in 1923, Haldane outlined how hydrogen would be produced from wind power via electrolysis, then liquefied and stored in huge reservoirs. He prophesied that in four centuries such a pathway would meet Britain's growing energy demand [13].

In Germany, the interest in hydrogen as a transport fuel moved from the conceptual stage to the practical application. The Germans were the first to exploit hydrogen as a booster fuel in the Zeppelins—a huge dirigible, which carried passengers across the Atlantic Ocean during the 1920s and the 1930s. The German Engineer Rudolf Erren, who was one of the best-known hydrogen advocates in the 1920s and the 1930s, made another fascinating accomplishment. Erren converted trucks, buses, submarines, and ICEs of all kinds to run on hydrogen in order to satisfy the German government's desire for energy self-sufficiency. His engines, which were patented in 1928, were

very popular, highly efficient, and were used to power a sizable number of vehicles in both Germany and England [13].

Interest in hydrogen as a fuel increased during the Second World War due to the threat of fuel supply cut-offs. This led many governments to consider industrial use of hydrogen. When the Australian government lost their oil fields to Japan, it authorised the construction of an experimental high-pressure electrolytic hydrogen plant using off-peak electricity. At the same time, the US government was looking into hydrogen use for its air force, army, and navy. However, the hydrogen progress was brought to a halt due to the Allies victory in 1945 and the return of cheap oil prices [13].

Even though the Welsh physicist Sir William Grove first conceived the principle of fuel cells* in 1839 [14], it was not until the 1950's when the first unit was manufactured. This great, revolutionary invention spurred the interest in hydrogen in many practical applications. The most worthy of mentioning is the development of the first pragmatic hydrogen-air fuel cell by the British scientist Francis T. Bacon. In the 1970s, the US programme of the National Aeronautics and Space Administration (NASA) used, for the first time, hydrogen-powered fuel cells in spacecrafts to produce electricity and drinkable water. The same year also marked the first use of the phrase "hydrogen economy", by General Motors (GM) who foresaw hydrogen as "the fuel for all types of transport." Despite GM's enthusiasm, their preliminary work on hydrogen research did not last for long [13].

The oil shock of 1973, the growing environmental awareness and the desire for energy security all boosted the investigation of hydrogen as an all-purpose form of energy. Government agencies in the US, Europe, and Japan started to fund hydrogen programmes. The year of the oil shock also marked the birth of the first scientific, monthly hydrogen journal, the *International Journal of Hydrogen Energy*, at the first International Conference on Hydrogen held in Miami Beach. In that delegation, the president of the association, T. Nejat Veziroglu, expressed his excitement that hydrogen "was a permanent solution to the depletion of conventional fuels, [and a] permanent solution to the global environmental problem." However, as energy prices declined later in the decade and the effect of the oil crisis began to fade, the government funding for hydrogen research cooled off again significantly [13].

**An electrochemical device that converts the chemical energy of a fuel directly into electrical energy.*

During the last decades, fluctuations in oil prices, environmental impacts of the existing energy system, and the breakthrough of fuel cell technology gave researchers the momentum to reconsider hydrogen as a promising future energy carrier. Since then, outstanding progress in hydrogen activities has taken place. Hoffmann highlighted in his 2001 book *Tomorrow's Energy* an excellent description of these activities from the late 1980s to the beginning of this century. Some of which will be discussed in more detail in the following sections [13].

Today, industry, government, and academic researchers are becoming seriously engaged in hydrogen and fuel cell technologies. The chairs of major oil and car companies have announced that the world is entering the oil endgame and the start of the hydrogen age. The Royal Dutch/Shell's company have also said that hydrogen would fuel a fourth of the vehicle fleet in the industrialised countries by 2025 [15]. More recently, President George W. Bush emphasised the commitment he had made earlier to develop hydrogen fuel cell cars and his support for other hydrogen-related technologies. In his January 2003 State of the Union Address, he announced:

"Tonight I'm proposing $1.2 billion in research funding so that America can lead the world in developing clean, hydrogen-powered automobiles. A single chemical reaction between hydrogen and oxygen generates energy, which can be used to power a car—producing only water, not exhaust fumes. With a new national commitment, our scientists and engineers will overcome obstacles to taking these cars from laboratory to showroom, so that the first car driven by a child born today could be powered by hydrogen, and pollution-free. Join me in this important innovation to make our air significantly cleaner, and our country much less dependent on foreign sources of energy" [16].

2.1.3 Why Hydrogen?

In the previous section, we traced back the history of hydrogen energy over time and briefly touched upon some of hydrogen's merits that caught the attention of many hydrogen enthusiasts. This section, however, explains in more detail why hydrogen is

at the top of the list of alternatives to fossil fuels. Why there is "a confluence of drivers that all point in the same direction—towards hydrogen," as stated by David Hart, one of the hydrogen advocators of the Imperial College Centre for Energy Policy and Technology [17].

Environmental Risks

Greenhouse gases are essential components of the atmosphere. They are mainly composed of CO_2 and other gases, including methane (CH_4), nitrous oxide (N_2O), and water (H_2O). The main effect of these gases is to allow some of the Sun's radiation into Earth to heat up its surface and preserve part of this heat from re-radiating back into space. This is defined as the greenhouse effect. Without the entrapment of heat by these gases, life on Earth would be difficult since the average temperature would not exceed –20 degrees Celsius (°C) [18].

Environmentalists and other energy practitioners blame the continuous emissions of greenhouse gases for changes in the global climate. This claim is based on the Second Assessment Report published by the Intergovernmental Panel on Climate Change (IPCC) in 1996 which concludes, "there could be a connection between anthropogenic greenhouse gas emissions and a possible increase in the average temperature of the atmosphere" [19]. The third report released by the same organisation confirms the earlier finding and shows that there was an average temperature increase of 0.6°C during the 20th century [20]. As a result, the 1990s was the warmest decade and 1998 was the warmest year since temperature records began. It has also been found that the average temperature will increase on land by about 0.15 degrees per decade and 0.05 degrees on the surface of the ocean [18].

Human activities are responsible for disrupting the natural CO_2 cycle [18, 21]. These activities include: the removal of forests which manage the level of CO_2 in the atmosphere through photosynthesis, as well as the discharge of destructive chemicals, such as chlorofluorocarbon gases which contribute towards intensifying the greenhouse effect. Of these activities, the most damaging is the burning of fossil fuels in our ever-increasing demanding machineries. Such processes have already increased

the concentration of the atmospheric CO_2 from 280 to 375 parts per million (ppm) over the course of the past 150 years, which is an increase of more than 30% [22]. The problem is that about two-thirds of this increment has occurred during the past 50 years [23]. Unfortunately, studies show that the CO_2 concentration could pass 550 ppm by this century [23]. The continuous, uncontrollable emissions of CO_2 would certainly trigger tremendous, unanticipated, and traumatic global climate change.

Currently, the UK's transport sector, including the aviation industry, generates nearly one-fourth of its total carbon emissions. Road transport, alone, contributes for 85% of this, with passenger cars accounting for about half of the total carbon emitted by the transport sector [7]. A similar trend is found in the US where the transport sector is projected to produce about half of the 40% rise in the US CO_2 emission forecast for 2025 [24]. Needless to say, tailpipe vehicle emissions are responsible for generating a large fraction of the smog and harmful pollutants in the air, including nitrogen oxides (NO_x), carbon monoxide (CO), and other un-reacted carbonaceous particulates. Such pollutants deteriorate air quality and pose a great threat to human health. This is why the transport sector is the main target for governments, researchers, and hydrogen enthusiasts.

Combusting hydrogen in the conventional ICEs produces virtually nothing other than water vapour. The exhaust effluent contains only some NO_x and tiny traces of other pollutants from the oxidation of the engine's lubricants. However, using hydrogen in fuel cells would be an even better choice. In fuel cells, hydrogen is electrochemically combined with oxygen in a clean, quite, efficient, and flameless process to produce electricity, heat, and pure distilled water. Unlike ICEs, fuel cells yield near-zero NO_x and zero noxious wastes [25, 26].

A further advantage of hydrogen fuel is that it can be produced from renewable resources, nuclear power, or clean fossil technologies. This "green" pathway could significantly reduce the build-up of greenhouse gases; hence lessen the effect of global warming. Moreover, hydrogen can serve as an agent in "greening" not only the transport sector but also all other sectors of the economy.

Energy Risks

Oil is an exhaustible, non-renewable energy source. Energy analysts predict that the world oil production will peak within the next few decades and will eventually diminish. According to the British Petroleum (BP) 2005 Energy Statistical Review [27], the total world oil reserve is expected to last for another 40 years. Also, the deposits of oil in the world are distributed unevenly. Over 80% of these oil reserves are available in nations within the OPEC—which are regions known with politically unstable conditions [27]. Furthermore, many energy-poor countries utilise almost their entire income from exports to import oil.

Despite these facts, oil is the predominant energy source used in today's energy market. Worldwide, there is a soaring appetite for oil. The world's oil production grew by more than 19% from 1994 to 2004, from 67 to 80 million barrels a day, and the competition for oil is expected to escalate steadily [27]. Developing countries, such as China and India, will lead the way of this competition due to their blooming economical and population growths. If these two super-giants continue to expand in energy demand at the current projection rate, they would consume more oil than the entire world did in 2003 [28]. Moreover, to quench the thirst for oil, a few countries will even go to war to secure the line of supplies. Other countries, like the UK, will shift slowly from being a net energy exporter to being a net energy importer as their domestic oil production declines and the growth rate of demand rises [7].

As the world oil production reaches its peak and demand keeps growing, oil prices will just keep going up until they reach a point where we are forced to adopt an alternative fuel. Many energy experts think that the price of oil could exceed 100 US dollars ($) in the coming few months [29]. The problem could become worse as Iran and Nigeria cut off their 5 million barrel worth of oil supplies from the market due to current political conflicts [30]. As a result, this would create a shortage in the oil supply worldwide, leading to another energy crisis.

Hydrogen could bring this crisis to an end. Unlike oil-based fuel, hydrogen can be produced in many different ways using different kinds of energy feedstocks, such as

biomass, or water utilising solar or wind power. It can also be produced on-site next to the demand source since the current production technologies allow such a decentralised option. Hydrogen could, therefore, offer independence and a more just distribution of resources as well as sustainability. This would lead to global, economical and social benefits.

Advances in Fuel Cells

Fuel cells are very efficient devices. They are significantly more efficient than the current combustion technologies. Regardless of the scale of the technology, fuel cells work efficiently under all circumstances, even at low load. For instance, typical combustion-based power plants generate electricity at efficiencies of 30% to 40%, whereas fuel cell power plants can generate electricity at efficiencies up to 60%. When fuel cells are combined with turbines to generate electricity and heat (co-generation), the efficiency of the system can reach up to 85%. Furthermore, conventional ICE vehicles convert less than 30% of the energy stored in petrol into mechanical energy. In contrast, electric vehicles powered by hydrogen fuel cells have much higher energy efficiency, utilising 40% to 60% of the hydrogen fuel's energy [31, 32].

The use of hydrogen-powered fuel cell vehicles was reinvigorated by the early 1990s when researchers at Los Alamos National Laboratory cut the amount of platinum catalyst in proton exchange membrane (PEM) fuel cells by almost a factor of ten [4]. This remarkable achievement slashed the cost of PEM fuel cells drastically because platinum is a very expensive metal. Another dramatic enhancement was accomplished by the leading Canadian fuel cell Company, Ballard Power Systems Inc. The company raised the power output of PEM fuel cells from around 170 Watts per litre of hydrogen fuel to more than 1300 Watts [33]. Since then, the interest in PEM fuel cells for transport purposes has increased substantially. Currently, the rapid technological progress in fuel cells signals the end of the 100-year reign of the ICE, as stated by the chairman of Ford Motor Company, William Clay Ford Jr., at the Greenpeace conference in late 2000 [33].

Advances in Hydrogen-Related Technologies

The last reason behind the expanding efforts in hydrogen research and development is the technological advances in hydrogen production technologies, especially carbon-free technologies. Impressive achievements have been made in developing on-site high-pressure electrolysers and in improving the efficiency of conventional electrolysis units. Heat is used in steam electrolysis, instead of electricity, to provide some of the energy required to split water molecules, making the process more energy efficient. Furthermore, novel hydrogen production technologies, such as biological hydrogen production by algae or bacteria in light-driven bioreactors, have been proposed [34]. In addition, there has been a sharp decline in the price of wind and solar energy in the past two decades [4]. Consequently, this renewed the interest in wind- and solar-based hydrogen production technologies since they offer zero carbon emissions as well as energy sustainability.

Another promising carbon-free hydrogen production pathway is the removal of CO_2 from the current fossil-based hydrogen production technologies and piping it deep underground. This process was suggested in the early 1990s by a Princeton University professor Bob Williams and was called CO_2 sequestration, or carbon capture and storage (CCS) [4]. Many researchers argue that CCS holds a great hope for the world as being a source of both cost-effective and clean hydrogen. Today, there is a considerable number of research and demonstration projects in the area of CCS around the globe. Some of these projects have already been completed, like the Weyburn project in Canada, while others are in progress [35].

In addition to the achievements in hydrogen production technologies, storage technologies have also witnessed major innovations. Researchers at Lawrence Livermore National Laboratory were successful in minimising the volume and weight of on-board liquid and compressed-gas hydrogen storage tanks by three-fold [36]. Moreover, lots of work has been conducted in developing innovative storage methods, such as storage of hydrogen in carbon nanotubes, in high-pressure glass microspheres, and in enhanced metal hydride materials [37]. A breakthrough in the subject of hydrogen storage could definitely speed the introduction of hydrogen as a fuel.

2.1.4 Hydrogen Uses

Hydrogen is valuable as a chemical feedstock. It is widely used in today's chemical industries to produce a wide range of products. According to the US Department of Energy (DOE) [38], approximately 500 billion normal cubic metres (Nm^3) of hydrogen are produced worldwide each year. About half of this quantity is used in ammonia production plants for fertiliser manufacture. Oil refineries alone consume 37% of the hydrogen produced for the removal of sulphur from the refined fuels and for other hydrotreating processes. Methanol production plants use about 8% of the total to manufacture synthesis gases necessary for making methanol. The remaining 5% is categorised as "merchant" hydrogen, which used in commercial sectors, such as space, pharmaceutical, food, electronics, and metals industries [39, 40]. One of the largest producers of merchant hydrogen in the world is Air Products and Chemicals Inc. Currently it operates more than 50 plants, producing over 25 million Nm^3 per day, and 7 pipeline systems [41].

For decades, researchers have been trying to find a means of storing electricity for time-displaced uses. Although a number of simple and advanced batteries have been suggested, none were able to cope with the vast variations in electricity demand. However, once produced, hydrogen can be stored using different storage methods and later converted to another energy form suited for the application. Besides being a convenient storage medium, hydrogen could also be used in transporting energy, even over long distances [42].

The transport sector is seen as the biggest market for hydrogen. Hydrogen may be used to power a vehicle in two ways: ICEs and fuel cells. Vehicles operating with hydrogen ICEs have potential benefits in terms of using conventional vehicle technologies that are well-understood and well-developed. However, it is unlikely to get substantial emission reductions from ICEs due to their inherent inefficiency [41].

Fuel cell-powered vehicles utilise an electrochemical process to convert pure hydrogen or hydrogen-rich fuel into electrical energy, which is used to drive the electric motors. Hydrogen can be stored in the vehicle either in a liquid or a gaseous form, or in a hydrogen rich fuel such as methanol or gasoline. Today, many different

car manufacturers are developing fuel cell prototypes. Daimler-Chrysler, for example, one of the biggest automobile manufacturers, has launched various types of fuel cell cars, NECARs (New Electric Car). NECAR1 was the first fuel cell vehicle ever built, NECAR2 works with compressed hydrogen, and NECAR3 has a methanol reformer to generate hydrogen. The most recent of the NECAR family, NECAR4, runs on hydrogen stored cryogenically [43].

The benefits of fuel cell vehicles are wide ranging but will not be fully apparent until these vehicles are in widespread use. With the use of hydrogen in fuel-cell vehicles there are zero or near-zero emissions of harmful ambient air substances like nitrogen dioxide (NO_2), sulphur dioxide (SO_2) or CO. Because of their low noise and high power qualities, fuel cell vehicles are ideal for eliminating noise pollution, which would be particularly beneficial in urban areas. Moreover, they offer high fuel efficiency, lower maintenance costs, and impressive driving range [43].

2.1.5 Hydrogen Economy

The world today is gradually moving from a hydrocarbon-based economy to a steady-state, clean, and secure hydrogen-based economy. The biggest challenge facing the hydrogen economy today is what is commonly referred to as the "chicken and egg" dilemma. Car manufacturers argue that they can mass produce hydrogen fuel cell vehicles but there is no infrastructure to support them. On the other hand, energy providers are reluctant to build hydrogen-fuelling stations since it is difficult to anticipate the size of future hydrogen demand. Some experts believe that this conundrum will delay the start-up of a hydrogen infrastructure because of the initial risk of investment. In contrast, other experts believe that there is no "chicken and egg" problem if governments, automakers, and energy companies are committed to the transition to a hydrogen economy. The feasibility of this idea is supported by the US National Renewable Energy Laboratory report which said, "If we really decided that we wanted a clean hydrogen economy, we could have it by 2010" [44].

Moving toward a sustainable hydrogen system at the peak of the oil age today seems far-fetched as many governments and industries have devoted more resources to the

gasoline- and methanol-based route than to the hydrogen path. However, there are a number of steps required to achieve this goal. In a paper published by Dunn [45], the author discussed at least ten generic elements of a hydrogen policy, or types of measures that could stimulate the transition. These basic elements are summarised in Table 2.1.

Table 2.1: Ten elements leading to a hydrogen economy [45]

• Research and development
• Demonstrations
• Feasibility studies
• Hydrogen economy target dates
• Public-private partnerships
• Full-cost energy pricing
• Environmental regulations
• Tax incentives
• Safety codes and standards
• Public education

Many researchers have investigated the deployment of the future hydrogen economy and a number of strategies have been suggested [46–50]. These strategies are classified into three terms: short (next 5 years), medium (10–20 years), and long (20–30 years). Over the next 5 years or so, governments should impose stringent environmental regulations on energy and automobile companies, and subsidise hydrogen ICEs. This would increase the incentive of automobile companies to mass-produce hydrogen ICE cars. The medium-term strategy should be the conversion of all governmental vehicles to fuel cell vehicles. This conversion should also include public transport such as buses and trains.

The long-term strategy leading to a hydrogen economy includes: shifting current petroleum fuel to hydrogen as well as using renewable energy sources to generate electricity and hydrogen fuel. The introduction of hydrogen-powered fuel cell vehicles is another foreseeable option towards a hydrogen economy. As emphasised in previous sections, hydrogen fuel cell vehicles have tremendous advantages over hybrids and ICE vehicles in terms of meeting our concerns over security of energy supply and climate change. However, fuel cell technology is still at the developing

stage and the commercialisation of the technology will require a considerable investment in research, development, and infrastructure.

Another long-term strategy was suggested by Lovins and Williams [46]. Although the proposed scheme relies on existing technologies, we categorised the strategy as long-term since the required technology is still undergoing rapid progress. The first stage of this strategy is the introduction of ultralight, supper-efficient hybrid vehicles, known as Hypercar®, which rely on fuel cell stacks and on-board tanks of compressed-gaseous hydrogen. The second stage is simultaneous integration of fuel cell market development between vehicles and buildings. The authors argued that we should start by deploying hydrogen and fuel cell technologies in a decentralised manner and then building up the hydrogen economy slowly until we reach the centralisation phase.

2.1.6 Hydrogen Safety

Like other fuels, hydrogen has its own pros and cons. On the negative side, hydrogen has wide flammability and detonability ranges when mixed with air. A volumetric mixture of hydrogen-and-air will have a flammability range between 4.0% and 75.0%, and a detonability range between 18.3% and 59.0%. The corresponding flammability and detonability limits for methane are 5.3% to 15.0% and 6.35% to 13.5% by volume, respectively. Petrol has an even narrower flammability and detonability limits, which are 1.0% to 7.6% and 1.1% to 3.3% by volume, respectively. To ignite a hydrogen flame, a very minute amount of energy is required—about 0.02 milli-joules (mJ). On the other hand, the minimum required ignition energy for a stoichiometric fuel-oxygen mixture is 0.29 mJ for methane and 0.24 mJ for petrol. Due to this minimal ignition energy, hydrogen can be ignited easily even by "electrical storms several miles away," as pointed out by James Hansel, a senior safety engineer for Air Products and Chemicals Inc. [47]. However, the explosion of hydrogen with a spark of heat or flame is almost impossible in an open area because of its high diffusivity rate. The hydrogen-air mixture can only be detonated by a strong initiator, such as a heavy blasting cap. However, detonation is more likely to happen in a completely confined volume, like a room or a storage tank [51–53].

Hydrogen is one of the most leak-prone of gases due to its tiny molecules. Hydrogen molecules tend to leak even from compact and strong materials, such as steel. To overcome this problem liquid hydrogen is used, however, a small fraction of it will boil-off every day. This poses a significant fire hazard. A hydrogen flame is nearly invisible in daylight and difficult to detect because of the absence of soot. According to James Hansel [47], "people have unknowingly walked into hydrogen flames." Hydrogen is also colourless and odourless unless special colorants and odorants are added. Furthermore, hydrogen is highly reactive causing many materials, including steel, to become brittle. Such an issue could lead to cracking or fissuring of materials resulting in structural defects of the system, hence catastrophic accidents [51, 52].

On the positive side, hydrogen has a high buoyant velocity at normal temperature and pressure (NTP), about 1.2–9.0 metre per second (m/s). Compared to hydrogen, methane travels at a slower rate of 0.8 to 6.0 m/s at NTP, while petrol is a non-buoyant fuel. Hydrogen also has a high diffusivity rate in air at NTP. It diffuses almost four times faster than methane, and about 12 times faster than petrol. Due to its high buoyancy and diffusivity, hydrogen spills quickly diffuse and escape away from its source into the atmosphere, minimising the risk of a fire. Contrary to methane and petrol flames, a hydrogen flame radiates at a very low energy meaning heat is not felt from a distance. Furthermore, hydrogen is non-explosive, non-toxic, and produces no smoke whereas petrol is explosive, slightly toxic, and awfully smoky [51–53].

Hydrogen has a bad reputation as a transport fuel in the general public perception. This reputation stemmed from the *Hindenburg* disaster. In May 1937, the *Hindenburg*—the largest airship ever built, nearly the size of the *Titanic*—burned while carrying 97 people at its dock in Lakehurst, New Jersey, after a voyage from Germany. Early investigations concluded that the cause of the accident was the presence of a highly flammable hydrogen-air mixture inside the dirigible's cover, which was ignited by the electrical storms that day. Sixty years later, in 1997, the former NASA scientist Addison Bain and the German scientist Ulrich Schmidtchen announced that the paint used on the skin of the airship, which contained flammable components, caused the ignition to occur by the aid of a storm's electrostatic charge. The scientists added that even though hydrogen contributed naturally to the disaster like any other fuel would, it was able to save the life of 62 passengers because of its

unique burning properties that kept the flame swirling harmlessly above the passengers' compartment. The 35 deaths were due to people jumping or falling from the compartment, or the burning of the airship's outer cover and on-board diesel [54].

Since the *Hindenburg* disaster, many experiments have been done to prove that hydrogen is not more dangerous than any hydrocarbon fuel [55]. Most of these tests revealed that hydrogen's hazards are different and generally more easily managed. Gas industries have also showed a good safety record in storing and handling hydrogen. For more than three decades, NASA has used and handled massive amounts of liquid hydrogen for fuelling space shuttles—more than 16 million gallons of liquid hydrogen for the Apollo-Saturn programme alone [55]. Despite some mishaps NASA had in dealing with liquid hydrogen, their experience offers an encouragement for utilising hydrogen as a safe future fuel.

The wide use of hydrogen as the ultimate fuel and energy carrier requires onerous safety codes and standards. The experience that the industry currently has is not enough and "inadequate to serve as a basis for decision-making," as asserted by a Stanford Research Institute study [55]. Therefore, "the critical path for a hydrogen economy must include major innovations in safety," says Joseph J. Romm in his recent book *The Hype about Hydrogen* [47]. However, this does not mean that hydrogen is more dangerous than other fuels, on the contrary and as discussed above, hydrogen, in many cases, is much safer.

2.1.7 Hydrogen Projects

The transition to a real-scale hydrogen economy mandates the emergence of new and novel hydrogen partnerships and pilot projects around the world. Through these partnerships, hydrogen and fuel cell technologies could be tested and technical, infrastructural, economical and environmental obstacles could be overcome. Due to the potential importance of such partnerships, many countries have lunched hydrogen programmes with the biggest players being the US, Japan, Germany, and Iceland. The US, as previously mentioned, had pledged $1.2 billion in launching a five-year initiative to commercialise hydrogen-powered cars by 2020. In March 2004, the

European Commission launched the first phase of a ten-year public-private partnership to develop hydrogen fuel cells with a budget of €2.8 billion ($3.4 billion). In Asia, Japan has also been aggressively progressing in the research and demonstration of hydrogen and fuel cell technologies with a 2002 budget of $240 million that increased to $268 million the following year [22, 56]. In addition to these proposals, many hydrogen partnerships and projects were established. To mention a few: London Hydrogen Partnership, Japan World Energy Network (WE-Net) programme, California Fuel Cell Partnership, Icelandic Hydrogen Transition Plan, and the Clean Urban Transport for Europe (CUTE) project. Of these partnerships, this section focuses on two: those in Iceland and California.

The Icelandic Hydrogen Transition Plan

Iceland enjoys considerable advantages, which make it an ideal place for the hydrogen experiment. The country has plentiful indigenous resources of inexpensive, clean geothermal and hydropower energy. Only a small fraction—about 15%—of these renewable energy sources is currently used, mainly for heating and power generation [57]. In a 2003 study published by the National Energy Authority of Iceland (known as Orkustofnun) [57], the potential for renewable electricity production has been estimated at 20 to 30 terawatt-hours per year (TWh/yr) for geothermal and hydropower energy, respectively. Being an independent island, Iceland also has the potential to generate electricity using wind turbines installed on the coastline or offshore. Moreover, the Icelandic government and its people are very supportive of the idea of introducing hydrogen as a fuel. With all these advantages, Iceland could soon become the "birthplace of the hydrogen economy," as stated by Thorsteinn Sigfusson, professor of physics at the University of Iceland in Reykjavík and founding chair of Icelandic New Energy Ltd [33].

Almost 21 years after the idea of developing a hydrogen economy in Iceland was suggested by a chemistry professor Bragi Arnason, the first Icelandic hydrogen partnership was established in 1999. The partnership involved a number of companies, including Shell Hydrogen, DaimlerChrysler, the Icelandic Holding Company VistOrka, and a well-known electrolyser producer Norsk Hydro. These

stakeholders formed what is known today as Icelandic New Energy Ltd. The mission of the company is "to investigate the potential for eventually replacing the use of fossil fuels in Iceland with hydrogen and create the world's first hydrogen economy," said Jon Bjorn Skulason, the General Manager of the company [58].

To fulfil its commitment, the company put forward a six-phase plan for the transition to a renewable hydrogen economy. The first phase was the opening of the world's first hydrogen fuelling station in the capital city Reykjavík on April 2003. The fuelling station is located on the site of a conventional fuelling station and was opened to the general public, even though the country has no privately owned hydrogen vehicles. Six months later, three hydrogen fuel cell buses arrived in Reykjavík for a two-year demonstration, as a part of the European Union (EU) funded Ecological City Transport System (ECTOS) project. The second phase is to gradually replace the current city bus fleet with PEM fuel cell buses. The third phase is to slowly introduce PEM fuel cells into passenger cars. The fourth phase is to demonstrate the viability of PEM fuel cells in the fishing fleet. The fifth phase is to gradually substitute the present fishing vessels with PEM vessels. Finally, the sixth phase is to export the surplus of hydrogen energy to the European continent [57–59]. The time framework for these phases depends mainly on the progress of the early stages and the breakthroughs in hydrogen technologies. The complete transition is predicted to take place by 2030–2040 [60].

The California Fuel Cell Partnership

Among the 50 US states, California was selected to be a "natural" laboratory for creating the first US hydrogen society for three main reasons. Firstly, California has one of the strictest environmental regulations in the country due to its poor air quality caused by the continuous emissions from the transport and industrial sectors. Secondly, California has mandated the introduction of zero emission vehicles and is aggressively pushing towards using them to improve air quality and reduce the dependence on foreign oil. Thirdly, most of the current Californian electricity is generated from renewable sources and low-carbon power generation technologies. The accessibility to an easy renewable electricity source offers an excellent

environment to produce "green" hydrogen. The above advantages give California the potential to be a real-scale test bed for learning all aspects of hydrogen and fuel cell demonstration projects [60, 61].

In April 1999, the California Fuel Cell Partnership (CaFCP) was set out in West Sacramento. The partnership consists of 32 members, including most major automakers, a number of energy providers, two fuel cell technology companies, several government agencies, and some authorities with specific areas of expertise. This collaboration would advance and evaluate hydrogen fuel cell vehicles under real-world conditions and bring the vehicle technology to the commercialisation stage. The CaFCP stated their goals as follows:

- Demonstrate fuel cell vehicle technology by testing and preparing the vehicles under real-world conditions in California,
- Demonstrate the feasibility of alternative fuel infrastructure technology through installing hydrogen and methanol fuelling stations,
- Explore and facilitate the path to commercialisation, and
- Enhance public awareness and understanding about alternative fuel technologies, focusing more on hydrogen and fuel cells [62].

Since its establishment, the CaFCP has contributed to the introduction of several dozen fuel cell vehicles. Presently, there are around 95 fuel cell vehicles on the roads of California—including both bus and light-duty vehicle fleets—and 16 fuelling stations to support them. According to the CaFCP 2004–2007 goals, the partnership members are planning to increase the number of fuel cell cars and buses up to 300 and 15 more fuelling stations are scheduled to be added all over California. The partnership is also committed to: (1) ensure "common fit" fuelling protocol, (2) promote practical safety codes and standards, (3) prepare and train communities for fuel cell vehicles and fuelling, and (4) exchange information and resources worldwide [62].

2.2 Hydrogen Supply Chain

2.2.1 Overview

In general, a supply chain can be viewed as a network comprising a number of facilities, such as suppliers, production sites, storage facilities and retailers. These facilities are integrated and connected together in a certain way seeking to: (1) acquire raw materials, (2) transform these raw materials into intermediate and finished products, and finally (3) distribute the finished products to retailers—customers or companies. The existence of supply chains is crucial in both service and manufacturing organisations; however the dimension and complexity of the chain may vary significantly from one industry to another [63, 64].

In a similar context, a hydrogen supply chain is defined as a network of integrated facilities, i.e. nodes, that are mutually connected and that work together in a specific way. These nodes include: (1) sources of energy, (2) production technologies, (3) storage facilities, (4) transportation modes, and (5) dispensing technologies—fuelling stations serving a quantified demand. The network begins with an energy source and terminates with fuelling stations. Between these end-nodes, there can be a series of production technologies, transportation modes, and storage facilities. The production and storage nodes are joined by the transportation modes.

In the subsequent sections, the abovementioned components of the hydrogen supply chain will discussed in more detail. Due to the wide range of hydrogen production, transportation, storage, and dispensing technologies that are currently available in the literature, only a number of these technologies will be considered in this thesis. If interested, the reader can view the extensive reviews by Ogden [37], Winter [65], and Padró and Putsche [66] for detailed discussions on hydrogen supply chain technologies.

2.2.2 Components of the Hydrogen Supply Chain

Primary Energy Sources

Despite the fact that hydrogen is the most abundant element in the universe, it does not exist freely on earth like oil or coal. It always combines with other elements such as oxygen and carbon. If hydrogen is to be used as the future fuel, it must be chemically separated and purified from hydrogen-containing compounds. This includes both non-renewable sources, such as oil, coal, or natural gas, and renewable sources, such as biomass, municipal solid wastes, sunlight, wind, geothermal, hydropower, or nuclear resources. Once hydrogen is freed from its source, it becomes a clean energy carrier.

Production Technologies

The diversity of hydrogen feedstocks gives rise to many production technologies that could be utilised. At present, there are a variety of commercial hydrogen production processes, including thermochemical methods, which are used to extract hydrogen from hydrocarbon resources, and electrolytic methods, which use electricity to split water to its constituent components—hydrogen and oxygen. Hydrogen can also be produced by photolytic methods, such as photobiological systems and photoelectrolysis. However, these promising methods are still being investigated at the laboratory level.

Hydrogen can be produced on a large-to-medium scale at dedicated, centralised hydrogen production plants, or on small-scale at local production facilities. Large-scale production facilities benefit from economies of scale and plants can be located near power and water sources. The main disadvantage of these facilities is the difficulties associated with hydrogen transport and distribution. Some methods of hydrogen production, such as its production from coal or biomass, are only feasible on a large-to-medium scale. On the other hand, small-scale production of hydrogen lessens the problems of hydrogen distribution by using the energy that is easily brought to the facility such as electricity, natural gas, or solar energy. However, the

total cost of the facility is generally high because cost is sensitive to the scale of production.

Steam Methane Reforming

Steam methane reforming—also known as steam reforming of natural gas since natural gas is mainly composed of methane—is the most common and least expensive method of hydrogen production. About half of the world's hydrogen and more than 90% of the US hydrogen is generated by steam methane reforming [67, 68]. The steam reforming technology can also be applied to other hydrocarbons such as ethane and naphtha. Heavier hydrocarbon feedstocks, however, cannot be used because they contain impurities and the feed of the reformer must be in the gaseous state. Other commercially available methods, such as partial oxidation, could be utilised for heavy hydrocarbons [66].

Reforming of methane to hydrogen is a multi-step process. In the first step, the feedstock is purified from impurities, which usually includes sulphur removal. The second step involves the reaction of methane and water vapour in tubes filled with a catalyst under a high pressure and temperature to form hydrogen and carbon monoxide:

$$CH_4 + H_2O \leftrightarrow CO + 3H_2 \tag{2.1}$$

After reforming, the resulting CO gas is shifted with steam to generate CO_2 and extra hydrogen via the water-gas shift reaction:

$$CO + H_2O \rightarrow CO_2 + H_2 \tag{2.2}$$

The flue gas exiting the shift reactors is 70%–80% hydrogen and the remainder consists of CO_2, CH_4, H_2O vapour, and CO. The hydrogen is then purified via a primary purification unit to remove any carbon oxides and water, followed by a secondary purification process to further eliminate any remnants of CO. The CO_2 stream is normally vented to the atmosphere [37, 69].

While steam reforming has been proven to be the cheapest route of producing hydrogen, natural gas is still a hydrocarbon-based fuel that emits CO_2 in the conversion process. As discussed previously, several studies have recommended that, in the future, CO_2 should be collected and sequestered in secure underground storage sites. Obviously, CCS would increase the costs of hydrogen production. In a recent study for British Energy, Watkiss and Hill [70] have estimated that sequestration would increase the costs of hydrogen production by 9%. The main advantage of a carbon-neutral fossil-to-hydrogen pathway is that the current energy infrastructure could be utilised to deliver natural gas to the processing facilities. In terms of energy supply security, however, the reliance on fossil fuel will continue.

Coal Gasification

In coal gasification, coal is gasified at a high temperature with the presence of oxygen to produce a synthesis gas, composed of H_2, CO_2, CO, CH_4, and H_2O. The synthesis gas leaving the gasifier is cooled and then quenched with water to remove particulates and any contaminates. Additional clean-up of sulphur compounds is required to prevent poisoning of the downstream catalyst. The synthesis gas is further processed, in the same way used to extract hydrogen from natural gas, to enrich the hydrogen content. Finally, the mixture is purified to produce hydrogen at the desired purity level through a sequence of purification steps. The reaction steps of gasification are shown by the following equations [37, 71]:

$$C_aH_b + a/2\ O_2 \rightarrow b/2\ H_2 + a\ CO \tag{2.3}$$

$$CO + H_2O \rightarrow CO_2 + H_2 \tag{2.4}$$

Hydrogen production from coal gasification is a well-established and well-practised commercial technology. However, it is only competitive with steam methane reforming in regions with scarce sources of oil and/or natural gas and abundant with coal deposits, such as South Africa, China and India [37]. Since coal gasification is a CO_2 generating process, coal plants can be efficiently coupled with CCS technology in a similar principle to steam methane reforming. This strategy is being pursed by the US DOE to make use of its vast coal reserves. The department planned state-of-the-art

coal-to-hydrogen demonstration projects and one project is already underway in North Dakota [72]. The project would explore the potential role of coal in the future hydrogen economy.

Biomass Gasification

The biomass gasification process resembles the process of producing hydrogen using coal gasification since biomass gasifiers are developed based on those for coal with minor technological modifications. However, biomass gasifiers operate at lower temperatures and the feedstock preparation requirements are different because biomass contains very little or no sulphur. Also, Biomass gasifiers can use a wide range of feedstock, including residues left over after the harvest of crops, trees, wastes from food processing plants, and sewage and municipal solid waste. The main drawbacks of biomass gasification are the availability of land to harvest the crops and the pre-treatment of the biomass feed. Furthermore, the technology is still not well-developed leading to a relatively expensive source of hydrogen, compared to previously mentioned methods [37, 71].

Water Electrolysis

In electrolysis, electricity is used to split water molecules into hydrogen and oxygen:

$$2H_2O + \text{electricity} \rightarrow 2H_2 + O_2 \tag{2.5}$$

Electrolysis is a well-proven process that has been industrially used for many decades, but on a small-scale. Only 4% of the annual global hydrogen production is derived from water electrolysis [66]. Electrolysis is a very clean, reliable process, and the hydrogen produced is very pure. It is the only process that does not rely on fossil fuels. Electrolysis combined with electrical energy produced from renewable sources, such as solar photovoltaic cells, wind turbines, geothermal energy, nuclear energy, or hydroelectric power, holds a great potential in the future to produce carbon-free hydrogen in a sustainable way.

The main drawback of this process is the intensive amount of electricity required, which makes it uncompetitive with steam reforming of natural gas. The cost of burning fossil fuels to generate electricity for electrolysis, for example, is three to five times more expensive than of reforming hydrogen directly from fossil fuels [69]. According to a study by the SFA Pacific Inc., the power consumption of the electrolytic process at 100% efficiency is about 40 kilowatt-hour per kilogram (kWh/kg) of hydrogen; however, in practice it is closer to 50 kWh/kg [73]. Despite this pitfall, there is growing interest in electrolysis technology since hydrogen can be produced locally where it is needed, i.e., decentralised production.

The production cost of hydrogen from water electrolysis is significantly higher than any other production technology. Electrolytic systems are generally only competitive with the steam methane reforming process in regions with cheap electricity—about 0.01–0.02 $/kWh [37].

Storage Technologies

The wide use of hydrogen as the future energy carrier requires it to be stored to meet time-varying demand. This includes large-scale, centralised bulk storage of hydrogen, medium-scale storage, and small-scale storage near the point of use. These different scales of hydrogen storage options are commonly used by today's chemical industry and may be utilised in the future hydrogen energy system. In the following sections, only two stationary storage technologies will be addressed: liquid hydrogen storage and aboveground compressed gas storage. Other hydrogen storage technologies are discussed by Ogden [37], Carpetis [74], Amos [75], and Padró and Putsche [66].

Liquid Hydrogen Storage

The storage of hydrogen as a cryogenic liquid has been used in industrial applications for many years. This is due to the fact that cryogenic storage is a much more weight-efficient means of storing hydrogen than compressed gas storage. Hydrogen is liquefied by reducing its temperature to very low levels—around −253°C at atmospheric pressure. Liquid hydrogen is stored in special super-insulated spherical

tanks to minimise heat loss. It cannot be stored in cylindrical tanks of the type used for liquefied natural gas due to the high boiling-off rate. NASA is presently the world's leader in storing and handling liquid hydrogen with the largest storage tank of a capacity up to 3800 m^3, which is about 22 metres in diameter [74, 76].

An advantage of liquid hydrogen over compressed gas is that the cryogenic tanks are more compact than pressure-cylindrical vessels, and thus truck delivery is less costly. For this reason, merchant hydrogen is often liquefied for storage and truck delivery. About one-third of merchant hydrogen is currently delivered by liquid-hydrogen tanker trucks and the rest is distributed by short-distance pipelines or compressed-gas tube trailers [37]. On the other hand, a key disadvantage of liquid hydrogen is the high capital cost associated with the liquefaction and storage equipment. Moreover, the energy required for liquefaction is by far the largest operating expense. The amount of electricity required to liquefy one kilogram of hydrogen is about 8.5–13.0 kWh/kg [41].

Compressed Gas Storage

Storing hydrogen in a compressed gas form is the simplest and the most common storage option used today. High compression is normally needed for this method to overcome the extremely low density of hydrogen gas, which is 0.08 kg/m^3 at ambient pressure [53]. Increasing the compression allows more hydrogen molecules to be contained within a specific volume and thus increasing the energy density. Hydrogen could be compressed up to a pressure of 70 mega-pascals (MPa) in order to achieve the desired storage content [47]. However, the typical storage pressure of commercially available pressurised vessels is 10–20 MPa with a holding capacity of 6000–9000 standard cubic feet (scf) [37].

The main technical challenges associated with compressed-gas storage systems are the tank volume and weight. This makes the storage system too bulky and difficult to transport or mount on a vehicle's body frame. Another drawback of compressed hydrogen storage is the high capital cost due to the high pressure required [47].

Transport and Distribution Options

Unlike the current energy infrastructure for electricity or natural gas, there is at present no widespread transmission and distribution system to bring hydrogen to consumers. The merchant hydrogen infrastructure that is in place today for delivering hydrogen to industrial users is very small, limited and inadequate to serve a large-scale hydrogen economy. As argued by Ogden [37], this infrastructure delivers fuel at perhaps 1% of the scale needed to serve major energy markets. The only well-developed hydrogen distribution infrastructure in the world exists in the US. The network is primarily utilised to supply the chemical and aerospace industries with their hydrogen demand via some 20,000 tanker trucks delivering about 80,000 metric tonnes of liquid hydrogen per year (t/yr) [77]. However, other parts of the world lack the existence of a decent hydrogen distribution infrastructure.

As with petrol, several options are available for transporting hydrogen, including trucks, pipelines, railways, and barges. This section discusses only the transport of hydrogen via truck and rail. The remaining options can be viewed in a report prepared by Amos [75].

Truck Transport

Liquid hydrogen is transported via trucks carrying special double-walled insulated tanks to minimise the boil-off rate. Some trucks use liquid nitrogen heat shields to cool the outer wall of the liquid hydrogen vessel to further reduce heat transfer. Tanker trucks can hold 360–4300 kg of liquid hydrogen with boil-off rates of 0.3%–0.6% per day [75]. On the other hand, compressed hydrogen gas is transported via tube trailers, which consist of several steel cylinders mounted on a protective framework. The holding capacity of tube trailers is a function of the number of tubes carried; however, a typical capacity of a tube trailer is 63–180 kg of hydrogen. The hydrogen gas inside these cylinders is normally pressurised to maximise the tank's capacity. The operating pressure varies between 20–60 MPa [75].

Rail Transport

As with tanker trucks, liquid hydrogen tanks can be mounted on a supporting framework and transported via railways. Similarly, a rail tube assembly could be configured to hold the desired amount of compressed hydrogen gas. The key difference between truck and rail transport is the storage capacity. Railcars usually have greater storage capacity due to the flexibility in the storage unit design. This is because, unlike trucks, railcars are not restricted by road infrastructure. The standard storage capacities of railway tank cars and railway tube cars are within the range of 2300–9072 kg and 180–454 kg of hydrogen, respectively [75].

Dispensing Technologies

The appearance of the future hydrogen fuelling stations will be similar to the existing petrol or diesel fuelling stations. However, the operation conditions for hydrogen fuelling stations will be different. Depending on the end-use applications, hydrogen stations will dispense hydrogen either in liquid or compressed gas form. If hydrogen is dispensed as a liquid, the fuelling stations would consist of liquid hydrogen storage tanks, pumps, and liquid dispensers. On the other hand, dispensing hydrogen as a compressed gas would require high-pressure storage vessels, compressors, and high-pressure hydrogen gas dispensers [73]. In the case of on-site hydrogen production at fuelling stations, the same fuelling components are needed, but there might be some reduction in compression energy since hydrogen is produced at a high pressure. Today, there are some 120 hydrogen fuelling stations in operation spread out over the world in connection with the present demonstration projects. This number is expected to reach 227 in the near future as more hydrogen fuel cell vehicles penetrate the transport market [78].

2.2.3 Design of Hydrogen Supply Chain

Design Factors

There are several factors that must be considered before designing the future hydrogen supply chain. The most crucial factor is characterising the demand level of hydrogen required for a particular region. This includes the consideration of the following important aspects: (1) the size of the hydrogen demand and its geographical location and concentration, (2) the proximity of demand, (3) daily and seasonal demand variations over time, and (4) the rate of demand growth. These aspects determine the number, size, type, and location of the production plants, distribution modes, and storage facilities [79].

The second main factor in designing a hydrogen supply chain is the location, availability, quantity, and cost of primary energy sources such as natural gas, biomass, or coal. These issues affect the decision of whether it is more favourable to establish a production facility on-site or to transport these resources to other production sites. The availability of land to accommodate the infrastructure for hydrogen production, storage and dispensing may also be an issue. This is an important aspect in metropolitan areas such as Greater London due to high prices and scarcity of suitable land. Moreover, secondary energy sources such as electricity as well as the availability and capacity of storage sites for carbon sequestration could greatly impact the choices made in establishing a hydrogen infrastructure [79].

The third important factor is technological breakthroughs in hydrogen production, delivery, storage, and end-user applications. For example, successful improvements in developing inexpensive and efficient small-scale steam methane reformers or high-pressure electrolysers could encourage the production of hydrogen at local fuelling stations [79]. In addition, a breakthrough in on-board hydrogen storage and advances in designing automotive fuel cell systems that are cost-effective, lightweight and compact would accelerate hydrogen deployment. As a result, this would increase the rate of demand growth, hence affecting the design of a hydrogen infrastructure. Other factors that would influence a hydrogen supply chain are government and industry

collaboration, public acceptance, the type of existing energy systems, and environmental and safety issues.

Due to the significance of identifying the appropriate demand volume, a number of attempts have been made to project the demand trend over time [39, 79–81]. The proposed analyses are mainly based on the rate of penetration of hydrogen vehicles into the current marketplace and rapid advancements in hydrogen technologies. An example of such analysis was the work carried out by the US DOE to predict the shape of a demand profile for four different scenarios. This profile is illustrated in Figure 2.2. Of these four demand scenarios, the bottom one depicts the demand outlook during a "business as usual" case in which hydrogen plays a minor impact on the transport market. The last three scenarios are developed for a plausible but optimistic vision of the penetration of hydrogen technologies into the fleet of light duty vehicles.

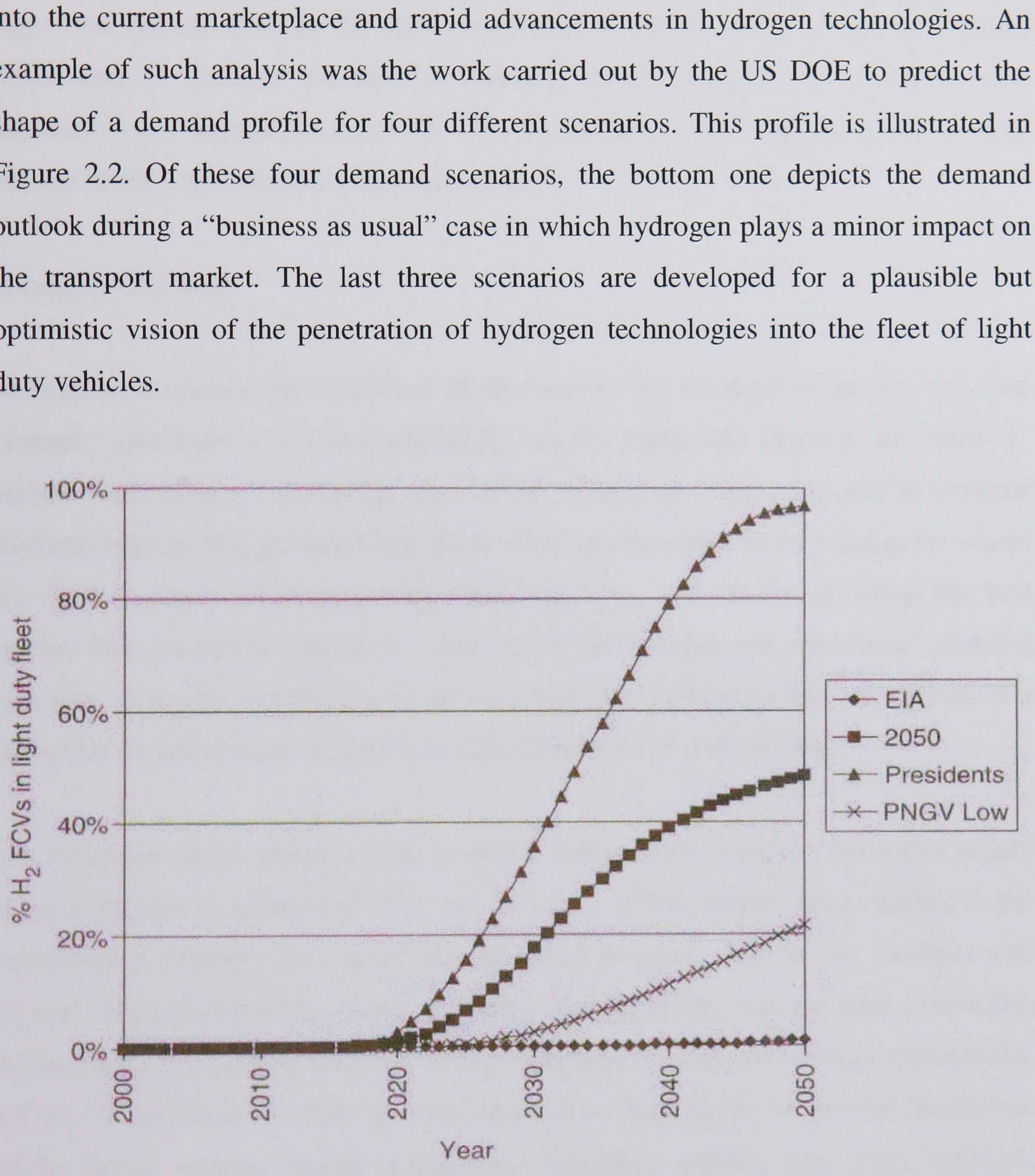


Figure 2.2: Hydrogen demand scenarios for vehicles considered by the US DOE [79].

Design Approaches

Designing a hydrogen supply chain network is a challenging task. This is due to the inherent complexity of the network, which stems from the presence of various processes and activities. As a result, there is a great necessity for paradigms to assist in designing a supply network based on performance objectives. Typical performance objectives include cost, profit, and environmental impact. Such a paradigm should either lead to the best configuration among various alternatives or improve the behaviour of a pre-specified system. The two widely used methods in engineering process design are simulation and optimisation.

Simulation Methods

Simulation examines the behaviour of the system and attempts to mimic, test, and compare alternatives. It relies essentially on the traditional question of "what if" versus "what is best". In reality, most of the simulation models are used to evaluate the performance of a pre-specified option. This can be achieved by running the model for several times eliminating undesired behaviour, and finally selecting the best option. The simulation approach is well suited for strategic and operational planning problems. It is also suitable for identifying potential bottlenecks and weaknesses of a particular design scheme as well as testing robustness of systems [82].

The literature shows that the most common approach in designing hydrogen supply chain networks is simulation. The key factor in differentiating these studies is the performance criteria—cost being the dominant measure. In a study, Simbeck and Chang [73] examined the entire hydrogen supply chain, starting with production technologies and ending with dispensing hydrogen for fuel cell vehicle applications. Of the 19 pathways studied, 15 were focused on large-scale centralised production plants using various energy feedstocks, including natural gas, coal, biomass, electricity, and petroleum coke and residue. The generated hydrogen was distributed as a compressed gas or liquid via tanker trucks or tube trailers. A pipeline was also considered for distributing compressed-gaseous hydrogen. The remaining four pathways relied on the production of hydrogen at local fuelling stations using small-

scale reformers or electrolysers. Based on the results obtained from these steady-state simulations, it was found that the cost-optimal pathway would be the production of hydrogen from natural gas in large-scale, centralised reforming plants with liquid hydrogen truck delivery.

A more recent comprehensive hydrogen supply chain cost analysis emerged from the committee of the National Research Council in the US [81]. The committee studied various combinations of feedstock, different scale of hydrogen production, two status of technology development (current versus possible future), and whether or not carbon sequestration is required at facilities processing hydrocarbon feedstock. These combinations formed 32 different hydrogen supply chain pathways. Out of the 32 pathways, nine involved large-scale central production plants using natural gas, coal and nuclear energy as a feedstock, with compressed-gaseous hydrogen distribution via a pipeline network. The next ten pathways considered the production of hydrogen in midsize facilities from natural gas, biomass, and electricity taken from the power grid. In this case, hydrogen was delivered to fuelling stations via tanker trucks in liquid form. The last 13 pathways were distributed options where hydrogen is produced on-site using small reformers or electrolysers. The committee also presented novel electrolytic distributed systems, including natural gas-assisted steam electrolysis, wind turbine-based electrolysis, photovoltaics solar-based electrolysis, and hybrid electrolysis utilising both renewable- and grid-derived electricity. For each pathway, the capital investment and operating cost for producing, distributing, and dispensing hydrogen were estimated. Similar to what was concluded by Simbeck and Chang [73], the committee found that the central large-scale production from natural gas offers the lowest hydrogen delivery cost.

A further cost analysis was carried out by Thomas *et al.* [83] to determine the delivery cost of hydrogen to fuel cell vehicle customers. The analysis provides a cost comparison between different hydrogen supply pathways, which utilise a number of production and transportation options. The analysis, moreover, investigates the effect of the size of hydrogen demand and the scale of production on the final hydrogen delivery cost. Based on discrete simulation, it was found that the most affordable and practical pathway to kick-off the hydrogen transport market is installing small-scale electrolysers and steam methane reformers. The authors asserted that fuelling

appliances could be added incrementally as time progresses to match the growth in fuel cell vehicle sales. Several hydrogen experts suggested this incremental additions and transitions strategy for initiating and developing the future hydrogen supply chain. The work of Ogden [61], Dunn [45], Lovins [15, 46], and Farrell *et al.* [84] represents a significant contribution in adopting such an approach.

Motivated by the concerns about urban air quality, Ogden [61, 79] examined the technical feasibility and economics of building a hydrogen vehicle refuelling infrastructure for the Los Angeles basin. Eleven different hydrogen supply options were proposed, analysed and compared in terms of the state of technology development, capital investment requirement, and hydrogen delivery cost. The examined systems use commercial and soon to be commercial technologies to produce, distribute and store compressed-gaseous hydrogen. The five near-term supply options are:

- Centralised steam reforming of natural gas with distribution of hydrogen via liquid hydrogen trucks or pipelines,
- Hydrogen recovered from chemical industry sources, such as petroleum refineries, with pipeline delivery to fuelling stations, and
- Production of hydrogen at local fuelling stations via small-scale steam reforming of natural gas or water electrolysis.

The six long-term supply options use a pipeline network to distribute hydrogen produced from the following technologies:

- Centralised production of hydrogen via electrolysis using CO_2-free electricity sources,
- Decentralised production of hydrogen via solar or wind powered electrolysis,
- Centralised production of hydrogen via gasification of biomass, coal, petroleum coke, or municipal solid wastes with CCS technology, and
- Hydrogen production via thermochemical water splitting powered by high temperature nuclear or solar heat.

Of these supply options, the most reasonable hydrogen pathway is to use the excess hydrogen from existing production facilities to facilitate the deployment of the infrastructure during its introductory phase.

Besides analysing the economics of the whole hydrogen supply chain network, Amos [75] and Padró and Putsche [66] evaluated the cost of individual components of the supply chain. Amos [75] extensively assessed the capital and operating costs associated with storing and transporting liquid and compressed-gaseous hydrogen. He studied different storage methods, including liquid hydrogen, compressed gas, metal hydride, and underground storage. He also investigated various modes of distribution, such as truck, railway, barge or pipeline. Padró and Putsche [66] surveyed more than 100 publications concerning the economics of current and near-term hydrogen technologies. This included production, storage, transport, and end-use technologies. For each technology, a detailed cost summary was presented.

In a study commissioned by the US DOE [85], Arthur D. Little, Inc. evaluate the energy efficiency, greenhouse gas emissions, cost, and safety of seven different well-to-wheel hydrogen supply chains. The performance of these chains was compared to that of methanol, ethanol, diesel, and gasoline supply chains. The study concluded that, despite the considerable differences in performance, risk, and cost of these various fuelling options, there is no clear winner to be identified. However, the hydrogen vehicular supply chain offered significant reduction in energy use and greenhouse gas emissions compared to ICE and gasoline hybrid-electric vehicles, but at a higher cost.

The design of a hydrogen supply chain has also received significant attention in the UK. Guy [86] examined the development of a transport hydrogen supply chain in London and the Southeast region and studied the challenges associated with establishing such an infrastructure. He proposed four different hydrogen pathways that could be implemented during the market development phase. These pathways were compared from technical, economical, market and environmental perspectives in order to select the most feasible option. He concluded that building a hydrogen supply chain in London and the Southeast region of the UK is feasible, environmentally beneficial and economically attractive. However, he also remarked that a number of technical challenges still need to be overcome in the future.

Joffe, Hart and Bauen [87] have also conducted a study to develop a refuelling hydrogen infrastructure in London due to the introduction of three hydrogen fuel cell

buses. The authors presented a methodology based on the technical modelling of hydrogen infrastructure technologies, as well as analysing the technical issues associated with the installation of an initial facility for bus refuelling in London. The proposed technical model characterises different technologies of the infrastructure to choose the best hydrogen configuration. After selecting the best configuration, the model makes decisions on the infrastructure's operation. From their discrete simulation, it was found that the choice of production technology has a great effect on when the infrastructure would be implemented, and the timing of hydrogen production and refuelling. While their work involves rigorous infrastructural assessment and operational simulation, the economics of the hydrogen infrastructure are not included in the model. The latter is an important issue in determining the optimal configuration of the future hydrogen supply chain.

It can be observed that all of the studies reviewed analyse each technology of the hydrogen supply chain individually. These technologies are then collectively connected to form a specific hydrogen pathway. Finally, individual pre-defined pathways are simulated and compared to select the "best" possible configuration based on a key performance indicator such as cost, pollutant emissions or energy efficiency. Also, most of these analyses are limited in their general applicability since they are based on a number of assumptions concerning the level of demand, distribution distance and geographic location. In addition, the studies do not consider the local availability or logistics network of energy sources, demand variation and different sizes of production plants and storage facilities, which are important factors in choosing the future hydrogen supply chain network. None of these studies looked at integrating the components of the hydrogen supply chain within a single framework to determine the optimal hydrogen pathway.

Optimisation Methods

The second method used in designing hydrogen supply networks is optimisation. While the simulation method evaluates the effectiveness of a pre-specified alternative, optimisation is designed to find the best course of actions among various decision alternatives according to some performance measures. These actions are represented by a set of mathematical expressions, referred to as an objective function and a set of

constraints. The last two elements constitute the optimisation problem. The objective function measures the behaviour of the system using some criteria such as minimising cost or maximising profit. On the other hand, constraints set the limits of the system and make sure that the generation of possible solutions fall within the defined feasible region by excluding the infeasible solutions [88].

Parameters and decision variables are the building blocks of optimisation problems. The former are known characteristics of the system such as production capacity, product flow rate, or operating conditions. Decision variables represent degrees of freedom in the optimisation. Often, they are further classified into: continuous, integer and binary variables. Integer variables might indicate the number of plants or storage facilities to be established, while binary variables represent decisions such as whether to install a transportation link or not [88].

Numerous techniques are currently available to formulate an optimisation problem [88, 89]. Choosing the appropriate method depends mainly on the way that was used to construct the objective function and constraints. For example, optimisation problems that have nonlinear variables in the objective and/or constraint functions are usually formulated as a nonlinear program problem. If the problem contains both integer and binary variables a mixed-integer nonlinear programme can be used. Since most of the models developed in this study exhibit a linear objective function and constraints with binary and integer variables, an MILP formulation is adopted. The MILP models will be solved with a commercial software tool known as General Algebraic Modelling System (GAMS). The software uses a branch and bound algorithm in order to search for the optimal solution.

To date, limited attention has been given to the role of optimisation techniques in designing and operating a future national hydrogen supply chain. Recently, Hugo [90] developed an optimisation-based formulation set in Germany that investigates different pathways for developing a hydrogen infrastructure. The generic model identifies the optimal infrastructure in terms of both investment and environmental criteria. While Hugo's work involves detailed mathematical modelling, it can be argued that the model fails to consider the issue of stationary storage of hydrogen in order to accommodate daily and seasonal time variations of demand. The model also

does not include the logistics network of energy sources, the concept of importing these resources from abroad if there is a shortfall, and the effect of demand uncertainty on the hydrogen infrastructure. Moreover, the high level of interactions between the different components of the hydrogen supply chain is not highlighted.

The use of an optimisation approach may provide a technological springboard for the early phases of developing a hydrogen supply chain network. It will predict the required investment in new hydrogen production plants, storage facilities and distribution networks. It will also enable governments to choose the optimum configurations for hydrogen production, storage and delivery systems before they develop organically. This may be of vital importance for national and international policy makers before any strategic industrial decisions are taken.

2.2.4 Uncertainty in Hydrogen Supply Chain

Types and Causes of Uncertainty

Uncertainty can be defined as the inability to predict future events or outcomes. In supply chain management, uncertainty is viewed as a plague propagating through the entire supply chain network. Such variability could affect the performance of suppliers and the reliability of production and transportation processes [91]. Thus, an immediate response to uncertainty in a supply chain network could lead to better performance in all supply chain activities as well as save considerable amount of capital. Ignoring uncertainty, however, may lead to inferior or simply wrong decisions and financial deficiency.

Due to the inherent and unavoidable nature of uncertainty, it is imperative to understand, measure, and analyse the main types of uncertainty in a supply chain. Geary *et al.* [92] classify supply chain uncertainty into four general categories: supply, manufacturing process, control, and demand. Uncertainty in these categories arises for many reasons; however, the focus of this thesis is uncertainty in demand. Therefore, only causes of demand uncertainty will be discussed in detail.

Product demand is a major type of uncertainty that occurs due to the difficulty of predicting the final product demand required by customers. This is because customers often tend to change their product specifications resulting in irregular orders, which in turn causes demand variability. As suggested by Davis [91], such perturbations can be avoided by keeping some inventories, i.e. stocks, to fulfil customer needs as required achieving an excellent customer satisfaction level. However, a build-to-order scenario is relatively rare and very costly. There are many factors on the demand side that must be considered when assessing demand uncertainty, including accuracy of demand forecasts, predictability of product demand, lead-time from design to production, rate of new product introduction, and number of sales channels.

Adding upon the causes of uncertainty highlighted in the previous discussion, Zimmermann [93] reported six general causes of uncertainty in supply chains. These causes are: lack of information or data, abundance of information, conflict of evidence, ambiguity (complexity), errors and noise in measurement, and belief. Such causes can affect any type of uncertainty mentioned earlier.

The literature reveals that demand is the most important and extensively studied type of uncertainty in supply chain design and operation [94–98]. The reason behind this is that managing demand in an effective and efficient manner would significantly improve customer satisfaction resulting in more profit. The source of demand variation analysed in this study stems from the inability to forecast the future hydrogen demand profile as fuel cell vehicles break through the near-term market. Handling this issue using appropriate modelling methods would aid decision makers in making meaningful and wise decisions.

Modelling Uncertainty

Uncertainty in supply chains can be classified into short-term and long-term [99]. Short-term uncertainty includes day-to-day variation in the supply chain activities such as cancelled/rushed orders, equipment failure, or sudden placed orders. This type of uncertainty can be modelled by a steady-state formulation of the problem by averaging each flow in the network over a sufficiently long period of time. On the

other hand, long-term uncertainty includes variation in supply chain activities over long timeframes such as seasonal demand variation, and raw materials and final product price fluctuation. This type of uncertainty requires a more direct modelling approach. Currently, numerous methods to model demand uncertainty exist. A few of them are: probability theory, scenario planning, evidence theory, fuzzy set theory, and rough set theory [93]. Despite the large number of uncertainty modelling methods, there is no method that is sufficient to model all kinds of uncertainty. However, the choice of the appropriate method is context dependent, as argued by Zimmermann [93].

The two distinct methods that are frequently used to represent uncertainty in supply chain modelling and optimisation are the probabilistic approach and the scenario planning approach. The former approach captures the stochastic aspect of the problem by treating one or more parameters as random variables with a known probability distribution [100]. In this approach, the demand is modelled through a normal distribution with a specified mean and standard deviation. Such an approach has commonly been used in literature and there are a number of studies which adopt this paradigm [101, 102]. However, the main hurdle associated with this approach is the difficulty to determine a probability distribution to describe the stochastic parameters. This difficulty leads to the use of a statistical procedure, which requires a huge amount of data that is almost never available. In this case "experts" will have to create the probability distribution using their experience and professional judgement [103].

The scenario planning approach captures uncertainty by representing a number of discrete realisations of the stochastic quantities. Each distinct realisation of all uncertain parameters gives rise to a scenario with an expected occurrence of particular outcomes. Each scenario can be viewed as quantitative descriptions of plausible future events. The objective of such an approach is to find robust solutions, which perform well under all scenarios. In some applications, scenario planning can replace forecasting since it takes into consideration potential changes in the business environment over a long-term planning horizon [100]. As stated by Owen *et al.* [100], there are at least three approaches to incorporate scenario planning into a supply chain model. These are: (1) optimising the expected performance over all scenarios, (2)

optimising the worst-case scenario, and (3) minimising the expected or worst-case "regret" across all scenarios.

Generating appropriate scenario sets in stochastic problems is a challenging task. Vanston Jr. *et al.* [104] presented a 12-step technique for generating scenario sets in stochastic planning applications. They reported that the method used in generating scenarios should depend on the intended use of the scenario, the nature of problem, and the personal preference of the researcher. However, regardless of the method used, each scenario should have distinct characteristics such as plausibility, self-consistency, inclusion of all critical and relevant events, and similarity between scenarios in form and scope. The well-known example of scenario use includes the work of Mulvey [105] to generate scenarios for the Towers Perrin* Investment System. The company uses a stochastic economic projection model called CAP:Link (capital market linkages) to generate economic factors and asset returns via a set of representative scenarios. Each scenario depicts a coherent set of outcomes over a long-term horizon of 10 to 40 years. The overall aim of the work was to construct a set of representative scenarios that are both optimistic and pessimistic for a risk investment strategy. Worldwide, Mulvey's software tool has been used in 12 countries in Europe, North America, and Asia.

In another work, Mulvey [106] also utilised a set of scenarios in the modelling framework of robust optimisation for several real-world applications. He elaborated on the notion of applying robust optimisation in large-scale planning problems that are subject to noisy, uncertain, or incomplete data. For advantages and disadvantages of scenario planning, interested readers can review the source. In addition, the scenario-based approach has been commonly used in many other mathematical programming problems [94–96, 100, 107]. For example, Tsiakis [95] considered a two-stage stochastic programming model for a multi-echelon supply chain network design under demand uncertainty. The uncertainty was captured via a number of representative scenarios resulting in a large-scale MILP model for this problem. The model was tested on a case study using a European supply chain network involving 14 products, 18 customer locations, 6 distribution centres, and 3 demand scenarios.

*A major international benefit and actuarial consulting company.

This work makes use of a scenario planning approach to capture uncertainty in hydrogen demand over a long-term planning horizon. The variation will be represented by a moderate number of scenarios for which a probability of occurrence will be specified. A multi-stage stochastic programming model is proposed to outline the plausible configurations of the future hydrogen supply chain network. As mentioned earlier, the goal of our formulation is to represent the possible future realisation of unknown problem parameters through a set of scenarios, and to consider the range of scenarios in determining a robust solution. The decisions incorporated in the presence of the stochastic behaviour are "here-and-now" decisions and "wait-and-see" decisions [94]. "Here-and-now" decisions have to be implemented prior to the realisation of the uncertainty and they are used to describe the first-stage variables. These decisions are associated with predicting the structure of supply chain network, for example the size, location, and capacity of production plants, before the actual demand to some future event is identified. On the other hand, "wait-and-see" decisions correspond to those decisions made after the uncertainty is unveiled and they relate to second-stage variables of the model. Examples of these decisions are production and transportation rates as well as network retrofits, which can often be revised when most up-to-date information is revealed.

The next chapter presents a novel optimisation approach for the structural design and operation of the future hydrogen supply chain network. The network is described as a static MILP model which is used to determine the supply chain of hydrogen production, transportation, and storage for vehicular use in Great Britain.

Chapter 3

Steady-State Design of Hydrogen Supply Chain

3.1 Problem Description

This chapter presents a model-based method to determine the design and operation of a steady-state hydrogen supply chain network. The examined network consists of production and storage facilities connected by transportation modes. The network is represented by a mathematical model which is formulated as an MILP optimisation problem. The construction of the network will be driven by hydrogen demand that is assumed to be both deterministic and time-independent. This leads to a snapshot representation of the network, which is revealed without deriving a migration pathway from the existing infrastructure. The migration pathways are considered in following chapters.

The proposed mathematical model is used to establish and investigate a number of strategic design decisions. These decisions include: (1) the geographical location, number, capacity, and type of production plants and storage facilities, (2) the transportation channels necessary, and (3) the amount of product to produce, store, and ship among plants and storage facilities. The objective of the model is to minimise the total cost of the network taking into account both infrastructural and operational costs. The applicability of the model is explored within a Great Britain context in order to study the potential hydrogen network configurations.

3.2 Model Structure and Components

The superstructure of the proposed hydrogen supply chain model is depicted in Figure 3.1. Within the figure, there are grid squares (g) enclosing different hydrogen production technologies and grids (g') enclosing different storage technologies. The grid squares represent different areas within Great Britain. While not all grids contain the different production technologies, all contain storage facilities. The grids containing the production technologies also contain storage facilities to satisfy the local hydrogen demand within the particular grid. Grids containing storage facilities only exist to satisfy regional demand of hydrogen. Production technology grids are connected to the storage technology grids via different transportation modes. The transportation modes are used to transport different product forms from production grids to storage grids, where hydrogen will be stored for market use.

As shown in Figure 3.1, the resulting model structure contains all possible configurations of the hydrogen supply chains as well as the interactions between the various supply chain components. From this structure, the optimisation algorithm will search for the best design option eliminating the undesired combinations of production/storage facilities and transportation links. In the following subsections, each component of the model structure will be addressed in greater detail, starting with grid squares and ending with storage facilities.

3.2.1 Grid Squares

An important step in designing a hydrogen supply chain model is identifying the geographical location required to map out all possible configurations. In this thesis, the mainland of Great Britain is considered as a scene for our study. The mainland is divided into grid squares of equal sizes. Each grid has a length of 108 kilometres (km), and represented by an index g in a set of indices from g_1 to g_n. The procedure used to construct these grids is provided in Appendix A.

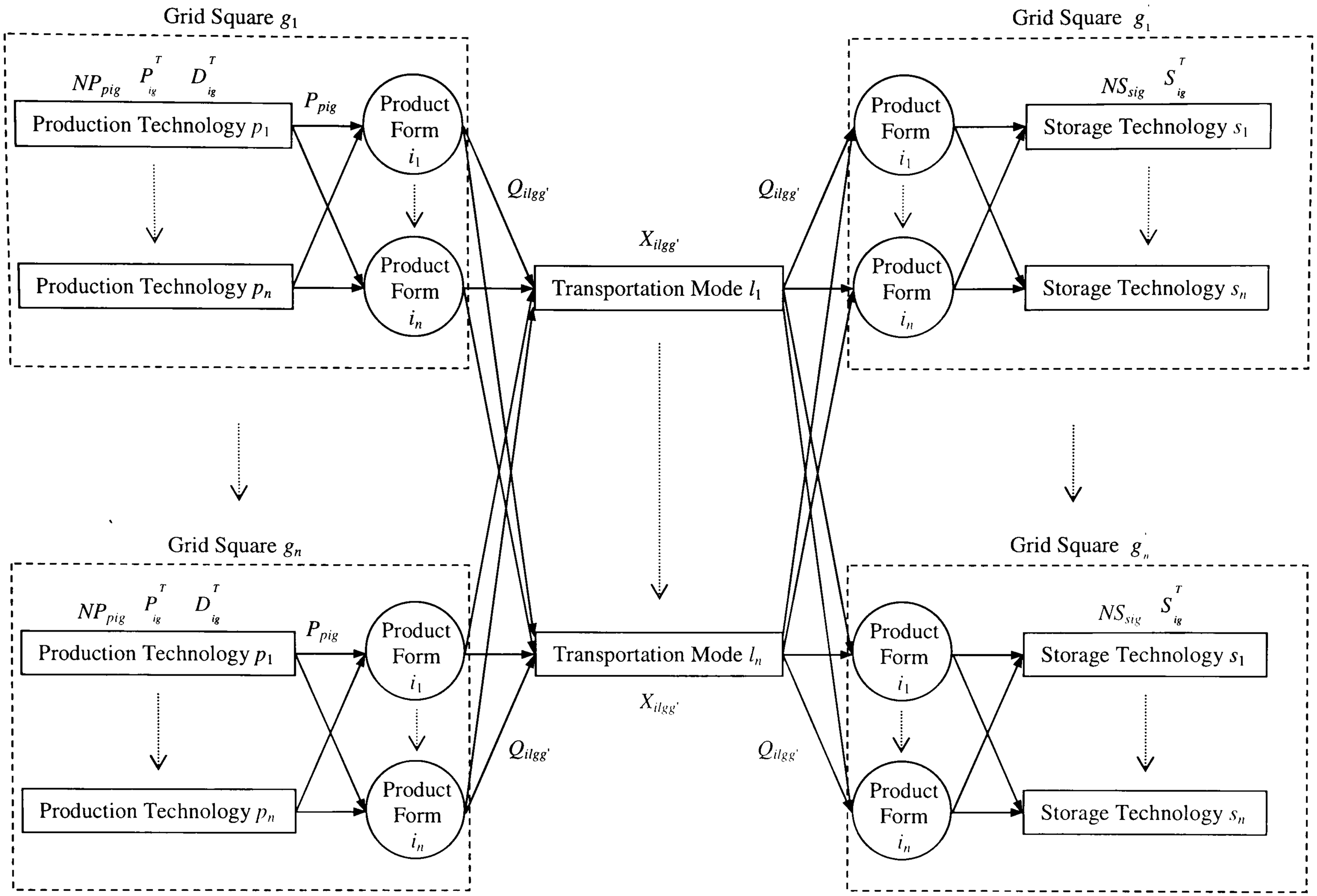


Figure 3.1: Superstructure of the steady-state model. The notations enclosed within the figure denote most of the decision variables involved in the model that need to be determined through optimisation.

After determining each grid's location, the geographic density of demand is characterised. The total equivalent hydrogen demand in Great Britain is estimated as a function of vehicle fuel economy, average distance travelled, and total number of vehicles available. The former factor is based on advanced hydrogen vehicles powered by PEM fuel cells, while the last two factors are based on data available for conventional ICE vehicles at 2002 levels. Two types of vehicles are considered: buses and private-and-light goods (PLG) vehicles, which include passenger cars and light vans. The demand for these mixed-modes is estimated based on the "asymptotic" assumption of 100% penetration in the transport market, i.e. saturated market. The procedure followed to calculate the demand is given in Appendix A.

3.2.2 Production Facilities

Since hydrogen can be produced from a wide variety of primary energy sources, a set of plant types with different production technologies can be used. The production technologies, including steam methane reforming, coal gasification, biomass gasification and electrolysis are designated by the index p. Each plant type has a production capacity which is bound between minimum and maximum limits. These limits determine the size of each type of the production facility. Also, each plant type incurs fixed capital and unit production costs. The establishment of plant types will be determined mainly by the demand of the grid, the failure of the grid to fulfil its needs from neighbouring grids, and the trade-offs between establishing plants or transportation links. The production decisions comprise of the number, location, and capacity of plant types. The total production rates in each grid are also included within the production decisions.

3.2.3 Product Physical Forms

Plants can produce different physical forms of product depending on customer requirements. These product forms are given the index i which represents the two common forms of hydrogen, gas or liquid. The form of the product is a key factor in

determining the transportation mode and the storage technology necessary, as well as the capital and operating costs concerning these technologies.

3.2.4 Transportation Modes

A number of transportation means could be utilised to deliver products from production facilities to storage sites. The corresponding options are given by the index l which can take a wide range of transportation options such as pipeline, truck, rail, etc. Each transportation option has a specific capacity, known delivery distance, minimum/maximum allowable flow rates, and capital and operating costs. The establishment of transportation links between various grids is determined by the cost of transportation mode versus the cost of establishing a new production facility. Transportation decisions include whether to establish a link between different grids and what the flow rate of product should be.

Since the delivery distance is a crucial factor in determining the type of transportation mode, a detailed assessment was carried to estimate the average distances within and between grids. The assessment can be viewed in Appendix B.

3.2.5 Storage Facilities

Storage facilities mark the final element of the proposed hydrogen supply chain model. Products delivered to the storage sites must be stored according to their physical form. Therefore, there are various types of storage technologies to select from. These storage technologies are indicated by the index s, taking potential alternatives such as cryogenic storage, compressed gas storage, metal hydride, etc. Each type of storage technology has upper and lower limits as well as different capital and unit storage costs. The stored product would be held in storage facilities for a certain number of days in order to serve demand and supply fluctuations, and plant interruptions. The products are then dispensed to customers according to their daily needs. The establishment of storage types is essential to satisfy the grid's demand and may be independent of the plant's location. The storage site could be located either

next to the production facilities within the vicinity of the grid or away from the production source, serving as distribution terminals. Storage decisions include determining the number, location and capacity of storage types, as well as the total average amount of product stored in each grid.

3.3 Model Formulation

The mathematical formulation is composed of nomenclature, constraints and objective function terms. The nomenclature includes indices, parameters, and decision variables, which are further categorised into: continuous, integer, and binary design variables. The corresponding notation and formulation are discussed below in more detail. The model proposed for this design problem is an MILP as described below.

3.3.1 Nomenclature

Indices

g	grid squares
g'	grid squares such that $g' \neq g$
i	product physical form
l	type of transportation modes
p	plant type with different production technologies
s	storage facility type with different storage technologies

Parameters

CCF	capital charge factor—payback period of capital investment (yr)
D_{ig}^{T}	total demand for product form i in grid g (kg/d)
DW_l	driver wage of transportation mode l ($/hr)
FE_l	fuel economy of transportation mode l (km/L)
FP_l	fuel price of transportation mode l ($/L)

GE_l general expenses of transportation mode l (\$/d)

$L_{gg'}$ delivery distance between grids g and g' (km)

LUT_l load/unload time of product for transportation mode l (hr)

ME_l maintenance expenses of transportation mode l (\$/km)

$PCap_{pi}^{\min}$ minimum production capacity of plant type p for product form i (kg/d)

$PCap_{pi}^{\max}$ maximum production capacity of plant type p for product form i (kg/d)

PCC_{pi} capital cost of establishing plant type p producing product form i (\$)

$Q_{il}^{\min}$ minimum flow rate of product form i by transportation mode l (kg/d)

$Q_{il}^{\max}$ maximum flow rate of product form i by transportation mode l (kg/d)

$SCap_{si}^{\min}$ minimum storage capacity of storage type s for product form i (kg)

$SCap_{si}^{\max}$ maximum storage capacity of storage type s for product form i (kg)

SCC_{si} capital cost of establishing storage type s storing product form i (\$)

SP_l average speed of transportation mode l (km/hr)

$TCap_{il}$ capacity of transportation mode l transporting product form i (kg/mode)

TMA_l availability of transportation mode l (hr/d)

TMC_{il} cost of establishing transportation mode l transporting product form i (\$/mode)

UPC_{pi} unit production cost for product form i produced by plant type p (\$/kg)

USC_{si} unit storage cost for product form i at storage type s (\$/kg/d)

α network operating period (d/yr)

β storage holding period—average number of days' worth of stock (d)

Continuous Variables

D_{ig}^{L} demand for product form i in grid g satisfied by local production (kg/d)

D_{ig}^{I} imported demand of product form i to grid g (kg/d)

FC fuel cost (\$/d)

FCC facility capital cost (\$)

FOC facility operating cost (\$/d)

GC general cost (\$/d)

LC	labour cost (\$/d)
MC	maintenance cost (\$/d)
P_{pig}	production rate of product form i produced by plant type p in grid g (kg/d)
P_{ig}^{T}	total production rate of product form i in grid g (kg/d)
$Q_{ilgg'}$	flow rate of product form i by transportation mode l between grids g and g' (kg/d)
S_{sig}	average inventory of product form i at storage type s in grid g (kg)
S_{ig}^{T}	total average inventory of product form i in grid g (kg)
TCC	transportation capital cost (\$)
TDC	total daily cost of the network (\$/d)
TOC	transportation operating cost (\$/d)

Integer Variables

NP_{pig}	number of plants of type p producing product form i in grid g
NS_{sig}	number of storage facilities of type s for product form i in grid g
NTU	number of transport units

Binary Variables

$X_{ilgg'}$	1 if product form i is to be transported from grids g to g' by transportation mode l, 0 otherwise
Y_{ig}	1 if product form i is to be exported from grid g, 0 otherwise
Z_{ig}	1 if product form i is to be imported into grid g, 0 otherwise

3.3.2 Constraints

Demand Constraints

As previously stated, each grid has its own deterministic demand. This demand must be fulfilled eventually by local production facilities or by importing products from

other neighbouring grids. The presence of production facilities within a particular grid will ensure this demand satisfaction. Therefore, the demand satisfied by local production of a product form i in grid g (D_{ig}^{L}) must by stipulated by the following constraint:

$$D_{ig}^{L} \leq P_{ig}^{T} \qquad \forall i, g \tag{3.1}$$

On the other hand, the demand for a product form i in a grid g satisfied by neighbouring grids (D_{ig}^{I}) is equal to the total flow imported to that grid by all types of transportation modes ($Q_{ilg'g}$):

$$D_{ig}^{I} = \sum_{l,g'} Q_{ilg'g} \qquad \forall i, g \tag{3.2}$$

The total grid demand (D_{ig}^{T}) must equal the demand satisfied by the local production plus the demand imported from other grids, as follows:

$$D_{ig}^{T} = D_{ig}^{L} + D_{ig}^{I} \qquad \forall i, g \tag{3.3}$$

Production Facility Constraints

A total mass balance on a grid must be written to determine the total daily production rate in a particular grid. Since steady-state operation is assumed, the sum of the total flow rate of each product entering grid g ($Q_{ilg'g}$) plus the total production rate of that same grid (P_{ig}^{T}) must equal the total flow rate leaving this grid ($Q_{ilgg'}$) plus the total demand required by grid g itself (D_{ig}^{T}):

$$P_{ig}^{T} = \sum_{l,g'} \left(Q_{ilgg'} - Q_{ilg'g} \right) + D_{ig}^{T} \qquad \forall i, g \tag{3.4}$$

The total production rate of a product form i in a grid g is equal to the production rate of all plants of type p established in that same grid:

$$P_{ig}^{T} = \sum_{p} P_{pig} \qquad \forall i, g \tag{3.5}$$

The production rate of a product form i produced by any plant of type p at a grid g (P_{pig}) cannot exceed certain limits. Thus, there is always a maximum production capacity for any product ($PCap_{pi}^{\max}$); moreover, there is often a minimum production rate ($PCap_{pi}^{\min}$) that must be maintained while the plant is operating:

$$PCap_{pi}^{\min} NP_{pig} \le P_{pig} \le PCap_{pi}^{\max} NP_{pig} \qquad \forall p, i, g \tag{3.6}$$

This means that the maximum daily production rate of product form i produced by plant of type p is constrained by the number of production facilities NP_{pig}.

Transportation Constraints

There must be a continuous flow of product between different grids in order to satisfy the required demand. The flow of a product form i from a grid g to a different grid g' will exist only if the transportation mode has been established. Therefore, there is always a minimum and a maximum flow rate of products ($Q_{il}^{\min}$ and $Q_{il}^{\max}$) needed to justify the establishment of a transportation mode between two grids in the network:

$$Q_{il}^{\min} X_{ilgg'} \le Q_{ilgg'} \le Q_{il}^{\max} X_{ilgg'} \qquad \forall i, l, g, g' : g \ne g' \tag{3.7}$$

Flow of a product form i between different grids can only occur in one direction. This is because if a grid can only satisfy its needs by importing from other grids it would not make sense for that grid to export to other grids. Therefore, a particular grid can only import product from neighbouring grids or export product to other grids, or neither but not both:

$$Y_{ig} \geq X_{ilgg'} \quad \forall i,l,g,g' : g \neq g' \tag{3.8}$$

$$Z_{ig} \geq X_{ilg'g} \quad \forall i,l,g,g' : g \neq g' \tag{3.9}$$

$$Y_{ig} + Z_{ig} \leq 1 \quad \forall i,g \tag{3.10}$$

Storage Facility Constraints

An important issue in the operation of this network is the ability of the storage facilities to hold the product for a certain period of time in order to accommodate for demand and supply fluctuations. Storage facilities could be built either locally within a specific grid or outside the grid boundary away from the production source.

During steady-state operation, the total average inventory of a product form *i* in a grid *g* (S_{ig}^T) is equal to a function of the corresponding total demand (D_{ig}^T) multiplied by the storage period (β), days of cover:

$$S_{ig}^T = \beta\, D_{ig}^T \quad \forall i,g \tag{3.11}$$

The parameter β in Equation 3.11 is introduced to cover uncertainties in both supply and demand as well as plant interruptions.

As the case with production plants, the average inventory of product form *i* stored in each storage facility of type *s* cannot exceed certain limits:

$$SCap_{si}^{\min} NS_{sig} \leq S_{sig} \leq SCap_{si}^{\max} NS_{sig} \quad \forall s,i,g \tag{3.12}$$

Constraint 3.12 implies that the average inventory of product form *i* stored in a grid *g* is constrained by the number of storage facilities NS_{sig}.

Similarly, the total average inventory of each product in each grid will be bound within certain limits:

$$\sum_{s} SCap_{si}^{\min} NS_{sig} \leq S_{ig}^{T} \leq \sum_{s} SCap_{si}^{\max} NS_{sig} \quad \forall i, g \tag{3.13}$$

Non-negativity Constraints

All decision variables must be non-negative:

$$D_{ig}^{L} \geq 0 \quad \forall i, g \tag{3.14}$$

$$D_{ig}^{I} \geq 0 \quad \forall i, g \tag{3.15}$$

$$NP_{pig} \geq 0 \quad \forall i, p, g \tag{3.16}$$

$$NS_{sig} \geq 0 \quad \forall i, s, g \tag{3.17}$$

$$P_{pig} \geq 0 \quad \forall i, p, g \tag{3.18}$$

$$P_{ig}^{T} \geq 0 \quad \forall i, g \tag{3.19}$$

$$Q_{ilgg'} \geq 0 \quad \forall i, l, g, g' : g \neq g' \tag{3.20}$$

$$S_{sig} \geq 0 \quad \forall i, s, g \tag{3.21}$$

$$S_{ig}^{T} \geq 0 \quad \forall i, g \tag{3.22}$$

3.3.3 Objective Function

The objective of the proposed model is to minimise the overall cost of a possible hydrogen supply chain network. This cost includes both capital and operating expenditure. The former are one-time costs associated with the establishment of production plants, storage facilities, and transportation links. Operating costs, however, are incurred on a daily basis and are associated with the cost of production at plants, the cost of storage, and the cost of transportation through the network. This study explores cost as the main objective, but a variety of metrics could be

investigated in a more detailed study, for example well-to-wheel analysis of greenhouse gas emissions.

In the subsequent sections, the cost terms used to estimate the overall cost of the hydrogen supply chain network are addressed in greater detail.

Facility Capital Cost

The facility capital cost is related to the establishment of production plants and storage facilities at candidate locations. It is calculated by multiplying the number of plants and storage facilities by their capital costs as follows:

$$FCC = \sum_{i,g}\left(\sum_{p} PCC_{pi} NP_{pig} + \sum_{s} SCC_{si} NS_{sig}\right) \tag{3.23}$$

Transportation Capital Cost

This thesis focuses primarily on mobile transport of hydrogen which includes truck and rail. Therefore, the cost functions used in estimating the capital and operating costs of transportation modes are only applicable for this purpose. The method of deriving these cost functions are detailed in Appendix C.

The capital cost of different types of transportation modes takes into account the number of transport units, i.e. trucks or railcars, required to satisfy the demand and cost of each unit. The number of transport units (NTU) depends significantly on the average distance travelled between different grids ($L_{gg'}$). Long delivery distances mean more trucks or railcars are required to deliver a given quantity of product, which can result in a higher transportation capital costs. The capacity of a transport container ($TCap_{il}$) is also an important factor, especially for long distances, since it determines the number of trips that must be made between the production plant and the storage facility. It is clear that large storage containers will reduce the cost of transportation as fewer trucks or railcars are required. In addition, the flow rate of products between

various grids ($Q_{ilgg'}$), transportation mode availability (TMA_l), average speed (SP_l), and loading/unloading time (LUT_l) are other main factors that affect the capital and operating costs of transportation. On the other hand, the cost of the transport unit (TMC_{il}) includes the cost of the transport container, the cost of the undercarriage and the cost of the cab. In the case of rail transport there will be no cab cost.

The number of trucks and/or railcars required to satisfy a certain flow between different grids are given by the following relationship:

$$NTU = \sum_{i,l,g,g'} \frac{Q_{ilgg'}}{TMA_l TCap_{il}} \left(\frac{2L_{gg'}}{SP_l} + LUT_l \right) \tag{3.24}$$

It can be noted from Equation 3.24 that $L_{gg'}$ is multiplied by two to account for the return journey.

Therefore, the transportation capital cost is given by the following equation:

$$TCC = NTU \times TMC_{il} \tag{3.25}$$

Facility Operating Cost

The facility operating cost is related to the cost required to operate the production plants and storage facilities efficiently. The plant operating cost is calculated by multiplying the unit production cost (UPC_{pi}) by the plant production rate (P_{pig}). Similarly, the storage operating cost is obtained by multiplying the unit storage cost (USC_{si}) by the average stored inventory (S_{sig}) in each grid. Thus, the corresponding cost terms in the objective function are of the form:

$$FOC = \sum_{i,g} \left(\sum_{p} UPC_{pi} P_{pig} + \sum_{s} USC_{si} S_{sig} \right) \tag{3.26}$$

Transportation Operating Cost

The transportation operating cost consists of fuel, labour, maintenance. and general costs. The daily fuel cost contributes significantly to the total operating cost. It is a function of daily fuel usage and fuel price:

$$FC = \sum_{i,l,g,g'} FP_l \left(\frac{2L_{gg'} Q_{ilgg'}}{FE_l TCap_{il}} \right) \tag{3.27}$$

where the first and second terms of the multiplication in Equation 3.27 represent fuel price and daily fuel usage, respectively.

The daily labour cost associated with transporting product forms between different grids is given as a function of the total delivery time and driver wage:

$$LC = \sum_{i,l,g,g'} DW_l \left(\frac{Q_{ilgg'}}{TCap_{il}} \left(\frac{2L_{gg'}}{SP_l} + LUT_l \right) \right) \tag{3.28}$$

Again, the first and second terms of the multiplication in Equation 3.28 represent driver wage and total delivery time, respectively.

The maintenance cost includes general maintenance of the transportation systems. It is a function of the total daily distance driven and the cost per unit distance travelled:

$$MC = \sum_{i,l,g,g'} ME_l \left(\frac{2L_{gg'} Q_{ilgg'}}{TCap_{il}} \right) \tag{3.29}$$

The last operating cost is the general cost. It consists of transportation insurance, license and registration, and outstanding finances. It depends on the number of transport units required to deliver products to the storage facilities and the corresponding general expenses:

$$GC = \sum_{i,l,g,g'} GE_l \left(\frac{Q_{ilgg'}}{TMA_l TCap_{il}} \left(\frac{2L_{gg'}}{SP_l} + LUT_l \right) \right) \tag{3.30}$$

Finally, the total transportation operating cost is equal to the sum of fuel, labour, maintenance, and general costs as follows:

$$TOC = FC + LC + MC + GC \tag{3.31}$$

3.3.4 Model Summary

Combining the cost terms derived in Section 3.3.3, the total daily cost of the hydrogen supply chain network can be expressed as follows:

$$TDC = \frac{FCC + TCC}{\alpha\, CCF} + FOC + TOC \tag{3.32}$$

The first term of the right-hand-side of Equation 3.32 is divided by the network operating period (α) in days and the annual capital charge factor (CCF) in order to find the cost per day.

Finally, the total daily cost of the network is minimised by the optimisation:

$$\min\ TDC \tag{3.33}$$

The above minimisation is subject to all constraints stated in Section 3.3.2.

3.4 Great Britain-Based Case Study

The mainland of Great Britain was chosen for several reasons. Great Britain has a fairly well established environmental culture with the potential to develop the infrastructure of a new source of energy such as hydrogen. Also, data that is required

to design such an infrastructure is easily accessible and available from different authorities. In addition, Great Britain has a long-term strategic initiative to promote a widespread use of hydrogen in the transport sector. For example, it is one of the European countries that are currently involved in the EU-funded CUTE project. The fruit of this project was the introduction of three fuel cell buses in London at the beginning of 2004 [108]. Considering the above features, Great Britain represents an ideal case study to outline all possible hydrogen supply chain networks.

The versatility of the examined model was tested using a number of production and storage technologies as well as a number of transportation modes. The types of production, storage, and transportation technologies are summarised in Table 3.1.

Table 3.1: Production, storage, and distribution technologies of the steady-state model

Production technology	• Steam methane reforming • Coal gasification • Biomass gasification
Storage technology	• Liquid hydrogen storage • Compressed gas storage
Transportation method	• Liquid hydrogen (LH_2) tanker truck • Liquid hydrogen railway tank car • Compressed-gaseous hydrogen (CH_2) tube trailer • Compressed-gaseous hydrogen railway tube car

Reforming and gasification technologies were selected because they are well-known and well-practised methods in today's industry [66, 67]. Also, these technologies can be built economically in medium-to-large production scales. Such an option is practical since most of the current hydrogen is produced in dedicated, centralised, large-scale plants. In addition, centralised reforming and gasification plants are well suited for CCS technology.

The purified hydrogen generated from the production facility has to either be liquefied or compressed before being stored or distributed. The form of hydrogen depends mostly on end-users. Liquid hydrogen is stored in large-scale super-insulated spherical tanks to minimise heat loss and boil-off rate, and then delivered via tanker trucks or railway tank cars. In contrast, compressed hydrogen gas is stored in large-scale pressurised cylindrical vessels to increase the energy density, and distributed by tube trailers or railway tube cars.

In summary, three different configurations of hydrogen networks are examined based on the physical form of hydrogen. These configurations are:

1. Production of hydrogen in medium-to-large, centralised plants and delivered to various stationary storage facilities as a liquid via tanker trucks and railway tank cars,
2. Production of hydrogen in medium-to-large, centralised plants and distributed to various stationary storage facilities as a compressed gas via tube trailers and railway tube cars, and
3. The last configuration is similar to the first one but only tanker trucks will be used.

3.4.1 Input Data

A key outcome of this exercise is the understanding of the data requirements for the application of a hydrogen supply chain design. Due to the existence of various processes in supply chain, data usually comes from diverse sources. In building the proposed model, a number of engineering-oriented methods were applied to validate the data as much as possible. These include comparison of similar data from alternative sources, comparison with petroleum supply chain data, first principles modelling, costing conventions, and thermodynamic and dimensional analysis. Such an attempt should help in the generation of a definitive data set for other researches.

The following subsections describe the input data required for the three configurations discussed above. Although data used below is based on theoretical assumptions and suggested purely for the sake of our analysis, they are still believed to be representative and valid for real cases.

Hydrogen Demand

The daily demand of hydrogen in the 34 grid squares is summarised in Table 3.2. The hydrogen supply network obtained from satisfying these demand values is assumed to operate at 100% utilisation rate, i.e. 365 d/yr, in order to cover daily and seasonal

variations of demand. The capital charge factor associated with this investment is assumed to be 3 years.

Table 3.2: Hydrogen demand in each grid square for the steady-state model

Grid, g	Hydrogen demand (t/d)
01	102
02	80
03	158
04	198
05	41
06	130
07	173
08	7
09	85
10	316
11	385
12	9
13	635
14	902
15	143
16	24
17	489
18	997
19	497
20	41
21	63
22	624
23	1047
24	861
25	356
26	63
27	394
28	879
29	2727
30	188
31	208
32	252
33	185
34	136

Production Facilities

The minimum and maximum production capacity of each plant type with respect to each hydrogen form ($PCap_{pi}^{\min}$ and $PCap_{pi}^{\max}$) are assumed to be 10 and 960 t/d, respectively. These values are based on commercial medium-to-large hydrogen plants that are currently in production [81]. The capital costs and the unit production costs of these plants are listed in Table 3.3. A detailed economic analysis was performed to estimates these cost figures. This analysis appears in Appendix C.

Table 3.3: Capital and unit production costs of hydrogen production technologies

Plant type, p	Steam reforming		Coal gasification		Biomass gasification	
Product form, i	LH_2	CH_2	LH_2	CH_2	LH_2	CH_2
Plant capital cost, PCC_{pi} (million \$)	903	644	1611	1331	1836	1558
Unit production cost, UPC_{pi} (\$/kg)	1.43	0.88	1.56	0.96	2.15	1.59

Transportation Modes

The maximum flow rate of liquid and compressed-gaseous hydrogen transported via trucks or railcars (Q_{il}^{max}) was assumed to be 960 t/d, while the minimum flow rate (Q_{il}^{min}) is assumed to be equal to the capacity of each transport mode (see Table 3.4). This means that the minimum allowable quantity of hydrogen flow between grids is equal to a fully-loaded transport unit. The maximum allowable quantity, however, is based on the assumption that individual modes cannot transport more than what is produced by a large production facility. The delivery distances travelled by these modes to deliver hydrogen to the point of storage were estimated and summarised in Table B.1 (Appendix B).

The capacity of the transport container and the capital cost of the transportation mode are shown in Table 3.4. Other parameters that are used to estimate the capital and operating costs for the different types of transportation modes are listed in Table 3.5. As appears in both tables, rail transport exhibits several advantages over truck transport in terms of container capacity, cheap fuel price, and low maintenance and general costs. On the other hand, truck delivery benefits from high delivery speed, high availability, and short load/unload time. Most of these data were obtained from a technical report by Amos [75]. However, the values for fuel price, driver wage, and maintenance and general costs were obtained from diverse sources as indicated in the tables.

Table 3.4: Capital cost and capacity of transportation modes

Transportation mode, l	Tanker truck	Tube trailer	Railway tank car	Railway tube car
Transport unit capacity, $TCap_{il}$ (kg/mode)	4,082	181	9,072	454
Tank unit cost (\$/mode)	350,000	100,000	400,000	200,000
Undercarriage cost (\$/mode)	60,000	60,000	100,000	100,000
Cab cost (\$/mode)	90,000	90,000	–	–
Transport mode cost, TMC_{il} (\$/mode)	500,000	250,000	500,000	300,000

Table 3.5: Characteristics of transportation modes

Transportation mode, l	Truck[1]	Rail[2]
Fuel economy, FE_l (km/L) [75]	2.55	4.25
Average speed, SP_l (km/hr) [75]	55	45
Transport mode availability, TMA_l (hr/d) [75]	18	12
Load/unload time, LUT_l (hr) [75]	2	12
Driver wage, DW_l ($/hr) [109]	23	23
Fuel price, FP_l ($/L) [110]	1.16	0.28
Maintenance expenses, ME_l ($/km) [111]	0.0976	0.0621
General expenses, GE_l ($/d) [112]	8.22	6.85

[1]Include both tanker trucks and tube trailers.
[2]Include both railway tank and tube cars.

Storage Facilities

The minimum and maximum storage capacities of each storage type with respect to each hydrogen form ($SCap_{si}^{min}$ and $SCap_{si}^{max}$) were assumed to be 10 and 540 t, respectively. The maximum value was estimated by doubling the size of the largest cryogenic tank available at NASA [113], while the minimum value was based on tanks available in today's gas industry. The capital cost for the establishment of different storage facility types and the unit storage costs are listed in Table 3.6 (see Appendix C for more detail). The average number of days' worth of stock (β) in these storage facilities is assumed to be 10 days.

Table 3.6: Capital and unit storage costs of hydrogen storage technologies

Storage type, s	Liquid hydrogen storage	Compressed gas storage
Product form, i	LH_2	CH_2
Storage capital cost, SCC_{si} (million $)	122	1894
Unit storage cost, USC_{si} ($/kg/d)	0.005	0.076

3.4.2 Results and Discussion

The aim of the proposed model was to satisfy the hydrogen demand listed in Table 3.2 by mapping out all possible hydrogen supply chain configurations. As mentioned, the model was tested with the supply of liquid and compressed-gaseous hydrogen via trucks and rail to various storage facilities. It was also constrained to deliver liquid hydrogen via tanker trucks only to study the effect of single- and multi-mode distribution options on the resulting network structures, as well as their costs. The

optimal solution of the three configurations led to the network structures shown in Figures 3.2–3.4. The number of production and storage facilities established in each grid of these figures is enclosed within a square or a circle, respectively. The number above each transportation link, i.e. arc, denotes the corresponding flow rate of liquid or compressed-gaseous hydrogen ($Q_{ilgg'}$) in t/d. The exact values of these flow rates between different grids with respect to transportation modes are listed in Tables E.1 and E.2 in Appendix E. In addition, a summary of the results found for the different continuous variables is tabulated in E.3 and E.4.

Figures 3.2 and 3.4 illustrate that tanker trucks are the main transport mode used to deliver liquid hydrogen from the point of production to the point of storage. This implies that tanker trucks are a preferable means of delivery for short distances and moderate hydrogen demand. For long distances and large quantities, railway tank cars become more attractive due to their low transportation operating cost and high storage capacity. However, in the case of the compressed-gaseous hydrogen network (see Figure 3.3) both railway tube cars and tube trailers are utilised since their storage capacity and cost does not differ significantly. Also there are fewer transportation links established in the compressed-gaseous hydrogen network than in the liquid hydrogen network. This is because of the high cost associated with distributing compressed hydrogen gas to various locations. Therefore, more production plants are established in order to fulfil the required demand.

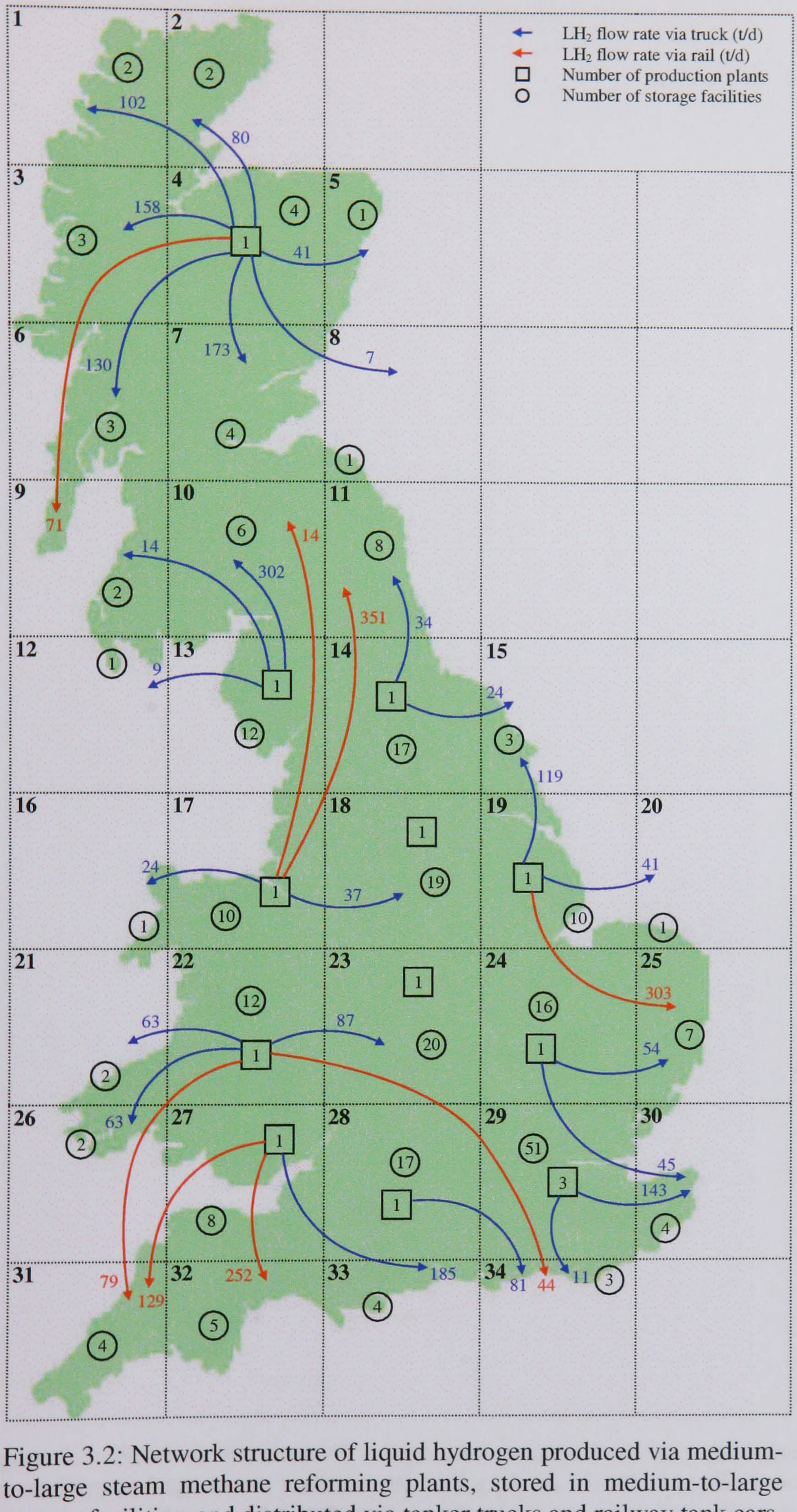


Figure 3.2: Network structure of liquid hydrogen produced via medium-to-large steam methane reforming plants, stored in medium-to-large storage facilities, and distributed via tanker trucks and railway tank cars.

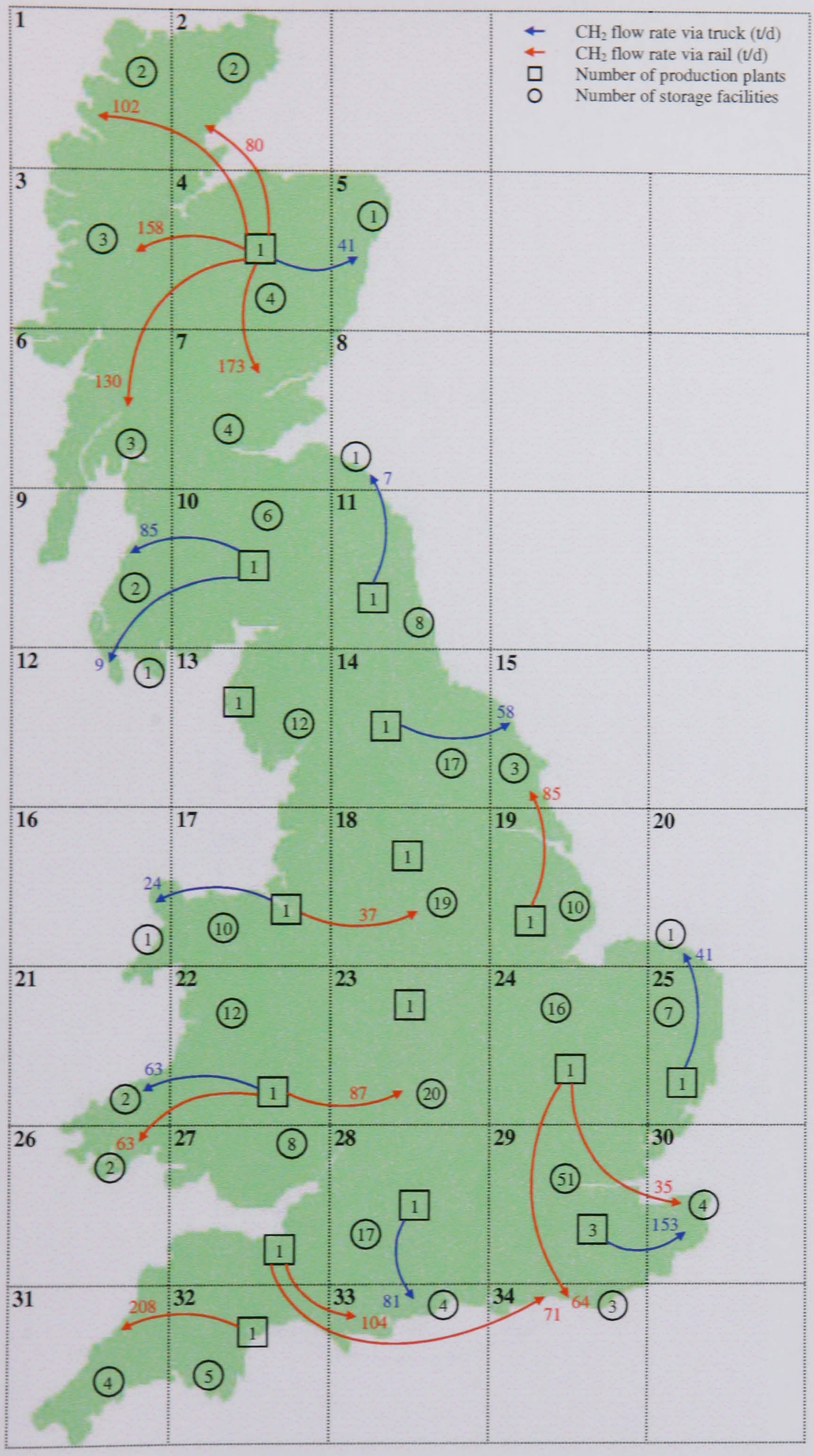


Figure 3.3: Network structure of compressed-gaseous hydrogen produced via medium-to-large steam methane reforming plants, stored in medium-to-large storage facilities, and distributed via tube trailers and railway tube cars.

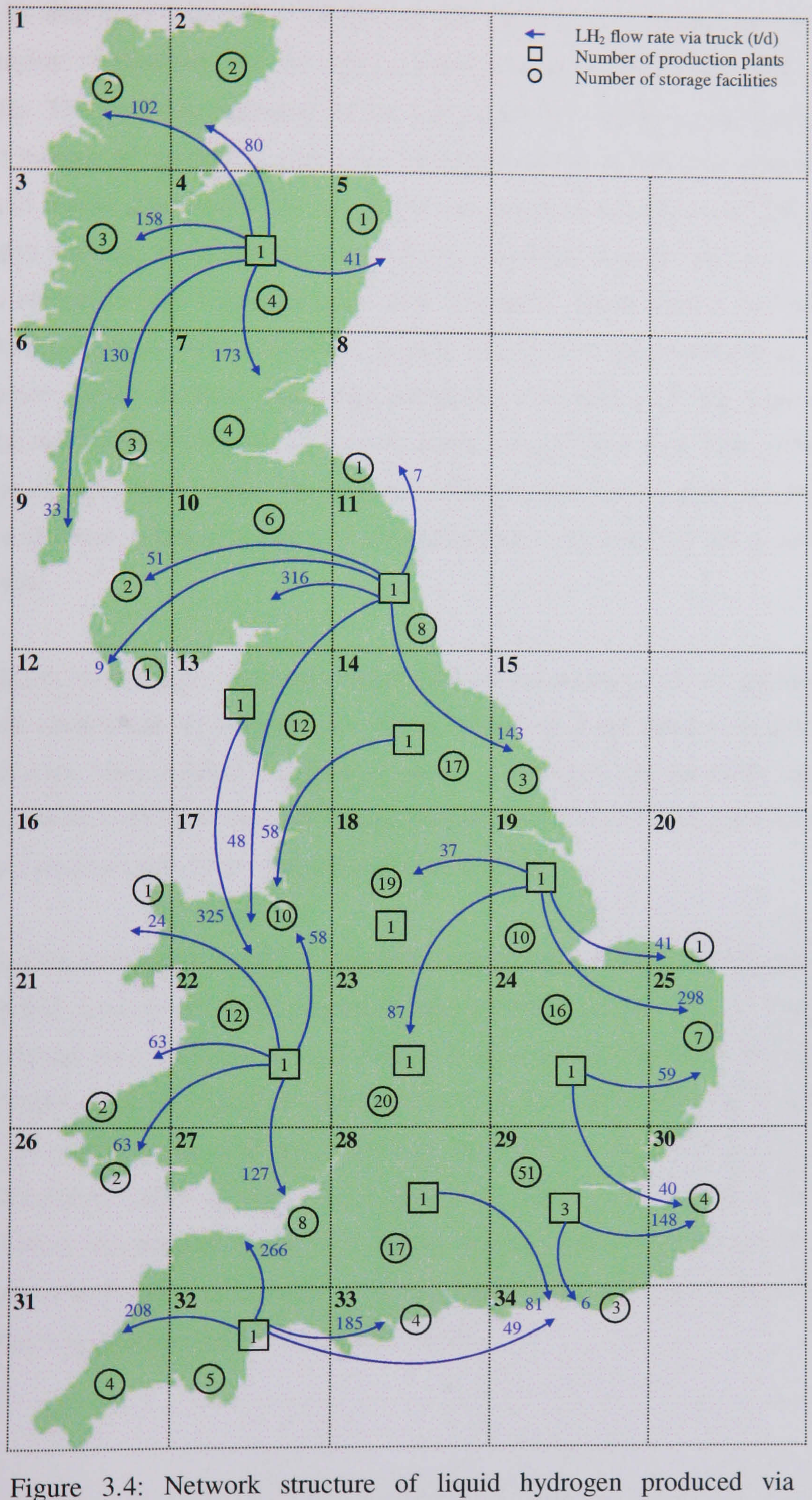


Figure 3.4: Network structure of liquid hydrogen produced via medium-to-large steam methane reforming plants, stored in medium-to-large storage facilities, and distributed via tanker trucks.

It can be seen from Figures 3.2–3.4 that grid 29, which covers London and the South East region of England, has the highest number of production plants and storage facilities. This could be explained by the high population density in this region. The fewest number of production plants and storage facilities are in grids covering the Scotland region. The reason for this is the low population density and thus a low hydrogen demand. It can also be observed that a number of grids, such as 1, 15 and 34, do not satisfy their local hydrogen needs. Therefore, the demand is fulfilled from neighbouring plants. This alternative is more economical than establishing a new production facility in those areas since demand is low. Moreover, the figures show that the mid and the southern parts of England contain more than 70% of the total number of production plants. This is due to the fact that these regions are the most populated areas in Great Britain and are considered to be a hub of heavy industrial activities.

In addition, these figures show that steam methane reforming plants are the only type of plant established. This is because steam reforming is the most widespread and currently the least expensive method to produce hydrogen. On the other hand, the establishment of different types of storage facilities is necessary in all grids in order to supply customers with their required hydrogen demand.

The cost for each of the examined network configurations is 61.29, 494.19 and 61.31 million $/d, respectively. A breakdown of these costs is listed in Table 3.7. In order to contextualise the cost values, the network costs are expressed in dollars per kilogram of hydrogen delivered ($/kg). In effect, the cost for the liquid and gaseous hydrogen based networks become 4.58 and 36.89 $/kg, respectively. Also, the respective costs for the networks are 0.29 and 2.35 in dollars per kilometre driven ($/km). Putting these values in perspective, the cost for an untaxed petrol network is 0.11 $/km assuming that the price of untaxed petrol is 0.5 pounds per litre (£/L). The exchange rate used was based on the 2002 figure of 1.5 $/£.

Table 3.7: Breakdown of total network costs for the steady-state model

Configuration	1	2	3
Capital cost			
Plants and storage facilities	44.97×10^{9}	513.50×10^{9}	44.97×10^{9}
Transportation modes	206.18×10^{6}	1.53×10^{9}	163.59×10^{6}
Total capital cost ($)	45.18×10^{9}	515.04×10^{9}	45.14×10^{9}
Operating cost			
Plants and storage facilities	19.82×10^{6}	21.97×10^{6}	19.82×10^{6}
Transportation modes			
Fuel cost	53.54×10^{3}	212.68×10^{3}	104.26×10^{3}
Labour cost	136.63×10^{3}	1.54×10^{6}	135.45×10^{3}
Maintenance cost	14.34×10^{3}	83.17×10^{3}	22.37×10^{3}
General cost	3.05×10^{3}	36.78×10^{3}	2.69×10^{3}
Total operating cost ($/d)	20.03×10^{6}	23.84×10^{6}	20.09×10^{6}
Total network cost ($/d)	*61.29×10^{6}*	*494.19×10^{6}*	*61.31×10^{6}*

It can be seen from Table 3.7 that the cost of the liquid hydrogen network is about eight times lower than the cost of the compressed-gaseous hydrogen network. Hugo [90] also demonstrated that if cost is used as an objective, the preferred form of the product is liquid hydrogen. One of the main contributors to the cost is the capacity of transport container which is approximately 20 times higher for liquid hydrogen than compressed gas. Certainly, this will increase the number of trips required between production plants and the storage facilities; therefore increasing the overall cost of the network.

Another major contributor is the storage and distribution cost of compressed hydrogen gas. This is due to the low energy density of gaseous hydrogen at atmospheric pressure—approximately 70 lower than that of liquid hydrogen [53]. To overcome this issue, high-pressure cylindrical vessels are used, hence increasing the cost of the system and the safety requirements. Also, the cost of medium-to-long term storage of compressed hydrogen gas is prohibitive because this storage method is too bulky, i.e. requiring many storage vessels. For example, based on studies by Amos [75] and Simbeck and Chang [73], the unit storage cost for liquid hydrogen is 18 $/kg compared to 281 $/kg for a pressure vessel. In summary, despite the high energy cost of liquefaction, large quantity storage and delivery of liquid hydrogen prevail over the high storage and distribution costs of compressed hydrogen gas.

Additionally, Table 3.7 shows that the difference in the overall cost difference between the single- and multi-mode liquid-based networks is insignificant. While this

negligible difference would imply that neither mode has a particular advantage over the other, the decision to use truck based distribution is still made. This is because it is more favourable to use tanker trucks instead of railway tank cars due to the flexibility in operations. Trucks are also easier to schedule, more efficient, and can be dispatched to users at any time, especially in emergencies. In addition, trucks use a road infrastructure which is well-established, whereas rail use a confined network that is shared by other users.

Table 3.7 also demonstrates that the capital cost of production and storage facilities for the compressed-gaseous network is much higher than that of the liquid-based network. This finding indicates that the former network has more production plants and hence fewer transportation links. To verify the outcome, the overall demand satisfied by local production facilities for both networks was calculated. The result shows that 75% and 85% of the overall demand is fulfilled by local production in the case of liquid and compressed-gaseous networks, respectively. These figures are an indicator of the degree of centralisation. Higher distribution and storage costs of compressed hydrogen gas result in a more decentralised solution, i.e. more plants established; thus more demand is being satisfied by local production.

The MILP models were solved by a Pentium 4, 1.8 GHz Dell machine via a modelling tool referred to as GAMS [114] using CPLEX v9.0 code. The corresponding computational statistics are summarised in Table 3.8. As can be seen from the results in Table 3.8, the short times required for solving the three different configurations and the low optimality gaps are satisfactory. This promising result is a good indication of having a model that is capable of mapping out the whole hydrogen supply network for Great Britain in a short time and a minimal optimality gap.

Table 3.8: Summary of computational results for the steady-state model

Configuration	1	2	3
Number of constraints	11807	11807	6197
Number of integer variables	2448	2448	1326
Number of continuous variables	2491	2491	1369
Optimality gap (%)	0.01	0.01	0.01
CPU time (sec)	425	7047	44

3.4.3 Concluding Remarks

The aims of this work were to:

- Develop quantitative tools that can support strategic decisions in hydrogen supply chain design and operation,
- Identify the main data requirements for such an activity, and
- Assess the capability of supply chain design models to address such problems.

The model of interest was utilised to indicate the optimal configurations of the future hydrogen supply chain before these configurations develop organically, amongst various potential options. The model considers a number of hydrogen production technologies in which different product forms are produced. The model also takes account of different storage technologies and flexible transportation modes. The derived supply chain network will be capable of supplying hydrogen for fuel cell vehicles in Great Britain during an entrenched transition from petroleum fuels to hydrogen.

In this work, three different network configurations concerned with the establishment of future hydrogen supply chain were studied. The results obtained manifest the usefulness of having a model that takes into account different existing components in these networks. Based on the data and assumptions inherent in the model, the production of hydrogen from natural gas in medium-to-large, centralised reforming plants presents the most optimal configuration. This is at the stage where hydrogen exists as an entrenched fuel for transportation. The hydrogen is then delivered to the storage facilities as a liquid via tanker trucks and railway tank cars. The resulting architecture is compatible with the existing petroleum supply chain in which petrol is produced from centralised refineries and distributed to several storage terminals by mostly trucks or rail as well as pipelines.

Besides the above hydrogen supply network, using only tanker trucks as the means of distributing liquid hydrogen seems to be the best option despite the insignificant difference in cost. This is because trucks benefit from a number of infrastructural and operational advantages. Also, truck-based distribution infrastructure of liquid

hydrogen produced from centralised reforming plants is a well-practised method used by many indusial gas companies since the 1960s [47].

A further feasible configuration of the hydrogen supply chain is the production of hydrogen from natural gas in medium-to-large, centralised reforming plants and transported to the users as a compressed gas. Based on the results obtained, this option is very expensive at the current stage due to the high capital cost of the storage facilities, as well as the high cost of medium-to-long term compressed gas storage. Another factor behind the high cost of compressed-gaseous hydrogen network is the distribution cost. This is due to the low hydrogen storage capacity per transport container. However, as novel storage technologies develop in the future, delivery of hydrogen via tube trailers and railcars will become cheaper than liquid hydrogen transport. This will lead to a gaseous hydrogen based network that is competitive because of the low production cost of compressed hydrogen gas.

At this stage, the computational results associated with the hydrogen supply chain problem were found to be promising. However, more detailed models for the design of the future hydrogen supply chain may be much larger, involving many alternatives to produce, store and distribute hydrogen.

In the next chapter, the steady-state model will be expanded to account for the availability of different primary energy feedstocks and the logistics associated with distributing these feedstocks throughout the supply chain network. The model will also consider different production and storage scales as well as the local distribution of hydrogen within grids.

Chapter 4

Design of an Extended Hydrogen Supply Chain

4.1 Problem Description

The model described in Chapter 3 addressed the strategic design of a hydrogen supply chain network with centralised, large-scale production and storage facilities. The model however neglects to take into consideration the availability of primary energy sources, and the scale of production and storage. These two aspects are important in determining the nature of production technologies and the appropriate feedstocks to be selected. In this chapter, these issues will be implemented by expanding the steady-state model. The resulting model will incorporate a number of primary energy sources to produce hydrogen in different production scales and finally store it in storage facilities of different sizes. The model will also account for distribution of hydrogen within the grid, i.e. local distribution, together with regional distribution, as well as the distribution of primary energy sources.

As with the steady-state model, the two essential characteristics of the hydrogen supply chain network are: demand-dependency and time-independency. The model is again represented by an optimisation problem formulated as an MILP. The main objective of the extended model is to explore whether centralised production and distribution of hydrogen is favoured over local or in-situ production using diversified primary energy feedstocks.

A number of new design decisions will be established by the model. These decisions are: (1) selection of primary energy sources, (2) assignment of different sizes of production and storage technologies, (3) allocation of transportation links necessary for distributing and importing energy sources, and (4) determination of resource surpluses in each location. Again, the network is designed for minimum total cost,

taking into account an optimisation of both capital investment and operating cost. This will be done by considering a snapshot of the network at one point in time.

4.2 Model Structure and Components

The superstructure of the extended model is shown in Figure 4.1. This figure resembles the one given for the steady-state model; however, an additional node for the primary energy sources was added. Also, the production and storage nodes were allowed to take different sizes. The main difference in this figure is that for small-scale, distributed production plants there will be no distribution activity since these plants are decentralised. Therefore, hydrogen will be dispensed directly to customers.

The components of the model are discussed below in more detail. Only information not mentioned in the steady-state model will be considered.

4.2.1 Primary Energy Sources

Hydrogen can be harnessed from a wide range of primary energy sources, including natural gas, oil, coal, biomass, and solar power, which are represented by the index *e*. These resources play an important role in determining the size, type, and location of the production technologies. Therefore, a comprehensive analysis was carried out to determine the geographical location, availability and quantities of the primary energy sources. The analysis can be found in Appendix D. The amount of energy sources consumed in each location depends mainly on the type and size of production technologies that are selected. Each type and size of production plants will have different rate of utilisation. The main decision associated with the primary energy sources is whether to import resources from neighbouring grids or from external sources, such as another country. Another decision is identifying the remaining amount of resources after some are used for hydrogen production.

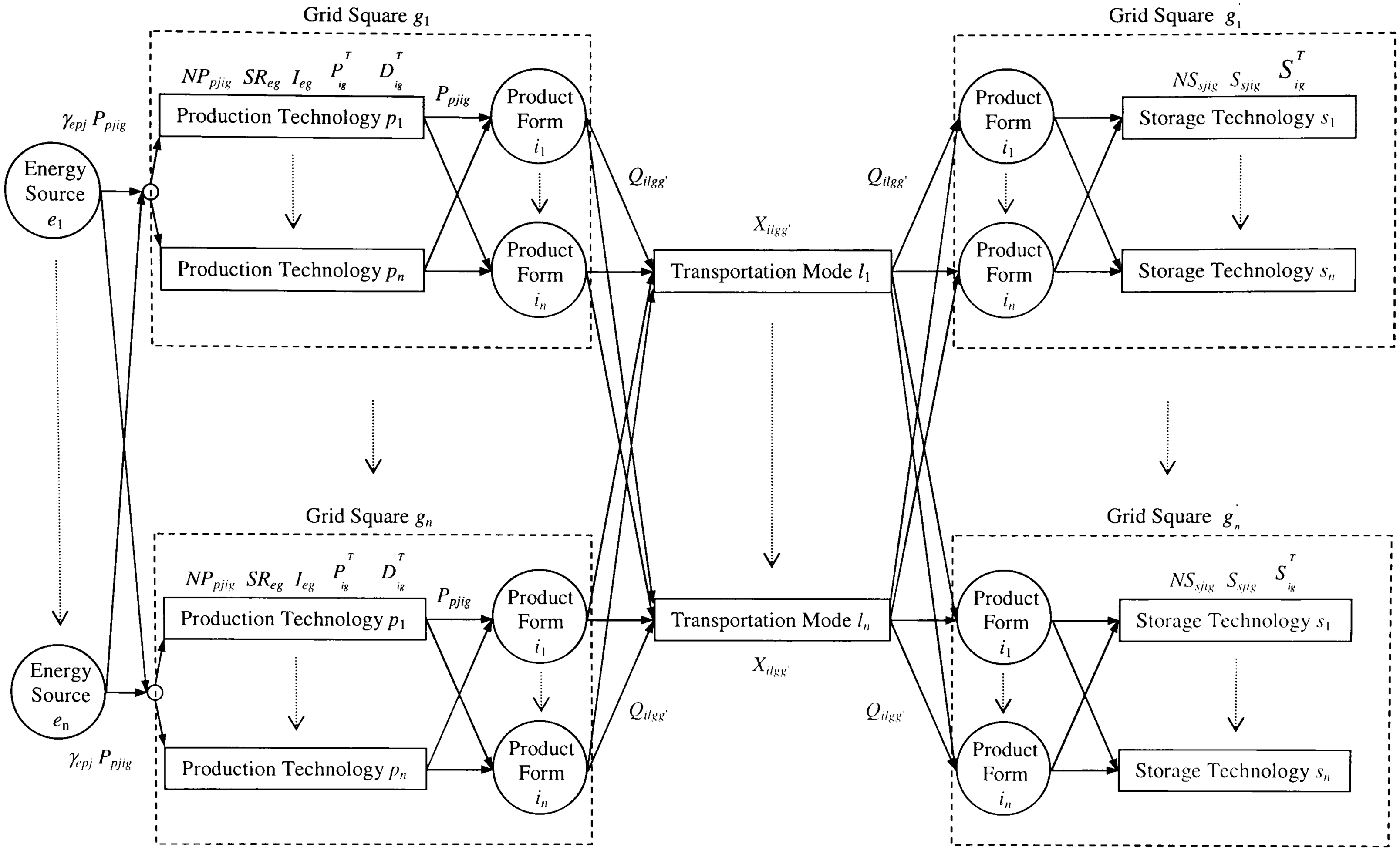


Figure 4.1: Superstructure of the extended model. Local transportation of product forms occurs when $g = g'$ whereas regional transportation occurs when $g \neq g'$.

4.2.2 Production and Storage Sizes

The different types of production and storage technologies given in the steady-state model are coupled with the index j in order to account for different sizes. Three production and storage sizes are considered, referred to as small, medium, and large. The establishment of a small production facility means that hydrogen is produced on-site at local fuelling stations (also known as forecourt production plants). A large production facility, on the other hand, indicates that hydrogen is produced at dedicated, centralised plants. However, the selection of different sizes of storage facilities is independent of the size of the installed production facilities. The reason behind installing different storage facility sizes is to accommodate for the unpredictable and uncontrollable demand variations. Each size of production and storage facility is bound between minimum and maximum limits, and has different capital and unit operating costs. The production and storage decisions comprise the number, location, and capacity of plant and storage types with respect to size. The total production rates and the average stored inventory for each size of these facilities are also contained within the production and storage decisions.

4.3 Model Formulation

Since this model is an extension of the steady-state model, the mathematical notation and formulation are similar to the one presented in Section 3.3. However, the complete notation and formulation will be described for ease of reference.

4.3.1 Nomenclature

Indices

e	primary energy sources
g	grid squares
g'	grid squares such that $g' \neq g$

i	product physical form
j	size of production plants and storage facilities
l	type of transportation modes
m	counter that determines total number of plants in a particular grid
p	plant type with different production technologies
s	storage facility type with different storage technologies

Parameters

A_{eg}	availability of primary energy source e in grid g (unit/d)
CCF	capital charge factor—payback period of capital investment (yr)
D_{ig}^{T}	total demand for product form i in grid g (kg/d)
DW_l	driver wage of transportation mode l ($/hr)
FE_l^L	fuel economy of transportation mode l within a grid (km/L)
FE_l^R	fuel economy of transportation mode l between grids (km/L)
FP_l	fuel price of transportation mode l ($/L)
GE_l	general expenses of transportation mode l ($/d)
L_g^L	local delivery distance within grid g (km)
$L_{gg'}^R$	regional delivery distance between grids g and g' (km)
L_g^{ave}	average delivery distance within grid g (km)
L^{max}	maximum delivery distance between grids (km)
LUT_l	load/unload time of product for transportation mode l (hr)
ME_l	maintenance cost of transportation mode l ($/km)
$PCap_{pji}^{min}$	minimum production capacity of plant type p and size j for product form i (kg/d)
$PCap_{pji}^{max}$	maximum production capacity of plant type p and size j for product form i (kg/d)
PCC_{pji}	capital cost of establishing plant type p and size j producing product form i ($)
Q_{il}^{min}	minimum flow rate of product form i by transportation mode l (kg/d)

Q_{il}^{max} maximum flow rate of product form i by transportation mode l (kg/d)

$SCap_{sji}^{min}$ minimum storage capacity of storage type s and size j for product form i (kg)

$SCap_{sji}^{max}$ maximum storage capacity of storage type s and size j for product form i (kg)

SCC_{sji} capital cost of establishing storage type s and size j for storing product form i ($)

SP_l^L average speed of transportation mode l within a grid (km/hr)

SP_l^R average speed of transportation mode l between grids (km/hr)

$TCap_{il}$ capacity of transportation mode l transporting product form i (kg/mode)

TMA_l^L availability of transportation mode l within a grid (hr/d)

TMA_l^R availability of transportation mode l between grids (hr/d)

TMC_{il} cost of establishing transportation mode l transporting product form i ($/mode)

UDC_e unit cost of distributing primary energy source e between grids ($/unit)

UEC_e unit cost of primary energy source e ($/unit)

UIC_e unit cost of importing primary energy source e from overseas ($/unit)

UPC_{pji} unit production cost of product form i by plant type p and size j ($/kg)

USC_{sji} unit storage cost of product form i at storage type s and size j ($/kg/d)

α network operating period (d/yr)

β storage holding period—average number of days' worth of stock (d)

γ_{epj} rate of utilisation of primary energy source e by plant type p and size j (unit resource/unit product)

μ coefficient for percentage of unit cost of primary energy source

π coefficient of a sufficiently large number to insure that there is no local demand when no plants are established

Continuous Variables

D_{ig}^L demand for product form i in grid g satisfied by local production (kg/d)

D_{ig}^{I} imported demand of product form i to grid g (kg/d)

DM_{mg}^{L} local demand satisfied by $m-1$ plants in grid g (kg/d)

ESC primary energy source cost ($/d)

FC fuel cost ($/d)

FCC facility capital cost ($)

FOC facility operating cost ($/d)

GC general cost ($/d)

I_{eg} import of primary energy source e to grid g from overseas (unit/d)

LC labour cost ($/d)

MC maintenance cost ($/d)

P_{pjig} production rate of product form i produced by plant type p and size j in grid g (kg/d)

P_{ig}^{T} total production rate of product form i in grid g (kg/d)

$Q_{ilgg'}$ flow rate of product form i by transportation mode l between grids g and g' (kg/d)

$QE_{egg'}$ flow rate of primary energy source e between grids g and g' (unit/d)

S_{sjig} average inventory of product form i at storage type s and size j in grid g (kg)

S_{ig}^{T} total average inventory of product form i in grid g (kg)

SR_{eg} surplus of primary energy source e in grid g (unit/d)

TCC transportation capital cost ($)

TDC total daily cost of the network ($/d)

TOC transportation operating cost ($/d)

Integer Variables

NP_{pjig} number of plants of type p and size j producing product form i in grid g

NS_{sjig} number of storage facilities of type s and size j storing product form i in grid g

NP_{g}^{T} total number of plants in grid g

NTU number of transport units

Binary Variables

U_{mg}	1 if there are $m-1$ plants in grid g, 0 otherwise
$X_{ilgg'}$	1 if product form i is to be transported from grids g to g' by transportation mode l, 0 otherwise
Y_{ig}	1 if product form i is to be exported from grid g, 0 otherwise
Z_{ig}	1 if product form i is to be imported to grid g, 0 otherwise

4.3.2 Constraints

Demand Constraints

The demand constraints will not be affected by the addition of primary energy sources. However, these constraints are listed below for convenience.

The demand satisfied by local production in a particular grid should be less than or equal to the total production rate of the grid itself:

$$D_{ig}^{L} \le P_{ig}^{T} \qquad \forall i, g \tag{4.1}$$

If demand is imported to a particular grid from neighbouring grids, the flow rate of product transported by all transportation modes must be equal to the corresponding demand:

$$D_{ig}^{I} = \sum_{l,g'} Q_{ilg'g} \qquad \forall i, g \tag{4.2}$$

The total grid demand must equal the sum of the demand satisfied by the local production facilities and the demand imported from other grids:

$$D_{ig}^{T} = D_{ig}^{L} + D_{ig}^{I} \qquad \forall i, g \tag{4.3}$$

Primary Energy Source Constraints

The establishment of different production plants in a particular grid is mainly governed by the local availability and quantity of primary energy sources, as well as the ability of the grid to import resources from overseas and/or nearby grids. Taking this into consideration, a total material balance on a grid can be written in the following form:

$$SR_{eg} = A_{eg} + I_{eg} + \sum_{g'} \left(QE_{eg'g} - QE_{egg'} \right) - \sum_{p,j,i} \gamma_{epj} P_{pjig} \qquad \forall e, g \tag{4.4}$$

Equation 4.4 implies that the surplus of primary energy sources in a grid (SR_{eg}) is equal to the daily local availability of resources (A_{eg}) plus the import of resources from overseas and neighbouring regions (I_{eg} and $QE_{eg'g}$), minus the local production rate (P_{pjig}) and the export of resources to another grid ($QE_{egg'}$). The coefficient γ_{epj} in the above equation expresses the amount of primary energy source e used by plant type p and size j to produce a unit amount of product.

Production Facility Constraints

A total mass balance on a grid square yields that the total daily production rate is:

$$P_{ig}^{T} = \sum_{l,g'} \left(Q_{ilgg'} - Q_{ilg'g} \right) + D_{ig}^{T} \qquad \forall i, g \tag{4.5}$$

Additionally, the total daily production rate is equal to the sum of all plants of type p and size j producing product form i:

$$P_{ig}^{T} = \sum_{p,j} P_{pjig} \qquad \forall i, g \tag{4.6}$$

The production rate of plant type p and size j producing product form i located in grid g is bound between minimum and maximum limits. These limits are multiplied by the

number of production facilities to determine the maximum daily production rate, as follows:

$$PCap_{pji}^{\min} NP_{pjig} \leq P_{pjig} \leq PCap_{pji}^{\max} NP_{pjig} \qquad \forall p, j, i, g \tag{4.7}$$

Since distributed production facilities are localised in nature, the production rate of these facilities must be less than or equal to the local demand:

$$\sum_{p} P_{pjig} \leq D_{ig}^{L} \qquad \forall i, g : j = \text{small plants} \tag{4.8}$$

Constraint 4.8 will guarantee that distributed plants will only fulfil the required local demand; hence no products will be exported to neighbouring grids.

Due to technical and economical barriers, certain types of production plants can only be constructed in fixed sizes. The following constraints insure these limitations:

$$NP_{pjig} = 0 \qquad \forall i, g : p = \text{coal gasification} \;\&\; j = \text{small plants} \tag{4.9}$$

$$NP_{pjig} = 0 \qquad \forall i, g : p = \text{biomass gasification} \;\&\; j = \text{small plants} \tag{4.10}$$

$$NP_{pjig} = 0 \qquad \forall i, g : p = \text{electrolysis} \;\&\; j = \text{large plants} \tag{4.11}$$

Transportation Constraints

The transportation constraints imposed upon the formulation of the distribution network will not be influenced by the addition of the primary energy sources. These constraints are again repeated below.

The flow of products will only be justified by the establishment of transportation links, as well as by the minimum and maximum allowable flow rates:

$$Q_{il}^{\min} X_{ilgg'} \leq Q_{ilgg'} \leq Q_{il}^{\max} X_{ilgg'} \qquad \forall i,l,g,g' : g \neq g' \tag{4.12}$$

Flow of a product form i between different grids by transportation mode l can only occur in one direction. A particular grid can only import products from nearby grids or export products to other grids. It can also do neither but not both. The corresponding consideration can be expressed as follows:

$$Y_{ig} \geq X_{ilgg'} \qquad \forall i,l,g,g' : g \neq g' \tag{4.13}$$

$$Z_{ig} \geq X_{ilg'g} \qquad \forall i,l,g,g' : g \neq g' \tag{4.14}$$

$$Y_{ig} + Z_{ig} \leq 1 \qquad \forall i,g \tag{4.15}$$

Storage Facility Constraints

The total average inventory of a product kept in each grid is equal to the total product demand multiplied by the number of days' worth of average demand required in the storage facility:

$$S_{ig}^{T} = \beta\, D_{ig}^{T} \qquad \forall i,g \tag{4.16}$$

In exactly the same way as the production facilities, the capacity of each storage type s and size j cannot exceed certain limits. This means that the average stored inventory at each grid g (S_{sjig}) is bound between a minimum and a maximum storage capacity as follows:

$$SCap_{sji}^{\min} NS_{sjig} \leq S_{sjig} \leq SCap_{sji}^{\max} NS_{sjig} \qquad \forall s,j,i,g \tag{4.17}$$

Constraint 4.17 implies that the maximum storage inventory is restricted by the number of storage facilities NS_{sjig}.

Similarly, the total average inventory of a product in each grid is bound within certain limits as expressed by the following constraint:

$$\sum_{s,j} SCap_{sji}^{\min} NS_{sjig} \le S_{ig}^{T} \le \sum_{s,j} SCap_{sji}^{\max} NS_{sjig} \qquad \forall i,g \tag{4.18}$$

Non-negativity Constraints

All continuous and integer variables presented in the model must be non-negative:

$$D_{ig}^{L} \ge 0 \quad \forall i,g \tag{4.19}$$

$$D_{ig}^{I} \ge 0 \quad \forall i,g \tag{4.20}$$

$$DM_{mg}^{L} \ge 0 \quad \forall m,g \tag{4.21}$$

$$I_{eg} \ge 0 \quad \forall e,g \tag{4.22}$$

$$NP_{pjig} \ge 0 \quad \forall p,j,i,g \tag{4.23}$$

$$NP_{g}^{T} \ge 0 \quad \forall g \tag{4.24}$$

$$NS_{sjig} \ge 0 \quad \forall s,j,i,g \tag{4.25}$$

$$P_{ig}^{T} \ge 0 \quad \forall i,g \tag{4.26}$$

$$P_{pjig} \ge 0 \quad \forall p,j,i,g \tag{4.27}$$

$$Q_{ilgg'} \ge 0 \quad \forall i,l,g,g' : g \ne g' \tag{4.28}$$

$$QE_{egg'} \ge 0 \quad \forall e,g,g' : g \ne g' \tag{4.29}$$

$$S_{sjig} \ge 0 \quad \forall s,j,i,g \tag{4.30}$$

$$S_{ig}^{T} \ge 0 \quad \forall i,g \tag{4.31}$$

$$SR_{eg} \ge 0 \quad \forall e,g \tag{4.32}$$

4.3.3 Objective Function

The goal that needs to be accomplished from the proposed optimisation problem is to minimise the total daily cost of the hydrogen supply chain network. The total cost comprises capital and operating costs. Capital cost is associated with the establishment of production plants, storage facilities, and transportation links. Operating cost, on the other hand, is associated with the cost of producing, storing, and transporting hydrogen locally and regionally. The capital and operating cost terms that constitute the overall cost function are presented in the subsequent subsections in more detail.

Facility Capital Cost

The facility capital cost is evaluated as follows:

$$FCC = \sum_{j,i,g} \left(\sum_{p} PCC_{pji} NP_{pjig} + \sum_{s} SCC_{sji} NS_{sjig} \right) \tag{4.33}$$

Transportation Capital Cost

Despite the various distribution options for hydrogen, this thesis only concentrates on truck and rail transport. The cost concerning these modes is divided into: capital and operating. These costs are further divided into local and regional. The local transportation cost represents the cost of distributing hydrogen within a particular grid square, while the regional transportation cost represents the cost of transporting hydrogen between various grids.

In approximating the local transportation cost, one should initially estimate the average delivery distance within the grid. The average distance is obtained by dividing the local delivery distance within a grid (L_g^L) by the total number of production plants established (NP_g^T):

$$L_g^{\text{ave}} = \frac{2L_g^L}{NP_g^T} \qquad \forall g \tag{4.34}$$

L_g^L is assumed to be the same for all grids (see Appendix B). It is multiplied by two to account for two-way journeys. Dividing the numerator by an integer variable, i.e. NP_g^T, results in a non-linear term. The non-linearity could be avoided by introducing a new binary variable U_{mg} and a counter m as follows:

$$NP_g^T = \sum_m (m-1)U_{mg} \qquad \forall g \tag{4.35}$$

where m is a counter that is equal to the number of plants established in a particular grid plus one ($m = 1, \ldots, NP^{max}+1$) and U_{mg} is a binary variable that determines if $m-1$ plants are established in grid g. The term $m-1$ in the right-hand-side of Equation 4.35 is introduced to allow some grids to have no production plants. On the other hand, the left-hand-side of the same equation is basically equal to the sum of all plant types and sizes producing product form i:

$$NP_g^T = \sum_{p,j,i} NP_{pjig} \qquad \forall g \tag{4.36}$$

The following constraint must be written to insure that only one term of the binary variables is valid:

$$\sum_m U_{mg} = 1 \qquad \forall g \tag{4.37}$$

Therefore, the average local delivery distance within a grid is equal to:

$$L_g^{\text{ave}} = \sum_m \frac{2L_g^L}{m-1} U_{mg} \qquad \forall g \tag{4.38}$$

Using Equation 4.38 in calculating the local transportation cost leads to the following relationship:

$$LTC_g = \sum_{i,m} \psi \frac{2L_g^L U_{mg} D_{ig}^L}{m-1} \quad \forall g \tag{4.39}$$

where ψ contains other parameters such as capacity, availability, and average speed of transportation mode. The variable D_{ig}^L is the demand satisfied by local production facilities, which is an important factor in estimating the local transportation cost.

Going back to Equation 4.39, it can be noticed that non-linearity arises again but in the numerator. Linearising the numerator can be achieved by defining a new variable as follows:

$$DM_{mg}^L \equiv U_{mg} D_{ig}^L \tag{4.40}$$

where DM_{mg}^L is the local demand satisfied by $m-1$ plants in grid g. The non-linearity can be prevented as follows:

$$DM_{mg}^L \geq D_{ig}^L - \pi(1-U_{mg}) \quad \forall i,m,g \tag{4.41}$$

The coefficient π is a sufficiently large number to assure that there is no local demand when no plants are established.

Summarising the above discussion, the local transportation cost in each grid is equal to:

$$LTC_g = \sum_{m} \psi \frac{2L_g^L DM_{mg}^L}{m} \quad \forall g \tag{4.42}$$

As mentioned in the steady-state model, the total capital cost of transportation is obtained by multiplying the number of transport units, i.e. truck or railcar, by the cost of each respective form and then summing up.

The number of transport units required to serve local and regional demand is given by the following relationship:

$$NTU = \sum_{i,l,m,g} \frac{DM_{mg}^{L}}{(m-1)TMA_{l}^{L}TCap_{il}}\left(\frac{2L_{g}^{L}}{SP_{l}^{L}} + LUT_{l}\right) + \sum_{i,l,g,g'} \frac{Q_{ilgg'}}{TMA_{l}^{R}TCap_{il}}\left(\frac{2L_{gg'}^{R}}{SP_{l}^{R}} + LUT_{l}\right) \tag{4.43}$$

The first term of the right-hand-side of Equation 4.43 represents the number of transport units within a grid, whereas the second term of the right-hand-side corresponds to the number of transport units between grids. The latter term is identical to the one given in Equation 3.24. However, in this formulation, the transportation mode speed, fuel economy, and availability for local and regional distributions are assumed to be different. This is because of traffic, speed limits, road layout, and delivery restrictions. Other parameters involved in the transportation cost estimations, including transport unit capacity, load/unload time, fuel price, driver wage, maintenance expenses and general costs, are assumed to be the same for both local and regional distributions.

As a result, the transportation capital cost is equal to:

$$TCC = NTU \times TMC_{il} \tag{4.44}$$

Facility Operating Costs

The facility operating cost is related to the cost required to operate production plants and storage facilities efficiently. The plant operating cost is calculated by multiplying the unit production cost (UPC_{pji}) by the plant production rate (P_{pjig}). Likewise, the

storage operating cost is obtained by multiplying the unit storage cost (USC_{sji}) by the average stored inventory (S_{sjig}) in each grid. Therefore, the corresponding cost terms in the objective function are of the form:

$$FOC = \sum_{j,i,g}\left(\sum_{p} UPC_{pji} P_{pjig} + \sum_{s} USC_{sji} S_{sjig}\right) \tag{4.45}$$

In Equation 4.45 the unit production and storage costs are directly proportional to the size of production and storage units, respectively. As shown in Figure 4.2, these unit costs benefit from economies of scale. Therefore, as the capacity of production or storage increases the unit cost decreases.

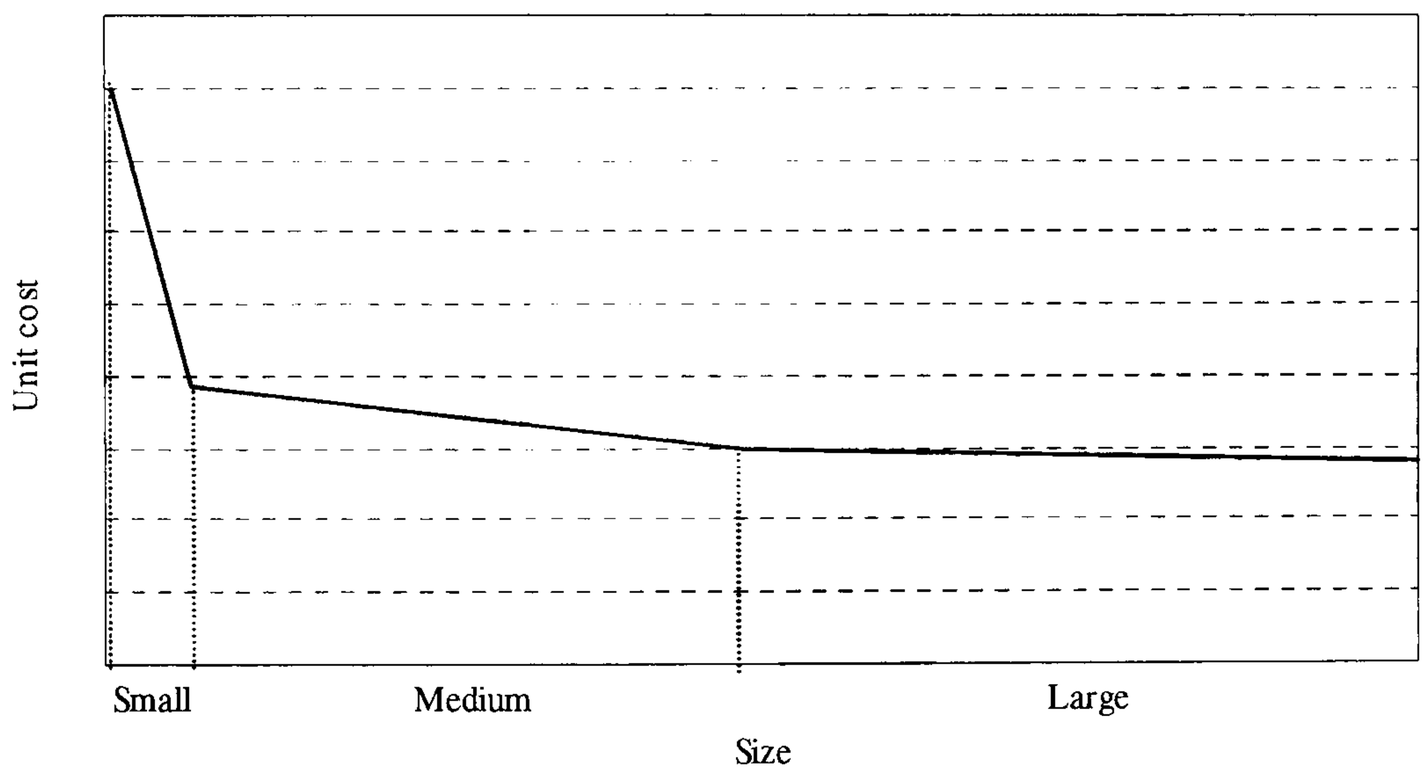


Figure 4.2: Unit cost versus size.

Transportation Operating Cost

The transportation operating cost used in the examined model consists of fuel, labour, maintenance, and general costs. In a similar manner to the transportation capital cost, the operating cost is further classified into local and regional costs. In the following five equations, the first term of the right-hand-side denotes the local operating cost while the second term of the right-hand-side denotes the regional cost.

The daily fuel cost for local and regional distributions is:

$$FC = \sum_{i,l,m,g} FP_l \left(\frac{2L_g^L DM_{mg}^L}{(m-1)FE_l^L TCap_{il}} \right) + \sum_{i,l,g,g'} FP_l \left(\frac{2L_{gg'}^R Q_{ilgg'}}{FE_l^R TCap_{il}} \right) \quad (4.46)$$

The daily labour cost associated with local and regional distributions is given as follows:

$$LC = \sum_{i,l,m,g} DW_l \left(\frac{DM_{mg}^L}{(m-1)TCap_{il}} \left(\frac{2L_g^L}{SP_l^L} + LUT_l \right) \right) + \sum_{i,l,g,g'} DW_l \left(\frac{Q_{ilgg'}}{TCap_{il}} \left(\frac{2L_{gg'}^R}{SP_l^R} + LUT_l \right) \right) \quad (4.47)$$

The maintenance cost is:

$$MC = \sum_{i,l,m,g} ME_l \left(\frac{2L_g^L DM_{mg}^L}{(m-1)TCap_{il}} \right) + \sum_{i,l,g,g'} ME_l \left(\frac{2L_{gg'}^R Q_{ilgg'}}{TCap_{il}} \right) \quad (4.58)$$

The general cost is:

$$GC = \sum_{i,l,m,g} GE_l \left(\frac{DM_{mg}^L}{(m-1)TMA_l^L TCap_{il}} \left(\frac{2L_g^L}{SP_l^L} + LUT_l \right) \right) + \sum_{i,l,g,g'} GE_l \left(\frac{Q_{ilgg'}}{TMA_l^R TCap_{il}} \left(\frac{2L_{gg'}^R}{SP_l^R} + LUT_l \right) \right) \quad (4.49)$$

Finally, the total transportation operating cost is equal to the sum of fuel, labour, maintenance, and general costs:

$$TOC = FC + LC + MC + GC \quad (4.50)$$

Primary Energy Source Cost

The cost of primary energy sources include the cost of importing energy sources from overseas plus the cost of importing energy sources from neighbouring grids:

$$ESC = \sum_{e,g} UIC_e I_{eg} + \sum_{e,g,g'} UDC_e L^R_{gg'} QE_{egg'} \tag{4.51}$$

In the first term of the right-hand-side of Equation 4.51, the unit cost of importing primary energy sources from overseas (UIC_e) is defined as the unit cost of primary energy sources (UEC_e) times an incremental factor μ. This factor takes into account the extra cost associated with importing primary energy sources from overseas and/or nearby grids. The unit cost of transporting primary energy sources between grids (UDC_e), which is represented by the second term of the right-hand-side of Equation 4.51, is defined as the UIC_e divided by the maximum distance travelled (L^{max}). This is because delivery distance is a crucial factor in determining the distribution cost of primary energy sources.

4.3.4 Model Summary

The total daily cost of the hydrogen supply chain network is obtained by combining the cost terms derived in Section 4.3.3 as follows:

$$TDC = \frac{FCC + TCC}{\alpha\, CCF} + FOC + TOC + ESC \tag{4.52}$$

Finally, the corresponding cost is minimised by the optimisation:

$$\min\ TDC \tag{4.53}$$

The above minimisation is subject to all constraints presented in Section 4.3.2.

4.4 Case Study Revisited

The case study given in Chapter 3 is revised to accommodate the availability of primary energy sources and their distribution, as well as different sizes of production and storage facilities. In this case study, hydrogen is assumed to be produced from four different primary energy sources, namely natural gas, coal, biomass, and electricity. These feedstocks will be utilised to produce hydrogen at different production scales via steam methane reforming, coal gasification, biomass gasification, and electrolysis, respectively. Three different production scales are included: small, medium, and large. Among these production technologies, coal and biomass gasification plants cannot be built at small-scale due to economical and environmental barriers [81]. In addition, it is economically infeasible to construct large-scale electrolysis plants since they suffer from diseconomies of scale [73, 81]. Once hydrogen is generated from these different types and sizes of production technologies, it will be distributed locally and regionally by truck and/or rail. Finally, hydrogen will be stored at stationary storage facilities of different sizes. Again, three different sizes of vessels will be used, referred to as small, medium and large.

This study examines only the production, storage, and distribution of liquid hydrogen. Liquid hydrogen is considered instead of its counterpart compressed-gaseous hydrogen because it is widely used in today's market. Liquid hydrogen enjoys considerable advantages over gas from a storage, distribution, and fuelling perspective. Compared with gaseous hydrogen, the liquid has a very high energy density which makes it easier to handle, transport, and store. In addition, the technologies used in generating, storing, and transporting liquid hydrogen are well-established and gas industries have a great deal of experience in dealing with it. From an economical viewpoint, however, designing a liquid hydrogen-based supply network is extensively cheaper than designing a gaseous-based network, as concluded in the previous chapter.

The model derived in this chapter will be used to analyse two different hydrogen supply chain configurations using Great Britain as a backdrop. These configurations are summarised in Table 4.1.

Table 4.1: Network configurations to be studied for the extended model

Configuration 1	Production of liquid hydrogen via steam methane reforming, coal and biomass gasification, and water electrolysis in large, medium, and small plants with tanker truck delivery. Different sizes of liquid hydrogen storage facilities will be used.
Configuration 2	Similar to the first scenario, however, both tanker truck and railway tank cars will be used for distribution.

4.4.1 Input Data

The addition of an extra node in the proposed model makes the process of collecting data even more complicated. This is due to the increase in the breadth of the hydrogen supply chain. Therefore, data must come from many disparate sources. The data that was used as an input to the model of interest is given below. A full discussion on how this data was gathered can be found in Appendices A to D.

Hydrogen Demand

The daily demand of hydrogen in each grid is listed in Table 4.2, which is identical to those values given for the steady-state model. Also, the hydrogen supply chain network resulting from satisfying these demand values is assumed to operate at 100% utilisation rate, i.e. 365 d/yr. The capital charge factor associated with this investment is 3 years.

Table 4.2: Hydrogen demand in each grid square for the extended model

Grid, *g*	Hydrogen demand (t/d)
01	102
02	80
03	158
04	198
05	41
06	130
07	173
08	7
09	85
10	316
11	385
12	9
13	635
14	902
15	143
16	24
17	489

Table 4.2 (*Continued*)

Grid, *g*	Hydrogen demand (t/d)
18	997
19	497
20	41
21	63
22	624
23	1047
24	861
25	356
26	63
27	394
28	879
29	2727
30	188
31	208
32	252
33	185
34	136

Primary Energy Sources

The daily availability of primary energy sources in each grid is summarised in Table 4.3. These figures are calculated by performing a detailed evaluation on the availability of primary energy sources in Great Britain (see Appendix D). The cost values associated with distributing these energy sources throughout the hydrogen supply chain network are listed in Table 4.4. It can be seen from the table that the unit cost of importing primary energy sources from another country is calculated by multiplying the unit cost of primary energy source at plant gate by 10%. This extra cost is added to account for the cost required to handle and distribute the primary energy sources. The unit distribution cost, however, is obtained by dividing the value of the unit import cost by the longest delivery distance, i.e. 983 km. The unit cost of primary energy sources which is used as a basis for the above calculations represents the price that is charged to industrial users.

Table 4.3: Availability of primary energy sources for the extended model (unit/d)

	Primary energy source, *e*			
Grid, *g*	Natural gas	Coal	Biomass	Electricity
01	0	0	2000	3000
02	0	0	2000	3000
03	0	0	2000	3000
04	0	0	2000	3000
05	110000	0	2000	3000
06	0	0	2000	3000

Table 4.3 (*Continued*)

Grid, g	Primary energy source, e			
	Natural gas	Coal	Biomass	Electricity
07	0	55000	2000	3000
08	0	0	2000	3000
09	0	55000	2000	3000
10	0	55000	2000	3000
11	0	82000	2000	3000
12	0	0	2000	3000
13	0	0	2000	3000
14	29000	0	685	3000
15	0	0	2000	3000
16	0	0	2000	3000
17	22000	164000	685	3000
18	0	164000	685	3000
19	29000	0	2000	3000
20	0	0	2000	3000
21	0	0	2000	3000
22	0	0	2000	3000
23	0	164000	685	3000
24	0	0	2000	3000
25	29000	0	2000	3000
26	0	0	2000	3000
27	0	82000	2000	3000
28	0	0	2000	3000
29	0	0	685	3000
30	0	0	2000	3000
31	0	0	2000	3000
32	0	0	2000	3000
33	0	0	2000	3000
34	0	0	2000	3000

Table 4.4: Costs associated with primary energy sources

Primary energy source, e	Natural gas	Coal	Biomass	Electricity
Unit cost of energy source, UEC_e ($/unit) [73, 110, 115]	0.12	0.03	0.05	0.05
Unit import cost of energy source, UIC_e ($/unit)	0.012	0.003	0.005	0.005
Unit distribution cost of energy source, UDC_e ($/unit/km)	1.22×10^{-5}	3.05×10^{-6}	5.09×10^{-6}	5.09×10^{-5}

Production Facilities

The minimum and maximum production capacities ($PCap_{pji}^{min}$ and $PCap_{pji}^{max}$) of each plant type with respect to size are given in Table 4.5. The capacity range assumed for the different sizes of steam methane reforming plants is based on commercial and near commercial processes that are available in industry today. Currently, single-train commercial steam methane reforming plants are being built with a production capacity of up to 480 t/d, which is equivalent to 200 million scf/d [81]. In fact, even

larger plants can be constructed using multiple trains. Small steam reformer units can also be built and companies have already provided units in the size range of interest. At least one company is constructing commercial steam methane reforming plants as small as 300 kg/d [81].

For medium and large coal and biomass gasification plants, the capacity range is assumed to be the same as the steam methane reforming plants. These figures are based on the assumption that future advancements in technology will lead to the commercialisation of these plants. An advantage of electrolysis plants is that they can be tailored to produce any size necessary ranging from home to industrial scale. Due to this flexibility in design, the capacity of electrolysis plants is assumed to range from 300 to 150,000 kg/d. As mentioned earlier, small-scale gasification units and large-scale electrolysis plants are not considered here because of technical and economical hurdles. It is worth noting that the capacity limits for the different sizes of production technologies are based on current and possible future plants obtained from various literature studies.

Table 4.5 also shows the amount of primary energy sources utilised by each type and size of the production technologies to generate a unit of hydrogen, i.e. rate of utilisation (γ_{epj}). As illustrated in the table, large plants benefit from a low rate of utilisation compared to small-scale plants since large plants have a relatively high energy efficiency. The rate of utilisation for both sizes of electrolysis plants are assumed to be identical because electrolyser efficiency is relatively independent of the plant size [116]. Moreover, the table lists the capital and the unit production costs (PCC_{pji} and UPC_{pji}) of the hydrogen production technologies mentioned earlier. The method adopted in estimating these costs is provided in Appendix C.

Table 4.5: Production capacities and costs of hydrogen plants

Plant type, p	Steam methane reforming			Coal gasification		Biomass gasification		Water electrolysis	
Plant size, j	Small	Medium	Large	Medium	Large	Medium	Large	Small	Medium
$PCap_{pji}^{min}$ (t/d)	0.3	10	200	10	200	10	200	0.3	10
$PCap_{pji}^{max}$ (t/d)	9.5	150	960	150	960	150	960	9.5	150
γ_{epj} [73, 81] (unit e/unit i)	4.02	3.34	3.16	5.64	5.33	18.43	11.26	52.49	52.49
PCC_{pji} ($\$\times10^6$)	29	224	903	389	1611	575	1836	61	663
UPC_{pji} (\$/kg)	3.36	1.74	1.43	2.03	1.56	3.52	2.15	6.82	5.03

Transportation Modes

The maximum allowable flow rate of liquid hydrogen by truck or rail is assumed to be equal to the maximum capacity of large plants, i.e. 960 t/d. The minimum flow rate, however, is assumed to be equal to a fully-loaded transport unit. Additional parameters concerning the capital and operating costs estimation are listed in Table 4.6. The table shows that each transportation mode transcends in certain aspects. Railway tank cars have large storage tanks which are capable of carrying almost double the amount of tanker trucks. Railway tank cars also benefit from high fuel economy, cheap fuel price, as well as low general and maintenance costs. In contrast, tanker trucks have the advantage of high speed, more frequent availability, and short load/unload time.

The table also shows that a few parameters depend mainly on whether hydrogen is distributed locally or regionally. These parameters include transport mode fuel economy, speed, and availability. It is obvious that these parameters would have a lower value than the regional ones. The reason behind this, as previously mentioned, is traffic, speed limits, road layout, and delivery restrictions are usually exist within a particular grid. Therefore, tanker trucks are an apt option for both local and regional distributions while railway tank cars are only suitable for regional distribution. In the case of rail delivery, the railway network is assumed to be in place and ready for use. This assumption is valid since Great Britain benefits from a huge national railway infrastructure. The average delivery distances required for these types of distribution modes are provided in Table B.1 in Appendix B.

As highlighted in the previous chapter, the capital cost of truck transport consists of the tank unit cost, the truck cab cost and the undercarriage cost. On the other hand, the capital cost of rail delivery includes the tank unit cost and the cost of the undercarriage. For rail delivery, there will be no cab cost since a prime mover is used to propel the carriages, for which the cost was not considered. The cost of these components for both modes is shown in Table 4.6.

Most of the values in Table 4.6 have been obtained from a report by Amos [75]. Some values, however, were assumed for the sake of the analysis.

Table 4.6: Costs and characteristics of transportation modes

Transportation mode, l	Tanker truck	Railway tank car
Transport unit capacity, $TCap_{il}$ (kg/mode)	4082	9072
Fuel economy within grid, FE_l^L (km/L)	2.30	3.83
Fuel economy between grids, FE_l^R (km/L)	2.55	4.25
Average speed within grid, SP_l^L (km/hr)	25	20
Average speed between grids, SP_l^R (km/hr)	55	45
Mode availability within grid, TMA_l^L (hr/d)	15	8
Mode availability between grids, TMA_l^R (hr/d)	18	12
Load/unload time, LUT_l (hr)	2	12
Driver wage, DW_l ($/hr)	23	23
Fuel price, FP_l ($/L)	1.16	0.28
Maintenance expenses, ME_l ($/km)	0.0976	0.0621
General expenses, GE_l ($/d)	8.22	6.85
Tank unit cost ($/mode)	350,000	400,000
Cab cost ($/mode)	90,000	–
Undercarriage cost ($/mode)	60,000	100,000
Transport mode cost, TMC_{il} ($/mode)	500,000	500,000

Storage Facilities

The minimum and maximum storage capacities of liquid hydrogen storage facilities for three different sizes are shown in Table 4.7. The maximum storage capacity of large facilities was assumed to be double that of the largest tank available today [113]. This was based on the assumption that future developments will lead to the construction of larger tanks. Due to the flexibility in storage facilities design, the other capacity limits can range from a few kilograms to several tonnes. However, these values were chosen for the sake of this study.

The table also shows the capital and unit storage costs for the different sizes of liquid hydrogen storage facilities. These values were obtained from a detailed economic analysis provided in Appendix C. The storage facilities were designed to hold 10 days' worth of stock of liquid hydrogen.

Table 4.7: Storage capacities and costs of liquid hydrogen storage facilities

Storage type, s	Liquid hydrogen storage		
Storage size, j	Small	Medium	Large
Minimum storage capacity, $SCap_{sji}^{min}$ (t)	0.5	10	200
Maximum storage capacity, $SCap_{sji}^{min}$ (t)	9.5	150	540
Storage capital cost, SCC_{sji} (million \$)	5	33	122
Unit storage cost, USC_{sji} (\$/kg/d)	0.032	0.010	0.005

4.4.2 Results and Discussion

The aim of the proposed model is to outline the optimal hydrogen supply chain network by satisfying the required demand. The model presented in Section 4.3 was constrained to examine two different hydrogen configurations summarised in Table 4.1. The production and storage technologies that lie behind the two configurations being examined are similar. However, the key difference lies in the way liquid hydrogen is distributed. The first network uses tanker trucks for hydrogen distribution while the second one uses both tanker trucks and railway tank cars. Transportation modes are varied to compare the difference in cost between the single- and multi-mode distribution networks, as well as to identify the distribution pattern obtained for such an exercise. The solutions of the two configurations lead to the network structures shown in Figures 4.3 and 4.4. As with the steady-state model, these figures encapsulate the number and location of hydrogen production and storage facilities as well as their types and sizes. The figures also depict the type of transportation modes established between grids and their flow rate. In addition, the flow rate of natural gas is shown within these figures. The exact values of hydrogen flow rate between grids with respect to transportation mode are summarised in Appendix E. The appendix also provides a summary of the results for the different continuous variables examined.

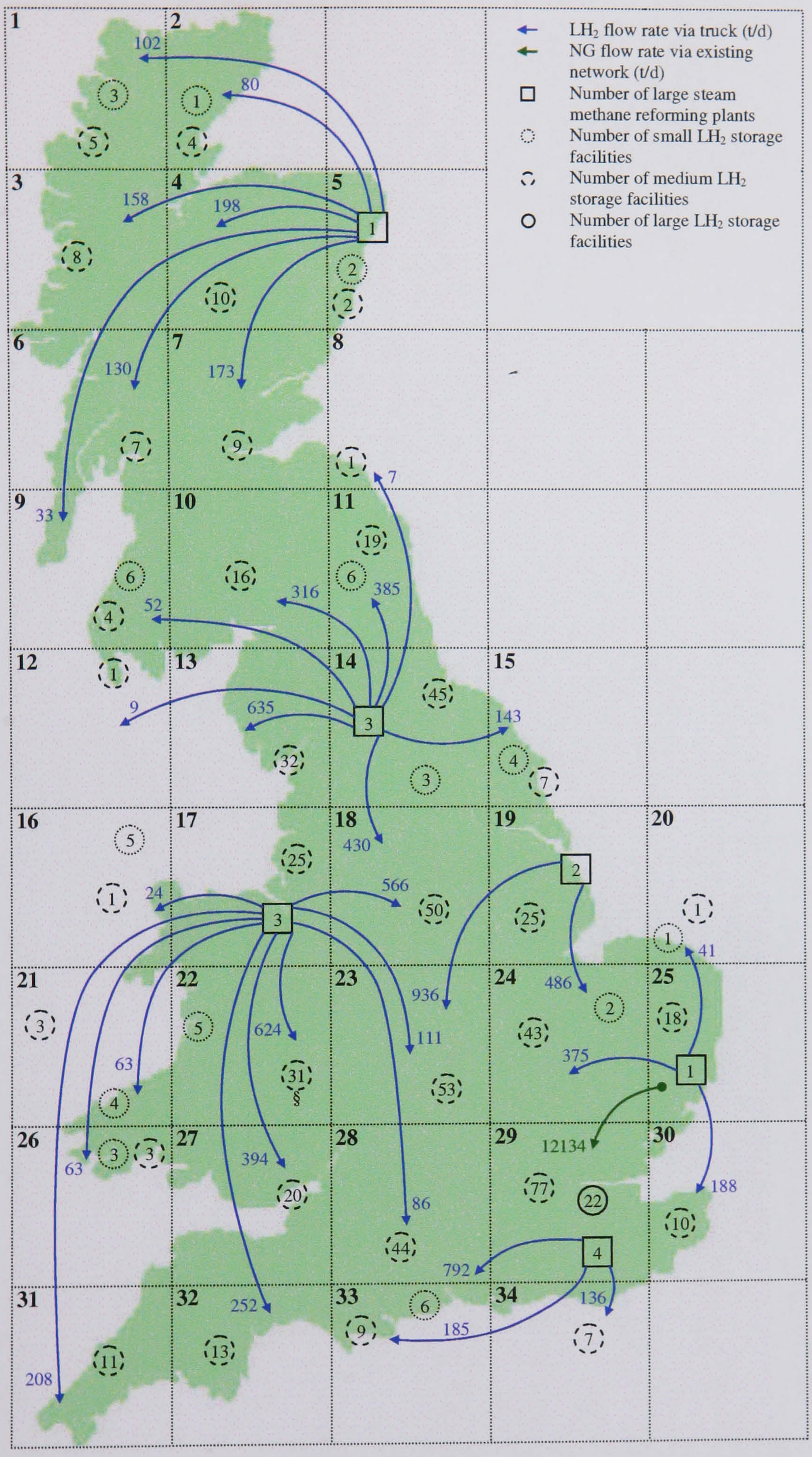


Figure 4.3: Network structure of liquid hydrogen produced via large-scale steam methane reforming plants. The hydrogen is stored in small, medium, and large liquid hydrogen storage facilities. Trucks are utilised as a means of distribution.

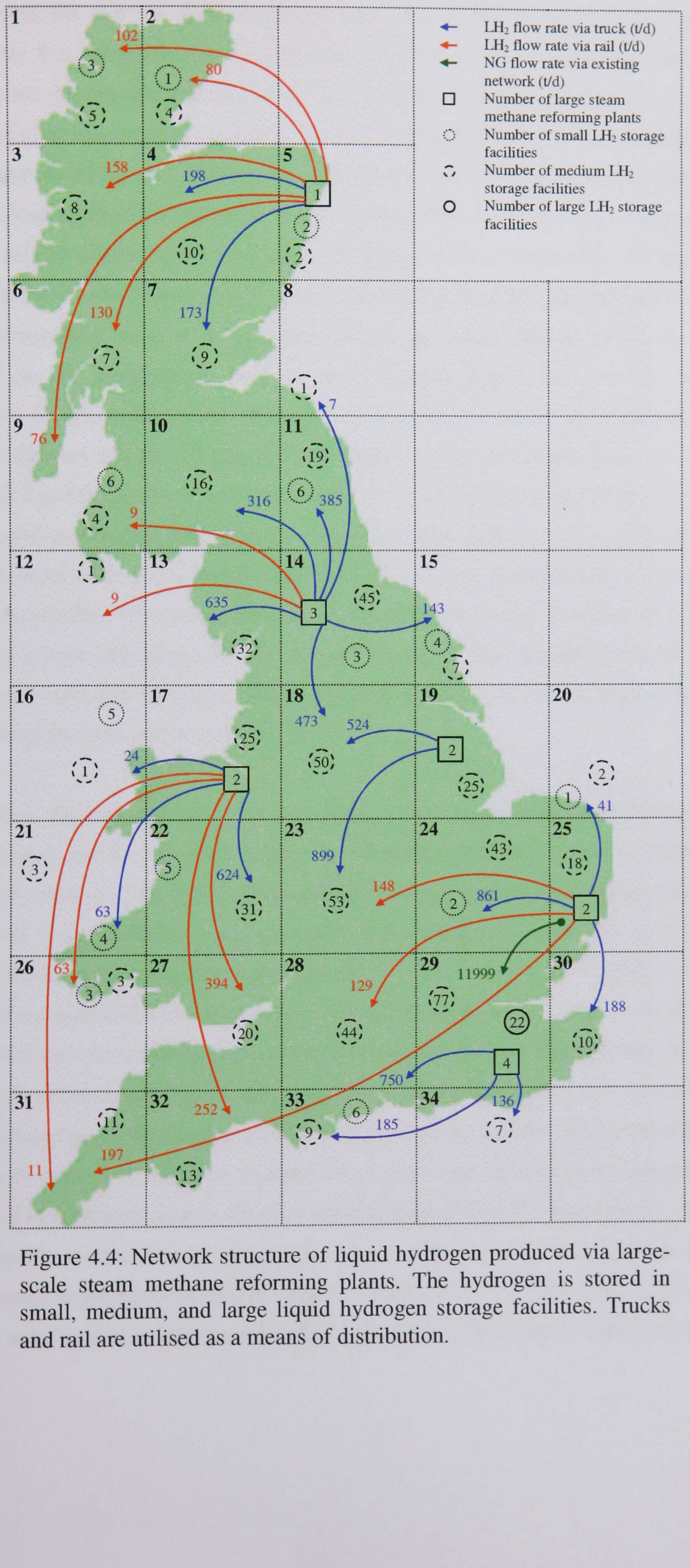


Figure 4.4: Network structure of liquid hydrogen produced via large-scale steam methane reforming plants. The hydrogen is stored in small, medium, and large liquid hydrogen storage facilities. Trucks and rail are utilised as a means of distribution.

Analysing the features of the network structures shown in Figures 4.3 and 4.4 indicates that the production arrangements for both figures are identical. The first reason for this similarity is the cost of hydrogen production technology. Since steam reforming of natural gas is currently the cheapest and the most common method for hydrogen production, all of the production plants established utilise such technology. The second cause of this similarity is the local availability of a primary energy source. Such factors influenced the geographical location of the production facility. It is evident that most of the production plants are built in locations abundant with natural gas to minimise the cost of importing natural gas from overseas or nearby grids. Based on our assumptions, these locations include grids 5, 14, 17, 19, and 25. Demand density marks the last reason behind the similarity of the optimised networks. This is illustrated in grid 29 which has the highest hydrogen demand because it covers Greater London and the South East region. As a result, four steam reforming plants are established in grid 29 despite the assumption that natural gas is unavailable. The feedstock for these plants is imported from grid 25 where a plentiful source of natural gas is accessible. This option minimises cost, as an alternative would be to transport hydrogen from grid 25 to grids 29, 33, and 34. Hence, it is inevitable that importing hydrogen from grid 25 would increase the transportation cost in that region therefore increasing the total cost of the network.

Although Figures 4.3 and 4.4 are alike in the production configuration, the distribution pattern for both figures is somewhat different. This discrepancy is primarily related to the types of transportation modes that are used. For instance, rail transport is well-suited for large quantities of hydrogen and long distances due to its high storage capacity and low operating cost. Trucks, however, are suitable for small-to-medium quantities and short delivery distances. Such observations can be clarified in Figure 4.4 where railway tank cars were mostly utilised for long delivery distances and high demand quantities. Comparing this to Figure 4.3, trucks seek to satisfy the grid demand using the shortest possible delivery distance and the minimum number of transport units. The types of transportation mode also influenced the geographical location of production plants. This is evident in grids 17 and 25. When trucks were the only means of transportation, it became more economical to build three plants in grid 17 because it provided the shortest path for truck delivery. In this case, fully loaded trucks were used to satisfy the nearby demand. On the other hand, allowing both truck

and rail transport resulted in two plants being built in grid 17 and two in grid 25. This is due to the fact that rail transport is inexpensive even at long delivery distances and low transport quantities (see Figure 4.4).

Even though the model incorporates different production scales, the decision to install large-scale plants was made. This is because it is more profitable to build large plants especially during a fully saturated hydrogen economy. Such an observation is expected when maturity is reached in the hydrogen market and hydrogen becomes the main transportation fuel. However, the size of the storage tanks varied according to the demand. The establishment of different sizes of storage facilities was necessary in order to fulfil customer needs. As shown in both figures, all grids contain medium size storage tanks since they have the right capacity to store the production. However, small-scale storage tanks were predominantly installed in grids with low demand or in a combination with midsize tanks to make sure that no storage capacity is wasted. This combination of different sizes seems to be cheaper than installing a large storage facility. Large-scale storage facilities were only built in locations where a large amount of hydrogen storage was needed as the case with grid 29.

The optimal costs for the single- and multi-mode network configurations are 54.69 and 54.63 million $/d, respectively. A breakdown of these costs is listed in Table 4.8. The negligible difference in the network costs indicates that neither mode has a particular advantage over the other. However, one can conclude that the single-mode network is favoured over the multi-mode one. This is due to the fact that trucks are more flexible in operation and have a well-established infrastructure. The table also shows that the regional transportation operating cost for the single-mode case is higher than that of the multi-mode case. The reason behind this is the high price of diesel, maintenance cost and general expenses. The difference in the local transportation operating cost of both modes is insignificant because of the assumption that only trucks can be used for local distribution. On the other hand, the capital cost of the multi-mode network is higher, especially for regional distribution, due to long load/unload times, low availability, and minimal average speed. Since both networks have the same number of production and storage facilities, the capital and operating costs of these facilities are similar.

Table 4.8: Breakdown of total network cost for the extended model

Configuration	1	2
Capital cost		
Plants and storage facilities	35.88×10^{9}	35.88×10^{9}
Local transportation cost	105.33×10^{6}	99.64×10^{6}
Regional transportation cost	406.01×10^{6}	466.76×10^{6}
Total capital cost ($)	36.39×10^{9}	36.44×10^{9}
Operating cost		
Plants and storage facilities	20.44×10^{6}	20.44×10^{6}
Transportation modes		
Local fuel cost	28.78×10^{3}	27.22×10^{3}
Local labour cost	72.68×10^{3}	68.75×10^{3}
Local maintenance cost	5.57×10^{3}	5.27×10^{3}
Local general cost	1.73×10^{3}	1.64×10^{3}
Regional fuel cost	262.94×10^{3}	174.61×10^{3}
Regional labour cost	336.18×10^{3}	334.01×10^{3}
Regional maintenance cost	56.41×10^{3}	42.29×10^{3}
Regional general cost	6.67×10^{3}	7.15×10^{3}
Primary energy source cost	247.68×10^{3}	244.91×10^{3}
Total operating cost ($/d)	21.46×10^{6}	21.35×10^{6}
Total network cost ($/d)	*54.69×10^{6}*	*54.63×10^{6}*

As mentioned earlier, the model described in this chapter was solved as an MILP problem using a Pentium 4, 1.8 GHz Dell machine incorporating CPLEX v9.0 code. A specialised modelling software, GAMS, was used to carry out this work. The computational results for the examined network configurations are summarised in Table 4.9. The table shows that the time required to solve these network configurations is reasonable in comparison to the number of constraints and decision variables involved in both networks. Also the optimality gap for these networks is minute. This optimality gap was assumed to be 0.01%—decreasing this percentage would have increased the accuracy slightly and decreased speed of computation.

Table 4.9: Summary of computational results for the extended model

Configuration	1	2
Number of constraints	8042	13652
Number of integer variables	2346	3468
Number of continuous variables	7328	8450
Optimality gap (%)	0.01	0.01
CPU time (sec)	11921	3844

4.4.3 Sensitivity Analysis

A sensitivity analysis was conducted to study the model's response to changes in the input parameters. To perform the analysis, the hydrogen supply chain network structures for the two configurations mentioned in Table 4.1 were obtained. Such determination was based on using the most probable values for the various parameters given in the input data section. This establishes the base case for analysis. After establishing the base case, the following four scenarios were employed to test the performance of the model by making use of the examined case study. These scenarios are summarised in Table 4.10.

Table 4.10: Scenarios testing the sensitivity of the extended model

Scenario 1	25% increase in transportation cost
Scenario 2	25% decrease in transportation cost
Scenario 3	No economy of scale in the production plants
Scenario 4	Economy of scale in the production plants

To achieve economies of scale in scenario 4 the relationship between unit cost and plant size was assumed to be non-linear; as the plant size increases unit cost decreases. However, in the case of no economy of scale in the production plants the relationship was assumed to be linear.

The above scenarios aim to show how sensitive the network structures are to parameter alterations. They also give some idea of the degree of risk involved in making judgements on the performance of the hydrogen supply chain network.

Four different benchmarks were utilised to describe the solution of the previously mentioned scenarios as well as the base case. These benchmarks are outlined as follows:

- Calculating the total number of each size of production plants, i.e. small, medium, and large,
- Calculating the percentage of grid squares which have a production plant,
- Calculating the percentage of grid squares which have at least one medium or large plant, and
- Calculating the overall percentage of demand met by local production.

These benchmarks provide an indication of the degree of centralisation, and were applied to five regions of Great Britain categorised as follows:

- Region A which includes Scotland and North of England (g_1–g_{15}),
- Region B which includes Wales, the Midlands, and East Anglia (g_{16}–g_{25}),
- Region C which includes South Wales and South West (g_{26}–g_{28} & g_{31}–g_{33}),
- Region D which includes South East and Greater London (g_{29}, g_{30}, g_{34}), and
- Region E which includes all regions covering Great Britain (g_1–g_{34}).

where g denotes grid square and the subscript denotes the number of grid shown in Figures 4.3 and 4.4.

As stated, the performance of the base case and the four different scenarios were studied by applying the above benchmarks on the five regions of Great Britain. The results for both network configurations are summarised in Tables 4.11 and 4.12, respectively. The tables will not include small- and medium-scale plants due to the fact that only large plants were established for the same reason mentioned in the results and discussion section.

Table 4.11: Sensitivity of the first network configuration

	Base case			
Region	Total number of large plants	% of grids with plant	% of grids with medium or large plant	% of local demand
A	4	12	12	28
B	6	18	18	27
C	0	0	0	0
D	4	12	12	89
E	14	41	41	37
	25% increase in transportation cost (scenario 1)			
Region	Total number of large plants	% of grids with plant	% of grids with medium or large plant	% of local demand
A	4	12	12	28
B	6	18	18	32
C	0	0	0	0
D	4	12	12	89
E	14	41	41	39
	25% decrease in transportation cost (scenario 2)			
Region	Total number of large plants	% of grids with plant	% of grids with medium or large plant	% of local demand
A	4	12	12	28
B	6	18	18	27
C	0	0	0	0
D	4	12	12	89
E	14	41	41	37

Table 4.11 (*Continued*)

Region	**No economy of scale (scenario 3)**			
	Total number of large plants	% of grids with plant	% of grids with medium or large plant	% of local demand
A	4	12	12	28
B	6	18	18	27
C	0	0	0	0
D	4	12	12	89
E	14	41	41	37
Region	**Economy of scale (scenario 4)**			
	Total number of large plants	% of grids with plant	% of grids with medium or large plant	% of local demand
A	4	12	12	28
B	6	18	18	27
C	0	0	0	0
D	4	12	12	89
E	14	41	41	37

Table 4.12: Sensitivity of the second network configuration

Region	**Base case**			
	Total number of large plants	% of grids with plant	% of grids with medium or large plant	% of local demand
A	4	12	12	28
B	6	18	18	27
C	0	0	0	0
D	4	12	12	89
E	14	41	41	37
Region	**25% increase in transportation cost (scenario 1)**			
	Total number of large plants	% of grids with plant	% of grids with medium or large plant	% of local demand
A	4	12	12	28
B	6	18	18	27
C	0	0	0	0
D	4	12	12	89
E	14	41	41	37
Region	**25% decrease in transportation cost (scenario 2)**			
	Total number of large plants	% of grids with plant	% of grids with medium or large plant	% of local demand
A	4	12	12	28
B	7	21	21	27
C	0	0	0	0
D	3	9	9	89
E	14	41	41	37
Region	**No economy of scale (scenario 3)**			
	Total number of large plants	% of grids with plant	% of grids with medium or large plant	% of local demand
A	4	12	12	28
B	6	18	18	27
C	0	0	0	0
D	4	12	12	89
E	14	41	41	37

Table 4.12 (*Continued*)

Region	Economy of scale (scenario 4)			
	Total number of large plants	% of grids with plant	% of grids with medium or large plant	% of local demand
A	4	12	12	28
B	6	18	18	27
C	0	0	0	0
D	4	12	12	89
E	14	41	41	37

The sensitivity measures applied to the studied network configurations show that the hydrogen demand was satisfied by dedicated, centralised production facilities. This means that the production plants are concentrated in certain grids rather than dispersed in many locations. The resulting degree of centralisation can be demonstrated by regions A and B for both networks, where less than 30% of the overall demand is met by local production plants. Due to the variation in population density, the number of plants established in these regions was different. Region A, which covers Scotland and the North of England, has four plants. Out of these four plants, only one is in Scotland and the rest are in the northern part of England. According to our calculation, the latter district is the third most populated area in Great Britain. On the other hand, grids that constitute region B have at least six plants. The reason behind this is the high concentration of population and industrial activities. Also region B is responsible for supplying region C, which has no plants, with its daily demand. It is evident that such an option is cheaper than establishing plants in region C due to the scarcity of natural gas in that region. As mentioned earlier, the highest number of production plants is expected in London and the South East region of the UK due to the high population density. Hence, four plants are built in this locality which assures about 90% of the required demand.

It can be observed from the first network configuration that increasing the transportation cost slightly affects the percentage of local production in region B. The region starts to move towards fulfilling its needs instead of importing hydrogen from other neighbouring grids. Conversely, decreasing the transportation cost gives rise to a longer distance delivery pattern. This can be clarified in region B of the second network configuration where seven plants are established instead of six. In this case, region B becomes as the main source of providing hydrogen to region D which has

only three plants. This option is more economical than building a plant in region D because of the low cost associated with distribution.

In summary, it can be concluded that the sensitivity measures used to describe the solution of the model had a slight influence on the network structure. However, these measures mostly affected the cost of the hydrogen supply chain networks. It can also be concluded that centralised, large-scale plants would be the main source of hydrogen during the long-term hydrogen economy.

4.4.4 Concluding Remarks

The model presented in Chapter 3 is extended to accommodate:

- Availability of primary energy sources,
- Different sizes of production and storage facilities,
- Local distribution of hydrogen, and
- Regional distribution of primary energy sources.

In addition to the decisions addressed in Chapter 3, the model of interest revealed a number of new decisions concerning the design and operational aspects of the hydrogen supply chain. At the design level, the model determined the appropriate energy feedstocks to be selected, the sizes of production and storage technologies to be built, and the local transportation links to be established. The operational decisions were the amount of feedstock, the average storage inventory level, and the flow rates of hydrogen and primary energy sources throughout the network. Using cost as a performance objective and formulating the problem as an MILP, the optimal design of the future hydrogen supply chain configuration was identified.

The feasibility of the model was examined using two different hydrogen supply chain configurations, which were applied within a Great Britain context. The results obtained illustrate the advantage of having a model that takes into consideration the interaction between various nodes of the hydrogen supply chain as well as the cost concerning these nodes. It has been shown from the results that the optimal configuration of the future hydrogen supply chain is the production of hydrogen from

natural gas in centralised, large-scale reforming plants. The local availability of natural gas is a focal point in determining the geographical location and the scale of production. The cost of production technologies and the density of demand are other important factors influencing the decision of production configuration. Once hydrogen is produced, tanker trucks and railway tank cars were used to deliver liquid hydrogen to storage facilities, where it would be stored in small-to-large tanks according to demand requirements. The derived configuration is similar to the existing petroleum supply chain. Such a supply chain produces a wide range of petroleum products from dedicated, centralised refineries. The product is then stored in different sizes of stationary storage facilities and distributed mostly via trucks or railway tank cars as well as pipelines.

A further feasible configuration of a future hydrogen supply chain is the production of liquid hydrogen from natural gas in large reforming plants with the use of tanker trucks as a means of distribution. Based on the obtained results, this pathway is slightly more expensive than the aforementioned configuration. However, at present this option is more feasible due to the flexibility of tanker trucks and the infrastructure already exist.

The performance of the previously discussed hydrogen configurations was assessed though several benchmarks. The sensitivity analysis revealed that the overall cost of the hydrogen network relies extensively on the cost of hydrogen production and distribution technologies. The analysis also showed that centralised, large-scale hydrogen plants are the best production option for vehicle transport sector fully dependent on hydrogen.

The subsequent chapter addresses the transition of the steady-state infrastructure to determining a pathway from now to high levels of adoption.

Chapter 5

Multi-Period Design of Hydrogen Supply Chain

5.1 Problem Description

The two mathematical models derived so far considered the design and operation of a snapshot of the hydrogen supply chain network at a point in time. This chapter, however, addresses the evolution of the network, i.e. the "pathway", over a long-term planning horizon. The model described here will build upon the one presented in Chapter 4 and will take into account this time evolution. An optimisation framework is used to capture the characteristics of the model. The resulting optimisation problem is framed as an MILP with the objective of minimising the overall network cost over the entire planning horizon. Due to the gradual growth of demand over time, a number of evolving networks will be determined from the optimisation procedure. The network at each time period is an expansion of the one obtained from the previous time period. The demand variation is driven by the penetration of hydrogen fuel cell vehicles into the transport market, as well as by the reduction of hydrogen production, storage, and delivery costs. In fact, it would take several decades for this penetration to happen widely and to consequently cause a large reduction in pollutant emissions and oil consumption.

A market penetration analysis of hydrogen fuel cell vehicles was performed to determine the shape of the demand profile over time and is shown in Figure 5.1 [39, 79–81]. This analysis was based on forecasting the percentage of hydrogen fuel cell vehicles entering the transport market. It can be observed from the figure that demand will have an S-shape trajectory. During the introductory stage of a hydrogen economy, demand will be limited to fleet vehicles with a fixed daily route and regular refuelling intervals at certain locations, e.g. buses. These fleet vehicles would probably be present in dense urban areas such as Greater London. When the cost of

manufacturing of hydrogen fuel cell vehicles becomes affordable and hurdles such as onboard storage are overcome, the demand trajectory might increase sharply. Eventually, as the market reaches a state of saturation, the demand trajectory will level off.

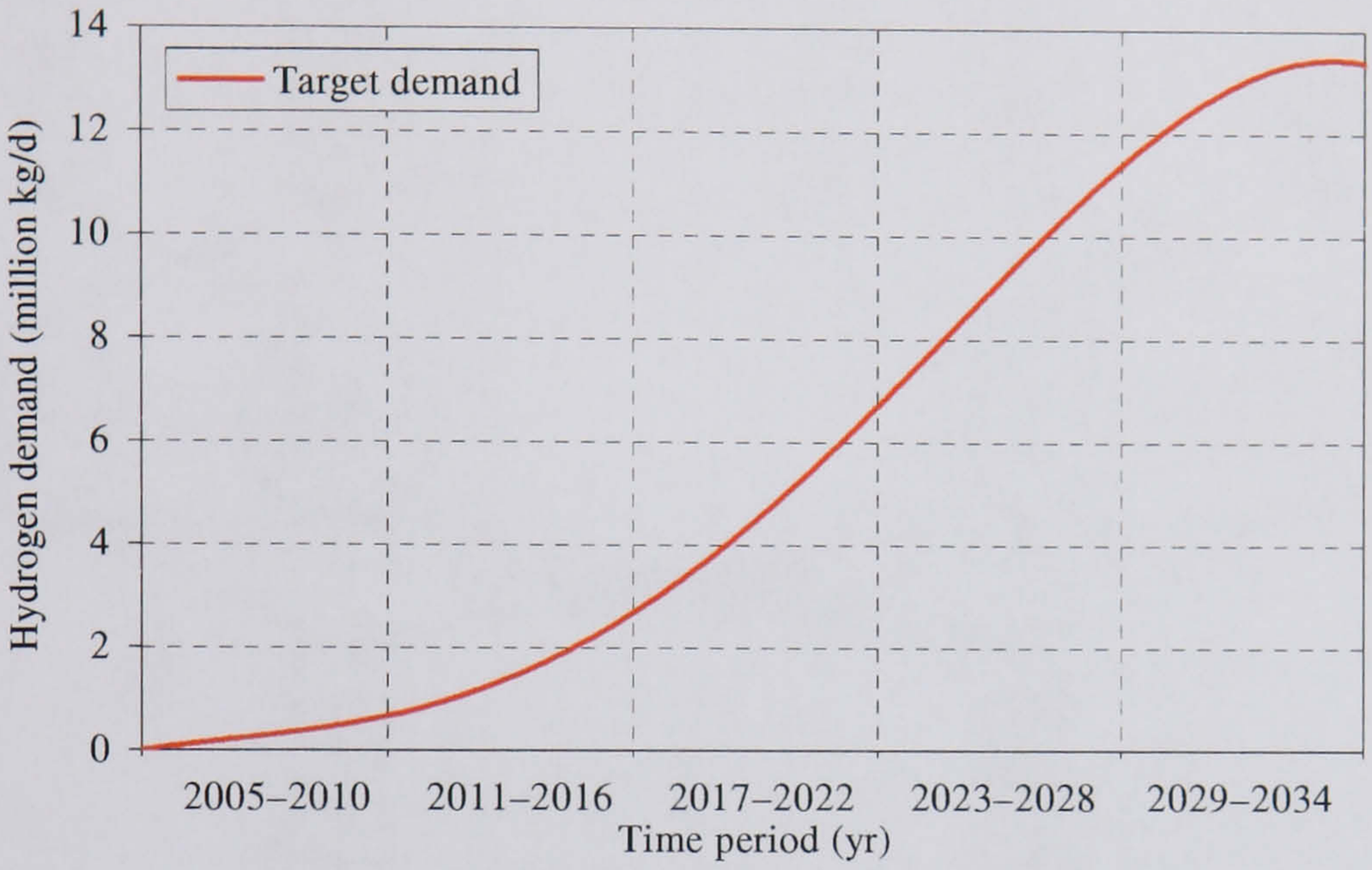


Figure 5.1: Hydrogen demand profile to be examined.

The multi-period model will outline the network structure at each time period of the planning horizon based on the demand profile provided. The strategic design decisions during each time period are: (1) selection of energy feedstocks for production technologies, (2) determination of location, number, type, and capacity of production and storage facilities, and (3) allocation of transportation modes. On the other hand, the operational decisions include: (1) utilisation rate of primary energy sources, (2) total average inventory of hydrogen, (3) flow rate of hydrogen and primary energy sources, and (4) import of resources from abroad.

5.2 Model Structure and Component

The superstructure of the model given in this chapter is exactly identical to the one presented in Chapter 4 in terms of the number of the nodes and their interactions (see Figure 5.2). However, the only difference is the addition of the time element to account for demand variations from one time period to another.

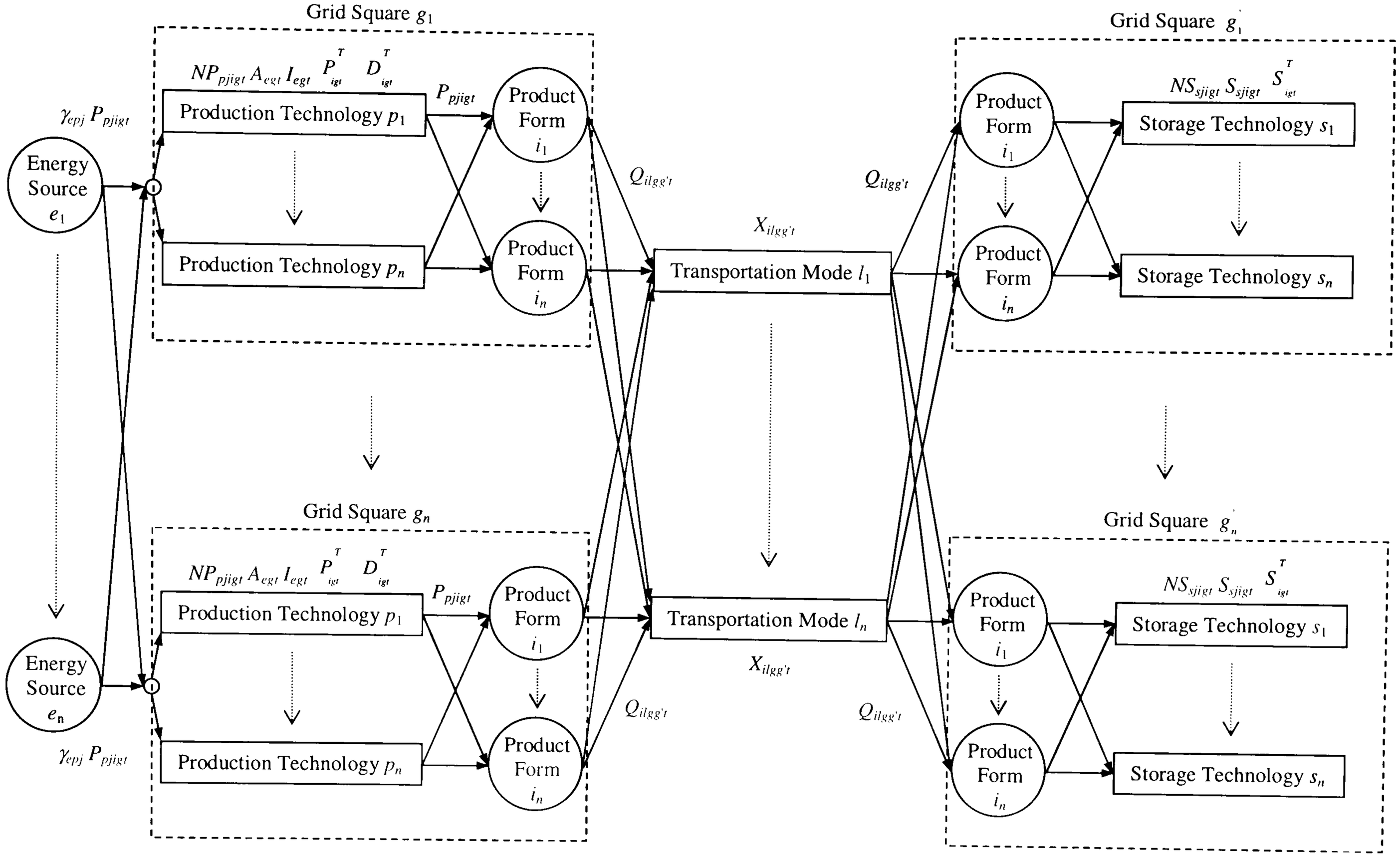


Figure 5.2: Superstructure of the multi-period model. Local transportation of product forms occurs when $g = g'$ whereas regional transportation occurs when $g \neq g'$.

This change to the model applies to all continuous and binary variables as well as demand parameters. Constraints were also modified and new ones were added to accommodate for this change. In addition, objective function terms responded to this alteration by seeking to minimise the average total daily cost of the network established.

The details concerning each component of the multi-period model are similar to the steady-state and the extended models, but within a time framework. The major distinction is demand evolution which is addressed below.

5.2.1 Demand Evolution

The planning investment horizon is divided into a number of time periods of equal length. Each time period is represented by an index t which starts from t_1 to t_n. The demand at the final time period (t_n) is assumed to be known in advance. This demand corresponds to a fully saturated vehicular market (see Appendix A for details). Using the demand value at t_n, the demand at previous time periods are predicted based on a fixed percentage of fuel cell vehicles penetration. The penetration percentage is assumed to follow an S-shape trajectory, which was shown earlier in Figure 5.1. Consequently, the demand at each time period is estimated.

5.3 Model Formulation

5.3.1 Nomenclature

The nomenclature used in this chapter is consistent with that used in Chapter 4. This section summarises only those symbols that are different from those listed in Section 4.3.1.

Index

t time periods of the planning horizon

Parameters

A_{eg}^{0} initial average availability of primary energy source e in grid g (unit/d)

D_{igt}^{T} total demand for product form i in grid g during time period t (kg/d)

LR learning rate—cost reductions as technology manufacturers accumulate experience (%)

NP_{pjig}^{0} initial number of plants of type p and size j producing product form i in grid g

NS_{sjig}^{0} initial number of storage facilities of type s and size j storing product form i in grid g

NTP number of time periods

PF_t penetration factor of hydrogen fuel cell vehicles during period time t (%)

SSF safety stock factor of primary energy sources within a grid (%)

Continuous Variables

A_{egt} Average availability of primary energy source e in grid g during time period t (unit/d)

D_{igt}^{L} demand for product form i in grid g satisfied by local production during time period t (kg/d)

D_{igt}^{I} imported demand of product form i to grid g during time period t (kg/d)

DM_{mgt}^{L} local demand satisfied by $m-1$ plants in grid g during time period t (kg/d)

I_{egt} import of primary energy source e to grid g from overseas during time period t (unit/d)

P_{pjigt} production rate of product form i produced by plant type p of size j in grid g during time period t (kg/d)

P_{igt}^{T} total production rate of product form i in grid g during time period t (kg/d)

$Q_{ilgg't}$ flow rate of product form i by transportation mode l between grids g and g' during time period t (kg/d)

$QE_{egg't}$ flow rate of primary energy source e between grids g and g' during time period t (unit/d)

S_{sjigt} average inventory of product form i stored in storage type s and size j in grid g during time period t (kg)

S_{igt}^{T} total average inventory of product form i in grid g during time period t (kg)

Integer Variables

IP_{pjigt} investment of plants of type p and size j producing product form i in grid g during time period t

IS_{sjigt} investment of storage facilities of type s and size j storing product form i in grid g during time period t

NP_{pjigt} number of plants of type p and size j producing product form i in grid g during time period t

NS_{sjigt} number of storage facilities of type s and size j storing product form i in grid g during time period t

Binary Variables

U_{mgt} 1 if there are $m-1$ plants in grid g during time period t, 0 otherwise

$X_{ilgg't}$ 1 if product form i is to be transported from grids g to g' by transportation mode l during time period t, 0 otherwise

Y_{igt} 1 if product form i is to be exported from grid g during time period t, 0 otherwise

Z_{igt} 1 if product form i is to be imported to grid g during time period t, 0 otherwise

5.3.2 Constraints

The mathematical constraints given in Chapter 4 are updated to account for the time effect and repeated briefly for ease of reference.

Demand Constraints

As mentioned earlier, demand will start at a low level and then sharply increase until it reaches the saturation point. Such a pattern can be described by the following equation:

$$D_{igt}^{T} = PF_t D_{ig}^{T} \tag{5.1}$$

where PF_t is a given coefficient expressing the percentage of penetration of hydrogen fuel cell vehicles during each time period t. D_{ig}^{T} is multiplied by PF_t to take into account the growth in demand during each time period of the planning horizon.

Each grid within the supply chain network will fulfil its needs by local production facilities or by importing products from other neighbouring grids. Therefore, the local demand, i.e. demand satisfied by local production, of a product form i in a grid g during time period t is expressed by the following constraint:

$$D_{igt}^{L} \leq P_{igt}^{T} \qquad \forall i, g, t \tag{5.2}$$

The imported demand of a product form i to a particular grid g and time period t is equal to the total flow imported to that grid by all transportation modes:

$$D_{igt}^{I} = \sum_{l,g'} Q_{ilg'gt} \qquad \forall i, g, t \tag{5.3}$$

The total product demand in each grid must equal the demand satisfied by the local production plus the demand imported from other grids as follows:

$$D_{igt}^{T} = D_{igt}^{L} + D_{igt}^{I} \qquad \forall i, g, t \tag{5.4}$$

Primary Energy Source Constraints

The average availability of primary energy sources in a grid g at the end of the first time period t_1 is given as a sum of four terms. These are the initial average availability of primary energy sources, the import of primary energy sources from overseas, the transportation of primary energy sources between grids, and the rate of consumption of these sources. The terms are expressed respectively by the following constraint:

$$A_{egt_1} = A_{eg}^{0} + I_{egt_1} + \sum_{g'} \left(QE_{eg'gt_1} - QE_{egg't_1} \right) - \sum_{p,j,i} \gamma_{epj} P_{pjigt_1} \qquad \forall e, g \tag{5.5}$$

The average availability of primary energy sources at the end of subsequent time periods is written as follows:

$$A_{egt} = A_{eg(t-1)} + I_{egt} + \sum_{g'} \left(QE_{eg'gt} - QE_{egg't} \right) - \sum_{p,j,i} \gamma_{epj} P_{pjigt} \qquad \forall e, g, t : t \neq t_1 \tag{5.6}$$

where $A_{eg(t\text{-}1)}$ is the average availability of primary energy sources at the end of previous time period.

The import and export of primary energy sources throughout the hydrogen supply network can take place only if a production plant exists and production takes place. This consideration will prevent any build up of primary energy sources in a grid, as follows:

$$\left(I_{egt} + \sum_{g'} QE_{eg'gt} \right) SSF = \sum_{g'} QE_{egg't} + \sum_{p,j,i} \gamma_{epj} P_{pjigt} \qquad \forall e, g, t \tag{5.7}$$

The first and second terms of the left-hand-side of Equation 5.7 represent the import of primary energy sources from overseas and neighbouring grids, respectively. These terms are multiplied by a safety stock factor (*SSF*) to store a small inventory of

primary energy sources as an insurance against unanticipated events. The first term of the right-hand-side of the same equation indicates the export of primary energy sources to nearby grids, while the second term indicates the amount of primary energy sources consumed by a production plant.

Production Facility Constraints

Assuming a steady-state operation during each time period, a total mass balance on a grid is written as follows:

$$P_{igt}^{T} = \sum_{l,g'} \left(Q_{ilgg't} - Q_{ilg'gt} \right) + D_{igt}^{T} \qquad \forall i, g, t \tag{5.8}$$

The total production rate of a product form i in a grid g and time period t is also equal to the production rate of all plants of type p and size j that are established:

$$P_{igt}^{T} = \sum_{p,j} P_{pjigt} \qquad \forall i, g, t \tag{5.9}$$

The production rate of plant type p and size j established in grid g during time period t is constrained by the number of production facilities and the minimum and maximum production limits:

$$PCap_{pji}^{\min} NP_{pjigt} \le P_{pjigt} \le PCap_{pji}^{\max} NP_{pjigt} \qquad \forall p, j, i, g, t \tag{5.10}$$

In the case of small-scale plants, products cannot be exported to neighbouring grids but can only satisfy local demand via the following constraint:

$$\sum_{p} P_{pjigt} \le D_{igt}^{L} \qquad \forall i, g, t : j = \text{small plants} \tag{5.11}$$

Some production technologies cannot be developed in certain sizes. This is due to inherent technical and economical limitations of the technology. The following constraints demonstrate such restrictions:

$$NP_{pjigt} = 0 \quad \forall i,g,t : p = \text{coal gasification} \;\&\; j = \text{small plants} \tag{5.12}$$

$$NP_{pjigt} = 0 \quad \forall i,g,t : p = \text{biomass gasification} \;\&\; j = \text{small plants} \tag{5.13}$$

$$NP_{pjigt} = 0 \quad \forall i,g,t : p = \text{electrolysis} \;\&\; j = \text{large plants} \tag{5.14}$$

Transportation Constraints

Local transportation of a product will only take place if the grid contains at least one production plant. This distribution depends significantly on the average delivery distance within a grid and local demand satisfied by the total number of plants established. The former factor is expressed by the following constraints:

$$L_{gt}^{\text{ave}} = \sum_{m} \frac{2L_g^L}{m-1} U_{mgt} \quad \forall g,t \tag{5.15}$$

The latter factor is given as follows:

$$DM_{mgt}^{L} \geq D_{igt}^{L} - \pi(1-U_{mgt}) \quad \forall i,m,g,t \tag{5.16}$$

Details on the derivation of the above equations are provided in Chapter 4, Section 4.3.3.

The constraints concerning regional transportation are similar to the ones given in Chapter 4 but the time element was introduced to the corresponding continuous and binary variables. These constraints are listed below without further discussion.

$$Q_{il}^{\min} X_{ilgg't} \leq Q_{ilgg't} \leq Q_{il}^{\max} X_{ilgg't} \quad \forall i,l,g,g',t : g \neq g' \tag{5.17}$$

$$Y_{igt} \geq X_{ilgg't} \quad \forall i,l,g,g',t : g \neq g' \tag{5.18}$$

$$Z_{igt} \geq X_{ilg'gt} \quad \forall i,l,g,g',t : g \neq g' \tag{5.19}$$

$$Y_{igt} + Z_{igt} \leq 1 \quad \forall i,g,t \tag{5.20}$$

Storage Facility Constraints

The total average inventory of product form i at grid g and time period t is:

$$S_{igt}^{T} = \beta D_{igt}^{T} \quad \forall i,g,t \tag{5.21}$$

The average inventory of product form i kept in grid g by storage type s and size j during time period t is subject to:

$$SCap_{sji}^{\min} NS_{sjigt} \leq S_{sjigt} \leq SCap_{sji}^{\max} NS_{sjigt} \quad \forall s,j,i,g,t \tag{5.22}$$

A similar concept can be imposed on the total average inventory:

$$\sum_{s,j} SCap_{sji}^{\min} NS_{sjigt} \leq S_{igt}^{T} \leq \sum_{s,j} SCap_{sji}^{\max} NS_{sjigt} \quad \forall i,g,t \tag{5.23}$$

Time Evolution Constraints

During the early stages of the transition to a hydrogen economy, hydrogen is expected to be supplied from existing petroleum refineries, chemical complexes or chlor-alkali plants. It could also be obtained from an existing storage facility. Taking these options into account, the number of production plants and storage facilities in a particular grid and during the first time period are given by the following constraints:

$$NP_{pjigt_1} = NP^0_{pjig} + IP_{pjigt_1} \qquad \forall p, j, i, g \tag{5.24}$$

$$NS_{sjigt_1} = NS^0_{sjig} + IS_{sjigt_1} \qquad \forall s, j, i, g \tag{5.25}$$

The parameters NP^0_{pjig} and NS^0_{sjig} are the number of existing production plants and storage facilities, respectively. The variables IP_{pjigt_1} and IS_{sjigt_1} are the number of new production plants and storage facilities that need to be built early during the first time period.

As the network evolves over time, new production plants and storage facilities will be invested in to meet the increased demand. Therefore, the number of production plants and storage facilities in each grid and during the subsequent time periods is equal to the number of the previously established facilities plus the number of new invested plants and storage facilities. This can be captured by the following constraints:

$$NP_{pjigt} = NP_{pjig(t-1)} + IP_{pjigt} \qquad \forall p, j, i, g, t : t \neq t_1 \tag{5.26}$$

$$NS_{sjigt} = NS_{sjig(t-1)} + IS_{sjigt} \qquad \forall s, j, i, g, t : t \neq t_1 \tag{5.27}$$

where $NP_{pjig(t\text{-}1)}$ and $NS_{sjig(t\text{-}1)}$ are the number of production plants and storage facilities at the end of the previous time period, respectively.

Non-negativity Constraints

All decision variables presented in the model must be non-negative:

$$A_{egt} \geq 0 \qquad \forall e, g, t \tag{5.28}$$

$$D^L_{igt} \geq 0 \qquad \forall i, g, t \tag{5.29}$$

$$D^I_{igt} \geq 0 \qquad \forall i, g, t \tag{5.30}$$

$$DM^L_{mgt} \geq 0 \qquad \forall m, g, t \tag{5.31}$$

$$I_{egt} \geq 0 \quad \forall e, g, t \tag{5.32}$$

$$IP_{pjigt} \geq 0 \quad \forall p, j, i, g, t \tag{5.33}$$

$$IS_{sjigt} \geq 0 \quad \forall s, j, i, g, t \tag{5.34}$$

$$NP_{pjigt} \geq 0 \quad \forall p, j, i, g, t \tag{5.35}$$

$$NS_{sjigt} \geq 0 \quad \forall s, j, i, g, t \tag{5.36}$$

$$P_{igt}^{T} \geq 0 \quad \forall i, g, t \tag{5.37}$$

$$P_{pjigt} \geq 0 \quad \forall p, j, i, g, t \tag{5.38}$$

$$Q_{ilgg't} \geq 0 \quad \forall i, l, g, g', t : g \neq g' \tag{5.39}$$

$$QE_{egg't} \geq 0 \quad \forall e, g, g', t : g \neq g' \tag{5.40}$$

$$S_{sjigt} \geq 0 \quad \forall s, j, i, g, t \tag{5.41}$$

$$S_{igt}^{T} \geq 0 \quad \forall i, g, t \tag{5.42}$$

5.3.3 Objective Function

The aim of the optimisation is to minimise the average total daily cost of the hydrogen supply chain network over a long-term planning horizon. This cost was obtained by dividing the sum of capital and operating costs during each time period by the total number of time periods. The cost terms associated with both capital and operating costs are elaborated in the following subsections. Again, some of these cost terms are generally similar to the ones presented in the previous models. However, a few modifications were made and will be addressed below.

Facility Capital Cost

The facility capital cost over the entire planning horizon is related to the establishment of new production plants and storage facilities at each time period *t*. The capital cost of the production plants is obtained by multiplying the plant capital costs by the total number of new plants. Likewise, the capital cost of storage facilities is obtained by multiplying the storage capital costs by the total number of new storage facilities. These costs are represented by the following objective function terms:

$$FCC = \sum_{j,i,g,t}\left(\frac{1}{LR}\left(\sum_{p} PCC_{pji} IP_{pjigt} + \sum_{s} SCC_{sji} IS_{sjigt}\right)\right) \tag{5.43}$$

where the first part of the right-hand-side of Equation 5.43 denotes the capital cost of production plants while the second part denotes the capital cost of storage facilities. The learning rate (LR) is introduced to take into account the reduction in the cost of production and storage technologies as experience accumulates with time. This coefficient is defined as follows:

$$LR = 1 + \left(\kappa(t-1)\right) \tag{5.44}$$

where the term $t-1$ represents the cost reduction with time and κ is the percentage of the corresponding reduction per year.

Transportation Capital Cost

The local and regional transportation capital costs are represented by the right-hand-side of the subsequent equation, respectively:

$$\begin{aligned} TCC = & \sum_{i,l,m,g,t} \frac{DM^{L}_{mgt} TMC_{il}}{(m-1) TMA^{L}_{l} TCap_{il}}\left(\frac{2L^{L}_{g}}{SP^{L}_{l}} + LUT_{l}\right) \\ & + \sum_{i,l,g,g',t} \frac{Q_{ilgg't}}{TMA^{R}_{l} TCap_{il}}\left(\frac{2L^{R}_{gg'}}{SP^{R}_{l}} + LUT_{l}\right) \end{aligned} \tag{5.45}$$

Facility Operating Cost

The facility operating cost over the entire planning horizon is given as follows:

$$FOC = \sum_{j,i,g,t}\left(\sum_{p} UPC_{pji} P_{pjigt} + \sum_{s} USC_{sji} S_{sjigt}\right) \tag{5.46}$$

Transportation Operating Cost

The transportation operating cost is categorised into: fuel, labour, maintenance, and general costs. The daily fuel cost during all time periods is equal to:

$$FC = \sum_{i,l,m,g,t} FP_l \left(\frac{2L_g^L DM_{mgt}^L}{(m-1)FE_l^L TCap_{il}} \right) + \sum_{i,l,g,g',t} FP_l \left(\frac{2L_{gg'}^R Q_{ilgg't}}{FE_l^R TCap_{il}} \right) \quad (5.47)$$

The daily labour cost for all time periods can be expressed as follows:

$$LC = \sum_{i,l,m,g,t} DW_l \left(\frac{DM_{mgt}^L}{(m-1)TCap_{il}} \left(\frac{2L_g^L}{SP_l^L} + LUT_l \right) \right) + \sum_{i,l,g,g',t} DW_l \left(\frac{Q_{ilgg't}}{TCap_{il}} \left(\frac{2L_{gg'}^R}{SP_l^R} + LUT_l \right) \right) \quad (5.48)$$

The maintenance cost is:

$$MC = \sum_{i,l,m,g,t} ME_l \left(\frac{2L_g^L DM_{mgt}^L}{(m-1)TCap_{il}} \right) + \sum_{i,l,g,g',t} ME_l \left(\frac{2L_{gg'}^R Q_{ilgg't}}{TCap_{il}} \right) \quad (5.49)$$

The general cost is:

$$GC = \sum_{i,l,m,g,t} GE_l \left(\frac{DM_{mgt}^L}{(m-1)TMA_l^L TCap_{il}} \left(\frac{2L_g^L}{SP_l^L} + LUT_l \right) \right) + \sum_{i,l,g,g',t} GE_l \left(\frac{Q_{ilgg't}}{TMA_l^R TCap_{il}} \left(\frac{2L_{gg'}^R}{SP_l^R} + LUT_l \right) \right) \quad (5.50)$$

Finally, the total transportation operating cost is:

$$TOC = FC + LC + MC + GC \quad (5.51)$$

Primary Energy Source Cost

The cost of primary energy sources over the entire planning horizon is:

$$ESC = \sum_{e,g,t} UIC_e I_{egt} + \sum_{e,g,g',t} UDC_e L^R_{gg'} QE_{egg't} \tag{5.52}$$

5.3.4 Model Summary

The average total daily cost is calculated by summing up all the cost terms derived in Section 5.3.3 in the following form:

$$TDC^{ave} = \frac{1}{NTP}\left(\frac{FCC + TCC}{\alpha\, CCF} + FOC + TOC + ESC\right) \tag{5.53}$$

The right-hand-side of Equation 5.53 is divided by the number of time periods (NTP) in order to find the average cost of the network over the entire planning horizon. Finally, the objective of the multi-period model is achieved by:

$$\min\ TDC^{ave} \tag{4.54}$$

subject to all the constraints given in Section 5.3.2.

5.4 Case Study Revisited

This section revisits the case study of Chapter 4 but takes into account demand variations over a long-term planning horizon. The proposed model will be used to examine the same network configurations postulated in Table 4.1.

5.4.1 Input Data

The following sections provide the input data required for the examined hydrogen supply chain networks. Since some of this data is already given in Section 4.4.1, only additional data is presented here.

Hydrogen Demand

As previously mentioned, the average daily demand of hydrogen in each time period is given as a function of the fuel cell vehicles penetration and the total equivalent demand at 100% market level. To estimate the demand in each period, the planning horizon is divided into five time periods from 2005 to 2034. The length of each period is assumed to be six years, resulting in 30 years in total. The fuel cell vehicle penetration percentage is assumed to start at 5% market share in the first period, growing to 20% in the second period, 50% in the third period, 85% in the fourth period, and reaching 100% in the last period. The values of the demand resulting from these penetration percentages for each grid are listed in Table 5.1.

Table 5.1: Hydrogen demand of each grid and period for the multi-period model (t/d)

	Time period, t				
Grid, g	t_1 (2005–2010)	t_2 (2011–2016)	t_3 (2017–2022)	t_4 (2023–2028)	t_5 (2029–2034)
01	5	20	51	87	102
02	4	16	40	68	80
03	8	32	79	134	158
04	10	40	99	168	198
05	2	8	21	35	41
06	6	26	65	110	130
07	9	35	86	147	173
08	0.4	1	4	6	7
09	4	17	43	72	85
10	16	63	158	269	316
11	19	77	192	327	385
12	0	2	5	8	9
13	32	127	318	540	635
14	45	180	451	767	902
15	7	29	71	121	143
16	1	5	12	21	24
17	24	98	244	415	489
18	50	199	498	847	997
19	25	99	249	423	497
20	2	8	20	35	41
21	3	13	32	54	63

Table 5.1 (*Continued*)

Grid, g	Time period, t				
	t_1 (2005–2010)	t_2 (2011–2016)	t_3 (2017–2022)	t_4 (2023–2028)	t_5 (2029–2034)
22	31	125	312	530	624
23	52	209	524	890	1047
24	43	172	431	732	861
25	18	71	178	303	356
26	3	13	31	53	63
27	20	79	197	335	394
28	44	176	439	747	879
29	136	545	1363	2318	2727
30	9	38	94	160	188
31	10	42	104	177	208
32	13	50	126	214	252
33	9	37	93	157	185
34	7	27	68	116	136

Primary Energy Sources

Due to the time effect, the initial average availability of primary energy sources considered in this model is slightly different from that given for the extended model. A full description on how these availabilities are estimated is provided in Appendix D. This section summarises only the results obtained from the evaluation; they are shown in Table 5.2.

Table 5.2: Initial availability of energy sources for the multi-period model (unit/d)

Grid, g	Primary energy source, e			
	Natural gas	Coal	Biomass	Electricity
01	0	0	2000	3000
02	0	0	2000	3000
03	0	0	2000	3000
04	0	0	2000	3000
05	92000	0	2000	3000
06	0	0	2000	3000
07	0	46000	2000	3000
08	0	0	2000	3000
09	0	46000	2000	3000
10	0	46000	2000	3000
11	0	68000	2000	3000
12	0	0	2000	3000
13	0	0	2000	3000
14	24000	0	685	3000
15	0	0	2000	3000
16	0	0	2000	3000
17	18000	137000	685	3000
18	0	137000	685	3000
19	24000	0	2000	3000
20	0	0	2000	3000
21	0	0	2000	3000

Table 5.2 (*Continued*)

Grid, *g*	Primary energy source, *e*			
	Natural gas	Coal	Biomass	Electricity
22	0	0	2000	3000
23	0	137000	685	3000
24	0	0	2000	3000
25	24000	0	2000	3000
26	0	0	2000	3000
27	0	68000	2000	3000
28	0	0	2000	3000
29	0	0	685	3000
30	0	0	2000	3000
31	0	0	2000	3000
32	0	0	2000	3000
33	0	0	2000	3000
34	0	0	2000	3000

Since this study allows for a small inventory of primary energy sources to be preserved, the safety stock factor (*SSF*) was given a percentage of 95. This means that at least 5% of the feedstock must be kept in grids for future use (beyond 2034).

Production Facilities

In the early phase of a hydrogen economy, hydrogen will be obtained from existing sources such as petrochemical plants, petroleum refineries, or chlor-alkali plants. Consequently, this study makes use of the Great Britain's existing refineries as a source of providing hydrogen during this introductory stage [117]. In these refineries, hydrogen will be produced via steam methane reforming since it is currently the cheapest and most common method of production. The scale of production, location, and number of these production sites are shown in Table 5.3.

Table 5.3: Number of existing hydrogen plants in each grid

Plant type, *p*	Steam methane reforming	
Plant size, *j*	Medium	Large
07	–	1
17	–	1
19	1	–
27	1	–
29	–	1

The parameter κ, which was introduced in the learning rate estimation, is assumed to be 5%/yr. This percentage will account for cost reduction in production technologies as advances in technology occur.

All other data concerning the production facilities is given in the input data section of Chapter 4.

Storage Facilities

Analogous to the production plants, this study assumes a number of storage facilities to be available at the start of the planning horizon. These storage facilities will be located within the same grids as the production plants. However, the scale of storage and the number of these facilities will be different as shown in Table 5.4. Also, there will be no small-scale storage facilities.

Table 5.4: Number of existing storage facilities in each grid

Storage type, s	Liquid hydrogen storage	
Storage size, j	Medium	Large
07	1	–
17	–	1
19	1	–
27	1	–
29	–	1

The reduction in cost of storage facilities through learning was given the same percentage as the one assumed for production plants, i.e. 5%/yr. Additional data for storage facilities is provided in Chapter 4, Section 4.4.1.

5.4.2 Results and Discussion

The model of interest is used to map out two different hydrogen supply chain network configurations. The configurations are similar in terms of primary energy feedstock requirements, as well as the type and size of production and storage technologies. However, they differ in the type of transportation modes, where the first configuration only utilised trucks for hydrogen distribution while the second utilised both trucks and

rail. Since these configurations capture the demand evolution over 34 years divided into five periods, five distinct network configurations were obtained. Each of these configurations is an expansion of the previous network as a transition occurs in the transport market. The optimal network structures for the first configuration for the five time periods of the planning horizon are depicted in Figures 5.3–5.7. The symbols of production, storage, and transportation technologies implemented in these figures are similar to ones given in previous chapters. Any differences in these symbols will be clarified in the figure key. Results that are not shown in the figures are provided in Appendix E.

Analysing the network structures shown in Figures 5.3–5.7 demonstrates that each network has a distinctive characteristic. The reason behind this is demand variation over a long-term planning horizon. As shown in Figure 5.3, the demand of hydrogen during the introductory stage of fuel cell vehicles is supplied largely by medium-to-large production plants. These plants represent petroleum refineries that are presently in operation in Great Britain. Such refineries are assumed to be equipped with steam methane reforming facilities and to exist in grids 7, 17, 19, 27, and 29, prior to the construction of a hydrogen infrastructure. Since most of the current hydrogen output of these plants is already committed, only the excess amount is assumed to be utilised for transportation fuel. Besides obtaining hydrogen from existing dedicated plants, new small-scale hydrogen plants were built in some grids. This is illustrated in grids with extremely low demand such as 2, 5, 8, 12, 16, 20, 21, and 26.

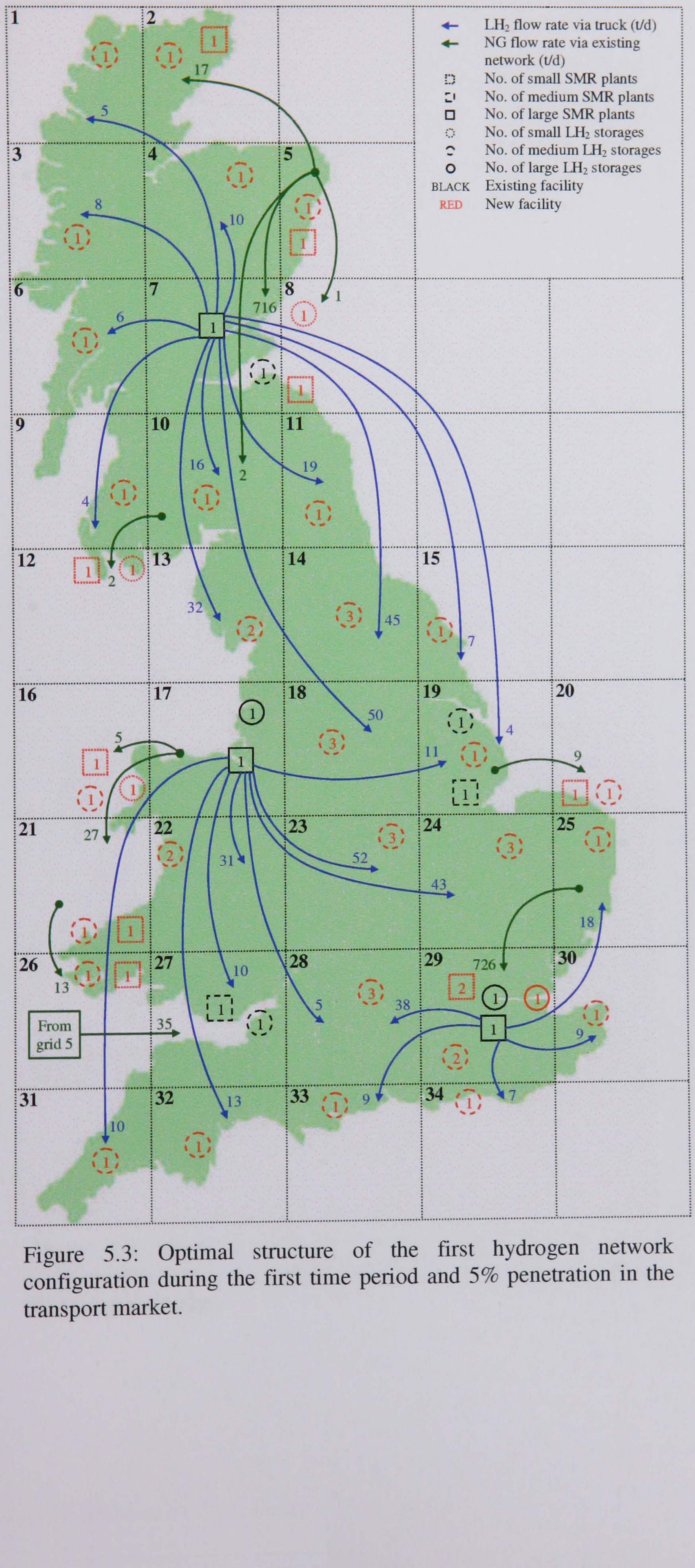


Figure 5.3: Optimal structure of the first hydrogen network configuration during the first time period and 5% penetration in the transport market.

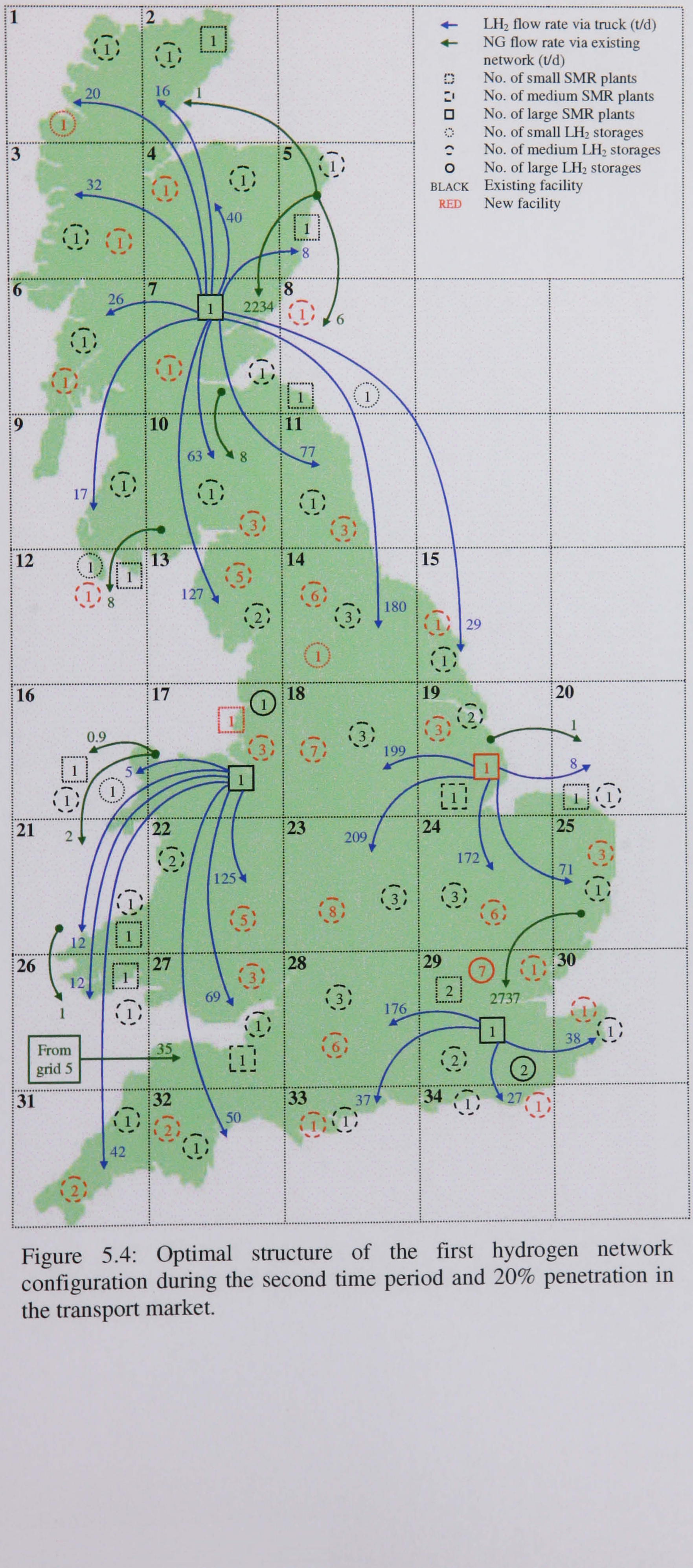


Figure 5.4: Optimal structure of the first hydrogen network configuration during the second time period and 20% penetration in the transport market.

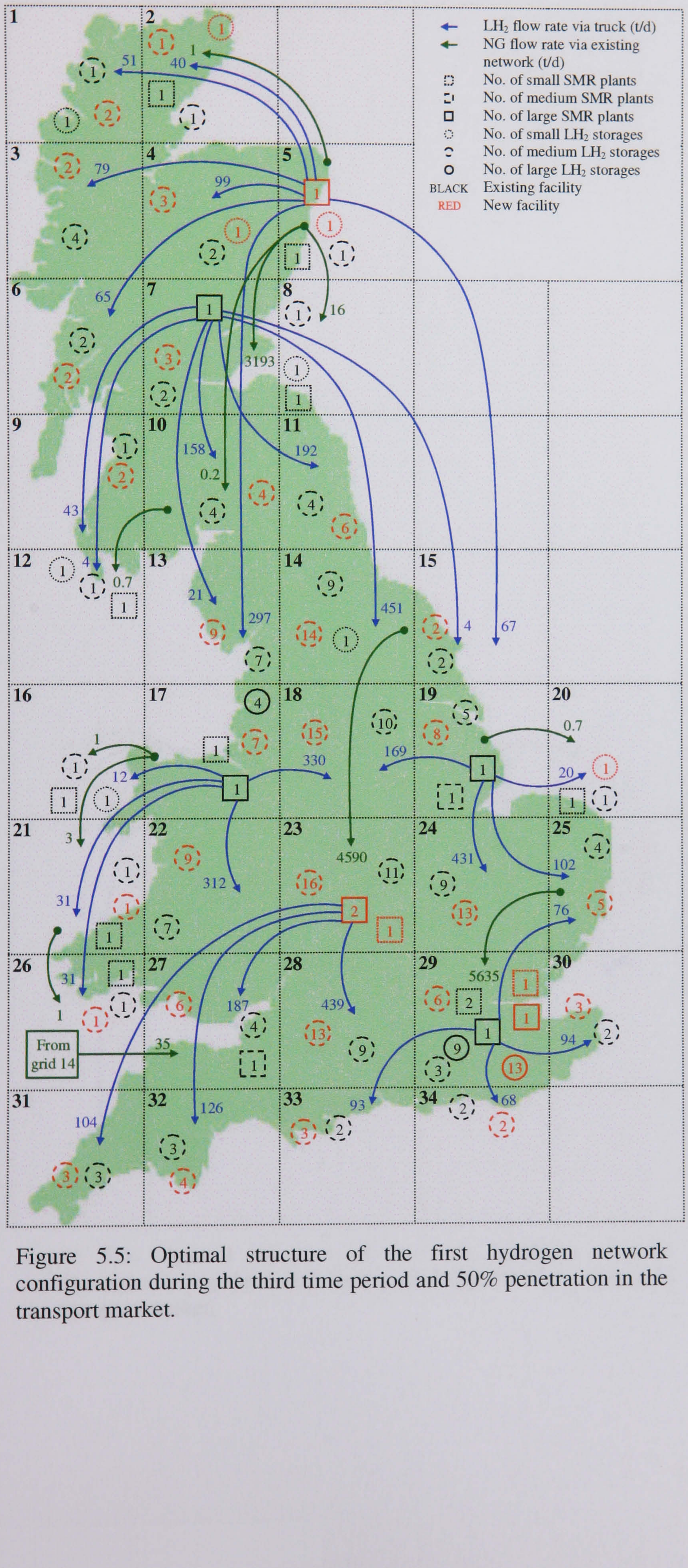


Figure 5.5: Optimal structure of the first hydrogen network configuration during the third time period and 50% penetration in the transport market.

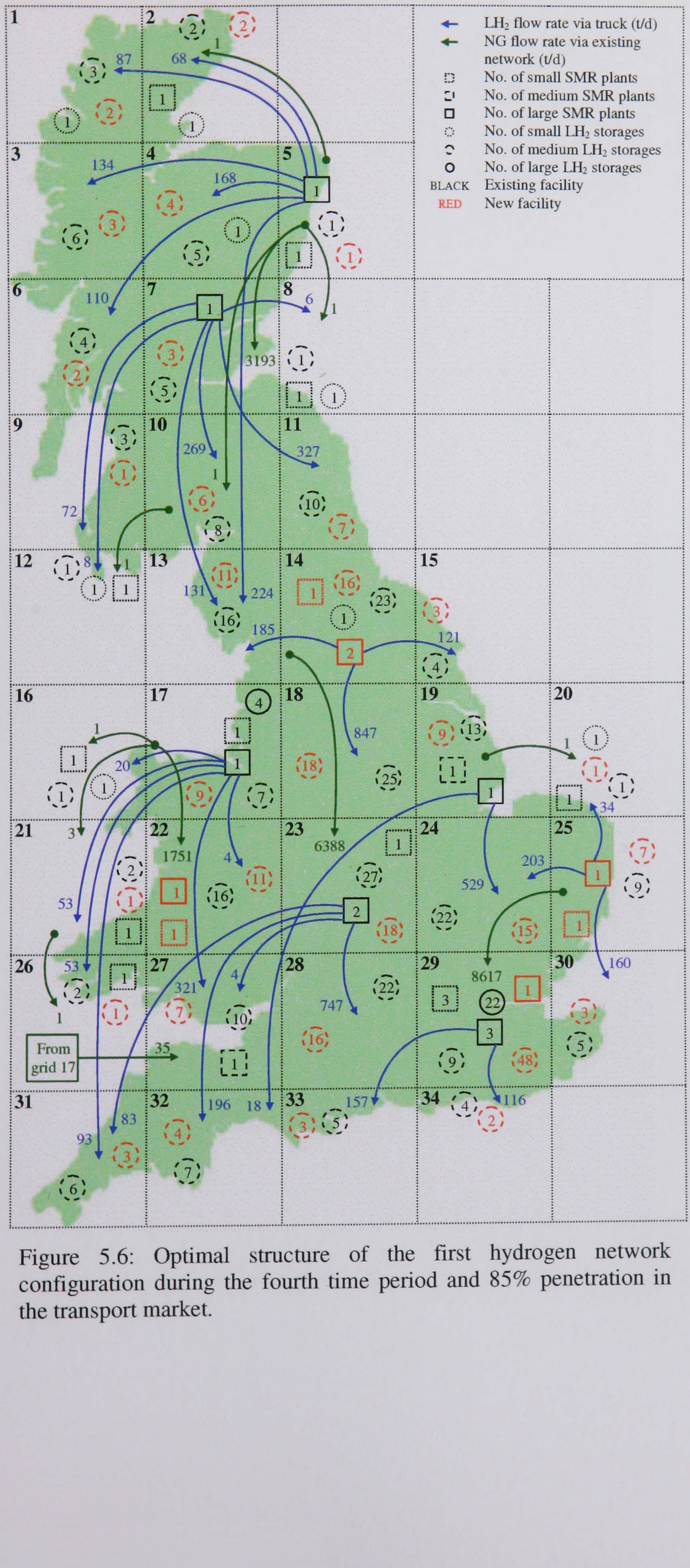


Figure 5.6: Optimal structure of the first hydrogen network configuration during the fourth time period and 85% penetration in the transport market.

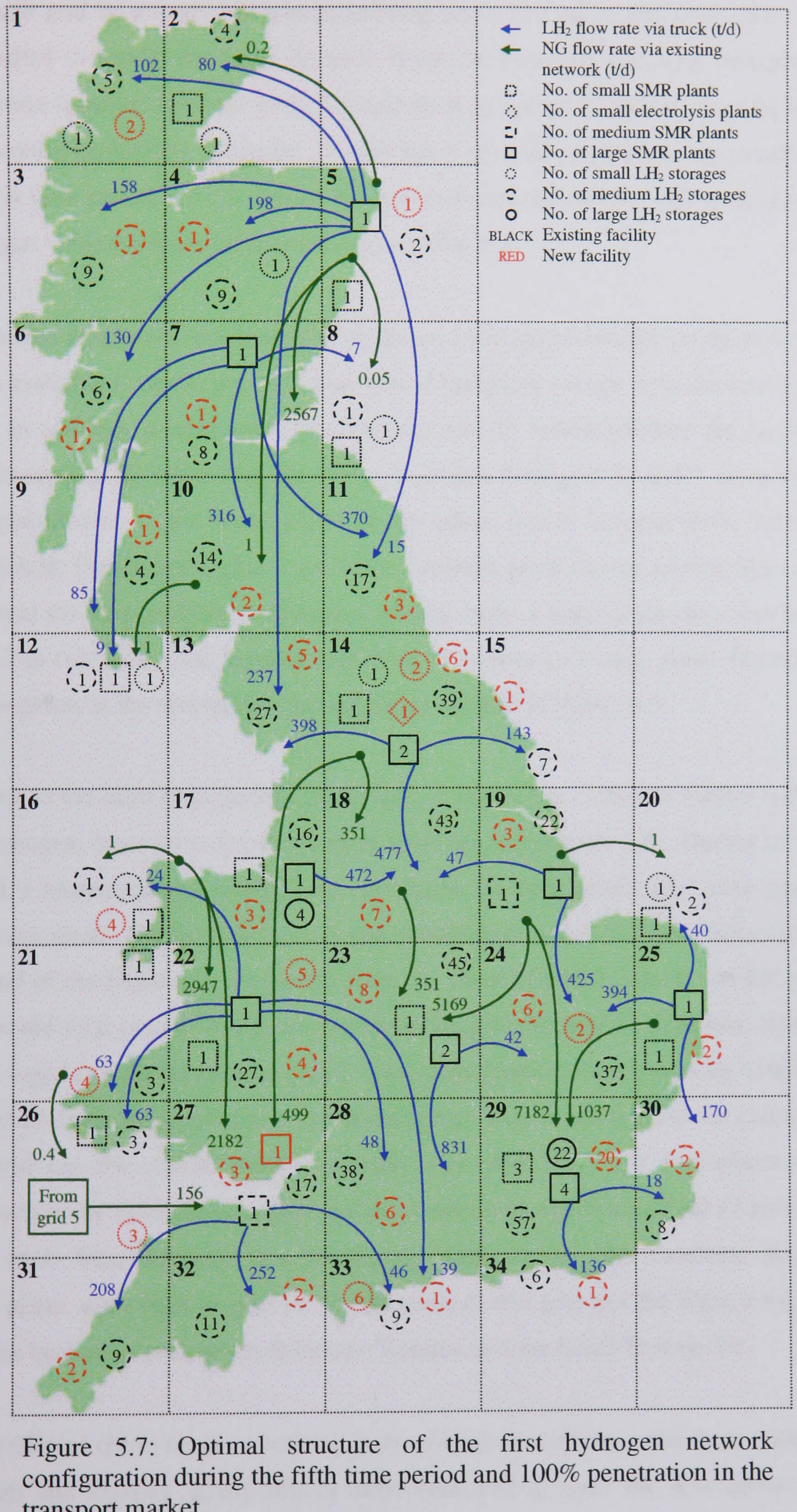


Figure 5.7: Optimal structure of the first hydrogen network configuration during the fifth time period and 100% penetration in the transport market.

Although grid 29 already has a large existing plant, two additional small plants were established to handle the huge demand. It can be observed that long transportation links were installed between grids because such an option is cheaper than building a new production facility. It can be realised that a centralised solution was obtained for the first time period. This is due to the low grid demand and the ability of obtaining hydrogen "over the fence" from existing oil refineries.

As demand progresses, reaching 20% at the second time period, the production rate of plants available from the previous time period increased to cope with the new demand level. In addition, a large plant was built in grid 19 which satisfies the demand of neighbouring grids rather than importing hydrogen from grid 17 and 7, as in the first time period. Due to the introduction of this plant, shorter transportation links were established. For instance, grid 7 no longer supplies grids 18 and 19, the links which exhibited the longest delivery distances. Furthermore, a small-scale plant was built in grid 17 to fulfil the local demand despite the existence of a large plant. The addition of new plants in the second time period can be viewed in Figure 5.4.

Moving to the third time period, where half of the current transport market is fuelled by hydrogen, leads to a denser network structure (see Figure 5.5). During this time period, a number of new plants were introduced. Of these plants, four were large and two were small. The first large plant was established in grid 5. This plant covers the demand of the Highlands instead of using the plant in grid 7, which was the case in the second time period. The plant also provides grids 13 and 15 with their hydrogen needs together with the plant in grid 7. Two large plants were additionally established in grid 23 since this grid covers the Birmingham area. According to our calculation, this grid has the second highest demand after grid 29. These two plants supply hydrogen to the South West region and the southern part of Wales. Grid 23 also fulfils some of its local demand via a small-scale plant. Finally, the remaining large and small plants were built in grid 29. As mentioned, this grid has the highest hydrogen demand because it encloses both Greater London and the South East region.

When 85% of the hydrogen economy is developed, it is obvious that more plants will be built and existing plants will be debottlenecked to meet the new demand (see Figure 5.6). The new plants were installed in grids with high demand and in close

proximity to an accessible source of natural gas. This can be shown in grids 14, 25, 22, and 29. The latter two grids have no natural gas; that is why they import natural gas from nearby grids, i.e. 17 and 25. It is interesting to observe that all the new plants were established in England and Wales. None of these plants were built in Scotland because the demand of this region was fully satisfied by the existing large and small plants. The establishment of three plants in grid 14 substitutes the long transportation links that used to provide hydrogen to the Northern part of England from Scotland. In addition, grid 29 stopped supplying grids 25 and 30 since the new large plant built in grid 25 covers its own demand and the demand of grid 30. Moreover, the flow rate of hydrogen between grids 17 and 22 decreased significantly due to the presence of new plants in grid 22.

During the fifth time period, all PLG vehicles and buses in Great Britain are assumed to be powered by hydrogen creating a fully saturated hydrogen economy. The network structure that describes such behaviour is shown in Figure 5.7. It is remarkable to note that the distribution network has changed drastically compared to the one for time period four. Most of these changes took place in England and Wales regions. The main reason behind this is the high population density and industrial activities that are present in these regions. In effect, one large-scale plant was being built in grid 27 which covers the demand of the South East region. Such an option is more economical than importing hydrogen from grids 17, 19, 23, and 29 which results in longer transportation links. Also, it turns out to be cheaper to build a small-scale plant in grid 14 instead of importing hydrogen from neighbouring grids. However, in this occasion an electrolysis small plant was built since it is more profitable than installing a stream reforming plant due to the abundance of electrical energy.

From the examined five network structures, it can be inferred that hydrogen demand at an early stage will be supplied mainly by: (1) distributed, small-scale plants installed at local fuelling stations, and (2) from existing production facilities with uncommitted capacity. The obtained strategies are analogous with the one suggested by several research institutes and energy professionals [46, 47]. As time progresses and more fuel cell vehicles are deployed, centralised hydrogen production via large-scale plants will be introduced gradually especially in areas with high population

density and industrial activities. At 100% hydrogen economy, a combination of small and large plants will be utilised to meet the daily demand of hydrogen fuel.

Almost all production plants established in Figures 5.3–5.7 utilised steam reforming of natural gas as a means of producing hydrogen. This method is currently the cheapest hydrogen production technology and the most practised worldwide. Apart from steam methane reforming plants, grid 14 shows an exception where electrolysis technology was used due to the availability of a plentiful source of electricity. Despite the high cost of an electrolysis plant, such an option seems to be more profitable than importing natural gas from overseas or nearby girds.

In exactly the same way as the production plants, a number of storage facilities are assumed at the introductory phase of hydrogen in order to replenish customers with their hydrogen needs. These storage facilities were located in the vicinity of the existing production plants (see Figure 5.3). As the network evolves from one time period to the next, new sizes of cryogenic tanks will be established. The size of these tanks will be tailored in accordance to the grid demand. It is evident that a grid with high demand will have the highest number of storage facilities.

Examining the distribution network of natural gas in Figures 5.3–5.7 depicts that steam reforming plants were built in grids abundant with natural gas or near grids with a natural gas terminal. The natural gas terminals were assumed to exist in grids 5, 14, 17, 19, and 25 [117]. The distribution of natural gas from these terminals was assumed to take place via the current national natural gas transmission system. Taking grid 7 as an example, it can be seen that this grid imports a large amount of natural gas from nearby grid 5 in order to operate the existing large-scale plant. A similar phenomenon occurs in grid 29, which is being supplied by grid 25. In grid 17, however, the plant was built in the vicinity of the natural gas platform eliminating the cost associated with importing natural gas.

The figures also show that the small plant established in grid 26 imports its feedstock from grid 17 through a two stage process. The first stage provides the plant in grid 21 with its natural gas needs and then, in the second step, the remaining amount of natural gas is transported to grid 26. Based on the delivery distances calculated in this

study, the two-stage process results in a shorter distance compared to importing natural gas directly from grid 17. Such logistics are also practical in today's industry since it is cheaper than carrying out two individual distribution pathways. Viewing the amount of natural gas transported between grids 17 and 21 indicates that a small fraction of natural gas is kept in grid 21 as a safety stock against uncertainties. In addition, one can observe from Figures 5.3, 5.4 and 5.7 that grid 27 imports natural gas from grid 5, where plenty of natural gas is locally available. Due to the fact that the model looks over the whole planning horizon, this option seems to be more profitable during the first, second and fifth time periods despite the availability of nearby natural gas resources. Also, the widespread natural gas transmission infrastructure in the UK makes such delivery sensible in practice. However, during the third and fourth time periods it becomes more economical for grid 27 to import natural gas from grids 14 and 17.

So far, the main focus of the discussion was on examining the network structure obtained from using trucks as the only means of hydrogen transport. The second network structure of interest studies the effects of utilising both trucks and rail on the arrangement of production plants and transportation links. The resulting network structures during the five time periods of the planning horizon are shown in Figures 5.8–5.12, respectively.

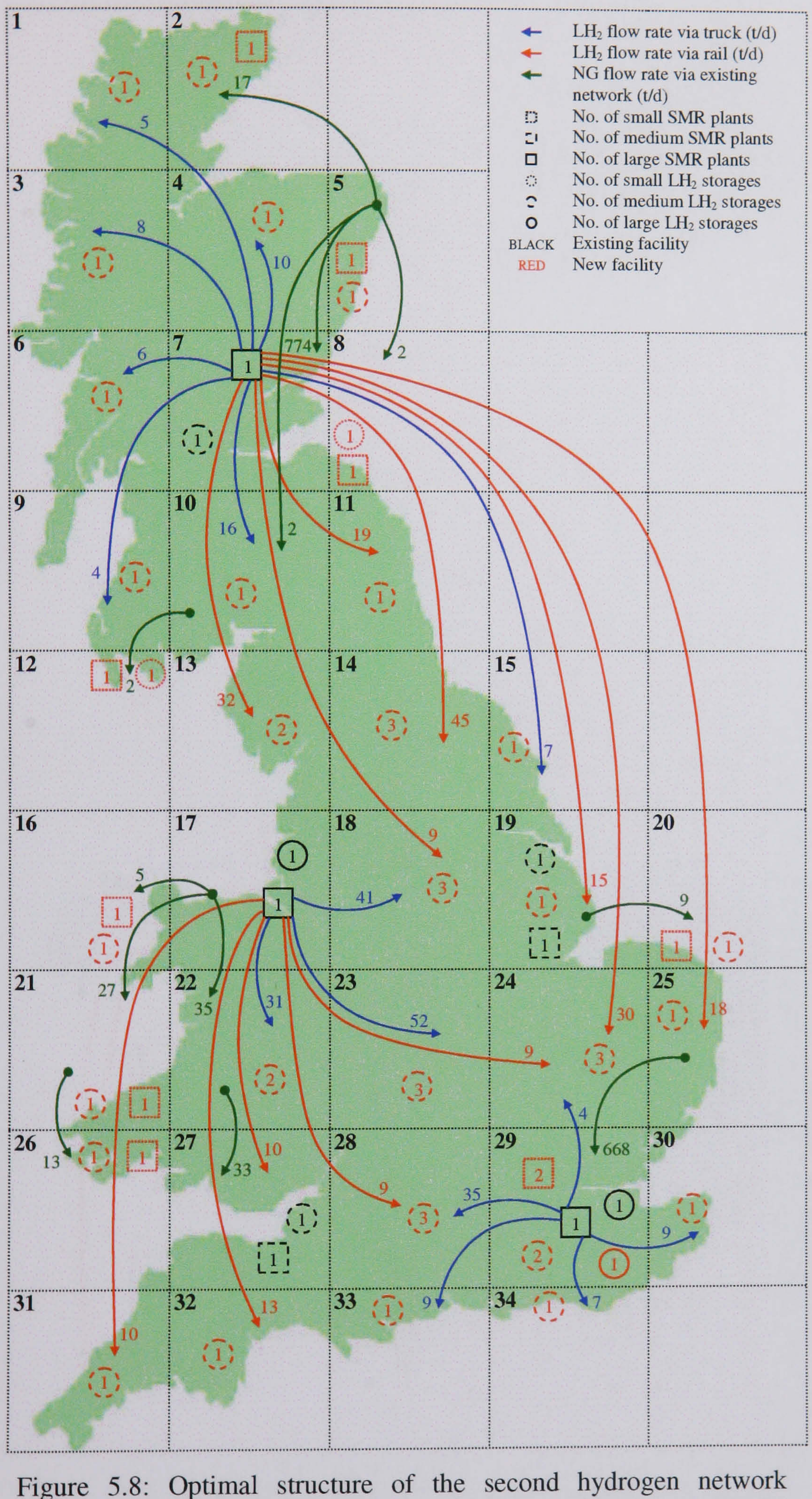


Figure 5.8: Optimal structure of the second hydrogen network configuration during the first time period and 5% penetration in the transport market.

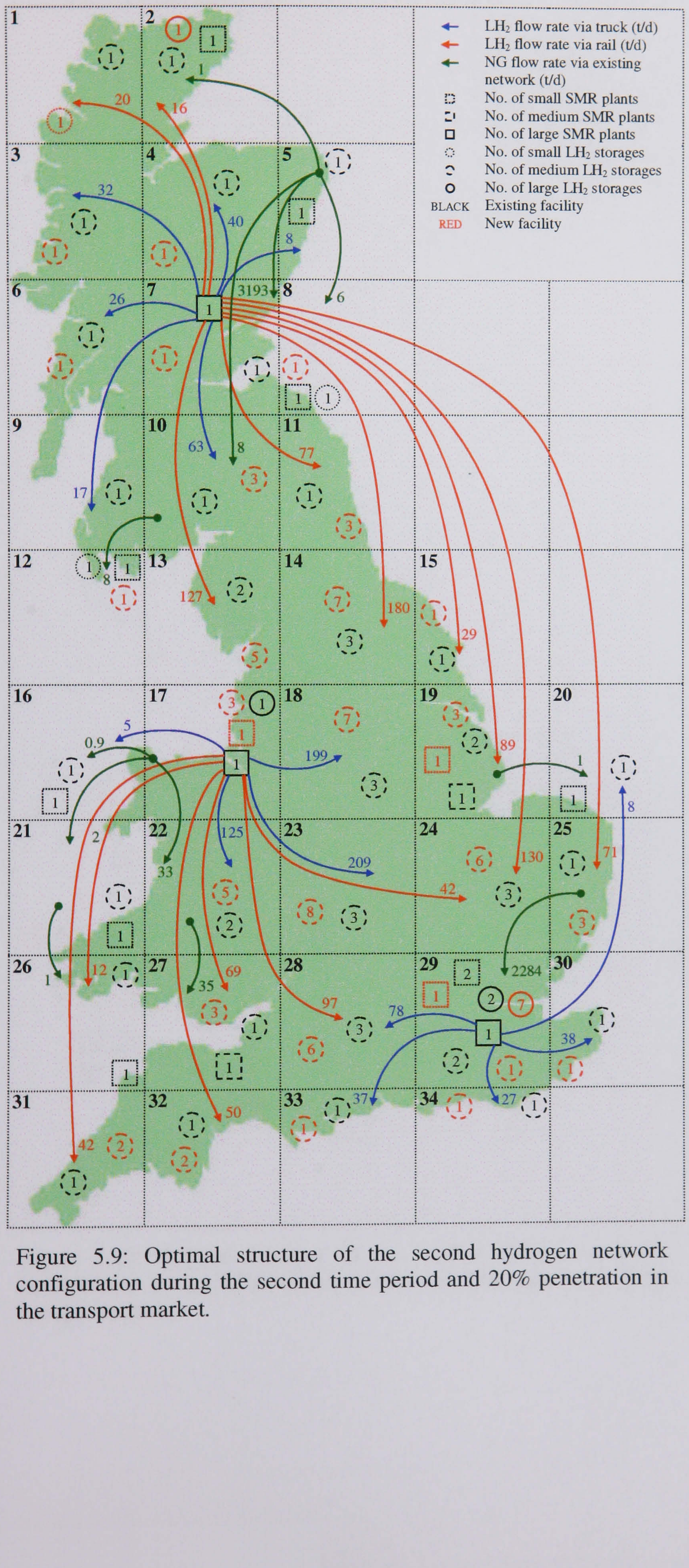


Figure 5.9: Optimal structure of the second hydrogen network configuration during the second time period and 20% penetration in the transport market.

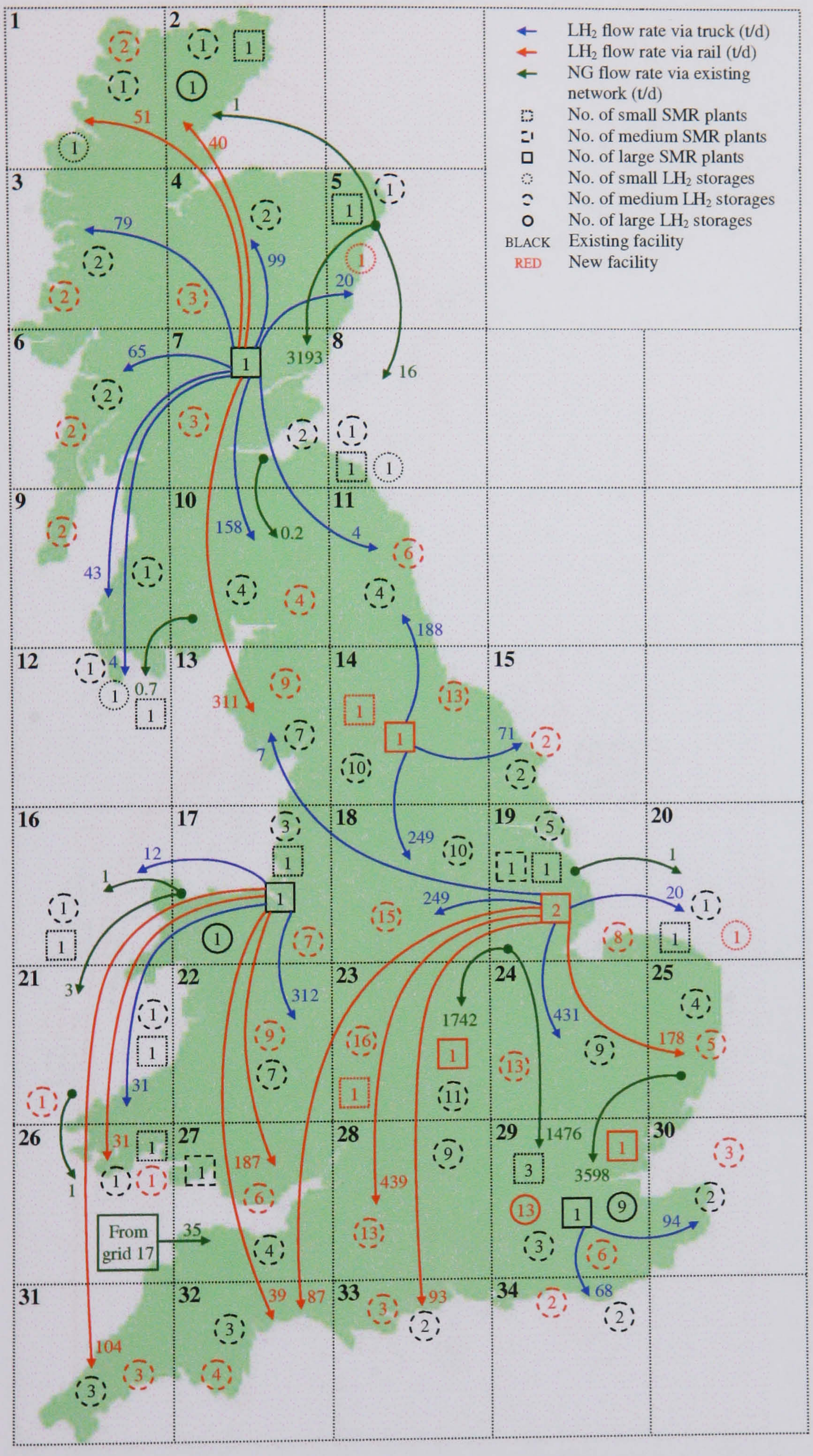


Figure 5.10: Optimal structure of the second hydrogen network configuration during the third time period and 50% penetration in the transport market.

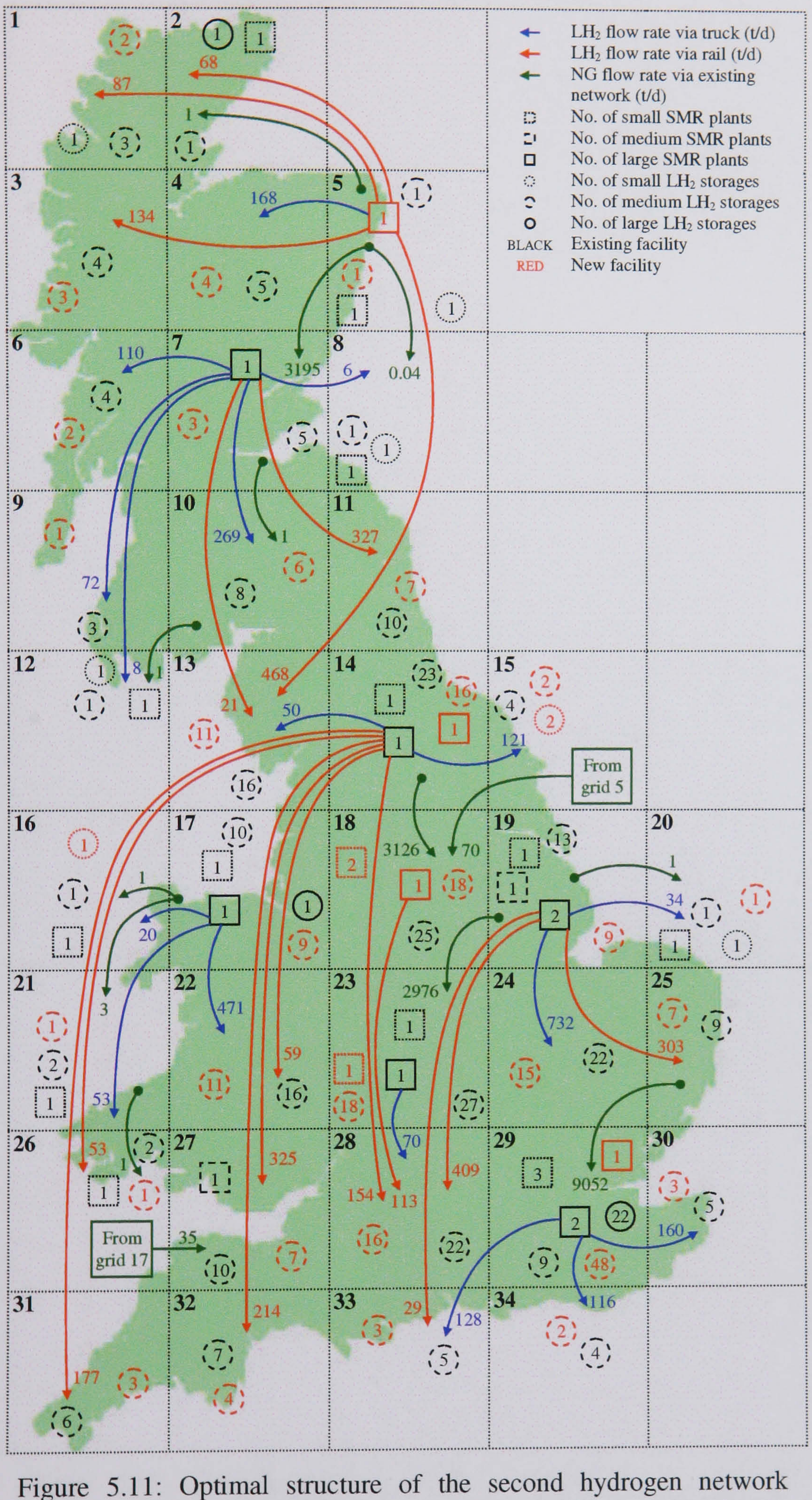


Figure 5.11: Optimal structure of the second hydrogen network configuration during the fourth time period and 85% penetration in the transport market.

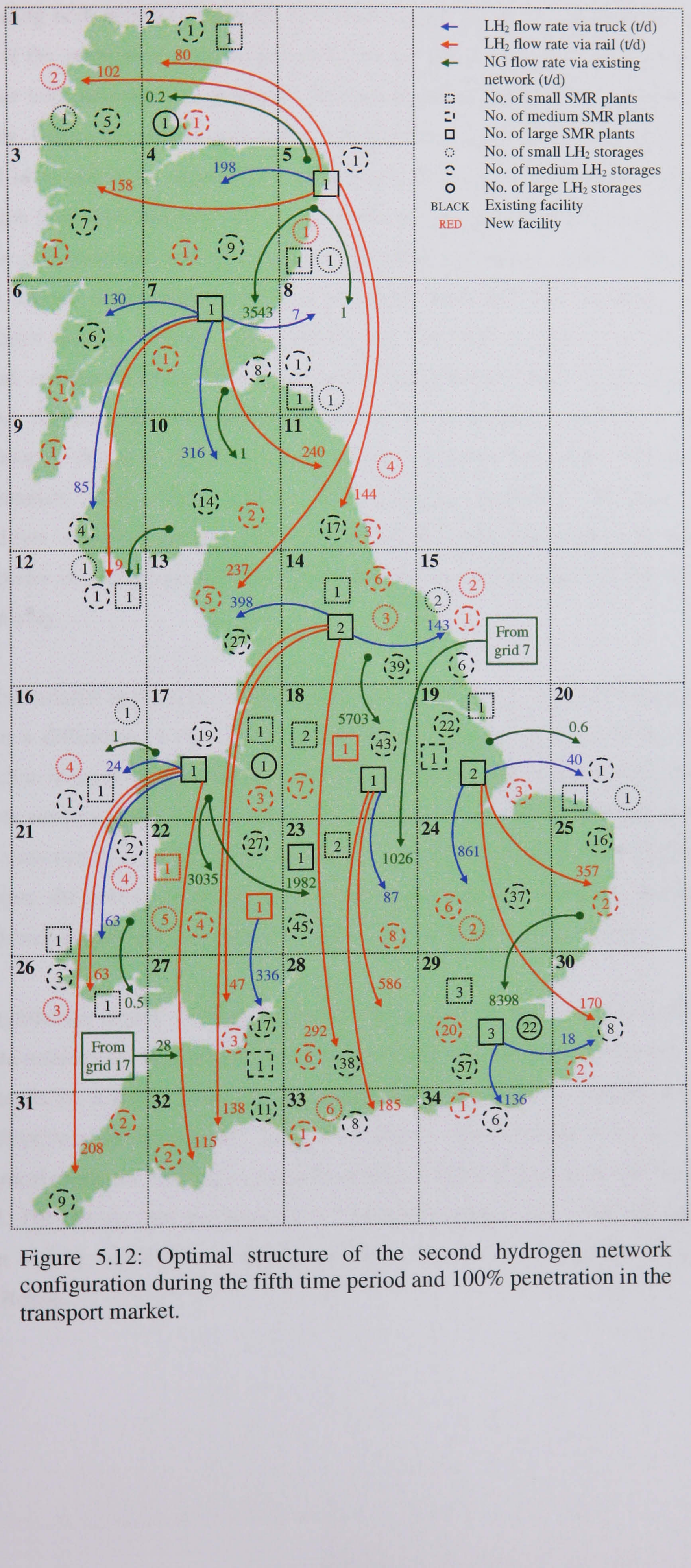


Figure 5.12: Optimal structure of the second hydrogen network configuration during the fifth time period and 100% penetration in the transport market.

Comparing both network structures, it is evident that there are major differences in terms of the position of production plants and transportation links. To illustrate this, consider both network configurations for the second and fourth time periods as an example. During the second time period of the first configuration, a large plant is built in grid 19 to satisfy the demand of nearby grids. This option is better than importing hydrogen from grids far away, as the case in the second network configuration. Due to the low cost associated with rail transport, importing hydrogen to grids 19, 24, and 25 in the second configuration seems to be more profitable than installing a new production facility. Instead, only a small plant was built in grid 19 to meet local demand. Another difference between network configurations 1 and 2 is the decision to use rail for long delivery distances because of economical benefits. A similar behaviour is shown in the fourth time period. It is clear from both networks that configuration 1 has a higher number of large plants established. The main reason behind this is the high cost of truck transport. On the other hand, there is no need for extra plants in configuration 2 in order to minimise the distribution costs due to cheap rail delivery.

The dissimilarity in plant locations between the examined networks will consequently lead to a difference in the distribution network of natural gas. The most obvious distinction is the flow rate of natural gas between grids 5 and 27, as shown in the first network structure. This transport link was eliminated in the second configuration due to the presence of a lower number of production plants in Wales and South England. Therefore, the amount of natural gas available in this region is sufficient for all plants established; hence there is no need for importation of natural gas from grid 5.

To describe the degree of centralisation in both networks, the overall percentage of demand satisfied by local production facilities during each time period was calculated. The results are listed in Table 5.5. As appears in the table, there is a higher degree of centralisation at the introductory phase of hydrogen. The percentage starts to increase as demand increases leading to a higher degree of decentralisation at the final time period. This means that the demand of hydrogen during a fully saturated transport market will be supplied by a number of production facilities dispersed throughout Great Britain.

Table 5.5: Overall percentage of demand met by local production plants

Configuration	Time period, t				
	t_1	t_2	t_3	t_4	t_5
1	31	30	37	51	54
2	31	26	44	51	55

The values of the cost terms that constitute the objective function of the first and second network configurations are summarised in Tables 5.6 and 5.7, respectively. These cost values are given for each time period. The table also shows the total daily cost of the network at each time period as well as the average daily cost of the network for the entire planning horizon.

Table 5.6: Itemisation of cost for the first configuration of the multi-period model

Cost element	Time period, t				
	t_1	t_2	t_3	t_4	t_5
Capital cost					
Plants and storage facilities	2×10^9	4×10^9	10×10^9	11×10^9	3×10^9
Local transportation	7×10^6	19×10^6	47×10^6	115×10^6	141×10^6
Regional transportation	29×10^6	101×10^6	226×10^6	278×10^6	286×10^6
Total capital cost ($)	2×10^9	4×10^9	10×10^9	11×10^9	4×10^9
Operating cost					
Plants and storage facilities	1×10^6	4×10^6	10×10^6	17×10^6	20×10^6
Transportation modes					
Local fuel cost	2×10^3	5×10^3	13×10^3	31×10^3	39×10^3
Local labour cost	5×10^3	13×10^3	33×10^3	79×10^3	98×10^3
Local maintenance cost	357	1×10^3	3×10^3	6×10^3	7×10^3
Local general cost	111	319	779	2×10^3	2×10^3
Regional fuel cost	21×10^3	67×10^3	152×10^3	183×10^3	182×10^3
Regional labour cost	24×10^3	83×10^3	187×10^3	230×10^3	237×10^3
Regional maintenance cost	4×10^3	14×10^3	33×10^3	39×10^3	39×10^3
Regional general cost	483	2×10^3	4×10^3	5×10^3	5×10^3
Primary energy source cost	31×10^3	96×10^3	302×10^3	439×10^3	530×10^3
Total operating cost ($/d)	1×10^6	4×10^6	11×10^6	18×10^6	22×10^6
Total network cost ($/d)	*3×10^6*	*8×10^6*	*20×10^6*	*29×10^6*	*25×10^6*
Network average cost ($/d)	*16.98×10^6*				

Table 5.7: Itemisation of cost for the second configuration of the multi-period model

Cost element	Time period, t				
	t_1	t_2	t_3	t_4	t_5
Capital cost					
Plants and storage facilities	2×10^9	3×10^9	10×10^9	10×10^9	4×10^9
Local transportation	7×10^6	14×10^6	62×10^6	101×10^6	130×10^6
Regional transportation	37×10^6	164×10^6	253×10^6	431×10^6	448×10^6
Total capital cost ($)	2×10^9	4×10^9	11×10^9	10×10^9	5×10^9
Operating cost					
Plants and storage facilities	1×10^6	4×10^6	10×10^6	17×10^6	20×10^6
Transportation modes					
Local fuel cost	2×10^3	4×10^3	17×10^3	27×10^3	36×10^3
Local labour cost	5×10^3	10×10^3	42×10^3	69×10^3	90×10^3
Local maintenance cost	355	741	3×10^3	5×10^3	7×10^3
Local general cost	111	232	1×10^3	2×10^3	2×10^3

Table 5.7 (*Continued*)

Cost element	Time period, t				
	t_1	t_2	t_3	t_4	t_5
Regional fuel cost	8×10^3	29×10^3	58×10^3	69×10^3	75×10^3
Regional labour cost	23×10^3	101×10^3	164×10^3	265×10^3	277×10^3
Regional maintenance cost	2×10^3	10×10^3	16×10^3	24×10^3	25×10^3
Regional general cost	538	2×10^3	4×10^3	6×10^3	6×10^3
Primary energy source cost	28×10^3	100×10^3	205×10^3	348×10^3	458×10^3
Total operating cost (\$/d)	1×10^6	4×10^6	11×10^6	18×10^6	21×10^6
Total network cost (\$/d)	3×10^6	8×10^6	21×10^6	28×10^6	26×10^6
Network average cost (\$/d)	16.93×10^6				

It can be seen from Tables 5.6 and 5.7 that the average daily cost of the multi-mode network is slightly cheaper than the single-mode one. As emphasised in the previous chapter, the main reason behind this is the low operating cost associated with rail delivery. Despite the minimal cost of the multi-mode network, it is believed that truck transport is more reasonable due to operational flexibility.

The MILP model used to outline the two examined network configurations was modelled by GAMS and solved using the CPLEX v9.0 code on a Pentium 4, 1.8 GHz Dell machine. The computational statistics for both networks as well as a summary of the results are given in Table 5.8. The table shows that the solution time is fixed at three days in order to find the optimal structure of the hydrogen configurations. This is because time can be compromised in designing such a large supply chain network. In addition, the resulting optimality gap for this size of problem looks very satisfactory.

Table 5.8: Summary of computational results for the multi-period model

Configuration no.	1	2
Number of constraints	43471	71521
Number of integer variables	14280	19890
Number of continuous variables	36671	42281
Optimality gap (%)	0.78	0.76
CPU time (d)	3	3

5.4.3 Concluding Remarks

The model developed within this chapter was used to capture the demand evolution of hydrogen over a 34 years planning horizon. The transition from one time period to the next was described by a pre-defined demand profile. This profile is a function of

hydrogen fuel cell vehicle penetration in the current transport market. During each time period of the planning horizon, the model was capable of predicting the investment required to establish the future hydrogen supply chain network. The model was also able to reveal the network configuration through a number of strategic decisions. These decisions include:

- Number, location, capacity, and type of production and storage facilities,
- Production rate of plants and average inventory in storage facilities,
- Flow rate and type of transportation links, and
- Utilisation rate of primary energy sources in each grid and their distribution throughout the network.

The above decisions were determined by formulating the model as an MILP problem.

To examine the applicability of the derived model, two different hydrogen network configurations were designed. The networks of interest incorporated the same types and sizes of production and storage facilities. However, the main difference emerged in the type of transport mode to be used. The solution obtained from of these networks illustrates that hydrogen will be supplied during the introductory phase from distributed plants at local fuelling stations as well as from the existing chemical plants. As more fuel cell vehicles penetrate the marketplace, the hydrogen demand increases gradually leading to a new investment in production and storage facilities. When most vehicles become powered by hydrogen, the vast demand of hydrogen will be met by both small- and large-scale plants, according to demand density. These plants would utilise steam methane reforming to generate hydrogen, which will be distributed via trucks and/or rail.

The solution of the proposed model gives a good indication of having a model that takes into account the evolution of hydrogen supply chain over a long-term planning horizon. Such realisation was deduced from the minute optimality gap and the reasonable solution time.

All of the designed hydrogen supply chains involved two echelons: production plants and storage facilities. The following chapter considers the design and operation of a multi-echelon hydrogen supply chain by adding fuelling stations.

Chapter 6

Extension to the Multi-Echelon Case

6.1 Problem Description

So far, the three models developed earlier address the design and operation of a two-echelon hydrogen supply chain. These echelons are: production plants and storage facilities linked together by transportation modes. Such models focused primarily on activities involved at the "upstream" level of the hydrogen supply chain, without concentrating on the activities downstream. The latter aspect is important since it ensures a complete design of the hydrogen supply chain network, starting from production plants and ending with fuelling stations. This chapter explores the concept of incorporating fuelling stations into the previous models. It also investigates the distribution pattern of hydrogen from the production plants or storage facilities to these fuelling stations. This is defined as "secondary distribution" compared with "primary distribution", which takes place between production and storage facilities only.

The addition of a new echelon to previous models will not affect the design decisions made for the upstream level. However, new decisions will be revealed. These decisions include the determination of the total number of fuelling stations required to be installed in a particular grid, as well as the cost associated with operating these fuelling stations. Another decision is estimating the investment needed for the secondary distribution of hydrogen within a grid. The determination of the number of fuelling stations will take place in response to the total equivalent demand of the grid. The establishment of secondary distribution links will be driven by the total equivalent demand, and the total number of production plants and storage facilities. As with previous models, the design of this network is formulated as an MILP problem. Again, the network is implemented within a Great Britain context.

6.2 Model Structure and Components

The multi-echelon model derived in this study comprises six nodes. These nodes are:

1. Primary energy sources,
2. Plants with different production sizes and technologies,
3. Storage facilities with different sizes and technologies,
4. Primary transportation modes connecting the above technologies together,
5. Fuelling stations, and
6. Secondary transportation modes connecting plants or storage facilities with fuelling stations.

Within the model, there are grids enclosing different hydrogen production and storage technologies as well as fuelling stations. The grids containing production technologies utilise various primary energy sources to produce different forms of hydrogen. The generated hydrogen will be transported to the different types and sizes of storage facilities via primary transportation modes. The hydrogen could also be transported directly to fuelling stations via secondary transportation modes, if these fuelling stations are in the vicinity of the production sites. The grids containing only storage facilities will make use of the surrounding fuelling stations to dispense the products to customers. In addition, grids containing distributed production plants will have no fuelling stations since the product will be generated on-site and will be dispensed directly to customers. However, fuelling stations will be "built" by petroleum-based ones being retrofitted if distributed plants do not satisfy the demand of the grid. This is due to the import of product from neighbouring grids in order to satisfy the corresponding demand deficiency.

As discussed above, the components that form the multi-echelon model are identical to that of the multi-period model. The only difference is the existence of fuelling stations and secondary transportation modes. Only these two components will be detailed below.

6.2.1 Fuelling Stations

The most important factors in the installation of fuelling stations is characterising the required demand and the form of product to dispense. These two factors will determine the size and type of fuelling stations. Since we assume that all grids encounter a finite deterministic demand, the establishment of fuelling stations is imperative to replenish consumers with their needs. Each type of fuelling station will have a fixed capacity as well as capital and operating costs. The fuelling decision includes the determination of the number of fuelling stations required to be installed in each grid.

6.2.2 Secondary Transportation Modes

The establishment of secondary transportation modes will take place between production plants or storage facilities and fuelling stations. Such establishment will happen in all grids due to the presence of production plants and/or storage facilities. The secondary transportation modes will have exactly the same characteristics as the primary transportation modes in terms of capacity, maximum/minimum flow rate, and capital and operating costs. They will also be represented by the same index l.

6.3 Model Formulation

The following subsections concentrate only on the addition of fuelling stations and secondary distribution, instead of repeating all of the mathematical details derived for the multi-period model.

6.3.1 Nomenclature

Index

n counter that determines total number of plants and storage facilities in a particular grid

Parameters

$FCap_i$ capacity of fuelling station for product form i (kg/d)

UFC_i unit fuelling cost of product form i ($/kg)

Integer Variables

NS_{gt}^{T} total number of storage facilities in grid g during time period t

NFS_{igt} number of fuelling stations dispensing product form i in grid g during time period t

Binary Variable

W_{ngt} 1 if there are $n-1$ plants and storage facilities in grid g during time period t, 0 otherwise

6.3.2 Constraints

Fuelling Constraints

The number of fuelling stations within a particular grid and time period depends on the total equivalent demand and the installed capacity of the fuelling stations, as follows:

$$NFS_{igt} = \frac{D^T_{igt}}{FCap_i} - \sum_p NP_{pjigt} \qquad \forall i, g, t : j = \text{small plants} \tag{6.1}$$

The second term of the right-hand-side of Equation 6.1 is brought in to account for the establishment of distributed plants with on-site production; otherwise the term will be taken as zero.

Non-negativity Constraints

The number of fuelling stations and the total number of storage facilities must be positive:

$$NS^T_{gt} \geq 0 \quad \forall g, t \tag{6.2}$$

$$NFS_{igt} \geq 0 \quad \forall i, g, t \tag{6.3}$$

6.3.3 Objective Function

The operating costs of fuelling stations and secondary distribution costs will be addressed below. The other cost terms have been discussed earlier in previous chapters and will be given here without further discussion.

Facility Capital Cost

There will be no capital cost associated with the establishment of fuelling stations. This is due to the assumption that current petrol stations will be converted to hydrogen stations. The conversion costs of these stations are assumed to be negligible. Therefore, the facility capital cost equation will remain the same:

$$FCC = \sum_{j,i,g,t} \left(\frac{1}{LR} \left(\sum_p PCC_{pji} IP_{pjigt} + \sum_s SCC_{sji} IS_{sjigt} \right) \right) \tag{6.4}$$

Transportation Capital Cost

The capital and operating transportation costs are divided into primary and secondary costs. All primary distribution cost terms are identical to those given in previous chapters. The secondary distribution cost terms, however, will be discussed in greater detail.

Since both local primary and secondary transportation costs take place within the boundary of a particular grid, the method used to estimate these costs is, to a certain extent, similar. The main difference is the method used to determine the average journey length. In approximating the local transportation cost, the average journey length was obtained by dividing the local delivery distance (L_g^L) by the total number of production plants. However, for secondary transportation, the average journey length is obtained by dividing L_g^L by the total number of production plants and storage facilities. This is due to the fact that a fuelling station could be supplied by nearby production plants as well as neighbouring storage facilities. Another difference is that the total equivalent demand (D_{igt}^T) should be used in estimating the cost functions rather than the local demand (D_{igt}^L). Such a consideration turns out to avoid non-linearities.

In the same way as for local transportation, the total number of plants and storage facilities must be expressed in term of a new counter and binary variable to avoid non-linearity in the cost functions:

$$NP_{gt}^T + NS_{gt}^T = \sum_n (n-1)W_{ngt} \qquad \forall g,t \tag{6.5}$$

The variables NP_{gt}^T and NS_{gt}^T are defined respectively as follows:

$$NP_{gt}^T = \sum_{p,j,i} NP_{pjigt} \qquad \forall g,t \tag{6.6}$$

$$NS_{gt}^{T} = \sum_{s,j,i} NS_{sjigt} \quad \forall g,t \tag{6.7}$$

The binary variable (W_{ngt}) in Equation 6.5 was introduced to determine if there are $n-1$ plants and storage facilities established in grid g and time period t (n = 1, ..., $NP^{max}+NS^{max}+1$). Again, one is subtracted from n to ensure that some grids can have no production plants.

The following constraint must be written to make sure that only one combination of the binary variables will have a value of one:

$$\sum_{n} W_{ngt} = 1 \quad \forall g,t \tag{6.8}$$

Therefore, the transportation capital cost for both primary and secondary distribution is given by the following relationship:

$$\begin{aligned} TCC = & \sum_{i,l,m,g,t} \frac{DM_{mgt}^{L} TMC_{il}}{(m-1)TMA_{l}^{L} TCap_{il}} \left(\frac{2L_{g}^{L}}{SP_{l}^{L}} + LUT_{l} \right) \\ & + \sum_{i,l,g,g',t} \frac{Q_{ilgg't}}{TMA_{l}^{R} TCap_{il}} \left(\frac{2L_{gg'}^{R}}{SP_{l}^{R}} + LUT_{l} \right) \\ & + \sum_{i,l,n,g,t} \frac{D_{igt}^{T} W_{ngt}}{(n-1)TMA_{l}^{L} TCap_{il}} \left(\frac{2L_{g}^{L}}{SP_{l}^{L}} + LUT_{l} \right) \end{aligned} \tag{6.9}$$

The first and second terms of the right-hand-side of Equation 6.9 represent the local and regional primary transportation costs, respectively. The third term represents the secondary transportation cost. W_{ngt} is introduced in this term to include the total number of production plants and storage facilities established and to exclude all other combinations.

Facility Operating Cost

The operating cost of production plants and storage facilities remains the same. For fuelling stations, the operating cost is estimated by multiplying the unit fuelling cost by the number of fuelling stations established and their capacities. This is shown by the third term of the equation below:

$$FOC = \sum_{i,g,t}\left(\sum_{p,j} UPC_{pji} P_{pjigt} + \sum_{s,j} USC_{sji} S_{sjigt} + UFC_i NFS_{igt} FCap_i \right) \tag{6.10}$$

Transportation Operating Cost

The transportation operating costs associated with primary and secondary distribution consist of fuel, labour, maintenance, and general costs. In the subsequent five equations, the first part of the right-hand-side denotes the local transportation operating cost, the second part denotes the regional transportation operating cost, and the third part denotes the secondary transportation cost.

The daily fuel cost is:

$$\begin{aligned} FC = & \sum_{i,l,m,g,t} FP_l \left(\frac{2L_g^L D_{mgt}^L}{(m-1)FE_l^L TCap_{il}} \right) \\ & + \sum_{i,l,g,g',t} FP_l \left(\frac{2L_{gg'}^R Q_{ilgg't}}{FE_l^R TCap_{il}} \right) \\ & + \sum_{i,l,n,g,t} FP_l \left(\frac{2L_g^L D_{igt}^T W_{ngt}}{(n-1)FE_l^L TCap_{il}} \right) \end{aligned} \tag{6.11}$$

The daily labour cost is:

$$LC = \sum_{i,l,m,g,t} DW_l \left(\frac{D^L_{mgt}}{(m-1)TCap_{il}} \left(\frac{2L^L_g}{SP^L_l} + LUT_l \right) \right) + \sum_{i,l,g,g',t} DW_l \left(\frac{Q_{ilgg't}}{TCap_{il}} \left(\frac{2L^R_{gg'}}{SP^R_l} + LUT_l \right) \right) + \sum_{i,l,n,g,t} DW_l \left(\frac{D^T_{igt} W_{ngt}}{(n-1)TCap_{il}} \left(\frac{2L^L_g}{SP^L_l} + LUT_l \right) \right) \quad (6.12)$$

The maintenance cost is:

$$MC = \sum_{i,l,m,g,t} ME_l \left(\frac{2L^L_g D^L_{mgt}}{(m-1)TCap_{il}} \right) + \sum_{i,l,g,g',t} ME_l \left(\frac{2L^R_{gg'} Q_{ilgg't}}{TCap_{il}} \right) + \sum_{i,l,n,g,t} ME_l \left(\frac{2L^L_g D^T_{igt} W_{ngt}}{(n-1)TCap_{il}} \right) \quad (6.13)$$

The general cost is:

$$GC = \sum_{i,l,m,g,t} GE_l \left(\frac{D^L_{mgt}}{(m-1)TMA^L_l TCap_{il}} \left(\frac{2L^L_g}{SP^L_l} + LUT_l \right) \right) + \sum_{i,l,g,g',t} GE_l \left(\frac{Q_{ilgg't}}{TMA^R_l TCap_{il}} \left(\frac{2L^R_{gg'}}{SP^R_l} + LUT_l \right) \right) + \sum_{i,l,n,g,t} GE_l \left(\frac{D^T_{igt} W_{ngt}}{(n-1)TMA^L_l TCap_{il}} \left(\frac{2L^L_g}{SP^L_l} + LUT_l \right) \right) \quad (6.14)$$

Finally, the total transportation operating cost is equal to:

$$TOC = FC + LC + MC + GC \quad (6.15)$$

Primary Energy Source Cost

The cost of primary energy sources is exactly the same as in previous chapters:

$$ESC = \sum_{e,g,t} UIC_e I_{egt} + \sum_{e,g,g',t} UDC_e L^R_{gg'} QE_{egg't} \tag{6.16}$$

6.3.4 Model Summary

By combining the cost terms derived in Section 6.3.3, the average total daily cost of the hydrogen supply chain network is minimised by the optimisation:

$$\min \ TDC^{ave} \tag{6.17}$$

where:

$$TDC^{ave} = \frac{1}{NTP}\left(\frac{FCC + TCC}{\alpha\, CCF} + FOC + TOC + ESC\right) \tag{6.18}$$

The above minimisation is subject to all the constraints presented in Section 6.3.2 of this chapter and Section 5.3.2 of Chapter 5.

6.4 Case Study Revisited

The mathematical formulation presented in this chapter is applied to a case study similar to the one presented in Chapter 5. However, this chapter additionally allows for secondary distribution of hydrogen and determination of the number of fuelling stations.

6.4.1 Input Data

The model data concerning primary energy sources, production plants, storage facilities, and primary transportation modes has already been presented in Sections 4.4.1 and 5.4.1. In this section, only additional data will be presented.

Fuelling Stations

The hydrogen fuelling station considered in this study is designed based on the average size of typical current petrol stations. The typical size of today's petrol stations ranges from 100,000 to 250,000 gallons per month [81]. For the purpose of this analysis, liquid hydrogen based fuelling stations will have a capacity of 5,000 kg/d and a utilisation rate of 90%. Since this study assumes the conversion of the current petrol fuelling stations to hydrogen, no significant capital investment will be required. However, there will be an operating cost which was estimated to be 0.39 $/kg. Appendix C shows the calculations used to estimate this unit cost.

Secondary Transportation Modes

Since secondary distribution resembles the local primary distribution, the same parameters were used to determine the capital and operating costs. The values of these parameters are shown in Table 4.6.

6.4.2 Results and Discussion

As has been mentioned throughout this chapter, the model presented was constrained to determine the number of fuelling stations required to replenish customers with hydrogen and the total costs of introducing these fuelling stations. The costs would include the operating cost of the fuelling stations as well as the capital and operating costs of secondary distribution. Since the model of interest is a continuation of the one given in Chapter 5 with the exception of some modifications, the optimal structures of

the first and second network configurations did not change drastically. As a result, these network structures will not be shown here. What will be shown is the number of fuelling stations in each grid and time period. Even though the demand value in each grid and time period is the same for both networks, the number of fuelling stations is different. This is due to the difference in the number of distributed, on-site production plants that were established. Table 6.1 lists the number of fuelling stations for network configurations 1 and 2, without adding the number of distributed plants to the presented values. The number of these plants is, however, given separately in Table 6.2 for both configurations. Only the newly established plants will be shown in Table 6.2. Of course, these plants would also exist at the subsequent time periods yet they are not demonstrated in the table.

Table 6.1: Number of fuelling stations for network configurations 1 and 2

Grid, g	Configuration 1					Configuration 2				
	t_1	t_2	t_3	t_4	t_5	t_1	t_2	t_3	t_4	t_5
01	1	5	11	18	21	1	5	11	18	21
02	0	3	7	13	15	0	3	7	13	15
03	2	7	16	27	32	2	7	16	27	32
04	2	8	20	34	40	2	8	20	34	40
05	0	1	4	6	8	0	1	4	6	8
06	2	6	13	22	26	2	6	13	22	26
07	1	6	17	29	34	1	6	17	29	34
08	0	0	0	1	1	0	0	0	1	1
09	1	4	9	15	18	1	4	9	15	18
10	4	13	32	54	64	4	13	32	54	64
11	4	16	39	66	77	4	16	39	66	77
12	0	0	0	1	1	0	0	0	1	1
13	7	26	64	108	127	7	26	64	108	127
14	7	35	88	151	178	7	35	89	152	179
15	2	6	15	25	29	2	6	15	25	29
16	0	0	2	4	4	0	0	2	4	4
17	3	18	47	82	96	3	18	47	82	96
18	10	40	100	168	198	10	38	98	167	197
19	4	19	49	84	99	5	19	49	84	99
20	0	1	4	6	8	0	1	4	6	8
21	0	2	6	10	12	0	2	6	10	12
22	7	23	61	105	123	7	24	61	105	123
23	8	39	102	175	206	11	42	105	178	208
24	9	35	87	147	173	9	35	87	146	172
25	4	15	36	61	72	4	15	46	60	71
26	0	2	6	10	12	0	2	6	10	12
27	4	16	40	67	79	4	16	40	67	79
28	6	33	85	147	173	9	36	88	150	176
29	24	106	269	460	542	24	106	269	460	542
30	2	8	19	32	38	2	8	19	32	38
31	3	9	21	36	42	3	9	21	36	42
32	3	11	26	43	51	3	11	26	43	51
33	2	8	19	32	37	2	8	19	32	37
34	2	6	14	24	28	2	6	14	24	28

Table 6.2: Number of new distributed plants for network configurations 1 and 2

Grid, g	Configuration 1					Configuration 2				
	t_1	t_2	t_3	t_4	t_5	t_1	t_2	t_3	t_4	t_5
02	1	–	–	–	–	1	–	–	–	–
05	1	–	–	–	–	1	–	–	–	–
07	1	–	–	–	–	1	–	–	–	–
08	1	–	–	–	–	1	–	–	–	–
12	1	–	–	–	–	1	–	–	–	–
14	2	–	1	–	–	2	–	–	–	–
16	1	–	–	–	–	1	–	–	–	–
17	2	–	–	–	–	2	–	–	–	–
18	–	–	–	2	–	–	2	–	1	–
19	1	–	–	–	–	–	1	–	–	–
20	1	–	–	–	–	1	–	–	–	–
21	1	–	–	–	–	1	–	–	–	–
22	–	2	–	–	–	–	1	1	–	–
23	3	–	–	1	–	–	–	–	1	1
24	–	–	–	–	–	–	–	–	1	–
25	–	–	–	–	–	–	–	–	1	–
26	1	–	–	–	–	1	–	–	–	–
28	3	–	–	–	–	–	–	–	–	–
29	4	–	–	–	–	4	–	–	–	–

In this section, attention will be directed towards the discussion of results for fuelling stations and secondary distribution. Analysis of the network structures will not be mentioned here due to minor changes in the configuration of production plants and transportation links. The latter issues were discussed in depth in Chapter 5.

It can be observed from Table 6.1 that the number of fuelling stations established in each grid and time period is related to the total equivalent demand of hydrogen for this particular location. For instance, this can be illustrated in grid 29 which has the highest number of fuelling stations due to the corresponding high demand level. The remaining grids will follow a similar behaviour in which the demand will determine the number of fuelling stations required to satisfy customers' needs. The tables also show that some grids, namely 2, 5, 8, 12, 16, 20, 21, and 26, will have no fuelling stations. This is due to the fact that each of these grids encapsulates distributed plants which act as fuelling stations (see Table 6.2). However, as the demand of these grids increase, new fuelling stations will be invested in since the demand cannot be fulfilled by the existing distributed plants.

The optimal average daily cost of configurations 1 and 2 is shown in Tables 6.3 and 6.4, respectively. The tables also list all other costs involved in the objective function. As appears in these tables, the operating cost of fuelling stations is included within the

facility operating cost, whereas the secondary transportation costs are given separately.

Table 6.3: Breakdown of total cost for configuration 1 of the multi-echelon model

Cost element	Time period, t				
	t_1	t_2	t_3	t_4	t_5
Capital cost					
Plants and storage facilities	2×10^9	5×10^9	11×10^9	9×10^9	3×10^9
Local transportation	4×10^6	12×10^6	48×10^6	103×10^6	115×10^6
Regional transportation	28×10^6	108×10^6	156×10^6	213×10^6	266×10^6
Secondary transportation	15×10^6	24×10^6	29×10^6	31×10^6	30×10^6
Total capital cost ($)	2×10^9	5×10^9	11×10^9	10×10^9	4×10^9
Operating cost					
Plants and storage facilities	1×10^6	5×10^6	13×10^6	22×10^6	26×10^6
Transportation modes					
Local fuel cost	1×10^3	3×10^3	13×10^3	28×10^3	31×10^3
Local labour cost	3×10^3	9×10^3	33×10^3	71×10^3	79×10^3
Local maintenance cost	224×10^3	660	3×10^3	5×10^3	6×10^3
Local general cost	70	205	797	2×10^3	2×10^3
Regional fuel cost	19×10^3	74×10^3	100×10^3	140×10^3	178×10^3
Regional labour cost	23×10^3	89×10^3	129×10^3	176×10^3	221×10^3
Regional maintenance cost	4×10^3	16×10^3	21×10^3	30×10^3	38×10^3
Regional general cost	458	2×10^3	3×10^3	4×10^3	4×10^3
Secondary fuel cost	4×10^3	7×10^3	8×10^3	8×10^3	8×10^3
Secondary labour cost	10×10^3	17×10^3	20×10^3	21×10^3	21×10^3
Secondary maintenance cost	767	1×10^3	2×10^3	2×10^3	2×10^3
Secondary general cost	239	393	479	503	500
Primary energy source cost	29×10^3	82×10^3	355×10^3	522×10^3	578×10^3
Total operating cost ($/d)	1×10^6	5×10^6	13×10^6	23×10^6	27×10^6
Total network cost ($/d)	3×10^6	10×10^6	23×10^6	32×10^6	30×10^6
Network average cost ($/d)	*19.76×10^6*				

Table 6.4: Breakdown of total cost for configuration 2 of the multi-echelon model

Cost element	Time period, t				
	t_1	t_2	t_3	t_4	t_5
Capital cost					
Plants and storage facilities	2×10^9	4×10^9	10×10^9	10×10^9	4×10^9
Local transportation	4×10^6	12×10^6	34×10^6	82×10^6	116×10^6
Regional transportation	37×10^6	154×10^6	350×10^6	471×10^6	415×10^6
Secondary transportation	16×10^6	25×10^6	30×10^6	31×10^6	32×10^6
Total capital cost ($)	2×10^9	4×10^9	10×10^9	11×10^9	5×10^9
Operating cost					
Plants and storage facilities	1×10^6	5×10^6	13×10^6	22×10^6	26×10^6
Transportation modes					
Local fuel cost	1×10^3	3×10^3	9×10^3	22×10^3	32×10^3
Local labour cost	3×10^3	8×10^3	23×10^3	57×10^3	80×10^3
Local maintenance cost	238×10^3	647	2×10^3	4×10^3	6×10^3
Local general cost	74	201	555	1×10^3	2×10^3
Regional fuel cost	8×10^3	24×10^3	53×10^3	75×10^3	77×10^3
Regional labour cost	23×10^3	94×10^3	213×10^3	289×10^3	260×10^3
Regional maintenance cost	2×10^3	8×10^3	19×10^3	25×10^3	24×10^3
Regional general cost	532	2×10^3	5×10^3	7×10^3	6×10^3
Secondary fuel cost	4×10^3	7×10^3	8×10^3	9×10^3	9×10^3
Secondary labour cost	11×10^3	17×10^3	21×10^3	22×10^3	22×10^3
Secondary maintenance cost	825	1×10^3	2×10^3	2×10^3	2×10^3

Table 6.4 (*Continued*)

Cost element	Time period, t				
	t_1	t_2	t_3	t_4	t_5
Secondary general cost	257	413	497	517	520
Primary energy source cost	28×10^3	87×10^3	124×10^3	306×10^3	368×10^3
Total operating cost (\$/d)	1×10^6	5×10^6	13×10^6	23×10^6	27×10^6
Total network cost (\$/d)	3×10^6	9×10^6	23×10^6	32×10^6	31×10^6
Network average cost (\$/d)	*16.68×10^6*				

The secondary transportation cost values for both networks are relatively similar (see Tables 6.3 and 6.4). The main reason behind this is the assumption that only tanker trucks will be used for hydrogen distribution. The small discrepancies between the cost values are related to the differences in the number of production plants established in each grid. This is because of the dependency of secondary transportation costs on the number of production and storage facilities. Since the latter factor is the same for both networks, the number of production plants is responsible for the minor differences in the cost figures. The tables also show that the average daily cost of the second network configuration is slightly lower than that of the first, for the reasons mentioned in previous chapters.

In order to compare the cost of the networks obtained with the existing petrol infrastructure, the networks' average daily cost were converted into \$/kg delivered and \$/km driven. The results found are displayed in Table 6.5. The table also presents the cost of the current petrol infrastructure assuming an untaxed petrol price of 0.5 £/L and an exchange rate of 1.5 \$/£.

Table 6.5: Comparison between hydrogen- and petrol-based supply chains

Configuration	1	2
Cost of hydrogen network (\$/kg)	2.84	2.83
Cost of hydrogen network (\$/km)	0.18	0.18
Cost of petrol network (\$/km)	0.11	

A summary of the computational results for network configurations 1 and 2 are given in Table 6.6. It appears from the table that the solution time and the optimality gap are reasonable for a problem of this size.

Table 6.6: Summary of computational results for the multi-echelon model

Configuration	1	2
Number of constraints	44017	72067
Number of integer variables	31110	36720
Number of continuous variables	36877	42487
Optimality gap (%)	0.89	0.69
CPU time (d)	3	3

6.4.3 Concluding Remarks

In this chapter, the multi-period model given in Chapter 5 was extended to accommodate fuelling stations and secondary distribution of hydrogen. The decisions associated with the resulting multi-echelon model includes: (1) determination of the total number of fuelling stations to be installed in each grid, and (2) outlining the secondary distribution pattern. The model was represented as an MILP problem. This formulation was used to examine two network configurations within a Great Britain context.

Analysing the results obtained for the network configurations studied shows that the establishment of fuelling stations is dependent on the total demand required for a particular region. The results also show that the secondary distribution pattern is related to the total number of production and storage facilities.

The next chapter will be concern with extending the two- and multi-echelon models to take into account demand uncertainty.

Chapter 7

Design of Stochastic Hydrogen Supply Chain under Demand Uncertainty

7.1 Problem Description

The aim of all of the previous models was to design a hydrogen network by satisfying a specific demand profile given beforehand. Deterministic demand is seldom the case in real life. Demand usually undergoes numerous variations relative to manufacturers' and customers' needs. These variations could largely affect the design and operation aspects of the future hydrogen supply chain. Consequently, this chapter considers the case where demand is not known exactly but subject to some uncertainty.

As highlighted in the literature review, a scenario-based approach is adopted to capture uncertainty in demand. This uncertainty is characterised by a set of distinct possible future realisations generating what is known as a scenario tree. A scenario tree comprises a number of nodes at which branching occurs. Each node determines the start and the end points of a particular time period. A path from the root to the leaf node, i.e. from first to last time period, represents a scenario. Each scenario encompasses a number of decisions that need to be resolved. Using the demand trajectory given in Figure 5.1, a scenario tree of the form shown in Figure 7.1 was obtained. Within the figure, only three time periods and nine distinctive scenarios were considered. Each scenario has a definite demand value and probability of occurrence. Based on these two measures, the hydrogen supply network for each of these scenarios was determined by the optimisation procedure. Having multiple scenarios gives a better representation of what the future network may look like as each scenario contributes towards the final network cost.

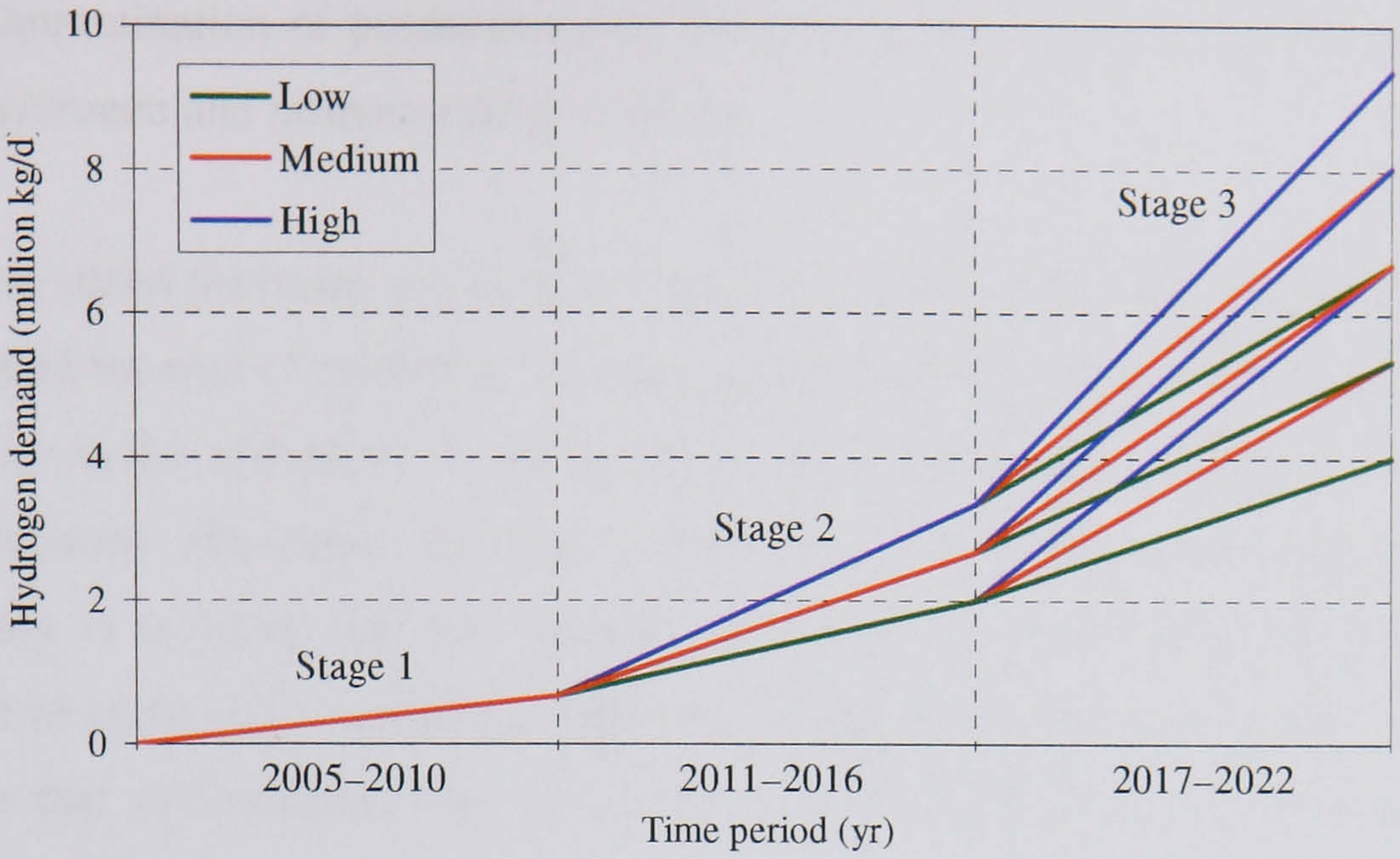


Figure 7.1: Demand scenario tree of interest.

Due to the stochastic nature of this problem, the demand path during the second time period was characterised into three unique paths known as: low, medium, and high. These paths are illustrated by the green, red, and blue lines in Figure 7.1, respectively. Similarly, each of these paths will lead to another low, medium and high path during the third time period. The scenario that includes a red line in both the second and third time periods is the "target" scenario (see Figure 5.1). All other scenarios are either an optimistic or pessimistic view of the demand profile. The high paths correspond to a higher hydrogen penetration than the expected target scenario, while the low paths represent the opposite outcome.

The stochastic behaviour of the demand is represented by a three-stage stochastic optimisation problem. The first stage assumes demand to be known while the second and third stages take into account demand variations over the planning horizon. These three stages are formulated as an MILP model. The model of interest is constructed in a way that can handle many scenarios. Such a formulation will allow the model to behave well under all demand fluctuations happening at some point during the life of the network. The decisions concerning each scenario within the model framework are:

1. Allocation of primary energy sources,
2. Assignment of location, number, type, and size of different production and storage facilities,
3. Establishment of different types of transportation links, and

4. Determination of production rate, average stored inventory, and flow rate of hydrogen and primary energy sources.

The above stated decisions are similar to the ones given for the multi-mode model but are repeated for ease of reference. The decisions associated with the first-stage will be made prior to the realisation of uncertainty and are usually referred to as "here-and-now" decisions. The future decisions correspond to those decisions made after the uncertainty is unveiled and are typically known as "wait-and-see" decisions. The objective of multi-stage modelling under uncertainty is to choose the optimal decision variables that will minimise the cost of the first-stage and the expected cost of the subsequent stages.

7.2 Model Structure and Components

The superstructure of the stochastic model proposed in this chapter is similar to that given for the multi-period model (see Figure 5.2). The only difference is the presence of demand uncertainty. This uncertainty will result in a number of network configurations in accordance to the demand variations during each time period. Due to the importance of demand variations, only this aspect will be addressed below. The remaining model components were discussed in depth in previous chapters.

7.2.1 Demand Uncertainty

In reality, it is unlikely that demand will follow the same pathway as the demand profile given in Figure 5.1. Instead, the demand curve will fluctuate deviating from the forecasted path. These fluctuations give rise to a large number of demand scenarios. However, only nine scenarios, represented by the index *k*, were considered.

7.3 Model Formulation

The formulation presented in Section 5.3 is modified to account for the multiple scenarios that are used to capture uncertainty. The modification will affect all decision variables, including continuous, integer and binary variables. Therefore, all of these variables will be augmented by the demand scenario index *k*. This addition will also take place in any mathematical constraints and objective function terms containing these variables. However, all parameters remain unchanged except for the demand parameters. The unchanged parameters will not be shown here since they were described in earlier chapters.

7.3.1 Nomenclature

Index

k	demand scenarios

Parameters

D^T_{igtk}	total demand for product form i in grid g during time period t under scenario k (kg/d)
PF_{tk}	penetration factor of hydrogen fuel cell vehicles during period time t under scenario k (%)
PR_k	probability of demand scenario k occurring during the lifetime of the network

Continuos Variables

A_{egtk}	availability of primary energy source e in grid g during time period t under scenario k (unit/d)

D^{L}_{igtk} demand for product form i in grid g satisfied by local production during time period t under scenario k (kg/d)

D^{I}_{igtk} imported demand of product form i to grid g during time period t under scenario k (kg/d)

DM^{L}_{mgtk} local demand satisfied by $m-1$ plants in grid g during time period t under scenario k (kg/d)

I_{egtk} import of primary energy source e to grid g from overseas during time period t under scenario k (unit/d)

P_{pjigtk} production rate of product form i produced by plant type p of size j in grid g during time period t under scenario k (kg/d)

P^{T}_{igtk} total production rate of product form i in grid g during time period t under scenario k (kg/d)

$Q_{ilgg'tk}$ flow rate of product form i by transportation mode l between grids g and g' during time period t under scenario k (kg/d)

$QE_{egg'tk}$ flow rate of primary energy source e between grids g and g' during time period t under scenario k (unit/d)

S_{sjigtk} average inventory of product form i stored in storage type s and size j in grid g during time period t under scenario k (kg)

S^{T}_{igtk} total average inventory of product form i in grid g during time period t under scenario k (kg)

Integer Variables

IP_{pjigtk} investment of plants of type p and size j producing product form i in grid g during time period t under scenario k

IS_{sjigtk} investment of storage facilities of type s and size j storing product form i in grid g during time period t under scenario k

NP_{pjigtk} number of plants of type p and size j producing product form i in grid g during time period t under scenario k

NS_{sjigtk} number of storage facilities of type s and size j storing product form i in grid g during time period t under scenario k

Binary Variables

U_{mgtk} 1 if there are $m-1$ plants in grid g during time period t under scenario k, 0 otherwise

$X_{ilgg'tk}$ 1 if product form i is to be transported from grids g to g' by transportation mode l during time period t under scenario k, 0 otherwise

Y_{igtk} 1 if product form i is to be exported from grid g during time period t under scenario k, 0 otherwise

Z_{igtk} 1 if product form i is to be imported to grid g during time period t under scenario k, 0 otherwise

7.3.2 Constraints

As cited before, nine different demand scenarios are considered during the three time periods of interest. These scenarios were amalgamated to form one and three unique scenarios during the first and second time periods, respectively (see Figure 7.1). The formation of the tree structure in Figure 7.1 was accomplished through using a condition known as non-anticipativity. This principle will be addressed later in the chapter. Due to the presence of the non-anticipativity condition, all of the subsequent constraints will have the index k regardless of the time period.

The incorporation of demand scenarios in the proposed constraints is straightforward. These constraints will be introduced in the following subsections with a brief discussion. Only new constraints will be discussed in detail.

Demand Constraints

The uncertainty in demand during each time period is described by the following equation:

$$D^T_{igtk} = PF_{tk} D^T_{ig} \qquad \forall i, g, t, k \tag{7.1}$$

where PF_{tk} is the penetration factor of hydrogen fuel cell vehicles during a particular time period t and demand scenario k. This factor is multiplied by the total equivalent demand in order to estimate the demand at the corresponding scenario and time period.

The local demand during each scenario k must be enforced by the following constraint:

$$D^L_{igtk} \leq P^T_{igtk} \qquad \forall i,g,t,k \tag{7.2}$$

The demand during scenario k satisfied by neighbouring grids should be equal to the sum of all flow rates entering the grid of interest during the same time period:

$$D^I_{igtk} = \sum_{l,g'} Q_{ilg'gtk} \qquad \forall i,g,t,k \tag{7.3}$$

The sum of Equations 7.2 and 7.3 gives the total demand for each scenario:

$$D^T_{igtk} = D^L_{igtk} + D^I_{igtk} \qquad \forall i,g,t,k \tag{7.4}$$

Primary Energy Source Constraints

The average availability of primary energy sources during the first time period t_1 and scenario k is:

$$A_{egt_1k} = A^0_{eg} + I_{egt_1k} + \sum_{g'} \left(QE_{eg'gt_1k} - QE_{egg't_1k} \right) - \sum_{p,j,i} \gamma_{epj} P_{pjigt_1k} \qquad \forall e,g,k \tag{7.5}$$

The average availability of primary energy sources for all other time periods is:

$$A_{egtk} = A_{egk(t-1)} + I_{egtk} + \sum_{g'} \left(QE_{eg'gtk} - QE_{egg'tk} \right) - \sum_{p,j,i} \gamma_{epj} P_{pjigtk} \qquad \forall e,g,t,k : t \neq t_1 \tag{7.6}$$

A mass balance on a particular grid is written for each primary energy source during time period t and scenario k:

$$\left(I_{egtk} + \sum_{g'} QE_{eg'gtk}\right) SSF = \sum_{g'} QE_{egg'tk} + \sum_{p,j,i} \gamma_{epj} P_{pjigtk} \qquad \forall e, g, t, k \tag{7.7}$$

where SSF is a safety stock factor which acts as a buffer against unpredicted contingencies in energy sources.

Production Facility Constraints

The total production rate for each scenario k is:

$$P^T_{igtk} = \sum_{l,g'} \left(Q_{ilgg'tk} - Q_{ilg'gtk}\right) + D^T_{igtk} \qquad \forall i, g, t, k \tag{7.8}$$

Additionally, the total production rate is equal to the production rate of all individual plants established:

$$P^T_{igtk} = \sum_{p,j} P_{pjigtk} \qquad \forall i, g, t, k \tag{7.9}$$

The production rate of each plant during scenario k must be constrained between lower and upper bounds:

$$PCap^{\min}_{pji} NP_{pjigtk} \le P_{pjigtk} \le PCap^{\max}_{pji} NP_{pjigtk} \qquad \forall p, j, i, g, t, k \tag{7.10}$$

Distributed plants established during scenario k can only fulfil local demand:

$$\sum_{p} P_{pjigtk} \le D^L_{igtk} \qquad \forall i, g, t, k : j = \text{small plants} \tag{7.11}$$

The following constraints make sure that plants with certain production technologies cannot be built in certain sizes:

$$NP_{pjigtk} = 0 \quad \forall i,g,t,k : p = \text{coal gasification} \;\&\; j = \text{small plants} \tag{7.12}$$

$$NP_{pjigtk} = 0 \quad \forall i,g,t,k : p = \text{biomass gasification} \;\&\; j = \text{small plants} \tag{7.13}$$

$$NP_{pjigtk} = 0 \quad \forall i,g,t,k : p = \text{electrolysis} \;\&\; j = \text{large plants} \tag{7.14}$$

Transportation Constraints

The total number of plants established in each grid g and at each scenario k is given as follows:

$$\sum_{p,j,i} NP_{pjigtk} = \sum_{m} (m-1) U_{mgtk} \quad \forall g,t,k \tag{7.15}$$

To obtain a meaningful result, the binary variable U_{mgtk} is constrained by:

$$\sum_{m} U_{mgtk} = 1 \quad \forall g,t,k \tag{7.16}$$

The local demand satisfied by the total number of plants established for each scenario k is expressed by the following constraint:

$$DM^{L}_{mgtk} \geq D^{L}_{igtk} - \pi(1 - U_{mgtk}) \quad \forall i,m,g,t,k \tag{7.17}$$

Equation 7.17 is written in this form to insure linearity (see Section 4.3.3).

The construction of a regional distribution network for each scenario k is stipulated by the following constraints:

$$Q_{il}^{\min} X_{ilgg'tk} \le Q_{ilgg'tk} \le Q_{il}^{\max} X_{ilgg'tk} \qquad \forall i,l,g,g',t,k : g \neq g' \tag{7.18}$$

$$Y_{igtk} \ge X_{ilgg'tk} \qquad \forall i,l,g,g',t,k : g \neq g' \tag{7.19}$$

$$Z_{igtk} \ge X_{ilg'gtk} \qquad \forall i,l,g,g',t,k : g \neq g' \tag{7.20}$$

$$Y_{igtk} + Z_{igtk} \le 1 \qquad \forall i,g,t,k \tag{7.21}$$

Storage Facility Constraints

The total average inventory of a product form *i* at scenario *k* is:

$$S_{igtk}^{T} = \beta\, D_{igtk}^{T} \qquad \forall i,g,t,k \tag{7.22}$$

The average inventory of a product during scenario *k* cannot exceed certain limits:

$$SCap_{sji}^{\min} NS_{sjigtk} \le S_{sjigtk} \le SCap_{sji}^{\max} NS_{sjigtk} \qquad \forall s,j,i,g,t,k \tag{7.23}$$

The same idea applies for the total average stored inventory during scenario *k*:

$$\sum_{s,j} SCap_{sji}^{\min} NS_{sjigtk} \le S_{igtk}^{T} \le \sum_{s,j} SCap_{sji}^{\max} NS_{sjigtk} \qquad \forall i,g,t,k \tag{7.24}$$

Time Evolution Constraints

The numbers of production and storage facilities in operation during scenario *k* and time period t_1 are respectively equal to:

$$NP_{pjigt_1k} = NP_{pjig}^{0} + IP_{pjigt_1k} \qquad \forall p,j,i,g,k \tag{7.25}$$

$$NS_{sjigt_1k} = NS_{sjig}^{0} + IS_{sjigt_1k} \qquad \forall s,j,i,g,k \tag{7.26}$$

For the subsequent time periods, the numbers of these facilities with in each scenario k is:

$$NP_{pjigtk} = NP_{pjigk(t-1)} + IP_{pjigtk} \qquad \forall p, j, i, g, t, k : t \neq t_1 \tag{7.27}$$

$$NS_{sjigtk} = NS_{sjigk(t-1)} + IS_{sjigtk} \qquad \forall s, j, i, g, t, k : t \neq t_1 \tag{7.28}$$

Non-anticipativity Constraints

The non-anticipativity principle, which was introduced initially by Wets [118], states that if a set of scenarios have the same available information up to time period t then the values of the variables corresponding to these scenarios are identical up to that time period. Since the demand trajectory for the first time period is assumed to be deterministic, the non-anticipativity principle will lead to one discrete scenario. The decision variables associated with this discrete scenario will be similar up to the first time period. The following constraint guarantees this condition:

$$V_{ot_1k} = V_{ot_1(k+1)} \qquad \forall o, k : k < 9 \tag{7.29}$$

where V is any decision variable presented in the model. The index o denotes other indices incorporated in a particular variable such as e, g, g', i, p, j, s, and m. Obviously, the indices which appear will depend on the variable.

The demand uncertainty encountered in the second time period is represented by nine scenarios which are "lumped" together forming three different sets of scenarios. The decision variables involved in each of the three lumped scenarios are identical up to that time period. The similarity in these scenarios is ensured via the following non-anticipative constraints:

$$V_{ot_2k} = V_{ot_2(k+1)} \qquad \forall o, k : k < 3 \tag{7.30}$$

$$V_{ot_2k} = V_{ot_2(k+1)} \quad \forall o,k : 3 < k < 6 \tag{7.31}$$

$$V_{ot_2k} = V_{ot_2(k+1)} \quad \forall o,k : 6 < k < 9 \tag{7.32}$$

In the last time period, there will be a unique set of variables for each of the nine scenarios. These sets of variables will yield nine different network configurations.

Non-negativity Constraints

All decision variables must be non-negative:

$$A_{egtk} \geq 0 \quad \forall e,g,t,k \tag{7.33}$$

$$D^L_{igtk} \geq 0 \quad \forall i,g,t,k \tag{7.34}$$

$$D^I_{igtk} \geq 0 \quad \forall i,g,t,k \tag{7.35}$$

$$DM^L_{mgtk} \geq 0 \quad \forall m,g,t,k \tag{7.36}$$

$$I_{egtk} \geq 0 \quad \forall e,g,t,k \tag{7.37}$$

$$IP_{pjigtk} \geq 0 \quad \forall p,j,i,g,t,k \tag{7.38}$$

$$IS_{sjigtk} \geq 0 \quad \forall s,j,i,g,t,k \tag{7.39}$$

$$NP_{pjigtk} \geq 0 \quad \forall p,j,i,g,t,k \tag{7.40}$$

$$NS_{sjigtk} \geq 0 \quad \forall s,j,i,g,t,k \tag{7.41}$$

$$P^T_{igtk} \geq 0 \quad \forall i,g,t,k \tag{7.42}$$

$$P_{pjigtk} \geq 0 \quad \forall p,j,i,g,t,k \tag{7.43}$$

$$Q_{ilgg'tk} \geq 0 \quad \forall i,l,g,g',t,k : g \neq g' \tag{7.44}$$

$$QE_{egg'tk} \geq 0 \quad \forall e,g,g',t,k : g \neq g' \tag{7.45}$$

$$S_{sjigtk} \geq 0 \quad \forall s,j,i,g,t,k \tag{7.46}$$

$$S^T_{igtk} \geq 0 \quad \forall i,g,t,k \tag{7.47}$$

7.3.3 Objective Function

The objective of optimisation is to minimise the expected value of the cost of the network taken over all the scenarios during the operation of the network. This minimisation is achieved by assuming that each scenario k has a known probability of occurrence in practice denoted by PR_k. As mentioned throughout this thesis, the cost terms include both capital and operating costs. The capital cost is associated with the cost of establishing production plants, storage facilities, and transportation modes during all scenarios. The operating cost, however, is associated with the cost of operating the aforementioned technologies efficiently. It also includes the cost of distributing primary energy sources throughout the network. The following subsections briefly address these cost terms since they are detailed in previous chapters. The only difference here is the addition of the probability of occurrence of each demand scenario.

Facility Capital Cost

The facility capital cost for all scenarios during the entire planning horizon is:

$$FCC = \sum_{j,i,g,t,k} \left(\frac{PR_k}{LR} \left(\sum_p PCC_{pji} IP_{pjigtk} + \sum_s SCC_{sji} IS_{sjigtk} \right) \right) \tag{7.48}$$

Transportation Capital Cost

The total transportation capital cost for all scenarios and time periods is:

$$TCC = \sum_{i,l,m,g,t,k} PR_k \left(\frac{DM^L_{mgtk} TMC_{il}}{(m-1) TMA^L_l TCap_{il}} \left(\frac{2L^L_g}{SP^L_l} + LUT_l \right) \right) + \sum_{i,l,g,g',t,k} PR_k \left(\frac{Q_{ilgg'tk}}{TMA^R_l TCap_{il}} \left(\frac{2L^R_{gg'}}{SP^R_l} + LUT_l \right) \right) \tag{7.49}$$

Facility Operating Cost

The facility operating cost for all scenarios during the entire planning horizon is given as follows:

$$FOC = \sum_{j,i,g,t,k} PR_k \left(\sum_p UPC_{pji} P_{pjigtk} + \sum_s USC_{sji} S_{sjigtk} \right) \tag{7.50}$$

Transportation Operating Cost

The fuel cost for all scenarios and time periods is:

$$FC = \sum_{i,l,m,g,t,k} PR_k FP_l \left(\frac{2L_g^L DM_{mgtk}^L}{(m-1)FE_l^L TCap_{il}} \right) + \sum_{i,l,g,g',t,k} PR_k FP_l \left(\frac{2L_{gg'}^R Q_{ilgg'tk}}{FE_l^R TCap_{il}} \right) \tag{7.51}$$

The labour cost for all scenarios and time periods is:

$$\begin{aligned} LC = & \sum_{i,l,m,g,t,k} PR_k DW_l \left(\frac{DM_{mgtk}^L}{(m-1)TCap_{il}} \left(\frac{2L_g^L}{SP_l^L} + LUT_l \right) \right) \\ & + \sum_{i,l,g,g',t,k} PR_k DW_l \left(\frac{Q_{ilgg'tk}}{TCap_{il}} \left(\frac{2L_{gg'}^R}{SP_l^R} + LUT_l \right) \right) \end{aligned} \tag{7.52}$$

The maintenance cost for all scenarios and time periods is:

$$MC = \sum_{i,l,m,g,t,k} PR_k ME_l \left(\frac{2L_g^L DM_{mgtk}^L}{(m-1)TCap_{il}} \right) + \sum_{i,l,g,g',t,k} PR_k ME_l \left(\frac{2L_{gg'}^R Q_{ilgg'tk}}{TCap_{il}} \right) \tag{7.53}$$

The general cost for all scenarios and time periods is:

$$GC = \sum_{i,l,m,g,t,k} PR_k GE_l \left(\frac{DM^L_{mgtk}}{(m-1)TMA^L_l TCap_{il}} \left(\frac{2L^L_g}{SP^L_l} + LUT_l \right) \right) + \sum_{i,l,g,g',t,k} PR_k GE_l \left(\frac{Q_{ilgg'tk}}{TMA^R_l TCap_{il}} \left(\frac{2L^R_{gg'}}{SP^R_l} + LUT_l \right) \right) \quad (7.54)$$

Summing up all the cost functions given above, the total transportation operating cost is:

$$TOC = FC + LC + MC + GC \quad (7.55)$$

Primary Energy Source Cost

The cost of primary energy sources for all scenarios during the entire planning horizon is:

$$ESC = \sum_k PR_k \left(\sum_{e,g,t} UIC_e I_{egtk} + \sum_{e,g,g',t} UDC_e L^R_{gg'} QE_{egg'tk} \right) \quad (7.56)$$

7.3.4 Model Summary

The expected total daily cost of the hydrogen supply chain network is given as follows:

$$TDC^{\exp} = \frac{1}{NTP} \left(\frac{FCC + TCC}{\alpha\, CCF} + FOC + TOC + ESC \right) \quad (7.57)$$

Finally, the objective of optimisation is to:

$$\min \; TDC^{\exp} \quad (7.58)$$

The optimisation is subject to all the constraints presented in Section 7.3.2.

7.4 Extension to Stochastic Multi-Echelon Case

The stochastic model described in this chapter is extended to take into account fuelling stations and secondary distribution. The addition of an extra echelon to the stochastic model is performed in a similar method to the one adopted in Chapter 6. The only difference is the introduction of the subscript k to the decision variables NFS_{igtk}, NS^{T}_{gtk} and W_{ngtk}. Any constraints and objective function terms containing these variables must also be enforced separately for each scenario.

The following sections list only the new constraints and objective function terms that should be incorporated in the formulation of the stochastic model in order to transform it to a multi-echelon model. All other constraints and cost terms are analogous to the one presented in Sections 7.3.2 and 7.3.3.

7.4.1 Constraint

The number of fuelling stations at each scenario k is:

$$NFS_{igtk} = \frac{D^{T}_{igtk}}{FCap_{i}} - \sum_{p} NP_{pjigtk} \qquad \forall i,g,t,k : j = \text{small plants} \tag{7.59}$$

where:

$$NFS_{igtk} \geq 0 \qquad \forall i,g,t,k \tag{7.60}$$

7.4.2 Objective Function

Transportation Capital Cost

Due to the existence of secondary distribution in each grid, the following cost term must be added to Equation 7.49:

$$TCC = \sum_{i,l,n,g,t,k} PR_k \left(\frac{D^T_{igtk} W_{ngtk}}{(n-1) TMA^L_l TCap_{il}} \left(\frac{2L^L_g}{SP^L_l} + LUT_l \right) \right) \tag{7.61}$$

The term $n-1$ is introduced to determine the average delivery distance within a grid and is expressed as follows:

$$\sum_{p,j,i} NP_{pjigtk} + \sum_{s,j,i} NS_{sjigtk} = \sum_{n} (n-1) W_{ngtk} \qquad \forall g,t,k \tag{7.62}$$

where the first and second term of the left-hand-side of Equation 7.62 denote the total number of production and storage facilities, respectively.

To assure that only one combination of the binary variables (W_{ngtk}) is active, the following constraint should be written:

$$\sum_{n} W_{ngtk} = 1 \qquad \forall g,t,k \tag{7.63}$$

Facility Operating Cost

The operating cost of fuelling stations that must be added to Equation 7.50 is:

$$FOC = \sum_{i,g,t,k} PR_k UFC_i NFS_{igtk} FCap_i \tag{7.64}$$

Transportation Operating Cost

The secondary transportation operating costs including fuel, labour, maintenance, and general cost are summarised below respectively. As stated, these terms must be added to the equations given for the stochastic model to account for multiple echelons.

$$FC = \sum_{i,l,n,g,t,k} PR_k FP_l \left(\frac{2L_g^L D_{igtk}^T W_{ngtk}}{(n-1) FE_l^L TCap_{il}} \right) \tag{7.65}$$

$$LC = \sum_{i,l,n,g,t,k} PR_k DW_l \left(\frac{D_{igtk}^T W_{ngtk}}{(n-1) TCap_{il}} \left(\frac{2L_g^L}{SP_l^L} + LUT_l \right) \right) \tag{7.66}$$

$$MC = \sum_{i,l,n,g,t,k} PR_k ME_l \left(\frac{2L_g^L D_{igtk}^T W_{ngtk}}{(n-1) TCap_{il}} \right) \tag{7.67}$$

$$GC = \sum_{i,l,n,g,t,k} PR_k GE_l \left(\frac{D_{igtk}^T W_{ngtk}}{(n-1) TMA_l^L TCap_{il}} \left(\frac{2L_g^L}{SP_l^L} + LUT_l \right) \right) \tag{7.68}$$

7.4.3 Model Summary

As with the stochastic model, the objective is to:

$$\min \ TDC^{\exp} \tag{7.69}$$

where:

$$TDC^{\exp} = \frac{1}{NTP} \left(\frac{FCC + TCC}{\alpha \, CCF} + FOC + TOC + ESC \right) \tag{7.70}$$

The optimisation is subject to all constraints given in Sections 7.3.2 and 7.4.1.

7.5 Case Study Revisited

The case studies examined in the previous chapters are revisited here but within a scenario perspective to capture the resulting demand uncertainty. The stochastic and the stochastic, multi-echelon models derived in this chapter are constraint to study the

design and operation of three different hydrogen supply chain networks. The first two network configurations are similar to the one presented in Chapter 5, whereas the third configuration is identical to the one presented in Chapter 6. For convenience, these network configurations are summarised in Table 7.1.

Table 7.1: Network configurations to be examined under demand uncertainty

Configuration 1	Production of liquid hydrogen in small, medium, and large plants via steam methane reforming, coal and biomass gasification, and water electrolysis technologies. Tanker trucks are used to deliver hydrogen to three different sizes of stationary storage facilities referred to as small, medium, and large liquid hydrogen tanks.
Configuration 2	Similar to the first scenario, however, both tanker trucks and railway tank cars will be used for delivery.
Configuration 3	Similar to the first scenario in terms of production, storage, and transportation technologies but fuelling stations and secondary transportation are included.

7.5.1 Input Data

This section lists the input data required for both stochastic and stochastic, multi-echelon models. To prevent redundancy, only new data will be provided. Other data concerning primary energy sources, production and storage facilities, and transportation modes were fully detailed in previous chapters. Regarding fuelling stations and secondary distribution, the corresponding data was given in Section 6.4.1.

Hydrogen Demand

In this chapter, the planning horizon, starting from 2005 and ending in 2022, was divided into three equal time periods of six years. The penetration of hydrogen fuel cell vehicles for the three time periods was assumed to be 5%, 20%, and 50%, respectively. Due to the existence of uncertainty, the last two percentages were assumed possibly to fluctuate deviating from the predicted path. This will result in nine scenarios each with different penetration percentages. These percentages are summarised in Table 7.2.

Table 7.2: Scenario penetration factor during each time period

Time period, t (yr)	Scenario, k								
	k_1	k_2	k_3	k_4	k_5	k_6	k_7	k_8	k_9
t_1 (2005–2010)	5%	5%	5%	5%	5%	5%	5%	5%	5%
t_2 (2011–2016)	15%	15%	15%	20%	20%	20%	25%	25%	25%
t_3 (2017–2022)	30%	40%	50%	40%	50%	60%	50%	60%	70%

Since this study assumes deterministic behaviour in the first time period, the penetration factor remains the same for all scenarios. The nine scenarios during the second time period were partitioned into a set of three distinct scenarios. Each of these clustered scenarios has the same penetration factor. For the third time period, each of the nine scenarios was given a different penetration factor, as shown in the above table.

Based on the penetration percentages given in Table 7.2, the average daily demand of hydrogen during each scenario was estimated. This estimation was done by multiplying the corresponding percentages by the total equivalent demand, which was calculated at 100% market level. The values obtained are listed in Table 7.3.

Table 7.3: Hydrogen demand for each time period and scenario (t/d)

Time period, t (yr)	Scenario, k								
	k_1	k_2	k_3	k_4	k_5	k_6	k_7	k_8	k_9
t_1 (2005–2010)	670	670	670	670	670	670	670	670	670
t_2 (2011–2016)	2009	2009	2009	2679	2679	2679	3349	3349	3349
t_3 (2017–2022)	4018	5358	6697	5358	6697	8037	6697	8037	9376

As mentioned earlier, the nine demand scenarios considered here were assumed to have a known probability of occurrence. The probability for each demand scenario is shown in Table 7.4.

Table 7.4: Probability of demand scenarios

Scenario, k	Probability (%)
k_1	6.25
k_2	12.50
k_3	6.25
k_4	12.50
k_5	25.00
k_6	12.50
k_7	6.25
k_8	12.50
k_9	6.25

The hydrogen demand of each grid for the nine scenarios over the first, second, and third time periods are tabulated in 7.5 and 7.6, respectively.

Table 7.5: Grid hydrogen demand for all scenarios over first and second periods (t/d)

Time period, t	t_1	t_2		
Scenario, k	k_1–k_9	k_1–k_3	k_4–k_6	k_7–k_9
01	5	15	20	26
02	4	12	16	20
03	8	24	32	39
04	10	30	40	49
05	2	6	8	10
06	6	19	26	32
07	9	26	35	43
08	0.4	1	1	2
09	4	13	17	21
10	16	47	63	79
11	19	58	77	96
12	0.5	1	2	2
13	32	95	127	159
14	45	135	180	226
15	7	21	29	36
16	1	4	5	6
17	24	73	98	122
18	50	149	199	249
19	25	75	99	124
20	2	6	8	10
21	3	9	13	16
22	31	94	125	156
23	52	157	209	262
24	43	129	172	215
25	18	53	71	89
26	3	9	13	16
27	20	59	79	98
28	44	132	176	220
29	136	409	545	682
30	9	28	38	47
31	10	31	42	52
32	13	38	50	63
33	9	28	37	46
34	7	20	27	34

Table 7.6: Grid hydrogen demand for all scenarios over third period (t/d)

	Scenario, k								
Grid, g	k_1	k_2	k_3	k_4	k_5	k_6	k_7	k_8	k_9
01	31	41	51	41	51	61	51	61	71
02	24	32	40	32	40	48	40	48	56
03	47	63	79	63	79	95	79	95	111
04	59	79	99	79	99	119	99	119	139
05	12	16	21	16	21	25	21	25	29
06	39	52	65	52	65	78	65	78	91
07	52	69	86	69	86	104	86	104	121
08	2	3	4	3	4	4	4	4	5
09	26	34	43	34	43	51	43	51	60
10	95	126	158	126	158	190	158	190	221
11	115	154	192	154	192	231	192	231	269

Table 7.6 (*Continued*)

Grid, g	Scenario, k								
	k_1	k_2	k_3	k_4	k_5	k_6	k_7	k_8	k_9
12	3	4	5	4	5	6	5	6	7
13	191	254	318	254	318	381	318	381	445
14	271	361	451	361	451	541	451	541	632
15	43	57	71	57	71	86	71	86	100
16	7	10	12	10	12	15	12	15	17
17	147	195	244	195	244	293	244	293	342
18	299	399	498	399	498	598	498	598	698
19	149	199	249	199	249	298	249	298	348
20	12	16	20	16	20	24	20	24	28
21	19	25	32	25	32	38	32	38	44
22	187	250	312	250	312	374	312	374	437
23	314	419	524	419	524	628	524	628	733
24	258	344	431	344	431	517	431	517	603
25	107	143	178	143	178	214	178	214	250
26	19	25	31	25	31	38	31	38	44
27	118	157	197	157	197	236	197	236	276
28	264	351	439	351	439	527	439	527	615
29	818	1091	1363	1091	1363	1636	1363	1636	1909
30	56	75	94	75	94	113	94	113	132
31	62	83	104	83	104	125	104	125	145
32	76	101	126	101	126	151	126	151	177
33	56	74	93	74	93	111	93	111	130
34	41	54	68	54	68	82	68	82	95

Table 7.5 shows that the demand of hydrogen in each grid during the first time period is equal for all scenarios due to the deterministic assumption. However, for the second time period, only the same cluster of scenarios (k_1–k_3, k_4–k_6, and k_7–k_9) will have the same demand. Moreover, the demand value of each grid and scenario in Table 7.6 varies according to the penetration percentage assumed.

7.5.2 Results and Discussion

For each of the examined network configurations, the network structure for only three demand scenarios over the planning horizon will be illustrated. These demand scenarios are referred to as the "worst", "middle", and "best" paths. The paths of interest are represented by scenario number 1, 5, and 9 respectively. The network structures of these paths over the first, second and third time periods for the first network configuration are shown in Figures 7.2–7.8.

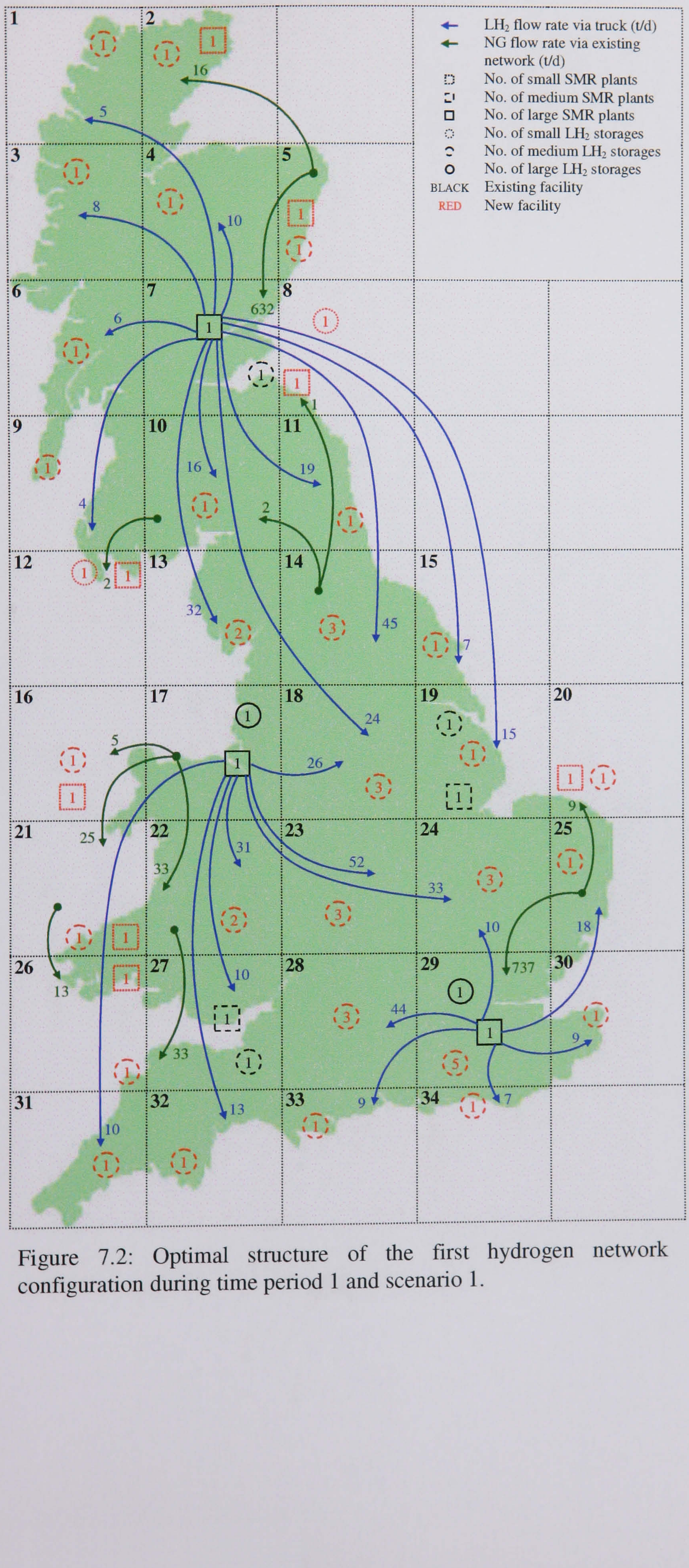


Figure 7.2: Optimal structure of the first hydrogen network configuration during time period 1 and scenario 1.

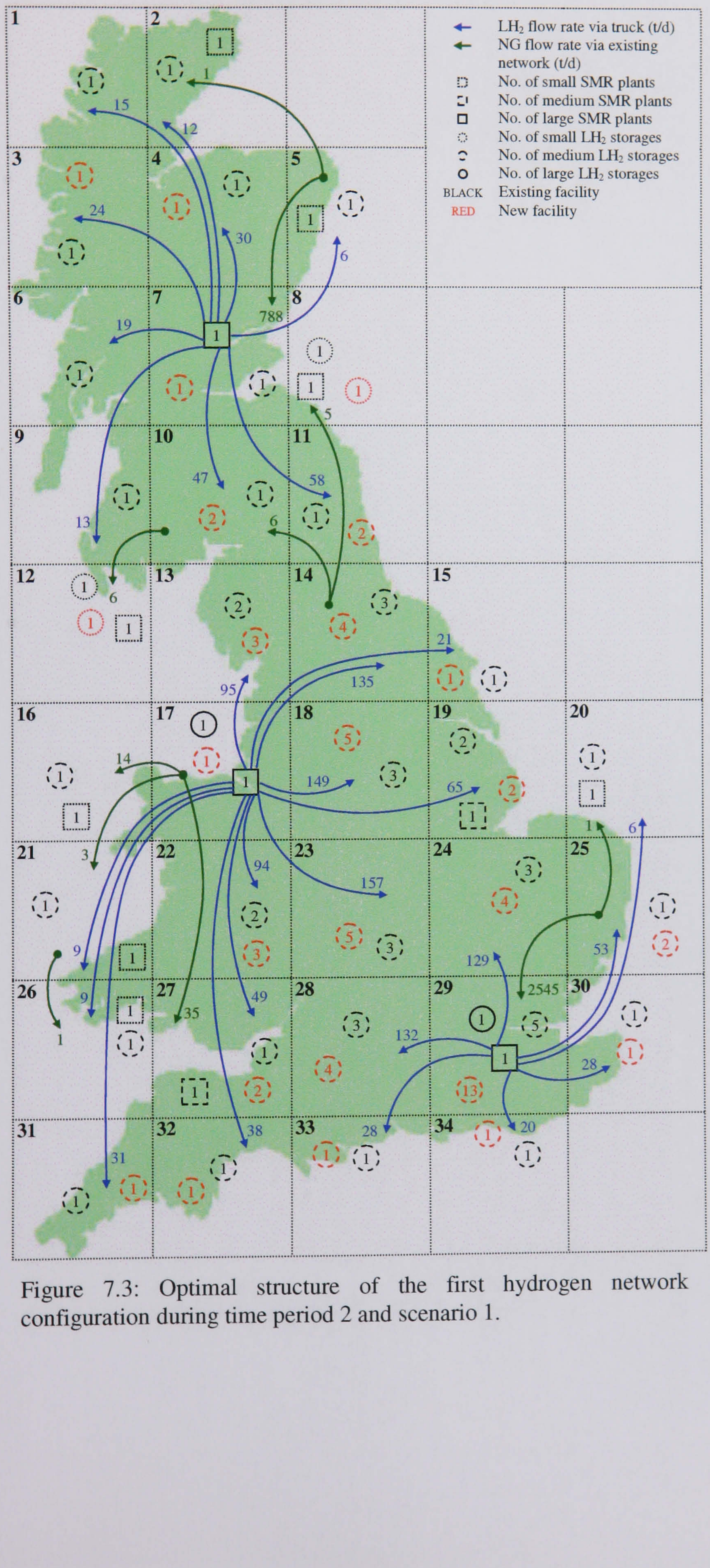


Figure 7.3: Optimal structure of the first hydrogen network configuration during time period 2 and scenario 1.

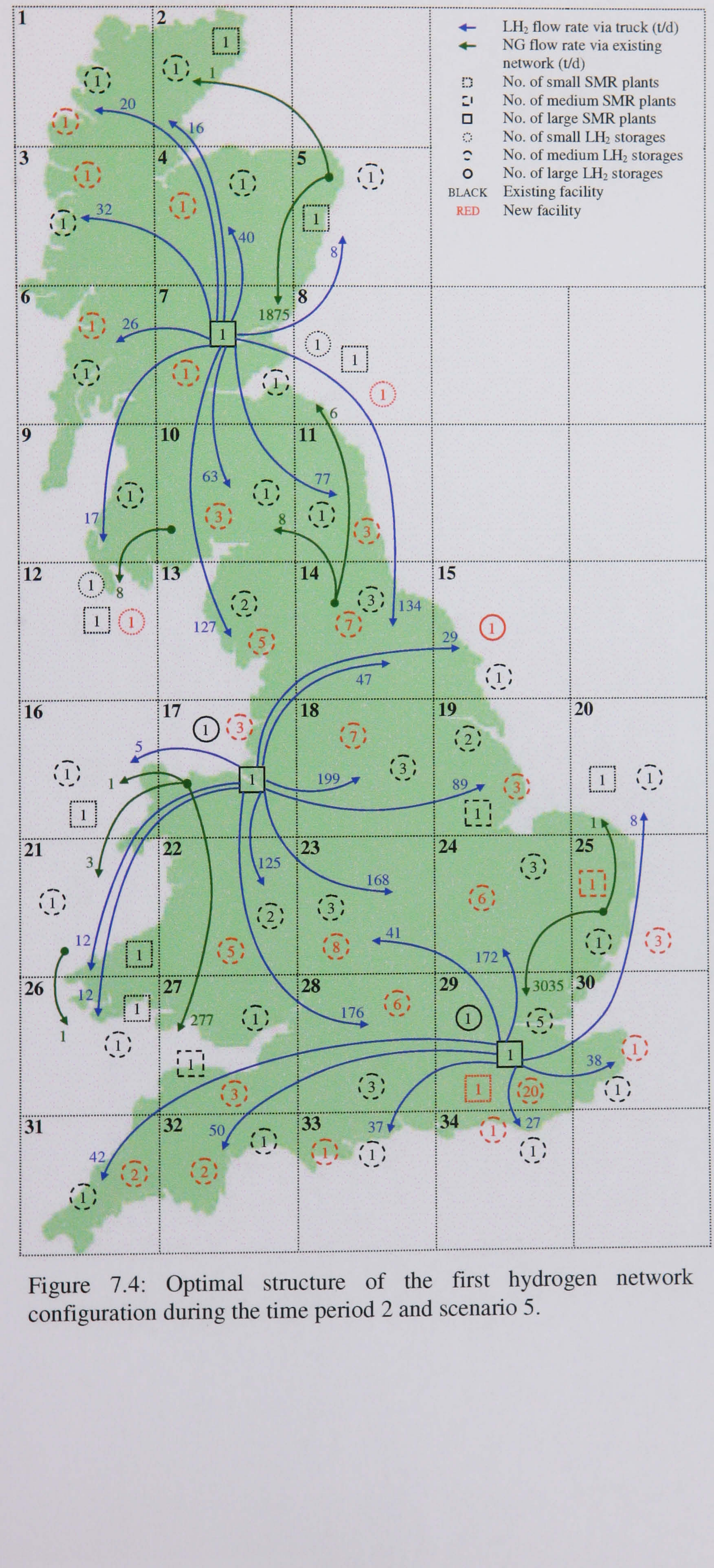


Figure 7.4: Optimal structure of the first hydrogen network configuration during the time period 2 and scenario 5.

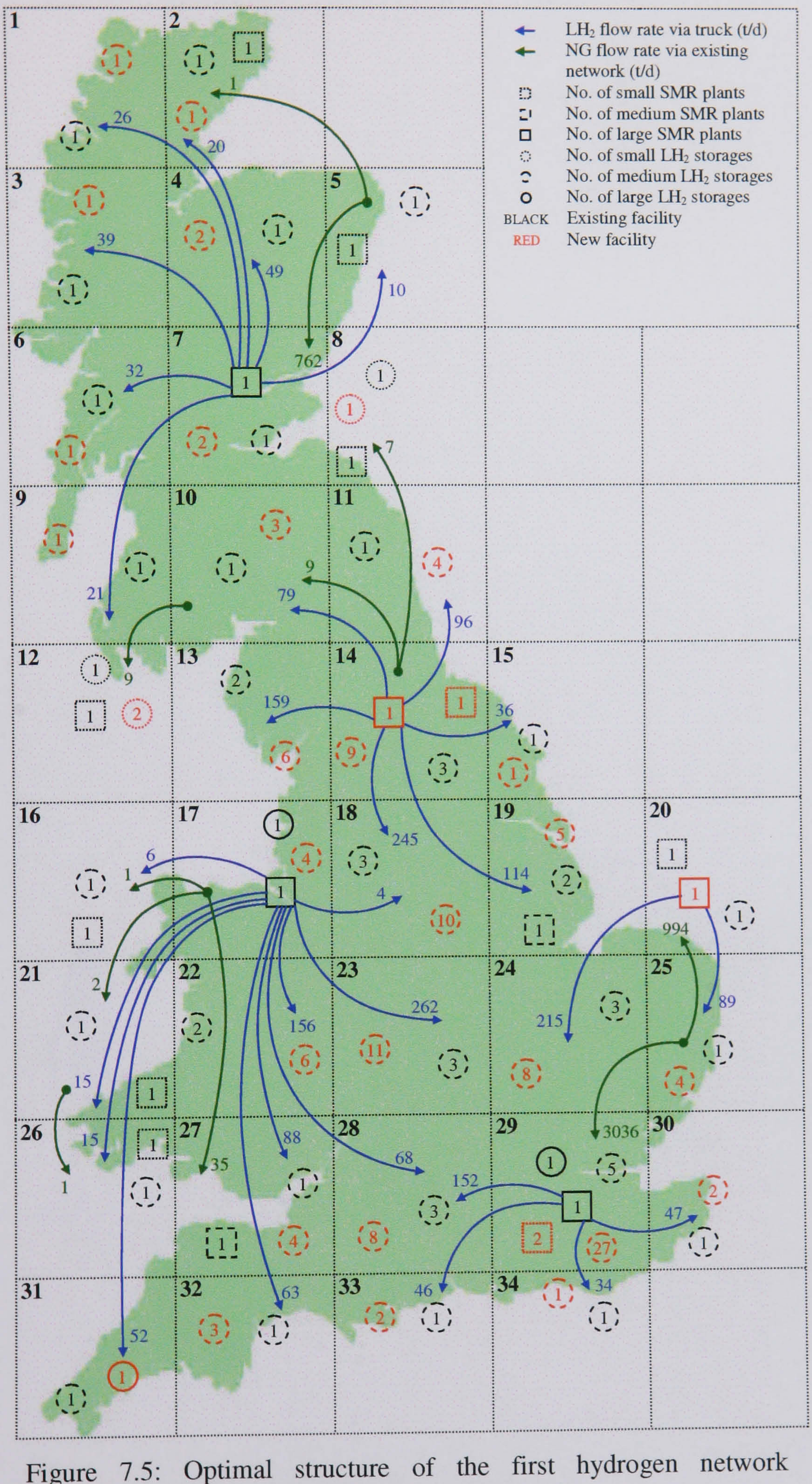


Figure 7.5: Optimal structure of the first hydrogen network configuration during time period 2 and scenario 9.

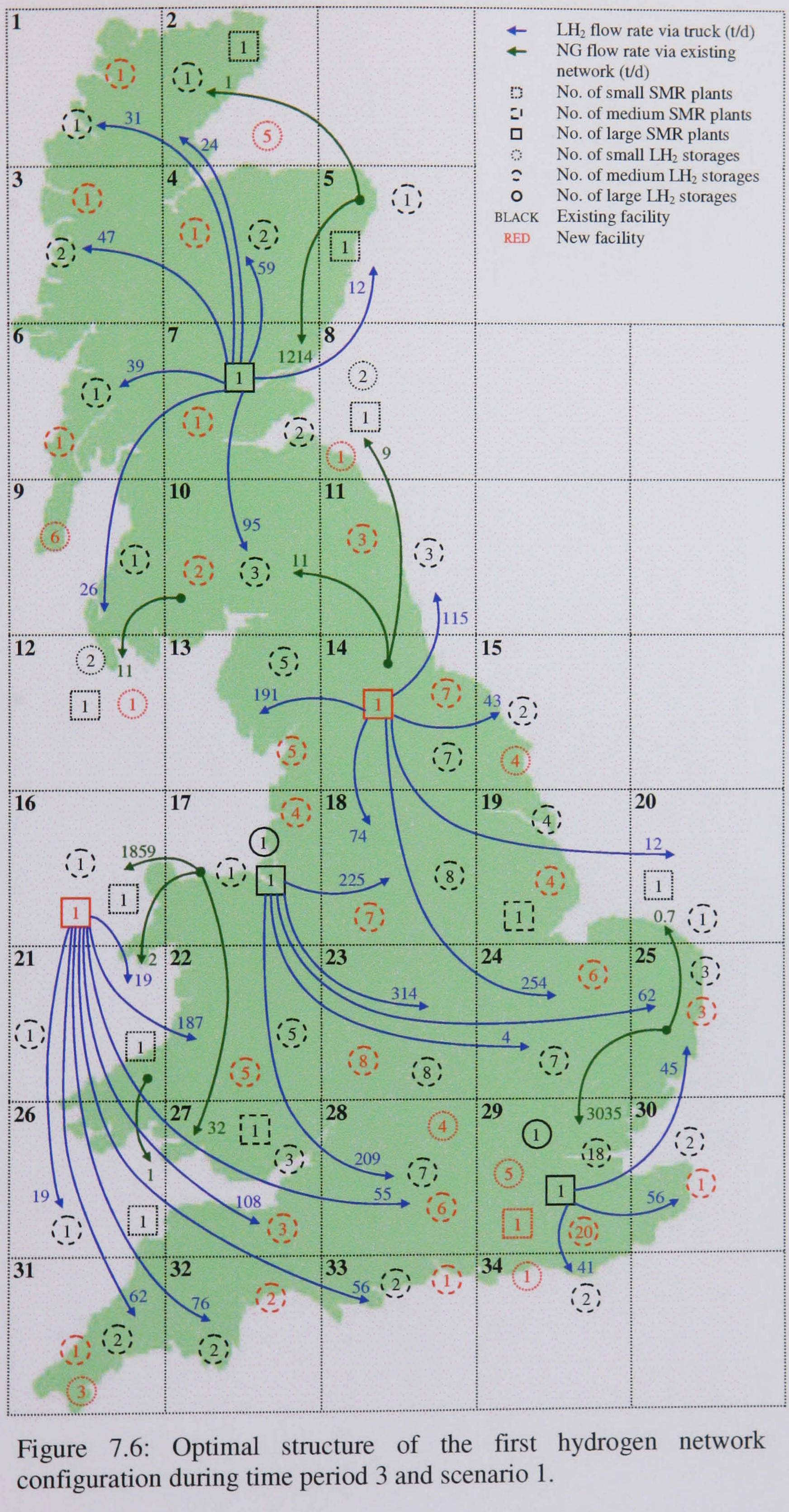


Figure 7.6: Optimal structure of the first hydrogen network configuration during time period 3 and scenario 1.

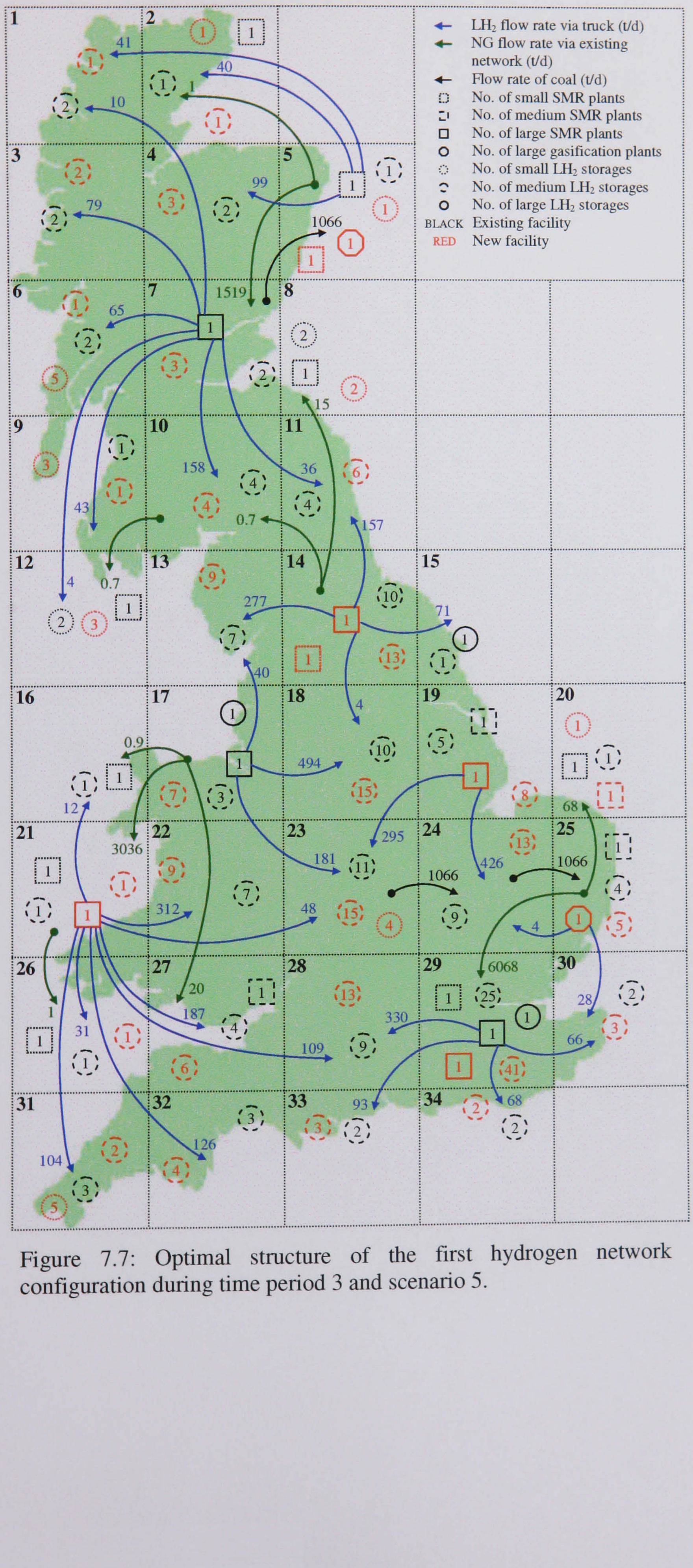


Figure 7.7: Optimal structure of the first hydrogen network configuration during time period 3 and scenario 5.

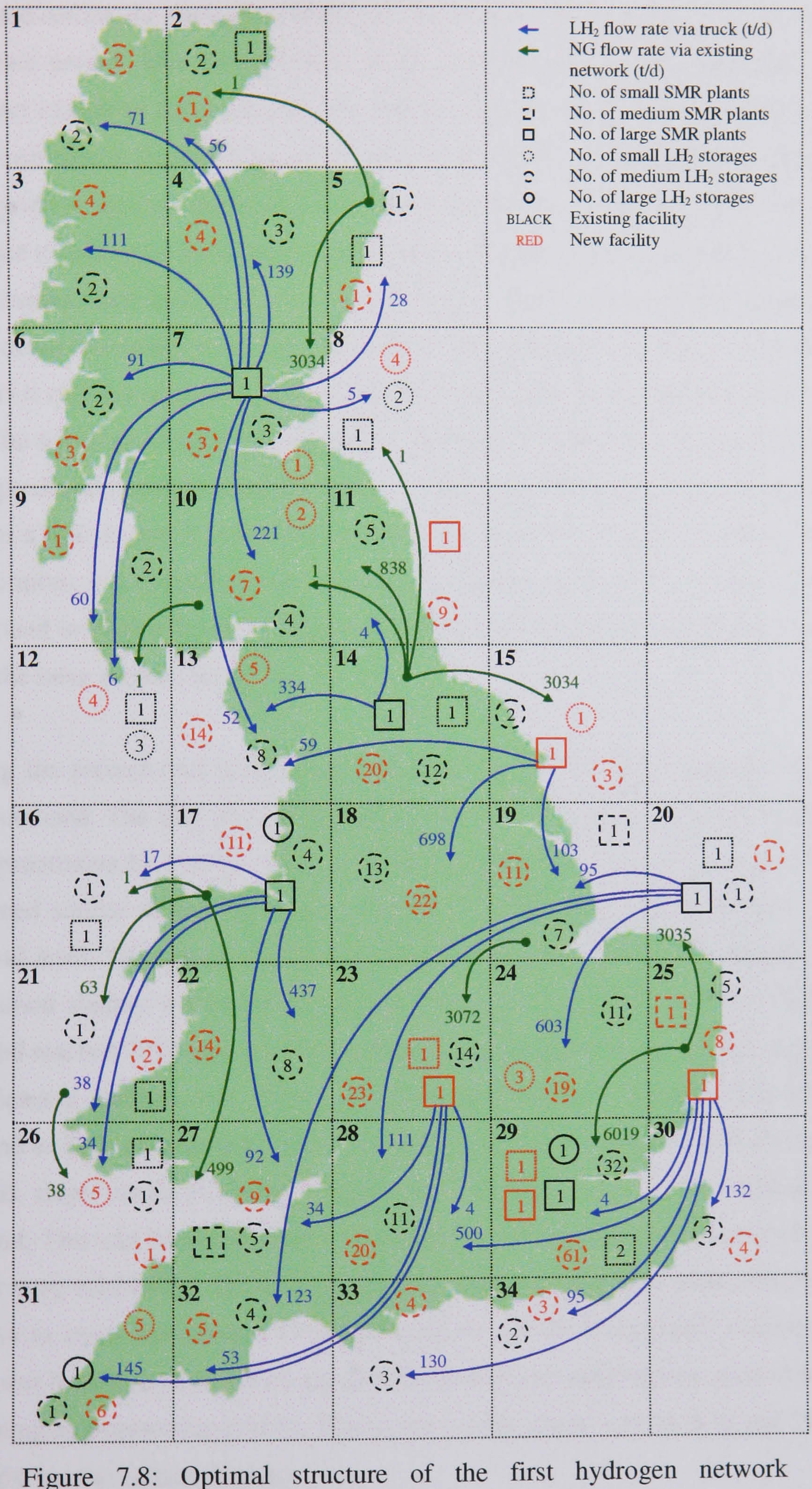


Figure 7.8: Optimal structure of the first hydrogen network configuration during time period 3 and scenario 9.

As stated earlier, the demand of hydrogen was assumed to be deterministic during the first time period. This demand level is the consequence of 5% penetration of the transport market by hydrogen fuel cell vehicles. The network structure resulting from this penetration is shown in Figure 7.2. It is evident from the figure that the demand in most grids is met by medium-to-large steam methane reforming plants, which are assumed to exist prior to the hydrogen economy. Besides these large plants, grids with low demand, such as 2, 8, 12, 20, and 26, satisfy their needs by establishing small-scale steam reforming plants. The feedstock of these plants is obtained from the grid itself if it contains a natural gas terminal, or from nearby grids abundant with natural gas. The figure also shows that the overall demand of hydrogen is mainly fulfilled by three production sources located in grids 7, 17, and 29. This observation suggests that there is a high degree of centralisation during the initial phase of the hydrogen market. Furthermore, it is interesting that the network structure in Figure 7.2 is identical to the one found in Figure 5.3 (see Chapter 5). This is due to the fact that these networks have the same demand level.

During the second time period, the network structures for three demand scenarios were outlined. The first network structure, which is depicted in Figure 7.3, assumes 15% penetration by hydrogen fuel cell vehicles. In this figure, the network structure remained similar to the one given in Figure 7.2 due to the minor increase in the demand level. To manage this increment, the production rate of the existing plants was raised slightly without installing new production facilities. However, when the demand reached 20%, only one small steam reforming plant was enough to cope with this demand addition (see Figure 7.4). The third network structure describes the demand at 25% of hydrogen fuel cell vehicles entering the current transport market. At this stage, more production plants were required to meet the corresponding demand. This can be demonstrated in Figure 7.5 where five extra steam reforming plants were established. Of these plants, one small and one large plant were built in grid 14 to cover the demand of South Scotland and North England. Another large plant was built in grid 20 which satisfies the demand of neighbouring grids instead of importing hydrogen from grid 29. The last two small plants were built in grid 29 since this grid has the highest demand.

The network structure for the middle demand scenario, i.e. Figure 7.4, is compared to the one obtained in Figure 5.4. This is because both networks were designed to satisfy the hydrogen demand at 20% penetration of fuel cell vehicles. It can be seen from both figures that the network configurations are somewhat similar, especially the network structure covering Scotland. The main difference is the establishment of a large plant in grid 19 in Figure 5.4, which provides grids 18, 20, 23, 24, and 25 with their hydrogen needs. However, in the case of Figure 7.4, the demand of these grids was met by the plants in grid 29. Such unlikeness indicates that building a plant in grid 19 during the second time period seems to be more economical than constructing the plant at the forthcoming time periods. Yet, this option could not give the optimal cost for the network structure in Figure 7.4 due to the effect of multiple demand scenarios.

The remaining Figures 7.6–7.8 demonstrate the network structures at 30, 50, and 70 percent demand level, respectively. Out of the nine demand scenarios studied, these network structures were chosen because they represent the worst, middle and best paths during the third time period. When the demand grows to 30%, a new large steam methane reforming plant is installed in grid 16. This plant covers the demand of Wales and the South West of England instead of utilising the plants in grid 17, as in Figure 7.5. Additionally, grid 14 has another large plant in order to meet the required demand. Moving to the middle network configuration, it is interesting to note that the production sources were increased from five nodes in Figure 7.6 to eight in Figure 7.7. Hence, the hydrogen network started to become more decentralised as demand level increased. Also at this stage, building a coal gasification plant becomes attractive with respect to producing hydrogen via steam methane reforming due to the availability of large quantities of coal. This example is shown in grids 5 and 25 where each grid has a large-scale coal gasification plant. The feedstock of these plants was imported from nearby coal mines located at grids 7, 23 and 24. The last network structure describes the demand of hydrogen when it reaches 70%. As expected, satisfying this demand will lead to a solution with high a degree of decentralisation (see Figure 7.8).

The second network configuration examined in this chapter is related to transporting liquid hydrogen via tanker trucks and railway tank cars. As with the first network

configuration, only the network structures for demand scenarios 1, 5, and 9 over the three time periods will be discussed. These network structures are shown in Figures 7.9–7.15, respectively.

To avoid repetition, the network structures depicted in Figures 7.9–7.15 will not be analysed in depth as was done with the first network configurations. However, the discussion will focus on the main factors that led to the differences between the single- and multi-mode network structures. The first factor behind this dissimilarity is the high storage capacity of railcars in comparison to tanker trucks. This implies that railcars would have fewer trips between the production sites and storage facilities. As a result, railcars could be dispatched to customers even at low-to-moderate utilisation tank capacity, whereas trucks will be sent only at full tank capacity. The second factor is the low operating transportation cost of railcars. Thus, this would make long delivery distances more favoured. In a multi-mode network, truck will be utilised only for short delivery distances.

Examining the network structures of the single- and multi-mode cases shows that the type of transportation modes has a great affect on the arrangement of production plants. In the single-mode network, production plants were usually located in a way that minimised the delivery distance between production sources and customers. Also plant production will be increased until demand cannot be met by existing capacity. On the other hand, these two issues are more flexible in the multi-mode network since delivery distance is not a critical factor due to the cheap transport cost. The previous discussion can be illustrated by looking at Figures 7.5 and 7.12. Figure 7.5 shows that there is no production plant in grid 5 because grid 7 together with grid 14 cover most parts of Scotland with the minimum possible delivery distances. However, in Figure 7.12, grids 5 and 14 provide neighbouring grids with hydrogen even though this results in longer delivery distances.

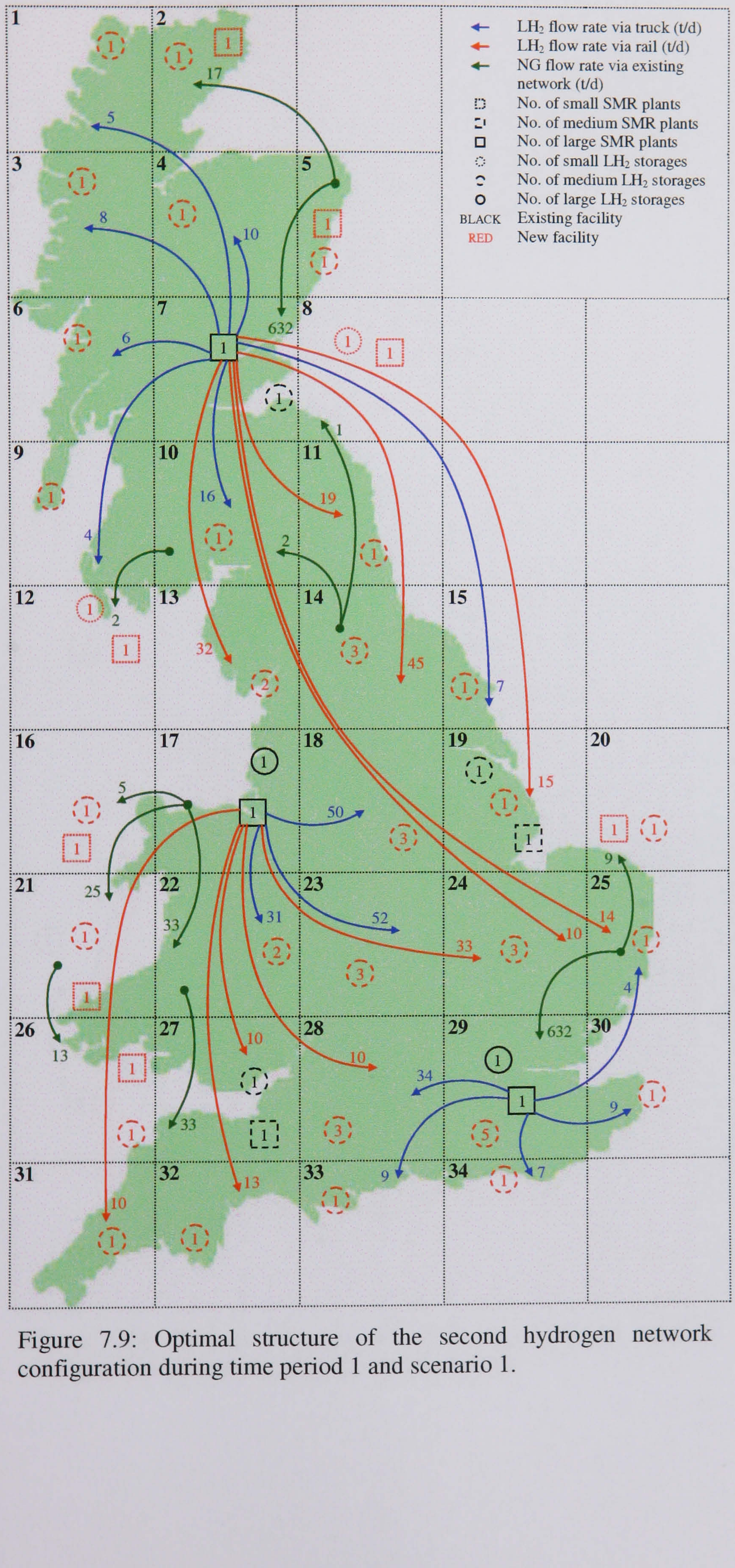


Figure 7.9: Optimal structure of the second hydrogen network configuration during time period 1 and scenario 1.

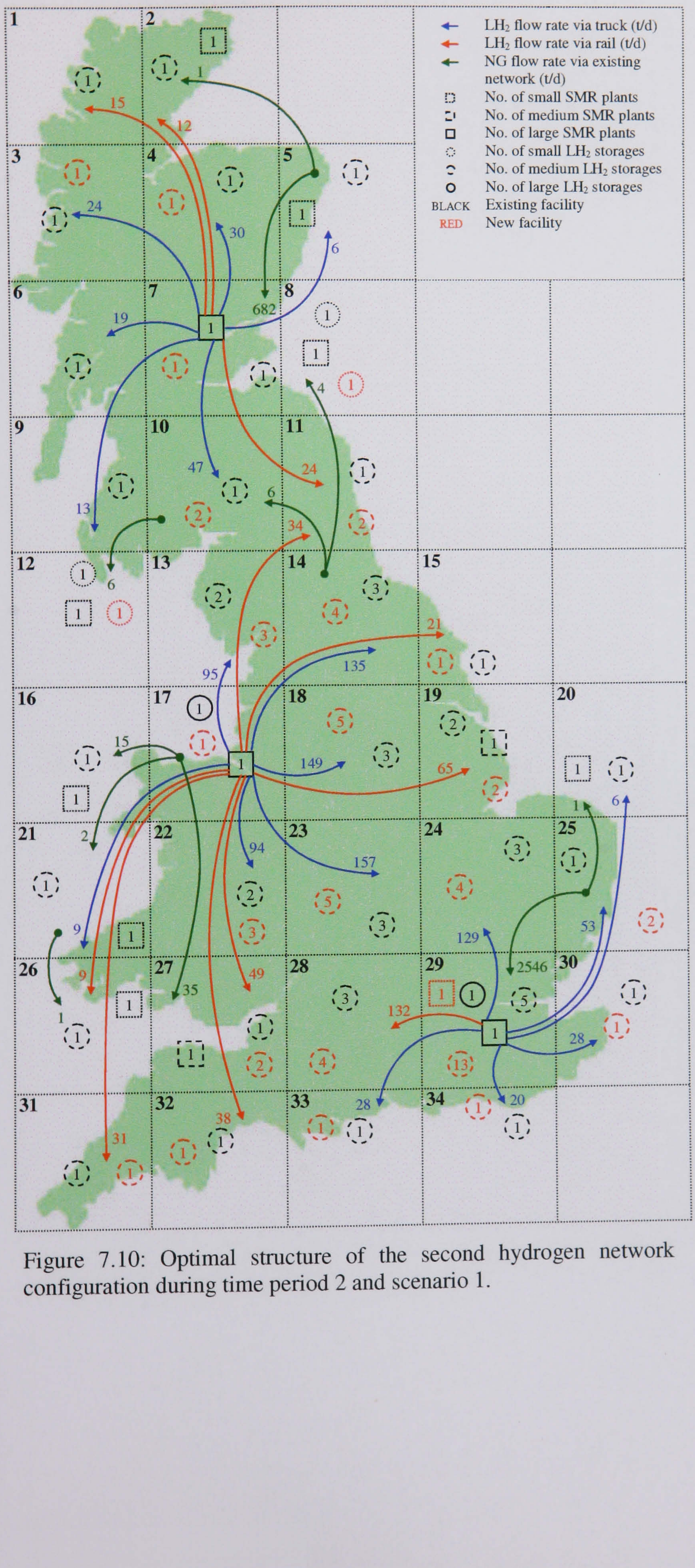


Figure 7.10: Optimal structure of the second hydrogen network configuration during time period 2 and scenario 1.

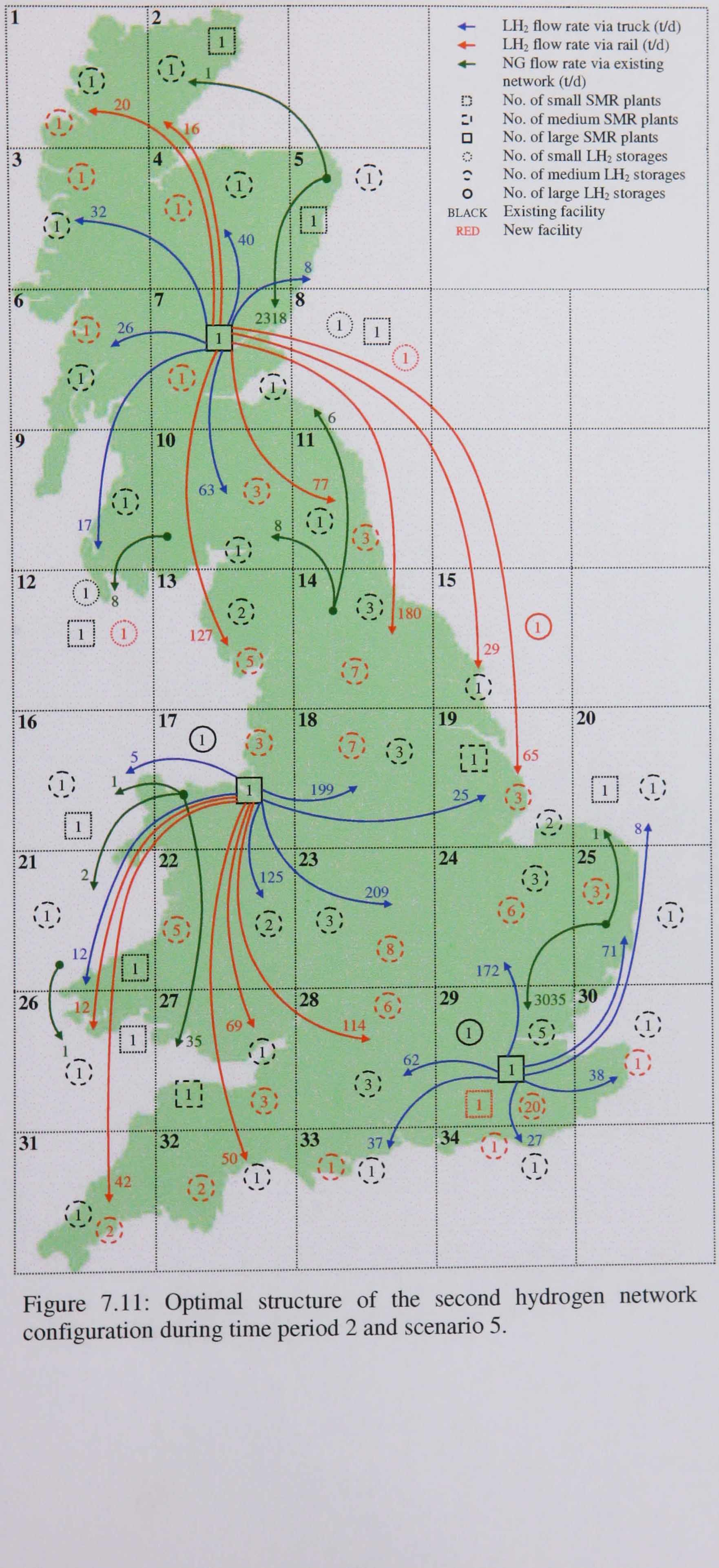


Figure 7.11: Optimal structure of the second hydrogen network configuration during time period 2 and scenario 5.

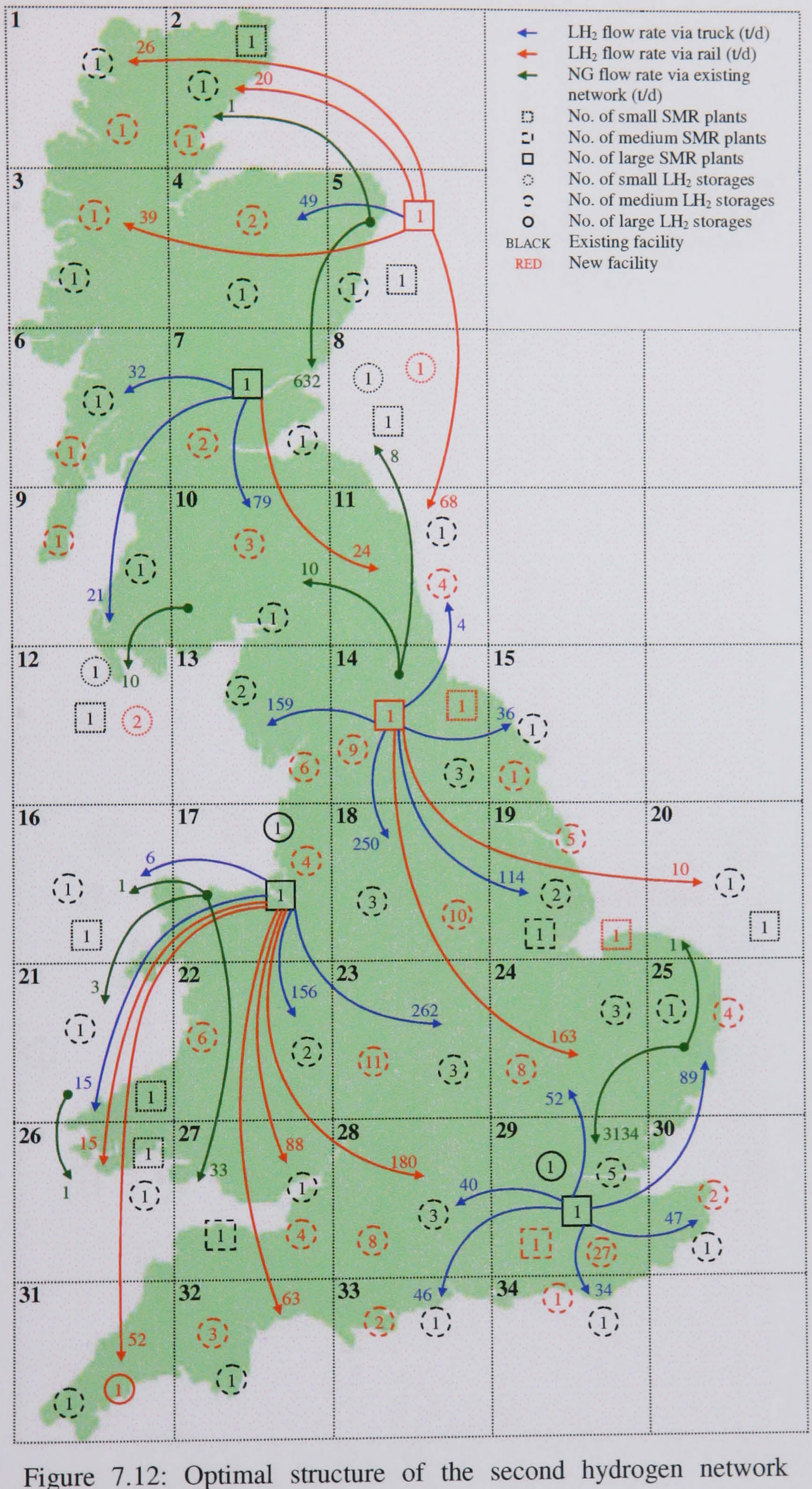


Figure 7.12: Optimal structure of the second hydrogen network configuration during time period 2 and scenario 9.

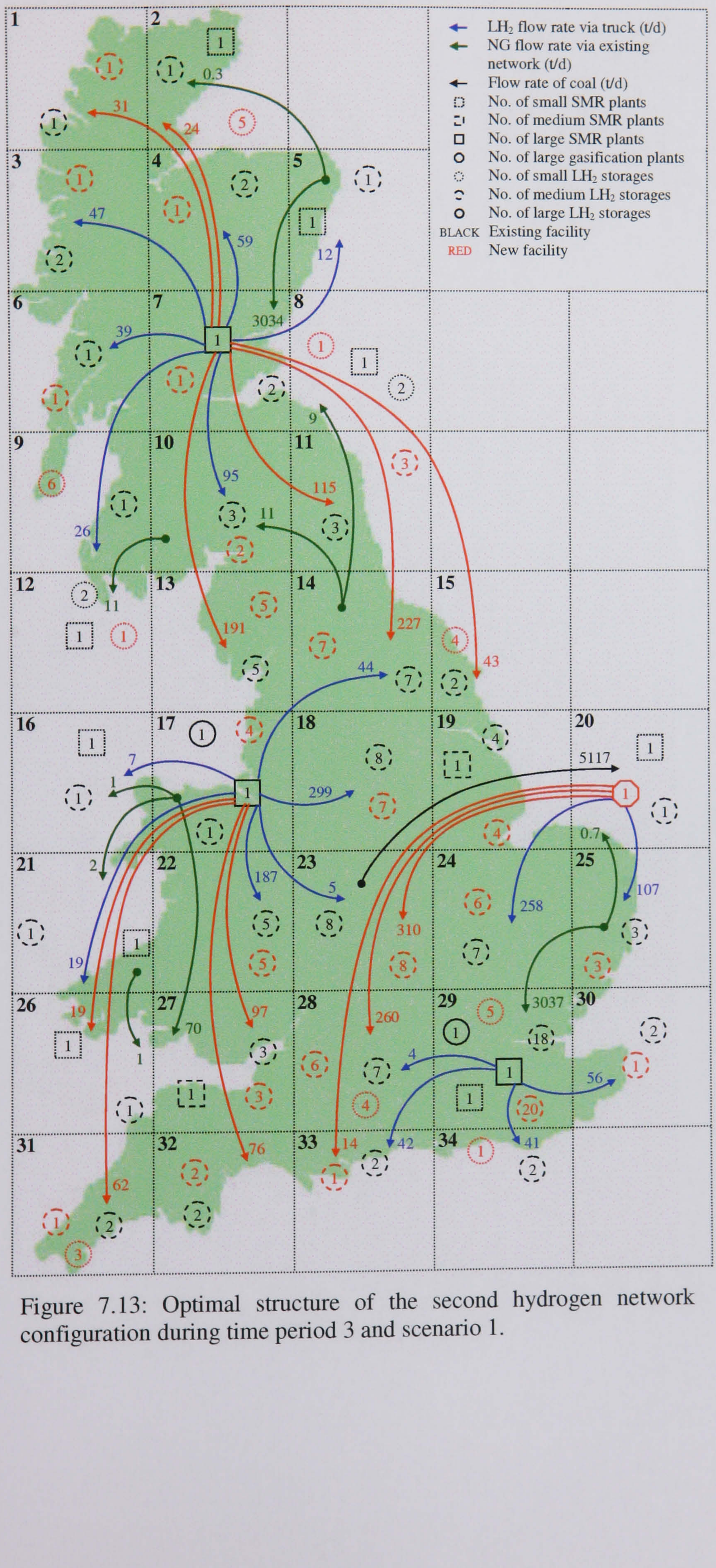


Figure 7.13: Optimal structure of the second hydrogen network configuration during time period 3 and scenario 1.

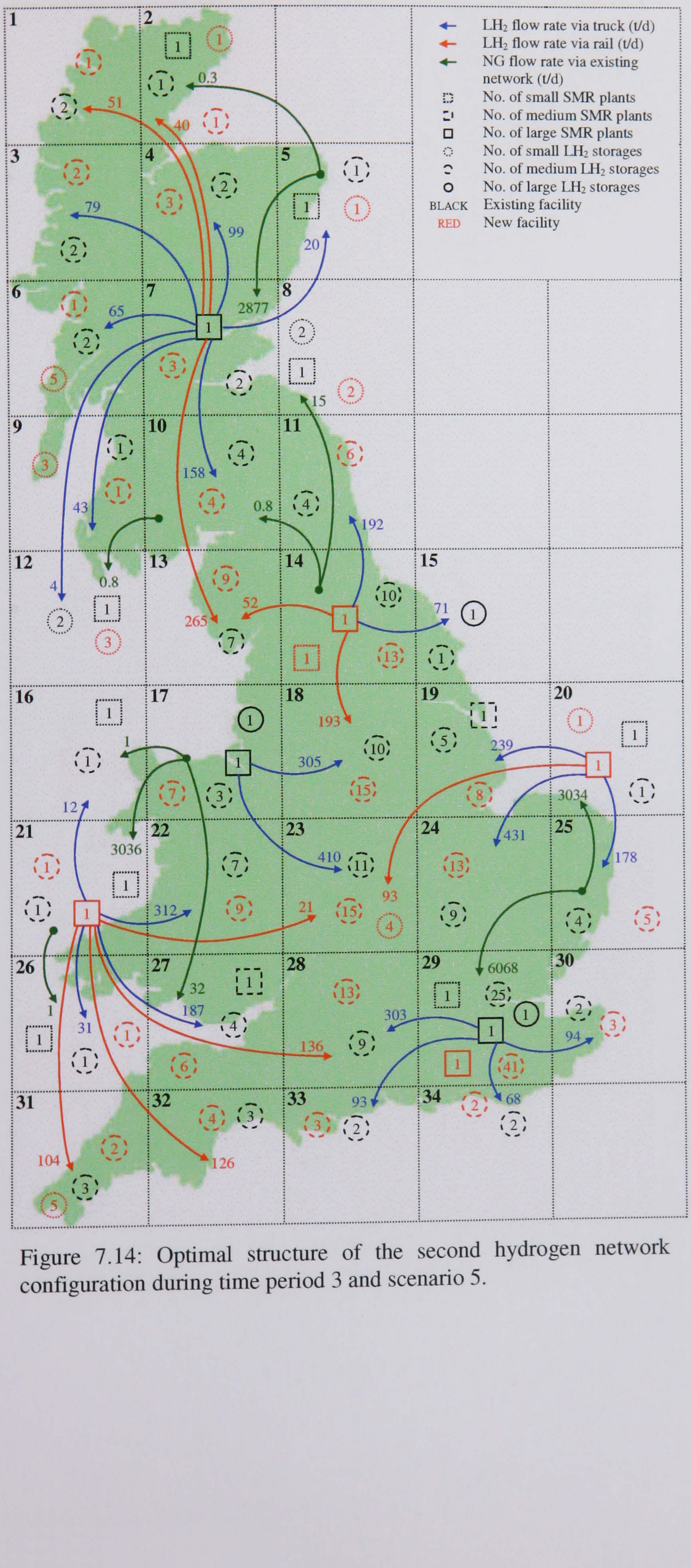


Figure 7.14: Optimal structure of the second hydrogen network configuration during time period 3 and scenario 5.

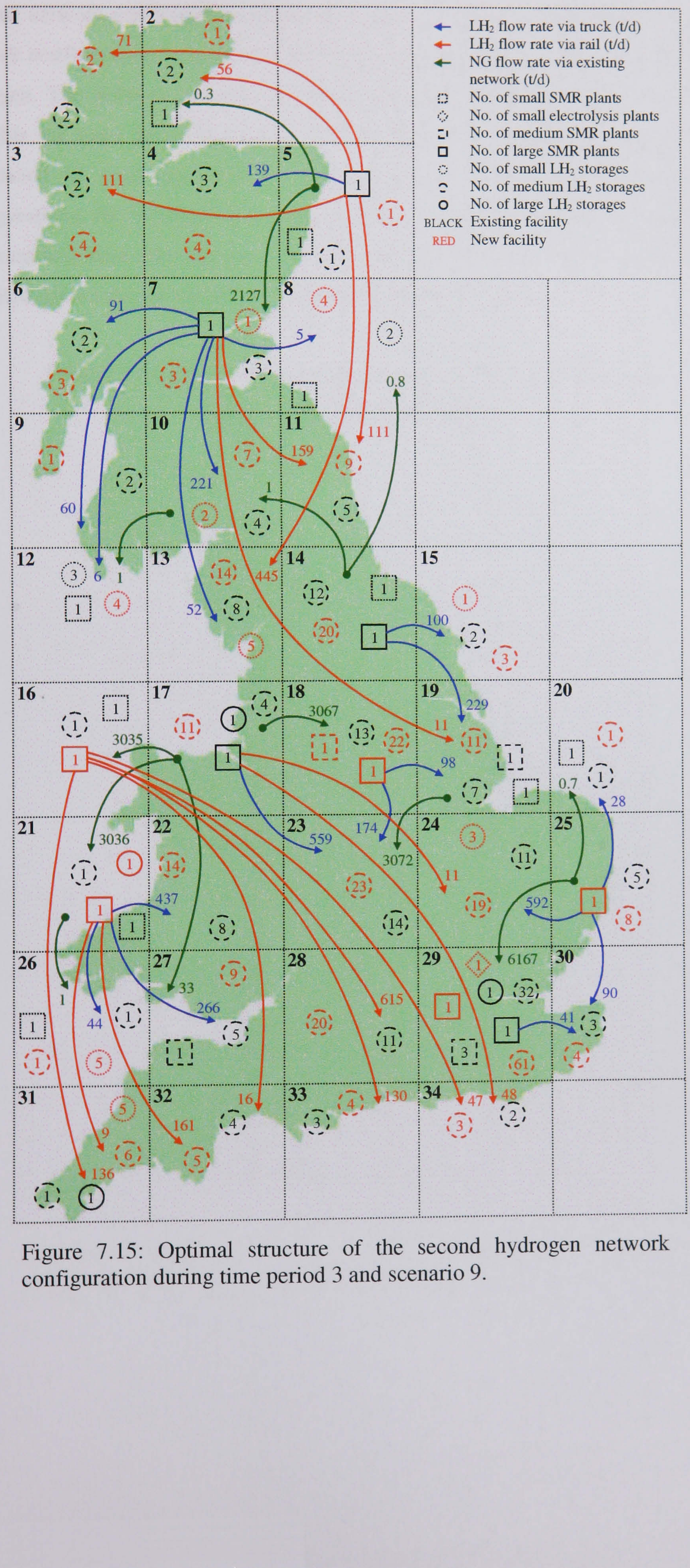


Figure 7.15: Optimal structure of the second hydrogen network configuration during time period 3 and scenario 9.

The last network configuration addressed in this chapter is the extension of the first network configuration to account for fuelling stations and secondary distribution of hydrogen. The network structures for this case study will not be shown since they resemble the ones given in Figures 7.2–7.8. Only the number of fuelling stations established in each grid will be given here. As with the previous network configurations, the corresponding results will be shown for scenarios 1, 5 and 9 over the examined three time periods. These numbers are tabulated in 7.7 and 7.8. The tabulated figures do not include the number of distributed plants.

Table 7.7: Number of fuelling stations during the first time period

Grid, g	No. of fuelling stations
01	1
02	1
03	2
04	2
05	0
06	1
07	2
08	0
09	1
10	3
11	4
12	0
13	6
14	9
15	1
16	0
17	5
18	10
19	5
20	0
21	0
22	6
23	10
24	9
25	4
26	0
27	4
28	9
29	27
30	2
31	2
32	3
33	2
34	1

Table 7.8: Number of fuelling stations during the second and third time periods

Time period, t	t_2			t_3		
Scenario, k	k_1	k_5	k_9	k_1	k_5	k_9
01	3	4	5	6	10	14
02	2	3	4	5	8	11
03	5	6	8	9	16	22
04	6	8	10	12	20	28
05	1	1	1	1	3	5
06	4	5	6	8	13	18
07	5	7	9	10	17	24
08	0	0	0	0	0	1
09	3	3	4	5	9	12
10	9	13	16	19	32	44
11	12	15	19	23	38	54
12	0	0	0	0	0	1
13	19	25	31	38	64	88
14	27	35	45	54	89	125
15	4	6	7	9	14	20
16	0	0	1	1	1	2
17	15	20	24	29	49	66
18	30	40	50	60	100	140
19	15	20	25	30	50	70
20	1	1	1	1	3	5
21	1	2	2	3	5	8
22	19	25	31	37	62	87
23	31	42	52	63	105	147
24	26	34	43	52	86	121
25	11	14	18	21	36	50
26	1	2	2	3	5	8
27	12	16	19	24	38	52
28	26	35	44	53	88	123
29	80	108	136	158	272	382
30	6	8	9	11	19	26
31	6	8	10	12	21	29
32	8	10	13	15	25	35
33	6	7	9	11	19	26
34	4	5	7	8	14	19

Tables 7.7 and 7.8 illustrate that grids with low demand, such as 8, 12, and 16, have no fuelling stations due to the presence of distributed plants. These plants replace the need for installing fuelling stations since they operate as fuelling source. However, as the demand of these grids increased, new fuelling stations were built due to the failure of existing plants to cope with the increased demand. In addition, the tables show that the number of fuelling stations is dependent upon the demand of individual grids. Therefore, grids with a high demand level will have a large number of fuelling stations.

For each of the examined network configurations, the average daily cost for the nine scenarios over the entire planning horizon is summarised in Table 7.9. The table also

shows the expected total daily cost of the network under all demand scenarios. It can be seen from the table that the middle scenario has the highest cost. This is because the middle scenario was assumed to have the highest probability value (see Table 7.4). This assumption was based on the fact that the demand trajectory is expected to follow this path during the dawn of hydrogen economy.

Table 7.9: Summary of cost for the studied network configurations (million $/d)

Scenario, k	Configuration		
	1	2	3
k_1	0.39	0.39	1.29
k_2	0.99	0.99	2.19
k_3	0.59	0.60	1.88
k_4	1.09	1.03	2.25
k_5	2.73	2.47	4.05
k_6	1.46	1.44	3.03
k_7	0.72	0.66	2.17
k_8	1.54	1.55	3.20
k_9	0.87	0.88	2.68
Total cost	*10.39*	*10.02*	*12.21*

As with the previous models, the three network configurations of interest were solved as MILP problems using GAMS with CPLEX v9.0 code. A Pentium 4, 1.8 GHz Dell machine was used to execute the run. The computational results of these configurations are summarised in Table 7.10. It can be observed that the size of the examined configurations increased by more than eight-fold when compared to the one addressed in Chapter 5. This is due to the introduction of demand uncertainty. Although the model has a large dimension, the optimality gap and time required for solving these configurations are promising.

Table 7.10: Summary of computational results for the stochastic model

Configuration	1	2	3
Number of constraints	379820	563658	430336
Number of continuous variables	200980	231886	202060
Number of integer variables	77724	108630	168606
Optimality gap (%)	6	3	9
CPU time (d)	3	3	3

7.5.3 Risk Analysis

A risk analysis was conducted to study the effect of demand uncertainty in the outcomes of the total network cost. The analysis would also describe the distribution of the cost profile for all demand scenarios. The shape of this profile will determine the degree of risk since a wider distribution means a more risky solution. To perform the analysis, the first network configuration was chosen as the base case for this study. Then, the probability of demand scenarios occurring during the network's lifetime was plotted versus the average total daily cost at each scenario. Figure 7.16 illustrates the cost histogram profile for the examined base case.

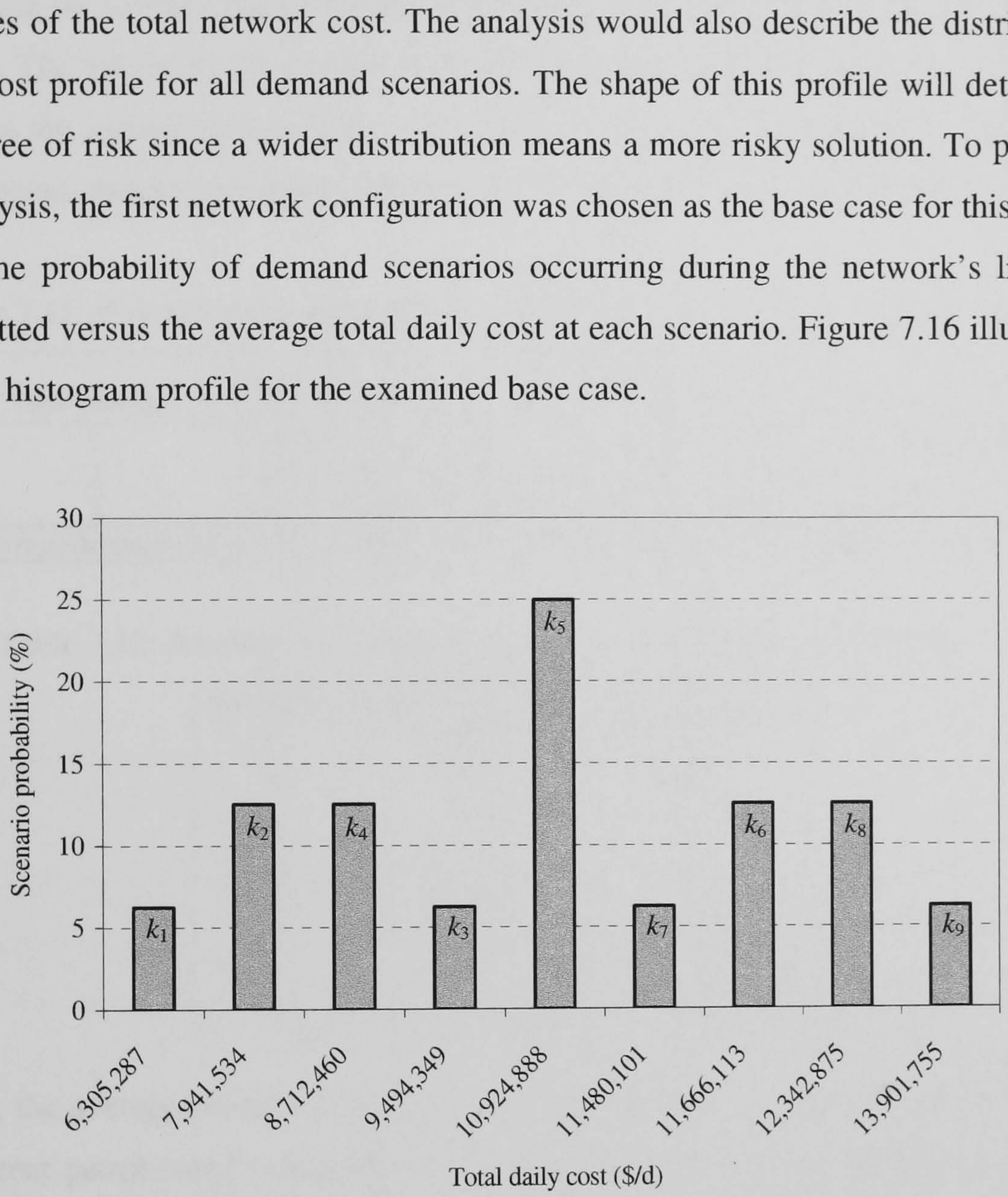


Figure 7.16: Cost profile of the base case.

It can be noticed from Figure 7.16 that the cost profile has a normal distribution. The middle histogram corresponds to scenario 5 which has the highest probability of occurrence, i.e. 25%. The average total daily cost of this scenario is about 11 million $/d. The worst-case scenario for this set of data has a cost of 6 million $/d with a probability of 6.25% while the best-case scenario has a cost of 14 million $/d with the same probability of occurrence. The last two cases represent scenarios 1 and 9, respectively. It can be inferred from the above figure that the width of the cost profile is reasonable despite the wideness of the demand range.

The average total cost of the hydrogen supply chain network for each scenario was given in $/d. In order to arrive to a meaningful unit given the demand variations, the $/d was converted to $/t of hydrogen delivered. This conversion was carried out by calculating the average daily demand of hydrogen for each scenario over the planning horizon. The values of the average daily demand for the three time periods and nine scenarios are summarised in Table 7.11. Then, these values were divided by the daily cost to obtain the cost per tonne delivered for each scenario, as shown in Table 7.12.

Table 7.11: Average daily demand of hydrogen for each scenario and time period

Time period, t	Scenario, k								
	k_1	k_2	k_3	k_4	k_5	k_6	k_7	k_8	k_9
1	670	670	670	670	670	670	670	670	670
2	2009	2009	2009	2679	2679	2679	3349	3349	3349
3	4018	5358	6697	5358	6697	8037	6697	8037	9376
Average demand (t/d)	2232	2679	3125	2902	3349	3795	3572	4018	4465

Table 7.12: Average total cost of hydrogen network per tonne delivered

Scenario, k	Probability (%)	Network cost ($/t)
k_1	6.25	2824
k_2	12.50	2964
k_4	12.50	3002
k_3	6.25	3038
k_8	12.50	3072
k_6	12.50	3074
k_9	6.25	3114
k_7	6.25	3214
k_5	25.00	3262

Finally, the average network cost was expressed in $/km to compare it to the cost of the current petrol supply chain network. This was achieved by multiplying the cost per tonne by the average fuel economy of PLG and buses, which is 0.0636 km/kg (see Appendix A). The results are listed in Table 7.13.

Table 7.13: Average total cost of hydrogen network per kilometre

Scenario, k	Probability (%)	Network cost ($/km)
k_1	6.25	0.180
k_2	12.50	0.189
k_4	12.50	0.191
k_3	6.25	0.193
k_8	12.50	0.195
k_6	12.50	0.196
k_9	6.25	0.198
k_7	6.25	0.204
k_5	25.00	0.208

To visualise the shape of the cost histogram profile, the probability of each scenario was plotted versus the cost per kilometre. Figure 7.17 depicts the obtained profile.

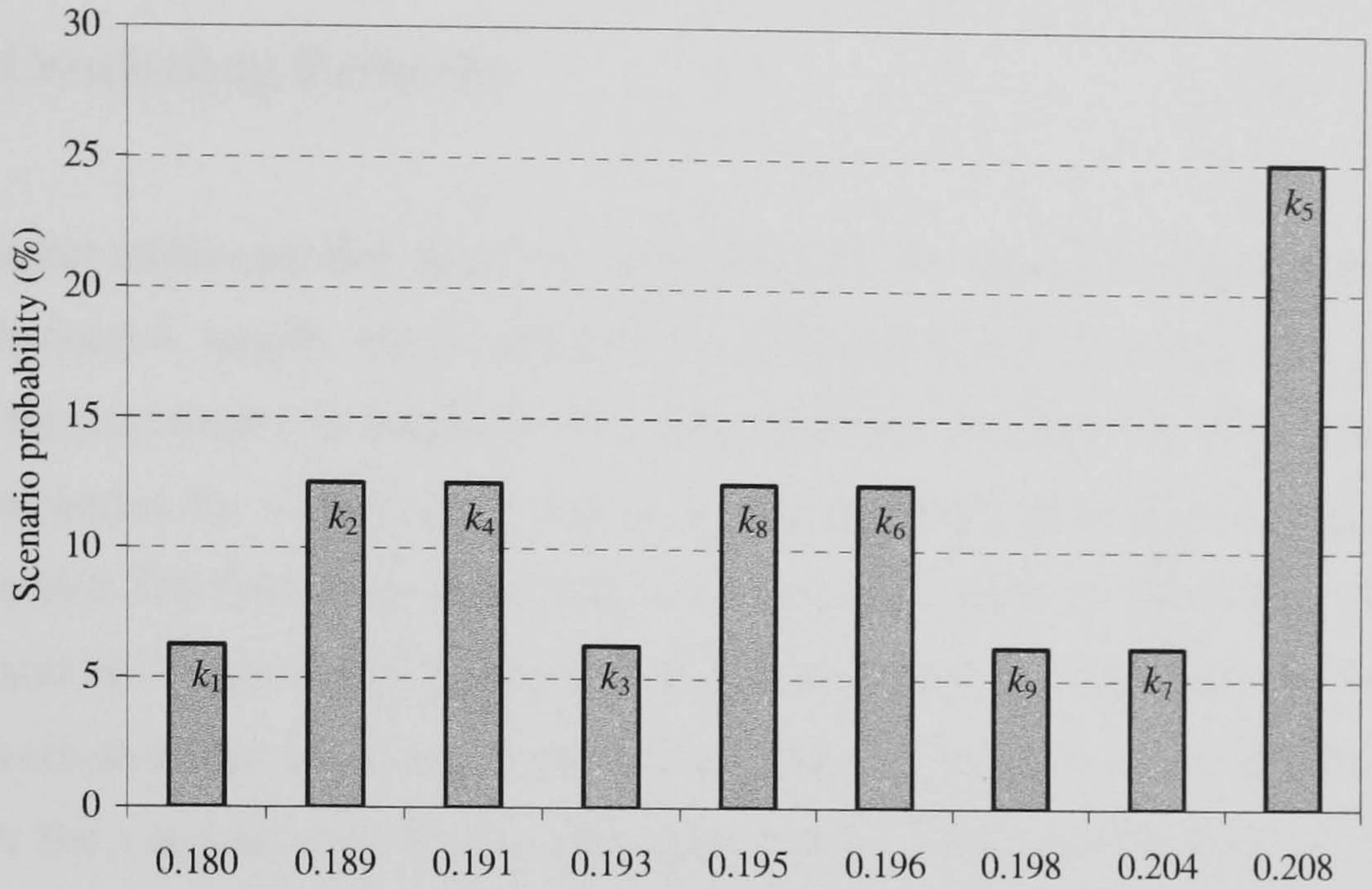


Figure 7.17: Probability versus the cost of hydrogen network per kilometre.

From the above Figure, the network cost for the middle-case scenario is 0.208 $/km. This value is compared to the cost of the existing petrol network. According to our calculation, the cost of a petrol network is 0.107 $/km, which is obtained based on the assumptions given in Table 7.14.

Table 7.14: Assumptions used to estimate the cost of the current petrol network

Parameter	Value
Average price of untaxed petrol ($/L)	0.75
Fuel economy of ICE car (km/L) [14]	12.69
Fuel economy of ICE bus (km/L) [119]	1.30
Average distance travelled (km/yr/mode) [120]	16605

Using the average annual distance travelled per vehicle, the cost of hydrogen and petrol infrastructures were estimated to be 3447 and 1780 $/yr/vehicle, respectively. It is evident from these figures that the cost of a hydrogen infrastructure is roughly twice that for untaxed petrol. The main reasons behind this are the high costs of hydrogen production, storage, and distribution technologies. However, it is expected that in the near future the cost of hydrogen technologies will decrease enough to compete with

its opponent. Despite the soaring cost of a hydrogen infrastructure, building such an infrastructure would improve the urban air quality and reduce foreign oil imports.

7.5.4 Concluding Remarks

This chapter addressed the effect of uncertainty on the design and operation of the future hydrogen supply chain network. A scenario-based approach was used to capture the uncertainty in demand over a long-term planning horizon. This uncertainty was represented by a three-stage stochastic optimisation problem formulated as an MILP model. The first stage was assumed to have a deterministic behaviour while the second and third stages were subject to demand variations. For each demand scenario, the network structure was revealed and its average total daily cost was determined. In addition, the expected cost of the hydrogen supply chain network over all demand scenarios was resolved. Since the problem of interest is a continuation of the multi-period model, the same strategic design decisions were determined but within a scenario-based context.

The second part of this chapter studied the extension of the stochastic model to accommodate fuelling stations and secondary distribution of hydrogen. As with the stochastic model, the resulting multi-echelon model was formulated as an MILP problem within a three-stage stochastic framework. The new decisions established by the stochastic, multi-echelon model were: (1) determining the number of fuelling stations installed in each grid and their operating cost, and (2) estimating the total cost associated with secondary distribution.

The feasibility of the derived models was tested by revisiting the case study presented in previous chapters but under demand uncertainty. As a result, the optimal network structures for three different configurations were outlined. In all of these network configurations, steam methane reforming technology was mostly chosen as a means of producing hydrogen due to its economical benefits. In the case of natural gas shortages, other production technologies such as coal gasification and water electrolysis were utilised because of their local availability. Such options were more profitable than importing natural gas from foreign countries. The size of these plants

varied according to the local demand of each grid. For instance, during the early phase of hydrogen introduction distributed plants were established for the most part. But as demand reached its saturation point more centralised facilities emerged.

The results obtained also show that the type of transportation mode has a great effect on the structure of hydrogen supply chain network. For example, the transport of hydrogen via trucks only resulted in short transportation links with high utilisation capacities. On the other hand, allowing both rail and truck for hydrogen delivery resulted in longer transportation links with low-to-high flow rates.

It has been shown from the examined network configurations that the consideration of demand uncertainty may lead to significant changes in the structure and cost of the optimal supply chain network. Due to this a risk analysis was carried out to evaluate the degree of risk during the existence of uncertainty. The solution found suggests a reasonable distribution profile despite the wide range of demand.

Chapter 8

Conclusions and Further Work

This chapter provides a summary of the main findings of this thesis. It also outlines some of the potential directions for future work in the area of hydrogen supply chain design.

8.1 Contribution of this Thesis

The design of the future hydrogen supply chain network is a difficult task due to several reasons. The first is the involvement of many hydrogen components within the design framework, including production plants, storage facilities, transportation modes, and fuelling stations. This involvement would increase the level of interactions between these sub-systems; hence increase the complexity of the hydrogen supply chain network. The degree of this complexity is increased by the considerable uncertainty in product demand. The second reason that affects the design of a future hydrogen supply chain is the stringent existing environmental regulations. This is characterised by the governments' pressure on automobile and energy companies to mitigate CO_2 emissions and other harmful pollutants. The third reason behind this difficulty is the concern to build a long-term viable hydrogen supply chain network. Viability and sustainability of the future energy infrastructure are crucial issues, especially for hydrogen since it can be produced from a variety of feedstocks at a wide range of sizes from city scale to household level. Collecting the necessary and right data marks the fourth reason for the difficulty in designing a hydrogen supply chain. This common problem stems from the breadth of the supply chain itself. In summary, all of the abovementioned reasons will significantly influence the strategic decisions involved in choosing the optimal configuration of a future hydrogen supply chain network.

In the past, the complexity of hydrogen supply chain design restricted research efforts to analysis of individual components of the supply chain such as production, storage, or distribution technologies. Also, this difficulty directed researchers towards using a simulation-based approach in designing the future hydrogen supply chain. Simulation is used to mimic the behaviour of pre-defined hydrogen pathways, test these pathways, and compare alternatives according to some performance measures such as cost and CO_2 emissions. Recently, however, attention has been increasingly drawn to focus on the design and operation of the hydrogen supply chain as a whole utilising an optimisation-based approach. Optimisation is a powerful and flexible technique for finding the best feasible solution for supply chain design problems, compared with the traditional "what if" approach. Making use of the optimisation method will assist in identifying the optimum configuration of the future hydrogen supply chain network before it develops organically. This may be of vital importance in forming national and international policy as well as strategic decisions in industry

The objective of this work has been to develop quantitative tools that can support strategic decisions in hydrogen supply chain design and operation. The proposed mathematical models outline the optimal configuration of hydrogen supply chain network for vehicular use in Great Britain. These models comprise: grid squares, storage facilities, transportation modes, fuelling stations, and production plants in which a number of product forms are produced. The decisions to be determined by these models were: (1) the location, number, and capacity of the previously mentioned components, (2) the production rate of plants and average stored inventory of hydrogen, (3) the flow rate of hydrogen and primary energy sources throughout the network, and (4) the local availability of primary energy sources. Moreover, these models were mainly driven by hydrogen demand, which was assumed to be known beforehand.

Within this thesis, five distinct models were developed to describe the design and operation of future hydrogen supply chain. The first model considered a steady-state formulation of the hydrogen network at one point in time with a deterministic demand. The model was then extended to account for local availability of primary energy sources as well as various sizes of production and storage facilities. The second model also took account of the local distribution of hydrogen within grids

together with regional distribution between different grids. Building upon the second model, the evolution of demand over a long-term planning horizon was introduced in the third model. During each time period, the optimal structure of hydrogen network was determined. The fourth model examined the uncertainty arising from long-term variations in hydrogen demand using a scenario-based approach. Finally, in the last model, the multi-period and the stochastic models were extended to a multi-echelon case. This extension took into consideration the establishment of fuelling stations as well as the secondary distribution of hydrogen from production plants or storage facilities to fuelling stations.

The versatility of the derived models was examined using different configurations of hydrogen supply chain. These configurations were applied to Great Britain due to its active involvement in the hydrogen and fuel cell programme, amongst others. The configurations of interest were alike in terms of the type and size of production and storage technologies. They also utilised the same type of primary energy sources. The key difference between these configurations lied in the type of transportation modes used. Some configurations used trucks and others used rail and trucks for hydrogen transport. The reason behind this variation was to study the effect of these modes on the design of a hydrogen network structure as well as to compare the differences in cost. All of these configurations dealt with the production, storage, and distribution of liquid hydrogen. The only exception was network configuration 2 discussed in Chapter 3 where compressed hydrogen gas was considered. This was to determine whether liquid- or gaseous-based hydrogen network is more cost-effective.

Based on our assumptions and taking cost as a performance measure, it is found that the optimal configuration of the future hydrogen supply chain is the production of liquid hydrogen in steam methane reforming plants. The size of these plants varies from one location to another according to the level of hydrogen demand. During a market fully dependent on hydrogen, centralised large-scale plants producing bulk quantities are the best feasible solution. However during the transition phase, local production of hydrogen at fuelling stations via distributed small-scale plants seems to be the best strategy. This option should be coupled with the usage of uncommitted hydrogen generated from the existing petroleum refineries or petrochemical plants. Between these two scenarios, the production of hydrogen can be tailored in

accordance to demand variation by installing small, medium, or large steam reforming plants. Since steam methane reforming technology is utilised mostly, the feedstock of these plants are obtained from natural gas terminals via the current national natural gas transmission network.

The second part of the optimal network configuration is the transportation of liquid hydrogen from the production sources to the storage terminals. Tanker trucks and railway tank cars were found to be the cheapest option for distributing hydrogen. Another option was to distribute hydrogen via tanker trucks only. Based on our assumptions, this method is slightly more expensive than using both trucks and rail. However, truck transport is preferable over rail since it enjoys considerable advantages from a logistics perspective, such as flexibility in operation and ease of accessibility to road infrastructure. In summary, it is expected that the future hydrogen supply chain would make use of both modes for distributing hydrogen in order to cover the wide range of demand levels. This is analogous with the current petroleum supply chain in which tanker trucks are used for short delivery distances and low-to-moderate quantities. On the other hand, railway tank cars are utilised for long delivery distances and large quantities.

The last part of the optimal network configuration is the storage of liquid hydrogen in super-insulated spherical tanks. Different sizes of storage tank were used ranging from small, medium, to large scales. The size of these tanks was determined by the volume of demand in each grid. These tanks were built to accommodate several days of storage in order to satisfy daily and seasonal demand fluctuations. Finally, the stored hydrogen was dispensed to customers through a number of fuelling stations.

From the obtained network configuration, it can be inferred that the future hydrogen supply chain network is somewhat similar to the existing petroleum supply chain in terms of production, distribution, and storage. In both supply chains, centralised production plants with truck and rail transport are found to be the best feasible solution. Also both configurations make use of small-to-large storage facilities. The main difference is that steam methane reforming plants can be used in forecourt production of hydrogen at local fuelling stations. This advantage is not possible in refineries due to economical and technical barriers.

A further possible configuration of the future hydrogen supply chain is the production of compressed hydrogen gas from natural gas in steam reforming plants. The hydrogen will then be transported to storage facilities via tube trailers and railcars, where it will be stored in its gaseous form. Based on the obtained results, this option is very expensive at the current stage. The main reason behind this is the high cost of pressurised tanks as well as the soaring cost associated with storing bulky quantities of hydrogen. Another factor for the high cost of a compressed hydrogen gas network is transportation costs. This is due to the low hydrogen storage capacity per transport container. However, as storage technologies develop in the future, stationary storage of hydrogen on a large scale will become competitive to liquid storage because of the intensive energy required for the liquefaction process. Also, since the delivery cost of hydrogen gas depends on the size of the transport unit, a decrease in storage technologies would result into a minimum distribution cost.

The performance of the studied models was evaluated using sensitivity and risk analyses. Both tests showed how changes in the numerical values of various problem parameters and/or the variations in demand uncertainty may lead to significant changes in the structure of the optimal hydrogen supply chain network. This confirms the impact of input data and demand variability on the design and operation of the future hydrogen supply chain network.

In conclusion, we believe that the work presented has resulted in quantitative tools that are capable of mapping out some of the future hydrogen supply chain configurations, as well as supporting in strategic decision making. However, it has to be remembered that real-life problems may be much larger and more complicated. This is due to the factors discussed earlier and the impact of uncertainty in supply chain network as a whole. In addition, other crucial factors will influence the design of the future hydrogen supply chain, including energy prices of fossil fuels, breakthroughs in hydrogen and fuel cell technologies, environmental- and infrastructural-related issues, as well as public acceptance and safety of hydrogen as a transportation fuel.

8.2 Potential Future Work

Although this thesis discussed a number of design issues concerning the future hydrogen supply chain, there are still several tasks that need further investigation. These tasks are classified into two main categories. The first category is related to the modelling of the hydrogen supply chain while the second category is related to solution algorithms. Each of these aspects will be separately addressed in greater detail below.

8.2.1 Hydrogen Supply Chain Modelling

Carbon Capture and Storage

Hydrogen will be produced initially from steam methane reforming plants. These plants usually produce a considerable amount of CO_2 which is currently released to the atmosphere. The continued emission of CO_2 has already shown a great impact on the environment in terms of global warming and sudden changes of climate conditions. As a result, it has been suggested that steam methane reforming plants should be coupled with a carbon capture and storage process in order to reduce CO_2 emissions. Such technology will capture, transport, and sequester CO_2 into depleted oil/gas fields or salt caverns.

The formulation presented in this work neglects to take into consideration the process of carbon capture and storage. However, the process of carbon sequestration should be taken into account in future work. This could be done by performing a well-to-wheel analysis of CO_2 emissions. The analysis should be used to develop a CO_2 supply chain network in which it can be integrated with the proposed hydrogen supply chain. Incorporating environmental impact within the derived hydrogen supply chain will lead to the design of a multi-objective optimisation based model, i.e. minimising both cost of CO_2 emissions.

Underground Hydrogen Storage

The proposed models only account for above-ground storage of liquid or compressed-gaseous hydrogen. The models, however, fail to address the issue of underground storage of compressed hydrogen gas. This option is considered to be the cheapest hydrogen storage method and can accommodate a huge quantity of hydrogen. However, the main drawback of underground storage is the availability of a suitable storage location. Furthermore, this option would increase the delivery cost because most of the underground storage facilities are located away from consumption sources. Therefore, to include underground storage in our model, we need to carry out an assessment identifying the potential locations in Great Britain that are appropriate for such application. We should also estimate the cost associated with storing gaseous hydrogen below ground.

Pipeline Transport

The cost functions presented in this thesis were mainly derived for container transport of hydrogen via trucks or rail. In order to allow for pipeline transport, new constraints should be added concerning the pressure drop along the pipeline and the number of compressors required for boosting the pressure. Also, the cost equations must be modified to account for the capital and operating costs of hydrogen distribution. Using a pipeline network for distributing hydrogen seems to be a feasible option in regions with a high demand concentration. In addition, pipeline transport insures continuous delivery of hydrogen compared to container transport which is often subject to a number of delays. Moreover, there is no need for storage facilities since pipelines act as flexible storage due to the compressibility of gas.

Hydrogen for Households

Currently, the supply chain network is only designed to provide hydrogen for automobiles. In the future, the network will be modified to take into account stationary energy demand. This can be obtained by calculating the total number of

households and other properties in Great Britain and the average hydrogen demand of each household and non-domestic property. The distribution of the stationary energy demand is likely to be correlated with the population density in each region.

Facilities Shutdown and Reinvestment

At present, the proposed models only invest in new production plants and storage facilities as transitions occur from one supply chain structure to another over time. In real life, the situation would involve the decommissioning of some production and storage facilities and reinvesting in others. For instance, a number of small-scale plants should be closed and a large-scale one should be built instead. Therefore, such feature has to be included into the model formulation.

8.2.2 Solution Algorithms

Throughout this work the capability of MILP formulation to model many components of hydrogen supply chain network has been demonstrated. However, as the number of mathematical expressions increase, the problem becomes large and time-consuming. This observation was made in the case of the multi-period and stochastic models, where multiple time periods and demand scenarios were introduced (see Chapters 5 and 7). To avoid such difficulty, the resulting models can be solved using some types of decomposition approach. Currently, there are a number of decomposition techniques that can be used to solve MILP problems, such as "branch-and-cut" and "branch-and-price". An overview of other decomposition strategies can be found in Nemhauser and Wolsey [121]. It is recommended to apply these techniques to minimise solution time and the problem dimensions.

References

1. Lovins, A.B., E.K. Datta, O.-E. Bustnes, J.G. Kommey, and N.J. Glasgow, *Winning the Oil Endgame: Innovation for Profits, Jobs, and Security*. 2004, Snowmass: Rocky Mountain Institute. 332.
2. Rigden, J.S., *Prologue*, in *Hydrogen: The Essential Element*. 2002, Harvard University Press: Cambridge. p. 1–5.
3. *Hydrogen*, in *The Columbia Encyclopedia*, P. Lagasse, Editor. 2001, Columbia University Press: New York. p. 1346–1347.
4. Romm, J.J., *Why Hydrogen? Why Now?*, in *The Hype about Hydrogen: Fact and Fiction in the Race to Save the Climate*. 2004, Island Press: Washington. p. 11–21.
5. U.S. Environmental Protection Agency (EPA), *US Emissions Inventory 2006: Draft Inventory of U.S. Greenhouse Gas Emissions and Sinks: 1990–2004*. 2006: Washington. p. 1–460.
6. Department of Trade and Industry (DTI), *UK Energy Sector Indicators 2005*. 2005: London. p. 1–121.
7. Department of Trade and Industry (DTI), *Energy White Paper: Our energy future—Creating a Low Carbon Economy*. 2003: London. p. 1–142.
8. Ausubel, J.H., *Where is Energy Going?*, in *The Industrial Physicist*. 2000. p. 16–19.
9. Hefner III, R.A., *The Age of Energy Gases: In the New Millennium*. 2002, Oklahoma City: The GHK Company. 25.
10. Hoffmann, P., *Hydrogen's Discovery: Phlogiston and Inflammable Air*, in *Tomorrow's Energy: Hydrogen, Fuel Cells and the Prospects for a Cleaner Planet*. 2002, The MIT Press: Cambridge. p. 19–25.
11. Wikipedia, *Hydrogen*. 28 February 2006, Wikipedia: The Free Encyclopedia. http://en.wikipedia.org/wiki/Hydrogen.
12. Verne, J., *The Mysterious Island*. 1986, New York: Signet Classic. 512.

13. Hoffmann, P., *A History of Hydrogen Energy: The Reverend Cecil, Jules Verne, and the Redoubtable Mr. Erren*, in *Tomorrows Energy: Hydrogen, Fuel Cells and the Prospects for a Cleaner Planet*. 2002, The MIT Press: Cambridge. p. 27–51.
14. Srinivasan, S., R. Mosdale, P. Stevens, and C. Yang, *Fuel Cells: Reaching the Era of Clean and Efficient Power Generation in the Twenty-First Century*. Annual Review of Energy and Environment, 1999. **24**: p. 281–328.
15. Lovins, A.B., *Twenty Hydrogen Myths*. 2003, Rocky Mountain Institute: Snowmass. p. 1–49.
16. Bush, G.W., *President Delivers "State of the Union"*. 1 February 2003, The White House. http://www.whitehouse.gov/news/releases/2003/01/20030128-19.html.
17. Hoffmann, P., *Why Hydrogen? Buckminster Fuller, Sheikh Yamani, and Bill Clinton*, in *Tomorrows Energy: Hydrogen, Fuel Cells and the Prospects for a Cleaner Planet*. 2002, The MIT Press: Cambridge. p. 1–18.
18. Kruse, B., S. Grinna, and C. Buch, *Hydrogen—Status and Possibilities*. 2002, The Bellona Foundation: Oslo. p. 1–53.
19. Intergovernmental Panel on Climate Change (IPCC), *IPCC Second Assessment Report: Climate Change 1995*. 1996: Geneva. p. 1–73.
20. Intergovernmental Panel on Climate Change (IPCC), *IPCC Third Assessment Report: Climate Change 2001*. 2001: Geneva. p. 1–34.
21. Hustad, C.-W. *A European Perspective on CO_2*. in *7th Annual CO_2 Conference*. 2001. Midland: CO_2-Norway AS.
22. Service, R.F., *Toward a Hydrogen Economy: The Hydrogen Backlash*, in *Science*. 2004. p. 958–961.
23. Intergovernmental Panel on Climate Change (IPCC), *Special Report on Emissions Scenarios*. 2001: Geneva. p. 1–169.
24. Energy Information Administration (EIA), *Annual Energy Outlook 2003*. 2003, U.S. Department of Energy (DOE): Washington. p. 1–267.
25. Cho, A., *Toward a Hydrogen Economy—Fire and ICE: Revving Up for H_2*, in *Science*. 2004. p. 964–965.
26. Pridmore, A. and A.L. Bristow, *The Role of Hydrogen in Powering Road Transport*. 2002, Tyndall Centre for Climate Change Research: Leeds. p. 1–31.

27. British Petroleum, *BP Statistical Review of World Energy 2005*. 2005: Surrey. p. 1–44.
28. Romm, J.J. and C.B. Curtis, *Mideast Oil Forever?*, in *The Atlantic Monthly*. 1996. p. 57–74.
29. BBC News, *Oil Prices Surge to New Records*. 1 April 2005, BBC MMVI. http://news.bbc.co.uk/go/pr/fr/-/2/hi/business/4399537.stm.
30. Alanazi, A., *Experts Expect Oil Prices to Reach $100 a Barrel*. 1 February 2006, Alriyadh Newspaper. http://www.alriyadh.com/2006/02/01/article127198.html.
31. British Petroleum Hydrogen Team, *BP Cleaner Energies/Hydrogen*. 19 May 2004, British Petroleum (BP). http://www.bp.com/liveassets/bp_internet/globalbp/STAGING/global_assets/images/renewables/hydro/hydrogen_brochure.pdf.
32. U.S. Department of Energy: Hydrogen Fuel Cells & Infrastructure Technologies Programme, *Why Are Hydrogen & Fuel Cells Important?* 21 February 2003. http://www.eere.energy.gov/hydrogenandfuelcells/.
33. Pearce, F., *Hydrogen: Fuel of the Future*. 12 November 2005, American Association for the Advancement of Science (AAAS): Population and Environment Issues. http://atlas.aaas.org/index.php?part=4&sec=hydro.
34. U.S. Department of Energy: Hydrogen Fuel Cells & Infrastructure Technologies Programme, *Hydrogen Basics: How is Hydrogen Produced?* 21 February 2003. http://www.eere.energy.gov/hydrogenandfuelcells/.
35. Service, R.F., *Toward a Hydrogen Economy: The Carbon Conundrum*, in *Science*. 2004. p. 962–963.
36. Smith, J.R., *This Hybrid Vehicle Uses Hydrogen*, in *Science & Technology Review*. 1995. p. 26–27.
37. Ogden, J.M., *Prospects for Building a Hydrogen Energy Infrastructure*. Annual Review of Energy and the Environment, 1999. **24**: p. 227–279.
38. U.S. Department of Energy: Hydrogen Fuel Cells & Infrastructure Technologies Programme, *Hydrogen: Frequently Asked Questions*. 21 February 2003. http://www.eere.energy.gov/hydrogenandfuelcells/.
39. Hart, D., A. Bauen, R. Fouquet, M.A. Leach, P.J. Pearson, and D. Anderson, *Hydrogen Supply for SPFC Vehicles*. 2000, Imperial College London: London. p. 1–69.

40. Hart, D., *Hydrogen and Sustainability*. 27 March 2003, Imperial College Centre for Energy Policy and Technology. www.forumforthefuture.org.uk/uploadstore/GenH_Hart.pdf.
41. Dutton, G., *Hydrogen Energy Technology*. 2002, Tyndall Centre for Climate Change Research: Oxon. p. 1–34.
42. Sørensen, B., *Implementation Scenarios*, in *Hydrogen and Fuel Cells: Emerging Technologies and Applications*. 2005, Elsevier Academic Press: London. p. 231–348.
43. Hoffmann, P., *Hydrogen for Cars and Buses: Steaming Tailpipes*, in *Tomorrow's Energy: Hydrogen, Fuel Cells and the Prospects for a Cleaner Planet*. 2002, The MIT Press: Cambridge. p. 99–139.
44. Ball, P., *Power Cells Get Warm*, in *Nature*. 2001. p. 1–2.
45. Dunn, S., *Hydrogen Futures: Toward a Sustainable Energy System.* International Journal of Hydrogen Energy, 2002. **27**(3): p. 235–264.
46. Lovins, A.B. and W. B.D. *A Strategy for the Hydrogen Transition.* in *10th Annual U.S. Hydrogen Meeting, National Hydrogen Association*. 1999. Virginia: Rocky Mountain Institute.
47. Romm, J.J., *Key Elements of a Hydrogen-Based Transportation System*, in *The Hype about Hydrogen: Fact and Fiction in the Race to Save the Climate*. 2004, Island Press: Washington. p. 89–114.
48. Smith, J.M., *Getting Along without Gasoline—The Move to Hydrogen Fuel*, in *Science & Technology Review*. 1996. p. 28–31.
49. Demirdöven, N. and J. Deutch, *Hybrid Cars Now, Fuel Cell Cars Later*, in *Science*. 2004. p. 974–976.
50. Chilton, C., *Driving into the Future*, in *Car*. 2005. p. 132–134.
51. Hydrogen Fuel Cell Engines and Related Technologies, *Module 1: Hydrogen Properties*. 2001, U.S. Department of Energy (DOE): Washington. p. 1–47.
52. Hydrogen Fuel Cell Engines and Related Technologies, *Module 6: Fuel Cell Engine Safety*. 2001, U.S. Department of Energy (DOE): Washington. p. 1–24.
53. Hord, J., *Is Hydrogen a Safe Fuel?* International Journal of Hydrogen Energy, 1978. **3**(2): p. 157–176.
54. U.S. Department of Energy: Hydrogen Fuel Cells & Infrastructure Technologies Programme, *Hydrogen and Fuel Cells:Safety, Codes and*

Standard: The Hindenburg Myth. 21 February 2003. http://www.eere.energy.gov/hydrogenandfuelcells/.

55. Hoffmann, P., *Safety: The Hindenburg Syndrome, or "Don't Paint Your Dirigible with Rocket Fuel"*, in *Tomorrow's Energy: Hydrogen, Fuel Cells and the Prospects for a Cleaner Planet*. 2002, Cambridge. p. 233–246.
56. European Commission, *Hydrogen Energy and Fuel Cells—A Vision of our Future*. 2003, Office for Official Publications of the European Commission: Luxembourg. p. 1–35.
57. Orkustofnun (National Energy Authority), *Towards a Sustainable Hydrogen Economy*. 2003, The Icelandic Ministry of Industry and Commerce, Orkustofnun, VistOrka: Reykjavík. p. 1–8.
58. Icelandic New Energy Ltd., *Icelandic New Energy: Preparing for a Hydrogen Future*. 2003, Icelandic New Energy Ltd.: Reykjavík. p. 1–8.
59. Árnason, B., T.I. Sigfússon, and J.B. Skúlason, *Creating a Non-Fossil Energy Economy in Iceland*. 2001, University of Iceland and Icelandic New Energy Ltd.: Reykjavík. p. 1–12.
60. Romm, J.J., *Hydrogen Partnerships and Pilots*, in *The Hype about Hydrogen: Fact and Fiction in the Race to Save the Climate*. 2004, Island Press: Washington. p. 175–186.
61. Ogden, J.M., *Developing an Infrastructure for Hydrogen Vehicles: A Southern California Case Study*. International Journal of Hydrogen Energy, 1999. **24**(8): p. 709–730.
62. California Fuel Cell Partnership (CaFCP), *California Fuel Cell Partnership*. 15 December 2005. http://www.fuelcellpartnership.org.
63. Ganeshan, R. and T.P. Harrison, *An Introduction to Supply Chain Management*. 3 October, Department of Management Science and Information Systems: The Pennsylvania State University. http://lcm.csa.iisc.ernet.in/scm/supply_chain_intro.html.
64. Beamon, B.M., *Supply Chain Design and Analysis: Models and Methods*. International Journal of Production Economics, 1998. **55**(3): p. 281–294.
65. Winter, C.-J. and J. Nitsch, *Hydrogen as an Energy Carrier: Technologies, Systems, Economy*. 1988, Berlin: Springer-Verlag. 377.
66. Padró, C.E.G. and V. Putsche, *Survey of the Economics of Hydrogen Technologies*. 1999, National Renewable Energy Laboratory: Golden. p. 1–53.

67. Gaudernack, B., *Hydrogen Production from Fossil Fuels*, in *Hydrogen Power: Theoretical and Engineering Solutions*, T.O. Saetre, Editor. 1998, Kluwer Academic Publishers: The Netherlands. p. 75–89.
68. Ogden, J.M., *Review of Small Stationary Reformers for Hydrogen Production.* 2001, Centre of Energy and Environmental Studies: Princeton. p. 1–52.
69. Hydrogen Fuel Cell Engines and Related Technologies, *Module 2: Hydrogen Use*. 2001, Department of Energy (DOE): Washington. p. 1–62.
70. Watkiss, P. and N. Hill, *The Feasibility, Costs, and Markets for Hydrogen Production*. 2002, AEA Technology Environment: Oxon. p. 1–27.
71. Williams, R.H., E.D. Larson, R.E. Katofsky, and J.S. Chen, *Methanol and Hydrogen from Biomass for Transportation*, in *Energy for Sustainable Development*. 1995, Center for Energy and Environmental Studies, School of Engineering and Applied Science, Princeton University: Princeton. p. 18–34.
72. Doctor, R.D. and J.C. Molburg, *Clean Hydrogen from Coal with CO_2 Capture and Sequestration*, in *The Hydrogen Energy Transition: Moving Toward the Post Petroleum Age in Transportation*. 2004, Elsevier Academic Press: London. p. 93–104.
73. Simbeck, D.R. and E. Chang, *Hydrogen Supply: Cost Estimate for Hydrogen Pathways—Scoping Analysis*. 2002, National Renewable Energy Laboratory: Golden. p. 1–69.
74. Carpetis, C., *Storage, Transport and Distribution of Hydrogen*, in *Hydrogen as an Energy Carrier: Technologies, System, Economy*, C.-J. Winter and J. Nitsch, Editors. 1988, Springer-Verlag: Berlin. p. 249–289.
75. Amos, W.A., *Costs of Storing and Transporting Hydrogen*. 1998, National Renewable Energy Laboratory: Golden. p. 1–216.
76. Taylor, J.B., J.E.A. Alderson, K.M. Kalyanam, A.B. Lyle, and L.A. Phillips, *Technical and Economic Assessment of Methods for the Storage of Large Quantities of Hydrogen.* International Journal of Hydrogen Energy, 1986. **11**(1): p. 5–22.
77. Moore, R.B. and V. Raman, *Hydrogen Infrastructure for Fuel Cell Transportation.* International Journal of Hydrogen Energy, 1998. **23**(7): p. 617–620.
78. Landinger, H., *Hydrogen Filling Stations Worldwide*. 15 January 2006, L-B-Systemtechnik GmbH. http://www.h2stations.org/.

79. Ogden, J.M., *Where Will the Hydrogen Come From? System Considerations and Hydrogen Supply*, in *The Hydrogen Energy Transition: Moving Toward the Post Petroleum Age in Transportation*, D. Sperling and J.S. Cannon, Editors. 2004, Elsevier Academic Press: London. p. 73–92.
80. Hart, D., M.A. Leach, R. Fouquet, P.J. Pearson, and A. Bauen, *Methanol Infrastructure—Will it Affect the Introduction of SPFC Vehicles?* Journal of Power Sources, 2000. **86**(1–2): p. 542–547.
81. National Research Council (NRC), *The Hydrogen Economy—Opportunities, Costs, Barriers, and R&D Needs*. 2004, Washington: The National Academies Press. 240.
82. D'este, G., *Freight and Logistics Modeling*, in *Handbook of Logistics and Supply Chain Management*, A.M. Brewer, K.J. Button, and D.A. Hensher, Editors. 2001, Elsevier Science Ltd.: Amsterdam. p. 521–534.
83. Thomas, C.E., J. Kuhn, I. F., B.D. James, J. Lomax, F. D., and G.N. Baum, *Affordable Hydrogen Supply Pathways for Fuel Cell Vehicles.* International Journal of Hydrogen Energy, 1998. **23**(6): p. 507–516.
84. Farrell, A.E., D.W. Keith, and J.J. Corbett, *A Strategy for Introducing Hydrogen into Transportation.* Energy Policy, 2003. **31**(13): p. 1357–1367.
85. Arthur D. Little Inc, *Guidance for Transportation Technologies: Fuel Choice for Fuel Cell Vehicles*. 2002, Arthur D. Little, Inc.: Cambridge. p. 1–345.
86. Guy, K.W.A., *The Hydrogen Economy—Developing the Infrastructure*. 2001, 6th World Congress of Chemical Engineering: Melbourne. p. 1–10.
87. Joffe, D., D. Hart, and A. Bauen, *Modelling of Hydrogen Infrastructure for Vehicle Refuelling in London.* Journal of Power Sources, 2004. **131**(1–2): p. 13–22.
88. Edgar, T.F., D.M. Himmelblau, and L.S. Lasdon, *Optimization of Chemical Processess*. 2nd ed. 2001, New York: McGraw-Hill Higher Education. 652.
89. Biegler, L.T., I.E. Grossmann, and A.W. Westerberg, *Systematic Methods of Chemical Process Design*. 1999, Upper Saddle River: Prentice-Hall PTR. 796.
90. Hugo, A., *Environmentally Conscious Process Selection, Design and Optimization*, in *Department of Chemical Engineering and Chemical Technology*. 2005, Imperial College London: London. p. 266.
91. Davis, T., *Effective Supply Chain Management.* Sloan Management Review, 1993. **Summer**: p. 35–46.

92. Geary, S., P. Childerhouse, and D. Towill, *Uncertainty and the Seamless Supply Chain.* Supply Chain Management Review, 2002. **July/August**: p. 52–61.

93. Zimmermann, H.-J., *An Application-Oriented View of Modeling Uncertainty.* European Journal of Operational Research, 2000. **122**(2): p. 190–198.

94. Guillén, G., F.D. Mele, M.J. Bagajewicz, A. Espuña, and L. Puigjaner, *Multiobjective Supply Chain Design under Uncertainty.* Chemical Engineering Science, 2005. **60**(6): p. 1535–1553.

95. Tsiakis, P., N. Shah, and C.C. Pantelides, *Design of Multi-echelon Supply Chain Networks under Demand Uncertainty.* Industrial and Engineering Chemistry Research, 2001. **40**(16): p. 3585–3604.

96. Chen, C.-L. and W.-C. Lee, *Multi-objective Optimization of Multi-echelon Supply Chain Networks with Uncertain Product Demands and Prices.* Computers and Chemical Engineering, 2004. **28**(6–7): p. 1131–1144.

97. Escudero, L.F., E. Galindo, G. Garcia, E. Gomez, and V. Sabau, *Schumann, a Modelling Framework for Supply Chain Management under Uncertainty.* European Journal of Operational Research, 1999. **119**(1): p. 14–34.

98. Petrovic, D., R. Roy, and R. Petrovic, *Modelling and Simulation of a Supply Chain in an Uncertain Environment.* European Journal of Operational Research, 1998. **109**(2): p. 299–309.

99. Subrahmanyam, S., J.F. Peknyt, and G.V. Reklaitis, *Design of Batch Chemical Plants under Market Uncertainty.* Industrial and Engineering Chemistry Research, 1994. **33**(11): p. 2688–2701.

100. Owen, S.H. and M.S. Daskin, *Strategic Facility Location: A Review.* European Journal of Operational Research, 1998. **111**(3): p. 423–447.

101. Cohen, M.A. and H.L. Lee, *Strategic Analysis of Integrated Production-Distribution Systems: Models and Methods.* Operations Research, 1988. **36**(2): p. 216–228.

102. Gupta, A. and C.D. Maranas, *Managing Demand Uncertainty in Supply Chain Planning.* Computers and Chemical Engineering, 2003. **27**(8–9): p. 1219–1227.

103. Wets, R.J.-B., *Challenges in Stochastic Programming.* Mathematical Programming, 1996. **75**: p. 115–135.

104. Vanston JR, J.R., W.P. Frisbie, S.C. Lopreato, and D.L. Poston JR, *Alternate Scenario Planning.* Technological Forecasting and Social Change, 1977. **10**: p. 159–180.

105. Mulvey, J.M., *Generating Scenario for the Tower Perrin Investment System.* Interfaces, 1996. **26**(2): p. 1–15.

106. Mulvey, J.M. and R.J. Vanderbei, *Robust Optimization of Large-Scale Systems.* Operations Research, 1995. **43**(2): p. 264–281.

107. Santoso, T., S. Ahmed, M. Goetschalckx, and A. Shapiro, *A Stochastic Programming Approach for Supply Chain Network Design under Uncertainty.* European Journal of Operational Research, 2005. **167**(1): p. 96–115.

108. Transport for London (TfL), *London Buses: Fuel Cell Buses*. 30 December 2004. http://www.tfl.gov.uk/buses/downloads/fuel-cell-buses.pdf.

109. Sinnott, R.K., *Costing and Project Evaluation*, in *Coulson & Richardson's Chemical Engineering: Chemical Engineering Design*. 2003, Butterworth-Heinemann: Oxford. p. 242–282.

110. Department of Trade and Industry (DTI), *Information and Statistics: Energy Prices*. 23 August 2004. http://www.dti.gov.uk/energy/inform/energy_prices/tables/table_531_mar04.xls.

111. Barnes, G. and P. Langworthy, *The Pre-mile Costs of Operating Automobiles and Trucks*. 2003, Minnesota Department of Transportation, Office of Research Services: St. Paul. p. 1–46.

112. Victoria Transport Policy Institute, *Transportation Cost and Benefits Analysis: Vehicle Costs*. 02 July 2004. http://www.vtpi.org/tdm/.

113. Peschka, W., *Thermal Insulation, Storage and Transportation of Liquid Hydrogen*, in *Liquid Hydrogen: Fuel of the Future*. 1992, Springer-Verlag: Wien. p. 71–103.

114. Brooke, A., D. Kendrick, A. Meeraus, and R. Raman, *GAMS: A User's Guide*. 1998, GAMS Development Corporation: Washington. p. 1–276.

115. British Petroleum, *BP Statistical Review of World Energy 2004*. 2004: Surrey. p. 1–44.

116. Turner, J.A., *Toward a Hydrogen Economy: Sustainable Hydrogen Production*, in *Science*. 2004. p. 972–974.

117. *Digest of United Kingdom Energy Statistics 2004*. 13 July 2005, The Department of Trade and Industry (DTI). http://www.dti.gov.uk/energy/inform/dukes/dukes2004/dukes04.pdf.

118. Wets, R.J.-B., *The Aggregation Principle in Scenario Analysis and Stochastic Optimisation*, in *Algorithms and Model Formulations in Mathematical Programming*, S.W. Wallace, Editor. 1989, Springer-Verlag: Berlin. p. 92–113.

119. Larson, E.D., E. Worrell, and J.S. Chen, *Clean Fuels from Municipal Solid Waste for Fuel Cell Buses in Metropolitan Areas.* Resources, Conservation and Recycling, 1996. **17**(4): p. 273–298.

120. Department for Transport (DfT), *Transport Trends: 2002 Edition*. 28 July 2004. http://www.dft.gov.uk.

121. Nemhauser, G.L. and L.A. Wolsey, *Integer and Combinational Optimization*. 1988, New York: John Wiley & Sons Inc. 782.

122. *Population Density, 2002: Regional Trends 38*. 28 July 2004, Office for National Statistics. http://www.statistics.gov.uk.

123. Philip, G., *Philip's Atlas of the World*. 2002, London: Philip's. 448.

124. Steinberg, M. and H.C. Cheng, *Modern and Prospective Technologies for Hydrogen Production from Fossil Fuels.* International Journal of Hydrogen Energy, 1989. **14**(11): p. 797–820.

125. Bockris, J.O.M., *The Economics of Hydrogen as a Fuel.* International Journal of Hydrogen Energy, 1981. **6**(3): p. 223–241.

126. Peter, M.S. and K.D. Timmerhaus, *Cost Estimation*, in *Plant Design and Economics for Chemical Engineers*, J.B. Clark and J.M. Morriss, Editors. 1991, McGraw-Hill: New York. p. 150–215.

127. Carpetis, C., *Estimation of Storage Costs for Large Hydrogen Storage Facilities.* International Journal of Hydrogen Energy, 1982. **7**(2): p. 191–203.

128. Schwarz, J.B. and K.A.G. Amankwah, *The Future of Energy Gases: Hydrogen Storage Systems*. 1993, U.S. Geological Survey Professional Paper 1570: Denver. p. 725–735.

129. *Chemical Composition of Natural Gas*. 16 January 2005, Union Gas. http://www.uniongas.com/aboutus/aboutng/composition.asp.

130. Lewis, J., *Oil—A Natural Resource: UK Oil and Gas*. 10 July 2005, The Institute of Petroleum. http://www.energyinst.org.uk/education/natural/5.htm.

131. *The Future of UK Gas Supplies*. 2004, The Parliamentary Office of Science and Technology: London. p. 1–4.

132. British Geological Survey, *Mineral Profile: Coal*. 2004: Nottingham. p. 1–24.

133. Nikolaou, A., M. Remrova, and I. Jeliazkov, *Biomass Availability in Europe*. 2003. p. 1–80.
134. Low Carbon vehicle partnership, *Biofuels for Road Transport*. 2005. p. 1–9.
135. Department of Trade and Industry (DTI), *UK Energy in Brief July 2004*. 2004: London. p. 1–19.

Appendix A

Hydrogen Demand

A.1 Introduction

In this appendix, the demand of hydrogen in Great Britain using the 2002 oil equivalent will be estimated. This estimation is based on the "asymptotic" assumption of 100% conversion of PLG vehicles and buses to be powered by hydrogen fuel. In some sections of the thesis, the gradual progress to this level is modelled. The following sections discuss in more detail the procedure used for this estimation.

A.2 Total Demand

The total equivalent demand of hydrogen is given as a function of: (1) total number of PLG vehicles and buses, (2) average distance travelled by these vehicles, and (3) fuel economy. The values of these parameters are listed in Table A.1. It is worth noting that some figures in the appendices used in calculations are more accurate than shown.

Table A.1: Parameters used in total hydrogen demand calculations

Parameter	PLG vehicles	Buses
Number of vehicles [120]	27.17×10^{6}	92.00×10^{3}
Average distance travelled (km/yr) [120]	16.47×10^{3}	56.52×10^{3}
Fuel economy (kg H_2/km) [81, 119]	0.0096	0.1177

Using the above values, the total daily demand of hydrogen for PLG vehicles and buses are given below respectively.

$$\left[27.17\times10^{6}\right]\left[16.47\times10^{3}\ \frac{\text{km}}{\text{yr}}\right]\left[0.0096\ \frac{\text{kg}}{\text{km}}\right]\left[\frac{1}{365}\ \frac{\text{yr}}{\text{d}}\right] = 11.72\times10^{6}\ \frac{\text{kg}}{\text{d}}$$

$$\left[92\times10^{3}\right]\left[56.52\times10^{3}\ \frac{\text{km}}{\text{yr}}\right]\left[0.1177\ \frac{\text{kg}}{\text{km}}\right]\left[\frac{1}{365}\ \frac{\text{yr}}{\text{d}}\right] = 1.68\times10^{6}\ \frac{\text{kg}}{\text{d}}$$

A.3 Demand Distribution

The determination of the geographical distribution of demand was carried out through dividing Great Britain's mainland into 45 grid squares of equal sizes. These grids were obtained by enclosing London and the South East region of the UK in a particular grid of reasonable size. This is because these regions have the largest population and traffic densities, as well as being the hub of many business activities [86]. Expanding upon this base grid, the remaining 44 grids were obtained. Of these grids, only 34 will be analysed in order to calculate the demand since they reside in the land area.

After determining the number of grids, the population density in each grid was estimated as follows:

1. Divide Great Britain into 11 regions. The name and population of these regions appear in Table A.2.
2. Divide each grid square into 196 grids of smaller sizes.
3. Determine the grids that cover each region. It is important to mention that some grids will cover more than one region. An example of this is grid 29 which covers London, most parts of the South East, and the Southern part of East Anglia (see Figure A.1).
4. Calculate the percentage of area that the grid covers from the corresponding regions. Using the percentage obtained, the population of grid per region is calculated by multiplying the percentage by the population of the region [122].
5. Since some grids lie in more than one region; in this case the population of each grid is calculated by summing up the corresponding population of each region that makes up this grid.

6. Find out the percentage of population in each grid with respect to the total number of Great Britain's population, i.e. population density.

To illustrate the above steps, take London and the South East region as an example. The results obtained from using these steps are summarised in Tables A.3 and A.4.

Table A.2: Population of Great Britain [122]

Region	Area (km^2)	Population density (Person/km^2)	Population (million)
Scotland	77925	65	5.07
North East	8573	293	2.51
North West	14106	480	6.77
Yorkshire & Humberside	15408	323	4.98
Wales	20732	141	2.92
West Midlands	12998	408	5.30
East Midlands	15607	270	4.21
East Anglia	19110	284	5.43
South West	23837	208	4.96
South East	19069	421	8.03
London	1572	4679	7.36
Total	470867		57.53

Table A.3: Grid population in London and the South East region

London			
Grid no. included	No. of small squares	% square/grid	Grid population/region
29	21	100	7.36×10^{6}
Total	21	100	7.36×10^{6}
South East			
Grid no. included	No. of small squares	% square/grid	Grid population/region
23	10	3.64	291.93×10^{3}
24	6	2.18	175.16×10^{3}
28	79	28.73	2.31×10^{6}
29	120	43.64	3.50×10^{6}
30	25	9.09	729.82×10^{3}
33	15	5.45	437.89×10^{3}
34	20	7.27	583.86×10^{3}
Total	275	100.00	8.03×10^{6}

Table A.4: Population density of the studied example

Grid, g	Population/grid	Population density
23	4.50×10^{6}	0.0782
24	3.70×10^{6}	0.0643
28	3.77×10^{6}	0.0656
29	11.71×10^{6}	0.2036
30	807.35×10^{3}	0.0140
33	794.77×10^{3}	0.0138
34	583.86×10^{3}	0.0101

A.4 Grid Demand

Using the population density given in Table A.4, the daily demand of hydrogen in each grid is calculated by multiplying these densities by the total equivalent demand of both PLG vehicles and buses (see Section A.2). The results are listed in Table A.5.

Table A.5: Hydrogen demand of the studied example

Grid, *g*	Hydrogen demand (t/d)
23	1047
24	861
28	879
29	2727
30	188
33	185
34	136

For the remaining grids that are not addressed in the studied example, the daily demand of hydrogen is shown in Figure A.1. The demand values are presented in a figure format to show the geographical location of each grid in Great Britain.

In determining a grid's demand, the assumption that people in different parts of Great Britain consume the same amount of fuel has been made. A more detailed model might also "zoom in" and use a denser grid in regions with high consumption. An alternative might be to use the 86 counties of Great Britain instead of employing the reported 34 grid squares. This would enable us to obtain more accurate statistics on, for example, the energy consumption.

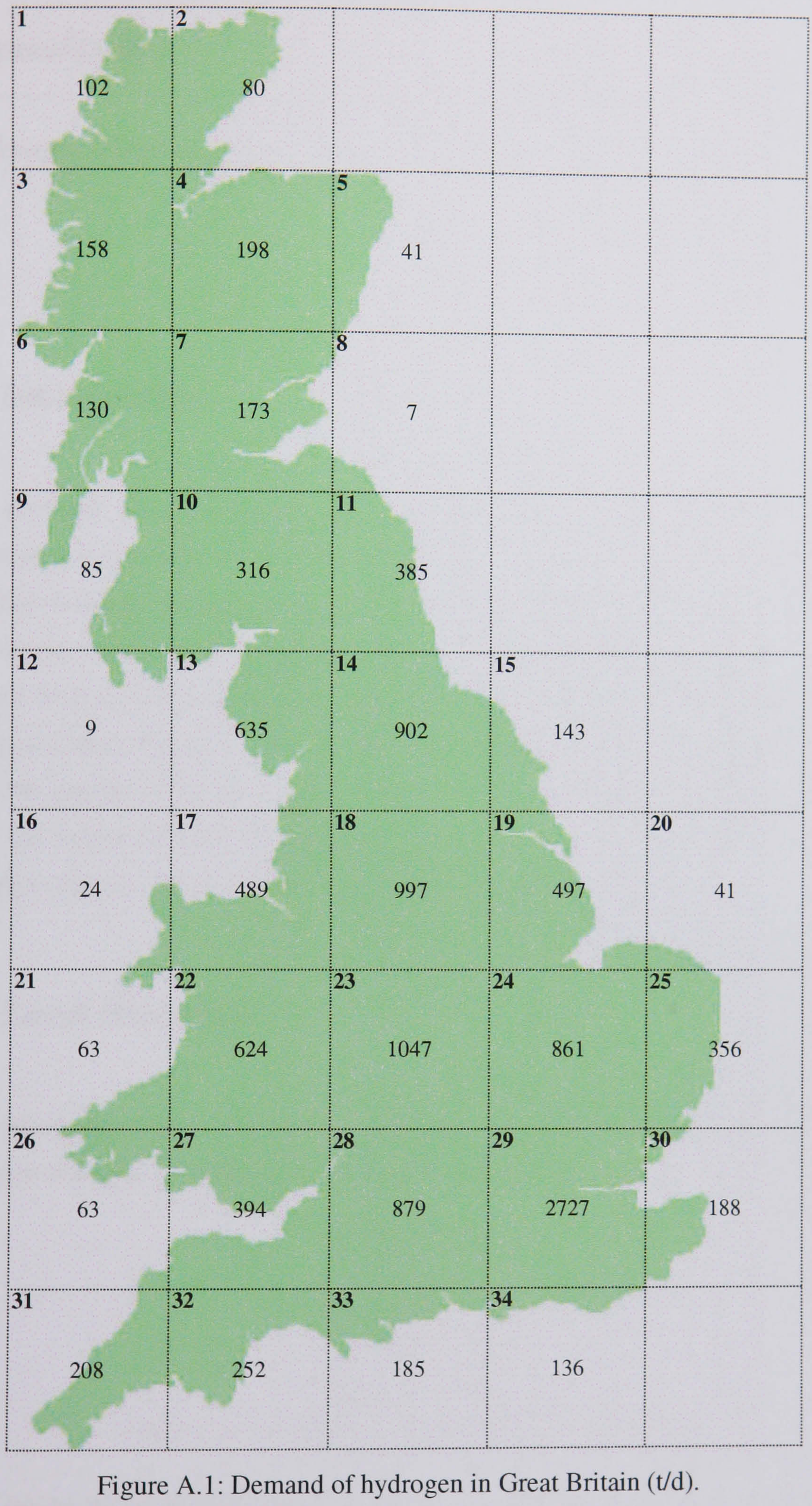


Figure A.1: Demand of hydrogen in Great Britain (t/d).

Appendix B

Delivery Distances

B.1 Introduction

This appendix describes an estimate of the average delivery distance within a particular grid (local distance) as well as the average distance between different grids (regional distance). As mentioned in Appendix A, Great Britain was divided into 34 grid squares. The area of each grid square was determined by measuring the vertical distance between the land ends, starting from the highest point in the Highlands and ending at Lizard Point in the South West. The distance obtained was 970 km [123]. Since the number of vertical grids is nine and their total height is 22.23 centimetres (cm), the height of each grid square is 2.47 cm which is equivalent to 108 km. Therefore, the area of each uniform grid square is 11616 km^2.

B.2 Local Distances

To estimate the average local delivery distance, we divided a grid square into eight triangular segments of equal sizes as shown in Figure B.1.

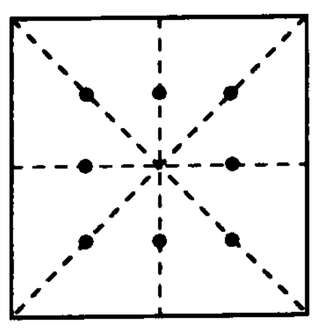


Figure B.1: Illustration of local distance calculation.

Since the length of the grid square is known, the distance between the grid's centre and the points illustrated in the figure can be calculated. This can be done by taking

the average of the distances between two points that lie on the same dotted line. Therefore, the average local delivery distance is estimated as follows:

$$\frac{(54\times2)+(76\times2)}{4} = 65 \text{ km}$$

where 54 is the distance between two vertical or horizontal points, as shown in Figure B.1. Also from the figure, the distance between the two points on the hypotenuse was calculated to be 76 km.

B.3 Regional Distances

The regional distances are estimated from the centre of one gird to the centre of the other bearing in mind the shortest land route. The centre of some grids will fall in water; in this case the distance is measured from the centre of one side of the grid or from the corner of the grid. An example of these two cases is shown in Figure B.2.

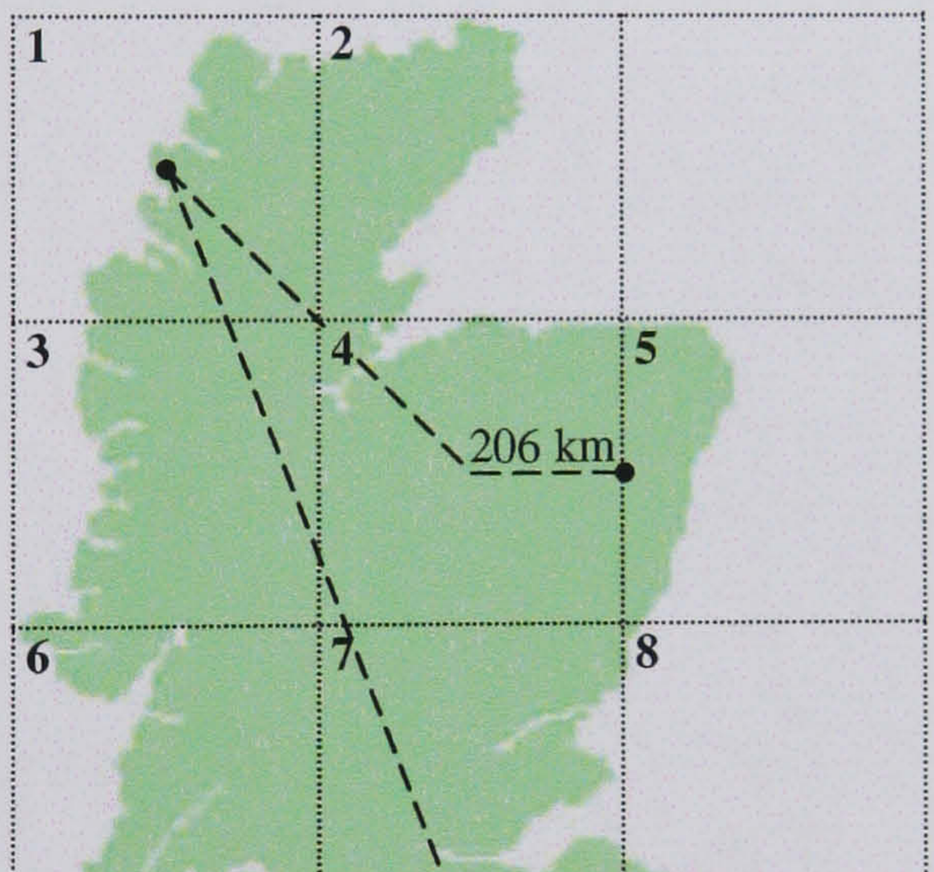


Figure B.2: Example of regional distance calculations.

A summary of the local and regional delivery distances for all grids are given in Table B.1. As shown in the table, the diagonal bold line represents the local delivery distances while the upper triangle of the matrix represents the regional delivery distances between different grids. Since we have a symmetric matrix, the lower triangle is similar to the upper one.

Table B.1: Local and regional delivery distances

Grid, *g*	**01**	**02**	**03**	**04**	**05**	**06**	**07**	**08**	**09**	**10**	**11**	**12**	**13**	**14**	**15**	**16**	**17**	**18**	**19**	**20**	**21**	**22**	**23**	**24**	**25**	**26**	**27**	**28**	**29**	**30**	**31**	**32**	**33**	**34**
01	**065**	108	108	152	206	216	241	344	328	341	415	404	446	482	536	664	587	580	631	730	706	682	682	723	831	791	788	785	821	843	972	899	837	852
02	*108*	**065**	152	152	197	247	247	352	346	351	459	408	457	492	529	673	597	587	648	746	715	691	691	749	835	802	795	795	827	853	983	909	848	861
03	*108*	*152*	**065**	108	162	108	152	248	222	241	323	298	344	389	421	563	487	482	539	637	655	581	580	628	736	743	689	685	723	749	870	796	735	751
04	*152*	*152*	*108*	**065**	054	152	108	216	222	216	282	290	323	349	390	533	457	449	496	596	577	553	552	590	663	663	656	656	688	710	843	769	709	722
05	*206*	*197*	*162*	*054*	**065**	194	120	228	241	228	291	314	332	361	399	548	471	461	509	609	590	566	565	602	675	677	670	670	701	723	856	783	723	735
06	*216*	*247*	*108*	*152*	*194*	**065**	108	170	120	152	241	197	248	305	345	476	400	389	457	551	510	492	484	539	617	606	597	597	629	658	787	713	650	662
07	*241*	*247*	*152*	*108*	*120*	*108*	**065**	108	120	108	174	194	216	241	283	427	351	341	389	488	469	445	444	482	555	556	550	550	580	602	736	662	602	614
08	*344*	*352*	*248*	*216*	*228*	*170*	*108*	**065**	120	076	076	194	170	170	194	368	292	275	314	415	403	381	381	410	482	502	488	488	511	531	679	605	542	550
09	*328*	*346*	*222*	*222*	*241*	*120*	*120*	*120*	**065**	054	162	076	130	194	241	359	283	271	345	435	401	375	366	421	502	489	448	480	514	540	670	596	533	537
10	*341*	*351*	*241*	*216*	*228*	*152*	*108*	*076*	*054*	**065**	108	054	108	152	194	323	247	241	305	399	365	343	341	389	466	451	444	444	482	508	629	555	497	511
11	*415*	*459*	*323*	*282*	*291*	*241*	*174*	*076*	*162*	*108*	**065**	222	152	108	130	323	247	216	248	344	361	341	323	341	411	451	444	431	444	460	629	555	485	488
12	*404*	*408*	*298*	*290*	*314*	*197*	*194*	*194*	*076*	*054*	*222*	**065**	162	228	278	390	314	302	377	467	423	406	406	453	533	507	500	500	542	571	686	612	552	568
13	*446*	*457*	*344*	*323*	*332*	*248*	*216*	*170*	*130*	*108*	*152*	*162*	**065**	108	162	229	152	152	241	323	271	247	247	305	390	359	351	351	389	421	540	466	404	410
14	*482*	*492*	*389*	*349*	*361*	*305*	*241*	*170*	*194*	*152*	*108*	*228*	*108*	**065**	054	229	152	108	152	248	271	241	216	241	361	349	341	323	341	361	522	448	377	381
15	*536*	*529*	*421*	*390*	*399*	*345*	*283*	*194*	*241*	*194*	*130*	*278*	*162*	*054*	**065**	269	194	120	120	224	305	269	222	222	343	381	361	328	328	341	535	461	381	377
16	*664*	*673*	*563*	*533*	*548*	*476*	*427*	*368*	*359*	*323*	*323*	*390*	*229*	*229*	*269*	**065**	076	170	275	323	054	076	170	275	381	130	170	229	314	361	389	315	269	305
17	*587*	*597*	*487*	*457*	*471*	*400*	*351*	*292*	*283*	*247*	*247*	*314*	*152*	*152*	*194*	*076*	**065**	108	216	276	120	108	152	241	341	197	216	241	305	345	416	343	290	314
18	*580*	*587*	*482*	*449*	*461*	*389*	*341*	*275*	*271*	*241*	*216*	*302*	*152*	*108*	*120*	*170*	*108*	**065**	108	174	194	152	108	152	241	269	241	216	241	269	416	343	**269**	275
19	*631*	*648*	*539*	*496*	*509*	*457*	*389*	*314*	*345*	*305*	*248*	*377*	*241*	*152*	*120*	*275*	*216*	*108*	**065**	108	290	241	152	108	174	361	305	241	216	224	464	389	290	275
20	*730*	*746*	*637*	*596*	*609*	*551*	*488*	*415*	*435*	*399*	*344*	*467*	*323*	*248*	*224*	*323*	*276*	*174*	*108*	**065**	328	275	170	076	076	392	314	229	170	162	464	381	269	241
21	*706*	*715*	*655*	*577*	*590*	*510*	*469*	*403*	*401*	*365*	*361*	*423*	*271*	*271*	*305*	*054*	*120*	*194*	*290*	*328*	**065**	054	162	269	377	076	120	194	290	341	347	273	229	269
22	*682*	*691*	*581*	*553*	*566*	*492*	*445*	*381*	*375*	*343*	*341*	*406*	*247*	*241*	*269*	*076*	*108*	*152*	*241*	*275*	*054*	**065**	108	216	323	120	108	152	241	290	315	241	194	229
23	*682*	*691*	*580*	*552*	*565*	*484*	*444*	*381*	*366*	*341*	*323*	*406*	*247*	*216*	*222*	*170*	*152*	*108*	*152*	*170*	*162*	*108*	**065**	108	216	222	152	108	152	194	315	241	162	170
24	*723*	*749*	*628*	*590*	*602*	*539*	*482*	*410*	*421*	*389*	*341*	*453*	*305*	*241*	*222*	*275*	*241*	*152*	*108*	*076*	*269*	*216*	*108*	**065**	108	328	241	152	108	120	389	**305**	194	170
25	*831*	*835*	*736*	*663*	*675*	*617*	*555*	*482*	*502*	*466*	*411*	*533*	*390*	*361*	*343*	*381*	*341*	*241*	*174*	*076*	*377*	*323*	*216*	*108*	**065**	434	341	241	152	130	484	415	269	229
26	*791*	*802*	*743*	*663*	*677*	*606*	*556*	*502*	*489*	*451*	*451*	*507*	*359*	*349*	*381*	*130*	*197*	*269*	*361*	*392*	*076*	*120*	*222*	*328*	*434*	**065**	120	222	328	381	**365**	291	**247**	290
27	*788*	*795*	*689*	*656*	*670*	*597*	*550*	*488*	*448*	*444*	*444*	*500*	*351*	*341*	*361*	*170*	*216*	*241*	*305*	*314*	*120*	*108*	*152*	*241*	*341*	*120*	**065**	108	216	269	248	174	130	174
28	*785*	*795*	*685*	*656*	*670*	*597*	*550*	*488*	*480*	*444*	*431*	*500*	*351*	*323*	*328*	*229*	*241*	*216*	*241*	*229*	*194*	*152*	*108*	*152*	*241*	*222*	*108*	**065**	108	162	241	174	054	076
29	*821*	*827*	*723*	*688*	*701*	*629*	*580*	*511*	*514*	*482*	*444*	*542*	*389*	*341*	*328*	*314*	*305*	*241*	*216*	*170*	*290*	*241*	*152*	*108*	*152*	*328*	*216*	*108*	**065**	054	341	276	120	076
30	*843*	*853*	*749*	*710*	*723*	*658*	*602*	*531*	*540*	*508*	*460*	*571*	*421*	*361*	*341*	*361*	*345*	*269*	*224*	*162*	*341*	*290*	*194*	*120*	*130*	*381*	*269*	*162*	*054*	**065**	392	329	170	120
31	*972*	*983*	*870*	*843*	*856*	*787*	*736*	*679*	*670*	*629*	*629*	*686*	*540*	*522*	*535*	*389*	*416*	*416*	*464*	*464*	*347*	*315*	*315*	*389*	*484*	*365*	*248*	*241*	*341*	*392*	**065**	108	222	275
32	*899*	*909*	*796*	*769*	*783*	*713*	*662*	*605*	*596*	*555*	*555*	*612*	*466*	*448*	*461*	*315*	*343*	*343*	*389*	*381*	*273*	*241*	*241*	*305*	*415*	*291*	*174*	*174*	*276*	*329*	*108*	**065**	162	216
33	*837*	*848*	*735*	*709*	*723*	*650*	*602*	*542*	*533*	*497*	*485*	*552*	*404*	*377*	*381*	*269*	*290*	*269*	*290*	*269*	*229*	*194*	*162*	*194*	*269*	*247*	*130*	*054*	*120*	*170*	*222*	*162*	**065**	054
34	*852*	*861*	*751*	*722*	*735*	*662*	*614*	*550*	*537*	*511*	*488*	*568*	*410*	*381*	*377*	*305*	*314*	*275*	*275*	*241*	*269*	*229*	*170*	*170*	*229*	*290*	*174*	*076*	*076*	*120*	*275*	*216*	*054*	**065**

Appendix C

Hydrogen Supply Chain Cost Analysis

C.1 Introduction

This appendix discusses in more detail the costs of various technologies that can be used to produce, store, distribute and dispense hydrogen. For each of these technologies, the total cost is divided into capital and operating costs. The former cost is a one-time investment associated with establishing production plants, storage facilities, transportation modes, and fuelling stations. This investment is usually made at the beginning of the project life. For production and storage technologies, the capital cost is subdivided into direct and indirect costs. Direct costs represent the cost required to install process equipment, purchase land, and other general facilities such as process and auxiliary buildings, building services, maintenance shops, and yard improvements. The indirect costs, however, represent engineering permits and start-up, contingency, and working capital.

The operating costs include all expenses that are made on a continuous basis over the life of the aforementioned technologies. They involve expenses that directly relate to the day-to-day operation of the processes as well as indirect expenses such as taxes, insurance, or depreciation. A typical classification of operating costs is given by:

1. Primary energy sources which represent feedstocks for the process that are consumed on a continuous basis.
2. Utilities which are required on a continuous basis such as steam, electricity, cooling water, or fuel oil.
3. Direct expenses which include labour, supervision, payroll, maintenance, and operating supplies such as catalysts, lubricants and solvents.

4. Indirect expenses which include depreciation, local taxes, interest, and insurance.

In this analysis, all cost terms were expressed in 2002 US dollars.

C.2 Hydrogen Production Technologies

This section presents estimates of the total cost of the following production technologies: (1) reforming natural gas (methane) to hydrogen, (2) conversion of coal to hydrogen via gasification, (3) production of hydrogen from biomass gasification, and (4) use of electrical energy to produce hydrogen via electrolysis. The hydrogen production facility for these different technologies consists of four steps shown in Figure C.1.

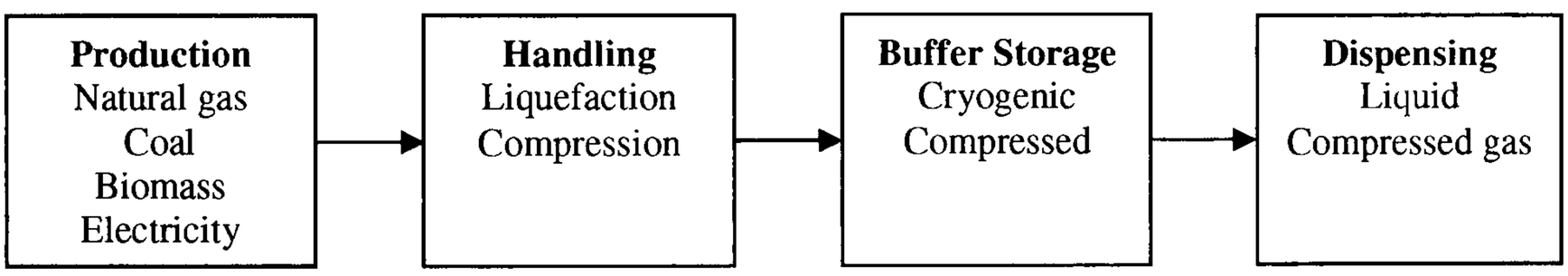


Figure C.1: Components of a generic hydrogen production.

Due to the nature of the production technologies and their economical barriers, some of these technologies will be restricted to certain sizes. For instance, we assume that steam methane reforming (SMR) can be built in three different sizes, referred to as large, medium, and small. Gasification plants, however, lack this advantage since the current technology does not support the establishment of small-scale plants. For electrolysis, small-scale and midsize plants are more favourable as electrolysis suffers from diseconomies of scale. In this study, the different plant sizes—small, medium and large—are assumed to have a production capacity range from 0.3 to 9.5, 10 to 150 and 200 to 960 t/d of hydrogen, respectively. Also, the average utilisation rates are 80% for small plants and 90% for both medium and large plants.

As noted throughout this thesis, the main focus was the production of liquid hydrogen via the abovementioned types and sizes of production technologies for the reasons discussed in earlier chapters. The production of compressed-gaseous hydrogen was also considered in Chapter 3 for large-scale plants only. The different plant types and sizes with the two possible hydrogen forms lead us to 12 different pathways summarised in Table C.1. The total cost for each pathway will be shown in Tables C.2–C.14. To understand how the total cost is calculated, we will take the production of liquid hydrogen in large SMR plants as an example (SMR-LRG-LH_2). For the remaining technologies, the same methodology will be followed and only a summary of the results will be shown.

A large amount of work [41, 66, 67, 70, 73, 81, 124, 125] has been published concerning the economics of current and near-term hydrogen production technologies. In a detailed survey, Padró and Putsche [66] examined most of these publications and presented a summary of the cost for six different hydrogen production options. These options are the production of hydrogen via SMR, noncatalytic partial oxidation, coal and biomass gasification, biomass pyrolysis, and electrolysis.

The results obtained from this cost analysis will be cross-checked with the analysis performed by Simbeck and Chang [73]. Since their study considers different input parameters, our results will differ slightly from their estimated ones. However, the values will give the reader a good indication about the accuracy of our economic analysis. For the sake of brevity, we will only show the unit capital and production costs. The corresponding values will be given in bold. Some of the examined production pathways will not have a reference data because the production of liquid hydrogen in medium and small facilities was not considered by Simbeck and Chang.

Table C.1: Hydrogen production pathways examined

Pathway name	Pathway description
SMR-LRG-LH_2	Production of liquid hydrogen via large steam methane reforming plant
SMR-MED-LH_2	Production of liquid hydrogen via medium steam methane reforming plant
SMR-SML-LH_2	Production of liquid hydrogen via small steam methane reforming plant
SMR-LRG-CH_2	Production of compressed hydrogen gas via large steam methane reforming plant
CG-LRG-LH_2	Production of liquid hydrogen via large coal gasification plant
CG-MED-LH_2	Production of liquid hydrogen via medium coal gasification plant
CG-LRG-CH_2	Production of compressed hydrogen gas via large coal gasification plant
BG-LRG-LH_2	Production of liquid hydrogen via large biomass gasification plant
BG-MED-LH_2	Production of liquid hydrogen via medium biomass gasification plant
BG-LRG-CH_2	Production of compressed hydrogen gas via large biomass gasification plant
WE-MED-LH_2	Production of liquid hydrogen via medium water electrolysis plant
WE-SML-LH_2	Production of liquid hydrogen via small water electrolysis plant

Table C.2: Data used for calculating the total cost of SMR-LRG-LH_2

Production			
Parameter	*Value*	*Remark*	*Source*
Design production capacity	960,000 kg/d	399 million scf/d	
Plant availability	329 d/yr	90% utilisation rate	
Annual actual production	315,360 t/yr	Calculated from above	
NG required per H_2 generated	360 Btu NG/scf H_2	76% LHV efficiency	[73]
NG consumed	126,260 kg/hr	Calculated from above	
Steam consumed	283,564 kg/hr	Material balance calculation	
CO_2 produced	346,362 kg/hr	Material balance calculation	
Production			
Parameter	*Value*	*Remark*	*Source*
Unit cost of SMR unit	\$312/kg/d H_2	At 100 t/d H_2 basis	[73]
Size factor of SMR unit	70%		[73]
Handling			
Parameter	*Value*	*Remark*	*Source*
Liquefaction energy	11 kWh/kg H_2		[75]
Liquefaction power	440,000 kW	Calculated from above	
Unit cost of liquefaction unit	\$700/kg/d H_2	At 100 t/d H_2 basis	[73]
Size factor of liquefaction unit	75%		[73]
Buffer Storage			
Parameter	*Value*	*Remark*	*Source*
Storage pressure	1–2 atm		[73]
Storage period	1 day	Assumption	
Storage capacity	960,000 kg	Calculated from above	
Unit cost of LH_2 storage	\$19/kg H_2	At 100 t/d H_2 basis	[73]
Size factor of LH_2 storage	70%		[73]
Dispensing			
Parameter	*Value*	*Remark*	*Source*
LH_2 dispenser rate	5,000 kg/hr/dispenser		[73]
Number of dispensers required	8	Calculated from above	
Cost of LH_2 dispenser	\$100,000/dispenser		[73]

Table C.3: Cost analysis of SMR-LRG-LH_2

Capital Cost			
Parameter	*Value (\$)*	*Remark*	*Source*
Direct Costs			
SMR unit	152,000,000	Calculated from above	
Liquefaction unit	382,000,000	Calculated from above	
LH_2 storage	9,000,000	Calculated from above	

Table C.3 (*Continued*)

Capital Cost			
Parameter	*Value ($)*	*Remark*	*Source*
LH_2 dispenser	800,000	Calculated from above	
Total process unit	543,000,000		
Land	27,000,000	5% of total process unit cost	[126]
General facilities	109,000,000	20% of total process unit cost	[126]
Total direct cost	679,000,000		
Indirect Costs			
Engineering permits & start-up	65,000,000	10% of direct cost excluding land	[126]
Total indirect cost	65,000,000		
Fixed capital investment (FCI)	745,000,000		
Contingency	74,000,000	10% of FCI	[126]
Working capital	84,000,000	3 months payable period	
Total capital investment	903,000,000		
Unit capital cost	$941/kg/d	Calculated from above	
	$1,534/kg/d	Reference data for comparison	[73]
Operating Cost			
Parameter	*Value ($/yr)*	*Remark*	*Source*
Direct Costs			
NG	122,000,000	$2.58/million Btu LHV	[115]
Electricity	180,000,000	$0.05/kWh	[110]
Steam	27,000,000	$12/t	[109]
Manpower (operating labour + general staff)	9,000,000	Labour wage = $26/hr Total personnel required = 160 Personnel availability = 2010 hr/yr	[109]
Maintenance & repairs	33,000,000	5% of direct cost excluding land	[126]
Operating supplies	7,000,000	1% of direct cost excluding land	[126]
Total direct cost	376,000,000		
Indirect Costs			
Interest	41,000,000	5% of FCI + contingency	[126]
Local taxes	25,000,000	3% of FCI + contingency	[126]
Insurance	8,000,000	1% of FCI + contingency	[126]
Total indirect cost	74,000,000		
Total operating cost	450,000,000		
Unit production cost	$1.43/kg	Calculated from above	
	$2.21/kg	Reference data for comparison	[73]

Table C.4: Summary of results for SMR-MED-LH_2

Parameter	*Value*	*Remark*	*Source*
Design production capacity	150,000 kg/d	62 million scf/d	
Plant availability	329 d/yr	90% utilisation rate	
Annual actual production	49,275 t/yr	Calculated from above	
NG required per H_2 generated	381 Btu NG/scf H_2	72% LHV efficiency	[81]
NG consumed	20,879 kg/hr	Calculated from above	
Steam consumed	46,891 kg/hr	Material balance calculation	
CO_2 produced	57,276 kg/hr	Material balance calculation	
Liquefaction energy	11 kWh/kg H_2		[75]
Liquefaction power	68,750 kW	Calculated from above	
Storage pressure	1–2 atm		[73]
Storage period	1 day	Assumption	
Storage capacity	150,000 kg	Calculated from above	
LH_2 dispenser rate	5,000 kg/hr/dispenser		[73]
Number of dispensers required	2	Calculated from above	
Unit cost of SMR unit	$312/kg/d H_2	At 100 t/d H_2 basis	[73]
Size factor of SMR unit	70%		[73]
Unit cost of liquefaction unit	$700/kg/d H_2	At 100 t/d H_2 basis	[73]

Table C.4 (*Continued*)

Parameter	*Value*	*Remark*	*Source*
Size factor of liquefaction unit	75%		[73]
Unit cost of LH_2 storage	\$19/kg H_2	At 100 t/d H_2 basis	[73]
Size factor of LH_2 storage	70%		[73]
Unit cost of LH_2 dispenser	\$100,000/dispenser		[73]
Cost of SMR unit	\$41,000,000	Calculated from above	
Cost of liquefaction unit	\$95,000,000	Calculated from above	
Cost of LH_2 storage	\$2,000,000	Calculated from above	
Cost of LH_2 dispenser	\$200,000	Calculated from above	
Cost of site for plant	\$7,000,000	5% of total process unit cost	[126]
General facilities cost	\$28,000,000	20% of total process unit cost	[126]
Engineering permits & start-up	\$17,000,000	10% of direct cost excluding land	[126]
FCI	\$190,000,000		
Contingency	\$19,000,000	10% of FCI	[126]
Working capital	\$14,000,000	3 months payback period	
Total capital cost	\$224,000,000		
Unit capital cost	\$1,491/kg/d	Calculated from above	
NG	\$20,000,000/yr	\$2.58/million Btu LHV	[115]
Electricity	\$28,000,000/yr	\$0.05/kWh	[110]
Steam	\$4,000,000/yr	\$12/t	[109]
Manpower (operating labour + general staff)	\$4,000,000	Labour wage = \$26/hr Total personnel required = 80 Personnel availability = 2010 hr/yr	[109]
Maintenance & repairs	\$8,000,000/yr	5% of direct cost excluding land	[126]
Operating supplies	\$2,000,000/yr	1% of direct cost excluding land	[126]
Interest	\$10,000,000/yr	5% of FCI + contingency	[126]
Local taxes	\$6,000,000/yr	3% of FCI + contingency	[126]
Insurance	\$2,000,000/yr	1% of FCI + contingency	[126]
Total operating cost	\$86,000,000/yr		
Unit production cost	\$1.74/kg	Calculated from above	

Table C.5: Summary of results for SMR-SML-LH_2

Parameter	*Value*	*Remark*	*Source*
Design production capacity	9,500 kg/d	4 million scf/d	
Plant availability	292 d/yr	80% utilisation rate	
Annual actual production	2,774 t/yr	Calculated from above	
NG required per H_2 generated	458 Btu NG/scf H_2	60% LHV efficiency	[81]
NG consumed	1,590 kg/hr	Calculated from above	
Steam consumed	3,570 kg/hr	Material balance calculation	
CO_2 produced	4,361 kg/hr	Material balance calculation	
Liquefaction energy	11 kWh/kg H_2		[75]
Liquefaction power	4,354 kW	Calculated from above	
Storage pressure	1–2 atm		[73]
Storage period	1 day	Assumption	
Storage capacity	9,500 kg	Calculated from above	
LH_2 dispenser rate	5,000 kg/hr/dispenser		[73]
Number of dispensers required	1	Calculated from above	
Unit cost of SMR unit	\$312/kg/d H_2	At 100 t/d H_2 basis	[73]
Size factor of SMR unit	70%		[73]
Unit cost of liquefaction unit	\$700/kg/d H_2	At 100 t/d H_2 basis	[73]
Size factor of liquefaction unit	75%		[73]
Unit cost of LH_2 storage	\$19/kg H_2	At 100 t/d H_2 basis	[73]
Size factor of LH_2 storage	70%		[73]
Unit cost of LH_2 dispenser	\$100,000/dispenser		[73]
Cost of SMR unit	\$6,000,000	Calculated from above	
Cost of liquefaction unit	\$12,000,000	Calculated from above	
Cost of LH_2 storage	\$359,000	Calculated from above	

Table C.5 (*Continued*)

Parameter	*Value*	*Remark*	*Source*
Cost of LH_2 dispenser	$100,000	Calculated from above	
Cost of site for plant	$922,000	5% of total process unit cost	[126]
General facilities cost	$4,000,000	20% of total process unit cost	[126]
Engineering permits & start-up	$2,000,000	10% of direct cost excluding land	[126]
FCI	$25,000,000		
Contingency	$3,000,000	10% of FCI	[126]
Working capital	$1,000,000	3 months payback period	
Total capital cost	$29,000,000		
Unit capital cost	$3,069/kg/d	Calculated from above	
NG	$2,000,000/yr	$2.58/million Btu LHV	[115]
Electricity	$2,000,000/yr	$0.05/kWh	[110]
Steam	$300,000/yr	$12/t	[109]
Manpower (operating labour + general staff)	$1,000,000	Labour wage = $26/hr Total personnel required = 20 Personnel availability = 2010 hr/yr	[109]
Maintenance & repairs	$1,000,000/yr	5% of direct cost excluding land	[126]
Operating supplies	$221,000/yr	1% of direct cost excluding land	[126]
Interest	$1,000,000/yr	5% of FCI + contingency	[126]
Local taxes	$834,000/yr	3% of FCI + contingency	[126]
Insurance	$278,000/yr	1% of FCI + contingency	[126]
Total operating cost	$9,000,000/yr		
Unit production cost	$3.36/kg	Calculated from above	

Table C.6: Summary of results for SMR-LRG-CH_2

Parameter	*Value*	*Remark*	*Source*
Design production capacity	960,000 kg/d	398 million scf/d	
Plant availability	329 d/yr	90% utilisation rate	
Annual actual production	315,360 t/yr	Calculated from above	
NG required per H_2 generated	360 Btu NG/scf H_2	76% LHV efficiency	[73]
NG consumed	126,260 kg/hr	Calculated from above	
Steam consumed	283,564 kg/hr	Material balance calculation	
CO_2 produced	346,362 kg/hr	Material balance calculation	
Compressor energy	1.5 kWh/kg H_2		[73]
Compressor power	60,000 kW	Calculated from above	
Storage pressure	215 atm		[73]
Storage period	1 day	Assumption	
Storage capacity	960,000 kg	Calculated from above	
CH_2 dispenser rate	300 kg/hr/dispenser		[73]
Number of dispensers required	134	Calculated from above	
Unit cost of SMR unit	$312/kg/d H_2	At 100 t/d H_2 basis	[73]
Size factor of SMR unit	70%		[73]
Unit cost of compressor	$2,000/kW H_2	At 100 t/d H_2 basis	[73]
Size factor of compressor	90%		[73]
Unit cost of CH_2 storage	$317/kg H_2	At 100 t/d H_2 basis	[73]
Size factor of CH_2 storage	70%		[73]
Unit cost of CH_2 dispenser	$30,000/dispenser		[73]
Cost of SMR unit	$152,000,000	Calculated from above	
Cost of compressor	$96,000,000	Calculated from above	
Cost of CH_2 storage	$144,000,000	Calculated from above	
Cost of CH_2 dispenser	$4,000,000	Calculated from above	
Cost of site for plant	$20,000,000	5% of total process unit cost	[126]
General facilities cost	$79,000,000	20% of total process unit cost	[126]
Engineering permits & start-up	$47,000,000	10% of direct cost excluding land	[126]
FCI	$541,000,000		
Contingency	$54,000,000	10% of FCI	[126]
Working capital	$49,000,000	3 months payback period	

Table C.6 (*Continued*)

Parameter	*Value*	*Remark*	*Source*
Total capital cost	$644,000,000		
Unit capital cost	$671/kg/d	Calculated from above	
	$884/kg/d	Reference data for comparison	[73]
NG	$136,000,000/yr	$2.58/million Btu LHV	[115]
Electricity	$24,000,000/yr	$0.05/kWh	[110]
Steam	$27,000,000/yr	$12/t	[109]
Manpower (operating labour + general staff)	$9,000,000	Labour wage = $26/hr Total personnel required = 160 Personnel availability = 2010 hr/yr	[109]
Maintenance & repairs	$24,000,000/yr	5% of direct cost excluding land	[126]
Operating supplies	$5,000,000/yr	1% of direct cost excluding land	[126]
Interest	$30,000,000/yr	5% of FCI + contingency	[126]
Local taxes	$18,000,000/yr	3% of FCI + contingency	[126]
Insurance	$6,000,000/yr	1% of FCI + contingency	[126]
Total operating cost	$278,000,000/yr		
Unit production cost	$0.88/kg	Calculated from above	
	$1.30/kg	Reference data for comparison	[73]

Table C.7: Summary of results for CG-LRG-LH_2

Parameter	*Value*	*Remark*	*Source*
Design production capacity	960,000 kg/d	399 million scf/d	
Plant availability	329 d/yr	90% utilisation rate	
Annual actual production	315,360 t/yr	Calculated from above	
Coal required per H_2 generated	405 Btu coal/scf H_2	75% LHV efficiency	[81]
Coal consumed	213,316 kg/hr	Calculated from above	
O_2 required per dry feed	1 kg O_2/kg feed		[81]
O_2 consumed	213,316 kg/hr	Calculated from above	
Steam required per dry feed	0.03 kg H_2O/kg feed		[71]
Steam consumed	6,399 kg/hr	Calculated from above	
CO_2 produced per H_2 generated	19 kg CO_2/kg H_2		[73]
CO_2 produced	759,206 kg/hr	Calculated from above	
Sulphur content	2%		[73]
Sulphur produced	4,266 kg/hr S	Calculated from above	
ASU energy	0.4 kWh/kg O_2	ASU = Air separation unit	[73]
ASU power	58,326 kW	Calculated from above	
Liquefaction energy	11 kWh/kg H_2		[75]
Liquefaction power	440,000 kW	Calculated from above	
Total power required	525,326 kW		
Storage pressure	1–2 atm		[73]
Storage period	1 day	Assumption	
Storage capacity	960,000 kg	Calculated from above	
LH_2 dispenser rate	5,000 kg/hr/dispenser		[73]
Number of dispensers required	8	Calculated from above	
Unit cost of coal handling & preparation	$20/kg/d coal	At 100 t/d H_2 basis	[73]
Size factor of coal handling & preparation	75%		[73]
Unit cost of Texaco coal gasifier	$25/kg/d coal	At 100 t/d H_2 basis	[73]
Size factor of Texaco coal gasifier	85%		[73]
Unit cost of ASU	$28/kg/d O_2	At 100 t/d H_2 basis	[73]
Size factor of ASU	75%		[73]
Unit cost of CO shift, coal & clean-up	$20/kg/d CO_2	At 100 t/d H_2 basis	[73]
Size factor of CO shift, coal & clean-up	75%		[73]
Unit cost of Sulphur recovery unit	$400/kg/d S		[73]

Table C.7 (*Continued*)

Parameter	*Value*	*Remark*	*Source*
Size factor of Sulphur recovery unit	80%		[73]
Unit cost of liquefaction unit	\$700/kg/d H_2	At 100 t/d H_2 basis	[73]
Size factor of liquefaction unit	75%		[73]
Unit cost of LH_2 storage	\$19/kg H_2	At 100 t/d H_2 basis	[73]
Size factor of LH_2 storage	70%		[73]
Unit cost of LH_2 dispenser	\$100,000/dispenser		[73]
Cost of coal handling & preparation	\$58,000,000	Calculated from above	
Cost of Texaco coal gasifier	\$182,000,000	Calculated from above	
Cost of ASU	\$81,000,000	Calculated from above	
Cost of CO shift, cool, clean-up	\$207,000,000	Calculated from above	
Cost of sulphur recovery unit	\$26,000,000	Calculated from above	
Cost of liquefaction unit	\$382,000,000	Calculated from above	
Cost of LH_2 storage	\$9,000,000	Calculated from above	
Cost of LH_2 dispenser	\$800,000	Calculated from above	
Cost of site for plant	\$47,000,000	5% of total process unit cost	[126]
General facilities cost	\$284,000,000	30% of total process unit cost	[126]
Engineering permits & start-up	\$123,000,000	10% of direct cost excluding land	[126]
FCI	\$1,401,000,000		
Contingency	\$140,000,000	10% of FCI	[126]
Working capital	\$69,000,000	3 months payback period	
Total capital cost	\$1,611,000,000		
Unit capital cost	\$1,678/kg/d	Calculated from above	
	\$2,989/kg/d	For comparison	[73]
Coal	\$53,000,000/yr	\$1/million Btu LHV	[115]
Electricity	\$214,000,000/yr	\$0.05/kWh	[110]
Steam	\$605,000/yr	\$12/t	[109]
Manpower (operating labour + general staff)	\$10,000,000	Labour wage = \$26/hr Total personnel required = 180; Personnel availability = 2010 hr/yr	[109]
Maintenance & repairs	\$62,000,000/yr	5% of direct cost excluding land	[126]
Operating supplies	\$12,000,000/yr	1% of direct cost excluding land	[126]
Interest	\$77,000,000/yr	5% of FCI + contingency	[126]
Local taxes	\$46,000,000/yr	3% of FCI + contingency	[126]
Insurance	\$15,000,000/yr	1% of FCI + contingency	[126]
Total operating cost	\$490,000,000/yr		
Unit production cost	\$1.56/kg	Calculated from above	
	\$3.06/kg	Reference data for comparison	[73]

Table C.8: Summary of results for CG-MED-LH_2

Parameter	*Value*	*Remark*	*Source*
Design production capacity	150,000 kg/d	62 million scf/d	
Plant availability	329 d/yr	90% utilisation rate	
Annual actual production	49,275 t/yr	Calculated from above	
Coal required per H_2 generated	428 Btu coal/scf H_2	73% LHV efficiency	[73]
Coal consumed	35,223 kg/hr	Calculated from above	
O_2 required per dry feed	1 kg O_2/kg feed		[81]
O_2 consumed	35,223 kg/hr	Calculated from above	
Steam required per dry feed	0.03 kg H_2O/kg feed		[71]
Steam consumed	1,057 kg/hr	Calculated from above	
CO_2 produced per H_2 generated	19 kg CO_2/kg H_2		[73]

Table C.8 (*Continued*)

Parameter	*Value*	*Remark*	*Source*
CO_2 produced	118,626 kg/hr	Calculated from above	
Sulphur content	2%		[73]
Sulphur produced	704 kg/hr S	Calculated from above	
ASU energy	0.4 kWh/kg O_2		[73]
ASU power	14,089 kW	Calculated from above	
Liquefaction energy	11 kWh/kg H_2		[75]
Liquefaction power	68,750 kW	Calculated from above	
Total power required	82,839 kW		
Storage pressure	1–2 atm		[73]
Storage period	1 day	Assumption	
Storage capacity	150,000 kg	Calculated from above	
LH_2 dispenser rate	5,000 kg/hr/dispenser		[73]
Number of dispensers required	2	Calculated from above	
Unit cost of coal handling & preparation	\$20/kg/d coal	At 100 t/d H_2 basis	[73]
Size factor of coal handling & preparation	75%		[73]
Unit cost of Texaco coal gasifier	\$25/kg/d coal	At 100 t/d H_2 basis	[73]
Size factor of Texaco coal gasifier	85%		[73]
Unit cost of ASU	\$28/kg/d O_2	At 100 t/d H_2 basis	[73]
Size factor of ASU	75%		[73]
Unit cost of CO shift, coal & clean-up	\$20/kg/d CO_2	At 100 t/d H_2 basis	[73]
Size factor of CO shift, coal & clean-up	75%		[73]
Unit cost of Sulphur recovery unit	\$400/kg/d S		[73]
Size factor of Sulphur recovery unit	80%		[73]
Unit cost of liquefaction unit	\$700/kg/d H_2	At 100 t/d H_2 basis	[73]
Size factor of liquefaction unit	75%		[73]
Unit cost of LH_2 storage	\$19/kg H_2	At 100 t/d H_2 basis	[73]
Size factor of LH_2 storage	70%		[73]
Unit cost of LH_2 dispenser	\$100,000/dispenser		[73]
Cost of coal handling & preparation	\$15,000,000	Calculated from above	
Cost of Texaco coal gasifier	\$40,000,000	Calculated from above	
Cost of ASU	\$21,000,000	Calculated from above	
Cost of CO shift, cool, clean-up	\$51,000,000	Calculated from above	
Cost of sulphur recovery unit	\$6,000,000	Calculated from above	
Cost of liquefaction unit	\$95,000,000	Calculated from above	
Cost of LH_2 storage	\$2,000,000	Calculated from above	
Cost of LH_2 dispenser	\$200,000	Calculated from above	
Cost of site for plant	\$12,000,000	5% of total process unit cost	[126]
General facilities cost	\$70,000,000	30% of total process unit cost	[126]
Engineering permits & start-up	\$30,000,000	10% of direct cost excluding land	[126]
FCI	\$343,000,000		
Contingency	\$34,000,000	10% of FCI	[126]
Working capital	\$12,000,000	3 months payback period	
Total capital cost	\$389,000,000		
Unit capital cost	\$2,595/kg/d	Calculated from above	
Coal	\$9,000,000/yr	\$1/million Btu LHV	[115]
Electricity	\$34,000,000/yr	\$0.05/kWh	[110]
Steam	\$100,000/yr	\$12/t	[109]
Manpower (operating labour + general staff)	\$5,000,000	Labour wage = \$26/hr Total personnel required = 100; Personnel availability = 2010 hr/yr	[109]

Table C.8 (*Continued*)

Parameter	*Value*	*Remark*	*Source*
Maintenance & repairs	$15,000,000/yr	5% of direct cost excluding land	[126]
Operating supplies	$3,000,000/yr	1% of direct cost excluding land	[126]
Interest	$19,000,000/yr	5% of FCI + contingency	[126]
Local taxes	$11,000,000/yr	3% of FCI + contingency	[126]
Insurance	$4,000,000/yr	1% of FCI + contingency	[126]
Total operating cost	$100,000,000/yr		
Unit production cost	$2.03/kg	Calculated from above	

Table C.9: Summary of results for CG-LRG-CH_2

Parameter	*Value*	*Remark*	*Source*
Design production capacity	960,000 kg/d	399 million scf/d	
Plant availability	329 d/yr	90% utilisation rate	
Annual actual production	315,360 t/yr	Calculated from above	
Coal required per H_2 generated	405 Btu coal/scf H_2	75% LHV efficiency	[81]
Coal consumed	213,316 kg/hr	Calculated from above	
O_2 required per dry feed	1 kg O_2/kg feed		[81]
O_2 consumed	213,316 kg/hr	Calculated from above	
Steam required per dry feed	0.03 kg H_2O/kg feed		[71]
Steam consumed	6,399 kg/hr	Calculated from above	
CO_2 produced per H_2 generated	19 kg CO_2/kg H_2		[73]
CO_2 produced	759,206 kg/hr	Calculated from above	
Sulphur content	2%		[73]
Sulphur produced	4,266 kg/hr S	Calculated from above	
ASU energy	0.4 kWh/kg O_2		[73]
ASU power	58,326 kW	Calculated from above	
Compressor energy	1.5 kWh/kg H_2		[73]
Compressor power	60,000 kW	Calculated from above	
Total power required	145,326 kW		
Storage pressure	215 atm		[73]
Storage period	1 day	Assumption	
Storage capacity	960,000 kg	Calculated from above	
CH_2 dispenser rate	300 kg/hr/dispenser		[73]
Number of dispensers required	134	Calculated from above	
Unit cost of coal handling & preparation	$20/kg/d coal	At 100 t/d H_2 basis	[73]
Size factor of coal handling & preparation	75%		[73]
Unit cost of Texaco coal gasifier	$25/kg/d coal	At 100 t/d H_2 basis	[73]
Size factor of Texaco coal gasifier	85%		[73]
Unit cost of ASU	$28/kg/d O_2	At 100 t/d H_2 basis	[73]
Size factor of ASU	75%		[73]
Unit cost of CO shift, coal & clean-up	$20/kg/d CO_2	At 100 t/d H_2 basis	[73]
Size factor of CO shift, coal & clean-up	75%		[73]
Unit cost of Sulphur recovery unit	$400/kg/d S		[73]
Size factor of Sulphur recovery unit	80%		[73]
Unit cost of compressor	$2,000/kW H_2	At 100 t/d H_2 basis	[73]
Size factor of compressor	90%		[73]
Unit cost of CH_2 storage	$317/kg H_2	At 100 t/d H_2 basis	[73]
Size factor of CH_2 storage	70%		[73]
Unit cost of CH_2 dispenser	$30,000/dispenser		[73]
Cost of coal handling & preparation	$58,000,000	Calculated from above	
Cost of Texaco coal gasifier	$182,000,000	Calculated from above	
Cost of ASU	$81,000,000	Calculated from above	

Table C.9 (*Continued*)

Parameter	*Value*	*Remark*	*Source*
Cost of CO shift, cool, clean-up	$207,000,000	Calculated from above	
Cost of sulphur recovery unit	$26,000,000	Calculated from above	
Cost of compressor	$96,000,000	Calculated from above	
Cost of CH_2 storage	$144,000,000	Calculated from above	
Cost of CH_2 dispenser	$4,000,000	Calculated from above	
Cost of site for plant	$40,000,000	5% of total process unit cost	[126]
General facilities cost	$239,000,000	30% of total process unit cost	[126]
Engineering permits & start-up	$104,000,000	10% of direct cost excluding land	[126]
FCI	$1,181,000,000		
Contingency	$118,000,000	10% of FCI	[126]
Working capital	$31,000,000	3 months payback period	
Total capital cost	$1,331,000,000		
Unit capital cost	$1,386/kg/d	Calculated from above	
	$2,263/kg/d	Reference data for comparison	[73]
Coal	$55,000,000/yr	$1/million Btu LHV	[115]
Electricity	$59,000,000/yr	$0.05/kWh	[110]
Steam	$605,000/yr	$12/t	[109]
Manpower (operating labour + general staff)	$10,000,000	Labour wage = $26/hr Total personnel required = 180; Personnel availability = 2010 hr/yr	[109]
Maintenance & repairs	$52,000,000/yr	5% of direct cost excluding land	[126]
Operating supplies	$10,000,000/yr	1% of direct cost excluding land	[126]
Interest	$65,000,000/yr	5% of FCI + contingency	[126]
Local taxes	$39,000,000/yr	3% of FCI + contingency	[126]
Insurance	$13,000,000/yr	1% of FCI + contingency	[126]
Total operating cost	$303,000,000/yr		
Unit production cost	$0.96/kg	Calculated from above	
	$2.09/kg	Reference data for comparison	[73]

Table C.10: Summary of results for BG-LRG-LH_2

Parameter	*Value*	*Remark*	*Source*
Design production capacity	960,000 kg/d	399 million scf/d	
Plant availability	329 d/yr	90% utilisation rate	
Annual actual production	315,360 t/yr	Calculated from above	
Biomass moisture content	15%		[73]
Biomass required per H_2 generated	451 Btu bio/scf H_2	80% LHV efficiency	[73]
Biomass consumed	450,552 kg/hr	Calculated from above	
Biomass gasifier feed	382,969 kg/hr dry	Calculated from above	
O_2 required per dry feed	0.8 kg O_2/kg feed		[73]
O_2 consumed	360,441 kg/hr	Calculated from above	
Steam required per dry feed	0.03 kg H_2O/kg feed		[71]
Steam consumed	13,517 kg/hr	Calculated from above	
CO_2 produced per H_2 generated	18 kg CO_2/kg H_2		[73]
CO_2 produced	700,806 kg/hr	Calculated from above	
ASU energy	0.4 kWh/kg O_2		[73]
ASU power	144,177 kW	Calculated from above	
Liquefaction energy	11 kWh/kg H_2		[75]
Liquefaction power	440,000 kW	Calculated from above	
Total power required	584,177 kW	Calculated from above	

Table C.10 (*Continued*)

Parameter	*Value*	*Remark*	*Source*
Storage pressure	1–2 atm		[73]
Storage period	1 day	Assumption	
Storage capacity	960,000 kg	Calculated from above	
LH_2 dispenser rate	5,000 kg/hr/dispenser		[73]
Number of dispensers required	8		
Unit cost of biomass handling & preparation	\$25/kg/d biomass	At 100 t/d H_2 basis	[73]
Size factor of biomass handling & preparation	75%		[73]
Unit cost of Shell biomass gasifier	\$20/kg/d biomass	At 100 t/d H_2 basis	[73]
Size factor of Shell biomass gasifier	80%		[73]
Unit cost of ASU	\$28/kg/d O_2	At 100 t/d H_2 basis	[73]
Size factor of ASU	75%		[73]
Unit cost of CO shift, coal & clean-up	\$15/kg/d CO_2	At 100 t/d H_2 basis	[73]
Size factor of CO shift, coal & clean-up	75%		[73]
Unit cost of liquefaction unit	\$700/kg/d H_2	At 100 t/d H_2 basis	[73]
Size factor of liquefaction unit	75%		[73]
Unit cost of LH_2 storage	\$19/kg H_2	At 100 t/d H_2 basis	[73]
Size factor of LH_2 storage	70%		[73]
Unit cost of LH_2 dispenser	\$100,000/dispenser		[73]
Cost of biomass handling & preparation	\$154,000,000	Calculated from above	
Cost of Shell biomass gasifier	\$234,000,000	Calculated from above	
Cost of ASU	\$138,000,000	Calculated from above	
Cost of CO shift, cool, clean-up	\$143,000,000	Calculated from above	
Cost of liquefaction unit	\$382,000,000	Calculated from above	
Cost of LH_2 storage	\$9,000,000	Calculated from above	
Cost of LH_2 dispenser	\$800,000	Calculated from above	
Cost of site for plant	\$53,000,000	5% of total process unit cost	[126]
General facilities cost	\$318,000,000	30% of total process unit cost	[126]
Engineering permits & start-up	\$138,000,000	10% of direct cost excluding land	[126]
FCI	\$1,569,000,000		
Contingency	\$157,000,000	10% of FCI	[126]
Working capital	\$110,000,000	3 months payback period	
Total capital cost	\$1,836,000,000		
Unit capital cost	\$1,912/kg/d	Calculated from above	
	\$3,017/kg/d	Reference data for comparison	[73]
Biomass	\$190,000,000/yr	\$3.22/million Btu LHV	[73]
Electricity	\$238,000,000/yr	\$0.05/kWh	[110]
Steam	\$1,000,000/yr	\$12/t	[109]
Manpower (operating labour + general staff)	\$10,000,000	Labour wage = \$26/hr Total personnel required = 180; Personnel availability = 2010 hr/yr	[109]
Maintenance & repairs	\$69,000,000/yr	5% of direct cost excluding land	[126]
Operating supplies	\$14,000,000/yr	1% of direct cost excluding land	[126]
Interest	\$86,000,000/yr	5% of FCI + contingency	[126]
Local taxes	\$52,000,000/yr	3% of FCI + contingency	[126]
Insurance	\$17,000,000/yr	1% of FCI + contingency	[126]
Total operating cost	\$678,000,000/yr		

Table C.10 (*Continued*)

Parameter	*Value*	*Remark*	*Source*
Unit production cost	\$2.15/kg **\$3.53/kg**	Calculated from above Reference data for comparison	[73]

Table C.11: Summary of results for BG-MED-LH_2

Parameter	*Value*	*Remark*	*Source*
Design production capacity	150,000 kg/d	62 million scf/d	
Plant availability	329 d/yr	90% utilisation rate	
Annual actual production	49,275 t/yr	Calculated from above	
Biomass moisture content	15%		[73]
Biomass required per H_2 generated	738 Btu bio/scf H_2	50% LHV efficiency	[81]
Biomass consumed	115,198 kg/hr	Calculated from above	
Biomass gasifier feed	97,918 kg/hr dry	Calculated from above	
O_2 required per dry feed	0.8 kg O_2/kg feed		[73]
O_2 consumed	92,158 kg/hr	Calculated from above	
Steam required per dry feed	0.03 kg H_2O/kg feed		[71]
Steam consumed	3,456 kg/hr	Calculated from above	
CO_2 produced per H_2 generated	18 kg CO_2/kg H_2		[73]
CO_2 produced	109,501 kg/hr	Calculated from above	
ASU energy	0.4 kWh/kg O_2		[73]
ASU power	36,863 kW	Calculated from above	
Liquefaction energy	11 kWh/kg H_2		[75]
Liquefaction power	68,750 kW	Calculated from above	
Total power required	105,613 kW		
Storage pressure	1–2 atm		[73]
Storage period	1 day	Assumption	
Storage capacity	150,000 kg	Calculated from above	
LH_2 dispenser rate	5,000 kg/hr/dispenser		[73]
Number of dispensers required	2	Calculated from above	
Unit cost of biomass handling & preparation	\$25/kg/d biomass	At 100 t/d H_2 basis	[73]
Size factor of biomass handling & preparation	75%		[73]
Unit cost of Shell biomass gasifier	\$20/kg/d biomass	At 100 t/d H_2 basis	[73]
Size factor of Shell biomass gasifier	80%		[73]
Unit cost of ASU	\$28/kg/d O_2	At 100 t/d H_2 basis	[73]
Size factor of ASU	75%		[73]
Unit cost of CO shift, coal & clean-up	\$15/kg/d CO_2	At 100 t/d H_2 basis	[73]
Size factor of CO shift, coal & clean-up	75%		[73]
Unit cost of liquefaction unit	\$700/kg/d H_2	At 100 t/d H_2 basis	[73]
Size factor of liquefaction unit	75%		[73]
Unit cost of LH_2 storage	\$19/kg H_2	At 100 t/d H_2 basis	[73]
Size factor of LH_2 storage	70%		[73]
Unit cost of LH_2 dispenser	\$100,000/dispenser		[73]
Cost of biomass handling & preparation	\$62,000,000	Calculated from above	
Cost of Shell biomass gasifier	\$87,000,000	Calculated from above	
Cost of ASU	\$56,000,000	Calculated from above	
Cost of CO shift, cool, clean-up	\$36,000,000	Calculated from above	
Cost of liquefaction unit	\$95,000,000	Calculated from above	
Cost of LH_2 storage	\$2,000,000	Calculated from above	
Cost of LH_2 dispenser	\$200,000	Calculated from above	
Cost of site for plant	\$17,000,000	5% of total process unit cost	[126]

Table C.11 (*Continued*)

Parameter	*Value*	*Remark*	*Source*
General facilities cost	$101,000,000	30% of total process unit cost	[126]
Engineering permits & start-up	$44,000,000	10% of direct cost excluding land	[126]
FCI	$501,000,000		
Contingency	$50,000,000	10% of FCI	[126]
Working capital	$24,000,000	3 months payback period	
Total capital cost	$575,000,000		
Unit capital cost	$3,834/kg/d	Calculated from above	
Biomass	$49,000,000/yr	$3.22/million Btu LHV	[73]
Electricity	$43,000,000/yr	$0.05/kWh	[110]
Steam	$327,000/yr	$12/t	[109]
Manpower (operating labour + general staff)	$5,000,000	Labour wage = $26/hr Total personnel required = 100; Personnel availability = 2010 hr/yr	[109]
Maintenance & repairs	$22,000,000/yr	5% of direct cost excluding land	[126]
Operating supplies	$4,000,000/yr	1% of direct cost excluding land	[126]
Interest	$28,000,000/yr	5% of FCI + contingency	[126]
Local taxes	$17,000,000/yr	3% of FCI + contingency	[126]
Insurance	$6,000,000/yr	1% of FCI + contingency	[126]
Total operating cost	$173,000,000/yr		
Unit production cost	$3.52/kg	Calculated from above	

Table C.12: Summary of results for BG-LRG-CH_2

Parameter	*Value*	*Remark*	*Source*
Design production capacity	960,000 kg/d	399 million scf/d	
Plant availability	329 d/yr	90% utilisation rate	
Annual actual production	315,360 t/yr	Calculated from above	
Biomass moisture content	15%		[73]
Biomass required per H_2 generated	451 Btu bio/scf H_2	80% LHV efficiency	[73]
Biomass consumed	450,552 kg/hr	Calculated from above	
Biomass gasifier feed	382,969 kg/hr	Calculated from above	
O_2 required per dry feed	0.8 kg O_2/kg feed		[73]
O_2 consumed	360,441 kg/hr	Calculated from above	
Steam required per dry feed	0.03 kg H_2O/kg feed		[71]
Steam consumed	13,517 kg/hr	Calculated from above	
CO_2 produced per H_2 generated	18 kg CO_2/kg H_2		[73]
CO_2 produced	700,806 kg/hr	Calculated from above	
ASU energy	0.4 kWh/kg O_2		[73]
ASU power	144,177 kW	Calculated from above	
Compressor energy	1.5 kWh/kg H_2		[73]
Compressor power	60,000 kW	Calculated from above	
Total power required	204,177 kW		
Storage pressure	215 atm		[73]
Storage period	1 day	Assumption	
Storage capacity	960,000 kg	Calculated from above	
CH_2 dispenser rate	300 kg/hr/dispenser		[73]
Number of dispensers required	134	Calculated from above	
Unit cost of biomass handling & preparation	$25/kg/d biomass	At 100 t/d H_2 basis	[73]
Size factor of biomass handling & preparation	75%		[73]
Unit cost of Shell biomass gasifier	$20/kg/d biomass	At 100 t/d H_2 basis	[73]

Table C.12 (*Continued*)

Parameter	*Value*	*Remark*	*Source*
Size factor of Shell biomass gasifier	80%		[73]
Unit cost of ASU	\$28/kg/d O_2	At 100 t/d H_2 basis	[73]
Size factor of ASU	75%		[73]
Unit cost of CO shift, coal & clean-up	\$15/kg/d CO_2	At 100 t/d H_2 basis	[73]
Size factor of CO shift, coal & clean-up	75%		[73]
Unit cost of compressor	\$2,000/kW H_2	At 100 t/d H_2 basis	[73]
Size factor of compressor	90%		[73]
Unit cost of CH_2 storage	\$317/kg H_2	At 100 t/d H_2 basis	[73]
Size factor of CH_2 storage	70%		[73]
Unit cost of CH_2 dispenser	\$30,000/dispenser		[73]
Cost of biomass handling & preparation	\$154,000,000	Calculated from above	
Cost of Shell biomass gasifier	\$234,000,000	Calculated from above	
Cost of ASU	\$138,000,000	Calculated from above	
Cost of CO shift, cool, cleanup	\$143,000,000	Calculated from above	
Cost of compressor	\$96,000,000	Calculated from above	
Cost of CH_2 storage	\$144,000,000	Calculated from above	
Cost of CH_2 dispenser	\$4,000,000	Calculated from above	
Cost of site for plant	\$46,000,000	5% of total process unit cost	[126]
General facilities cost	\$273,000,000	30% of total process unit cost	[126]
Engineering permits & start-up	\$119,000,000	10% of direct cost excluding land	[126]
FCI	\$1,349,000,000		
Contingency	\$135,000,000	10% of FCI	[126]
Working capital	\$74,000,000	3 months payback period	
Total capital cost	\$1,558,000,000		
Unit capital cost	\$1,623/kg/d	Calculated from above	
	\$2,411/kg/d	Reference data for comparison	[73]
Biomass	\$202,000,000/yr	\$3.22/million Btu LHV	[73]
Electricity	\$83,000,000/yr	\$0.05/kWh	[110]
Steam	\$1,000,000/yr	\$12/t	[109]
Manpower (operating labour + general staff)	\$10,000,000	Labour wage = \$26/hr Total personnel required = 180; Personnel availability = 2010 hr/yr	[109]
Maintenance & repairs	\$59,000,000/yr	5% of direct cost excluding land	[126]
Operating supplies	\$12,000,000/yr	1% of direct cost excluding land	[126]
Interest	\$74,000,000/yr	5% of FCI + contingency	[126]
Local taxes	\$45,000,000/yr	3% of FCI + contingency	[126]
Insurance	\$15,000,000/yr	1% of FCI + contingency	[126]
Total operating cost	\$501,000,000/yr		
Unit production cost	\$1.59/kg	Calculated from above	
	\$2.69/kg	Reference data for comparison	[73]

Table C.13: Summary of results for WE-MED-LH_2

Parameter	*Value*	*Remark*	*Source*
Design production capacity	150,000 kg/d	62 million scf/d	
Plant availability	329 d/yr	90% utilisation rate	
Annual actual production	49,275 t/yr	Calculated from above	
H_2O required per H_2 generated	9 kg H_2O/kg H_2		[73]
H_2O consumed	56,250 kg/hr	Calculated from above	
O_2 produced	49,956 kg/hr	Material balance calculation	
Electrolysis theoretical efficiency	39.37 kWh/kg H_2	At 100% efficiency	[73]
Electrolysis electrical efficiency	75%		[73]
Electrolysis actual power	52.19 kWh/kg H_2	Calculated from above	
Electrolysis power	328,083 kW	Calculated from above	
Liquefaction energy	11 kWh/kg H_2		[75]
Liquefaction power	68,750 kW	Calculated from above	
Total power required	396,833 kW		
Storage pressure	1–2 atm		[73]
Storage period	1 day	Assumption	
Storage capacity	150,000 kg	Calculated from above	
LH_2 dispenser rate	5,000 kg/hr/dispenser		[73]
Number of dispensers required	2	Calculated from above	
Unit cost of electrolyser	$800/kW	At 100 t/d H_2 basis	[73]
Size factor of electrolyser unit	90%		[81]
Unit cost of liquefaction unit	$700/kg/d H_2	At 100 t/d H_2 basis	[73]
Size factor of liquefaction unit	75%		[73]
Unit cost of LH_2 storage	$19/kg H_2	At 100 t/d H_2 basis	[73]
Size factor of LH_2 storage	70%		[73]
Unit cost of LH_2 dispenser	$100,000/dispenser		[73]
Cost of electrolyser	$315,000,000	Calculated from above	
Cost of liquefaction unit	$95,000,000	Calculated from above	
Cost of LH_2 storage	$2,000,000	Calculated from above	
Cost of LH_2 dispenser	$200,000	Calculated from above	
Cost of site for plant	$21,000,000	5% of total process unit cost	[126]
General facilities cost	$83,000,000	20% of total process unit cost	[126]
Engineering permits & start-up	$50,000,000	10% of direct cost excluding land	[126]
FCI	$565,000,000		
Contingency	$57,000,000	10% of FCI	[126]
Working capital	$42,000,000	3 months payback period	
Total capital cost	$663,000,000		
Unit capital cost	$4,422/kg/d	Calculated from above	
Water	$110,000/yr	$0.00025/kg (demineralised)	[109]
Electricity	$162,000,000/yr	$0.05/kWh	[110]
O_2 by-product (sale)	($4,000,000/yr)	($10/t O_2)	[73]
Manpower (operating labour + general staff)	$4,000,000	Labour wage = $26/hr Total personnel required = 80 Personnel availability = 2010 hr/yr	[109]
Maintenance & repairs	$25,000,000/yr	5% of direct cost excluding land	[126]
Operating supplies	$5,000,000/yr	1% of direct cost excluding land	[126]
Interest	$31,000,000/yr	5% of FCI + contingency	[126]
Local taxes	$19,000,000/yr	3% of FCI + contingency	[126]
Insurance	$6,000,000/yr	1% of FCI + contingency	[126]
Total operating cost	$248,000,000/yr		
Unit production cost	$5.03/kg	Calculated from above	

Table C.14: Summary of results for WE-SML-LH_2

Parameter	*Value*	*Remark*	*Source*
Design production capacity	9,500 kg/d	4 million scf/d	
Plant availability	292 d/yr	80% utilisation rate	
Annual actual production	2,774 t/yr	Calculated from above	
H_2O required per H_2 generated	9 kg H_2O/kg H_2		[73]
H_2O consumed	3,563 kg/hr	Calculated from above	
O_2 produced	3,164 kg/hr	Material balance calculation	
Electrolysis theoretical efficiency	39.37 kWh/kg H_2	At 100% efficiency	[73]
Electrolysis electrical efficiency	75%		[73]
Electrolysis actual power	52.19 kWh/kg H_2	Calculated from above	
Electrolysis power	20,779 kW	Calculated from above	
Liquefaction energy	11 kWh/kg H_2		[75]
Liquefaction power	4,354 kW	Calculated from above	
Total power required	25,133 kW		
Storage pressure	1–2 atm		[73]
Storage period	1 day	Assumption	
Storage capacity	9,500 kg	Calculated from above	
LH_2 dispenser rate	5,000 kg/hr/dispenser		[73]
Number of dispensers required	1	Calculated from above	
Unit cost of electrolyser	$1,000/kW	At 100 t/d H_2 basis	[73]
Size factor of electrolyser unit	90%		[81]
Unit cost of liquefaction unit	$700/kg/d H_2	At 100 t/d H_2 basis	[73]
Size factor of liquefaction unit	75%		[73]
Unit cost of LH_2 storage	$19/kg H_2	At 100 t/d H_2 basis	[73]
Size factor of LH_2 storage	70%		[73]
Unit cost of LH_2 dispenser	$100,000/dispenser		[73]
Cost of electrolyser	$26,000,000	Calculated from above	
Cost of liquefaction unit	$12,000,000	Calculated from above	
Cost of LH_2 storage	$359,000	Calculated from above	
Cost of LH_2 dispenser	$100,000	Calculated from above	
Cost of site for plant	$2,000,000	5% of total process unit cost	[126]
General facilities cost	$8,000,000	20% of total process unit cost	[126]
Engineering permits & start-up	$5,000,000	10% of direct cost excluding land	[126]
FCI	$53,000,000		
Contingency	$5,000,000	10% of FCI	[126]
Working capital	$3,000,000	3 months payback period	
Total capital cost	$61,000,000		
Unit capital cost	$6,436/kg/d	Calculated from above	
Water	$6,000/yr	$0.00025/kg (demineralised)	[109]
Electricity	$10,000,000/yr	$0.06/kWh	[110]
O_2 by-product (sale)	($222,000/yr)	($10/t O_2)	[73]
Manpower (operating labour + general staff)	$1,000,000	Labour wage = $26/hr Total personnel required = 20 Personnel availability = 2010 hr/yr	[109]
Maintenance & repairs	$2,000,000/yr	5% of direct cost excluding land	[126]
Operating supplies	$465,000/yr	1% of direct cost excluding land	[126]
Interest	$3,000,000/yr	5% of FCI + contingency	[126]
Local taxes	$2,000,000/yr	3% of FCI + contingency	[126]
Insurance	$584,000/yr	1% of FCI + contingency	[126]
Total operating cost	$19,000,000/yr		
Unit production cost	$6.82/kg	Calculated from above	

C.3 Hydrogen Storage Technologies

In this section, the storage cost of liquid and compressed hydrogen gas in stationary storage facilities will be estimated. The storage facility includes storage tanks and dispensers. For liquid hydrogen storage, three different sizes will be considered namely large, medium and small. However, only the large size of compressed-gaseous storage facility will be considered for the purpose of this study. The different sizes of storage facilities–small, medium, and large–are assumed to have a storage capacity range from 0.5 to 9.5, 10 to 150, and 200 to 540 tonnes of hydrogen, respectively, with a 100% average utilisation rate. The economic analysis for each type and size of these storage technologies are summarised in Tables C.15–C.18. The calculation procedure to be used in this analysis is consistent with the one used for production technologies.

Several comprehensive studies [66, 75, 76, 127, 128] have been carried out to evaluate the cost of stationary hydrogen storage systems. Taylor *et al.* [76] analysed the cost of storing hydrogen above-ground as a cryogenic liquid as well as high-pressure storage both above and below ground. Amos [75] examined the capital and operating costs of several storage options including compressed gas, liquid hydrogen, metal hydride, and underground storage. Carpetis and Schwarz *et al.* [127, 128] have also provided an economic evaluation of hydrogen stored in pressurised cylinders, on metal hydride, and in cryogenic vessel. In all of these studies, the cost of hydrogen storage depends on the quantity of hydrogen to be stored, the storage period, the type of technology, the required form of hydrogen to be used, and the required energy density.

Again, the unit capital costs obtained from our economic assessment will be cross-checked with the ones estimated by Amos [75], since he examined a range of storage capacities. The value will appear in bold. It is worth noting that we did not validate our unit storage cost with a reference data. This is due to the fact that most of the reviewed studies include the operating cost of compression and liquefaction in their calculations. However, in our case the compression and liquefaction costs were

included in the production cost as a part of the handling step (see Section C.2). Therefore, the reference data shows a significant difference from the calculated value.

Table C.15: Summary of results for large-scale liquid hydrogen storage

Parameter	*Value*	*Remark*	*Source*
Storage capacity	540,000 kg		
Storage availability	365 d/yr	100% utilisation rate	
Storage pressure	1–2 atm		[73]
Storage period	10 days	Assumption	
Boil-off rate	0.03%/d		[113]
LH_2 dispenser rate	5,000 kg/hr/dispenser		[73]
Number of dispensers required	8	Calculated from above	
Unit cost of LH_2 storage	$19/kg	At 100 t/d H_2 basis	[73]
Size factor of LH_2 storage	70%		[73]
Unit cost of LH_2 dispenser	$100,000/dispenser		[73]
Cost of LH_2 tank	$91,000,000	Calculated from above	
Cost of LH_2 dispenser	$800,000	Calculated from above	
Cost of site for storage	$5,00,000	5% of total process unit cost	[126]
General facilities cost	$9,000,000	10% of total process unit cost	[126]
Engineering permits & start-up	$5,000,000	5% of direct cost excluding land	[126]
FCI	$110,000,000		
Contingency	$11,000,000	10% of FCI	[126]
Working capital	$323,000	3 months payback period	
Total capital cost	$122,000,000		
Unit capital cost	$13/kg	Calculated from above	
	$21/kg	Reference data for comparison	[73]
Manpower (operating labour + general staff)	$1,000,000/yr	Labour wage = $26/hr Total personnel required = 24 Personnel availability = 2010 hr/yr	[109]
Maintenance & repairs	$5,000,000/yr	5% of direct cost excluding land	[126]
Operating supplies	$1,000,000/yr	1% of direct cost excluding land	[126]
Interest	$6,000,000/yr	5% of FCI + contingency	[126]
Local taxes	$4,000,000/yr	3% of FCI + contingency	[126]
Insurance	$1,000,000/yr	1% of FCI + contingency	[126]
Total operating cost	$18,000,000/yr		
Unit storage cost	$0.005/kg/d	Calculated from above	

Table C.16: Summary of results for medium-scale liquid hydrogen storage

Parameter	*Value*	*Remark*	*Source*
Storage capacity	150,000 kg		
Storage availability	365 d/yr	100% utilisation rate	
Storage pressure	1–2 atm		[73]
Storage period	10 days	Assumption	
Boil-off rate	0.06%/d	Double that of NASA's tank	
LH_2 dispenser rate	5,000 kg/hr/dispenser		[73]
Number of dispensers required	2	Calculated from above	
Unit cost of LH_2 storage	$19/kg	At 100 t/d H_2 basis	[73]
Size factor of LH_2 storage	70%		[73]
Unit cost of LH_2 dispenser	$100,000/dispenser		[73]
Cost of LH_2 tank	$25,000,000	Calculated from above	
Cost of LH_2 dispenser	$200,000	Calculated from above	
Cost of site for storage	$1,000,000	5% of total process unit cost	[126]
General facilities cost	$2,000,000	10% of total process unit cost	[126]
Engineering permits & start-up	$1,000,000	5% of direct cost excluding land	[126]
FCI	$30,000,000		

Table C.16 (*Continued*)

Parameter	*Value*	*Remark*	*Source*
Contingency	$3,000,000	10% of FCI	[126]
Working capital	$215,000	3 months payback period	
Total capital cost	$33,000,000		
Unit capital cost	$22/kg	Calculated from above	
	$43/kg	Reference data for comparison	[73]
Manpower (operating labour + general staff)	$861,000/yr	Labour wage = $26/hr Total personnel required = 16 Personnel availability = 2010 hr/yr	[109]
Maintenance & repairs	$1,000,000/yr	5% of direct cost excluding land	[126]
Operating supplies	$275,000/yr	1% of direct cost excluding land	[126]
Interest	$2,000,000/yr	5% of FCI + contingency	[126]
Local taxes	$994,000/yr	3% of FCI + contingency	[126]
Insurance	$331,000/yr	1% of FCI + contingency	[126]
Total operating cost	$5,000,000/yr		
Unit storage cost	$0.010/kg/d	Calculated from above	

Table C.17: Summary of results for small-scale liquid hydrogen storage

Parameter	*Value*	*Remark*	*Source*
Storage capacity	9,500 kg		
Storage availability	365 d/yr	100% utilisation rate	
Storage pressure	1–2 atm		[73]
Storage period	10 day	Assumption	
Boil-off rate	0.20%/d		[76]
LH_2 dispenser rate	5,000 kg/hr/dispenser		[73]
Number of dispensers required	1	Calculated from above	
Unit cost of LH_2 storage	$19/kg	At 100 t/d H_2 basis	[73]
Size factor of LH_2 storage	70%		[73]
Unit cost of LH_2 dispenser	$100,000/dispenser		[73]
Cost of LH_2 tank	$4,000,000	Calculated from above	
Cost of LH_2 dispenser	$100,000	Calculated from above	
Cost of site for storage	$185,000	5% of total process unit cost	[126]
General facilities cost	$369,000	10% of total process unit cost	[126]
Engineering permits & start-up	$203,000	5% of direct cost excluding land	[126]
FCI	$4,000,000		
Contingency	$445,000	10% of FCI	[126]
Working capital	$108,000	3 months payback period	
Total capital cost	$5,000,000		
Unit capital cost	$53/kg	Calculated from above	
	$85/kg	Reference data for comparison	[73]
Manpower (operating labour + general staff)	$431,000/yr	Labour wage = $26/hr Total personnel required = 8 Personnel availability = 2010 hr/yr	[109]
Maintenance & repairs	$203,000/yr	5% of direct cost excluding land	[126]
Operating supplies	$41,000/yr	1% of direct cost excluding land	[126]
Interest	$245,000/yr	5% of FCI + contingency	[126]
Local taxes	$147,000/yr	3% of FCI + contingency	[126]
Insurance	$49,000/yr	1% of FCI + contingency	[126]
Total operating cost	$1,000,000/yr		
Unit storage cost	$0.032/kg/d	Calculated from above	

Table C.18: Summary of results for large-scale compressed hydrogen storage

Parameter	*Value*	*Remark*	*Source*
Storage capacity	540,000 kg		
Storage availability	365 d/yr	100% utilisation rate	
Storage pressure	165 atm		[73]
Storage period	10 days	Assumption	
CH_2 dispenser rate	300 kg/hr/dispenser		[73]
Number of dispensers required	134	Calculated from above	
Unit cost of CH_2 dispenser	\$30,000/dispenser		[73]
Unit cost of CH_2 storage	\$298/kg	At 100 t/d H_2 basis	[73]
Size factor of CH_2 storage	70%		[73]
Cost of CH_2 tank	\$1,000,000,000	Calculated from above	
Cost of CH_2 dispenser	\$4,000,000	Calculated from above	
Cost of site for storage	\$73,000,000	5% of total process unit cost	[126]
General facilities cost	\$146,000,000	10% of total process unit cost	[126]
Engineering permits & start-up	\$73,000,000	5% of direct cost excluding land	[126]
FCI	\$2,000,000,000		
Contingency	\$146,000,000	10% of FCI	[126]
Working capital	\$323,000	3 months payback period	
Total capital cost	\$2,000,000,000		
Unit capital cost	\$197/kg	Calculated from above	
	\$283/kg	Reference data for comparison	[73]
Manpower (operating labour + general staff)	\$1,000,000/yr	Labour wage = \$26/hr Total personnel required = 24 Personnel availability = 2010 hr/yr	[109]
Maintenance & repairs	\$80,000,000/yr	5% of direct cost excluding land	[126]
Operating supplies	\$16,00,000/yr	1% of direct cost excluding land	[126]
Interest	\$95,000,000/yr	5% of FCI + contingency	[126]
Local taxes	\$57,000,000/yr	3% of FCI + contingency	[126]
Insurance	\$19,000,000/yr	1% of FCI + contingency	[126]
Total operating cost	\$268,000,000/yr		
Unit storage cost	\$0.076/kg/d	Calculated from above	

C.4 Hydrogen Distribution Technologies

As mentioned, this thesis addresses the distribution of hydrogen by trucks and rail. The derivation of the cost functions for both transport modes are illustrated below in greater detail.

C.4.1 Capital Cost

The transportation capital cost is calculated by multiplying the number of vehicles by the cost of the mode. The number of vehicles is calculated as follows:

1. Determine the daily number of journeys required between two destinations using the following equation:

$$\text{No. of journey} = \frac{\text{Demand per day}}{\text{Vehicle capacity}} \tag{C.1}$$

2. Determine the duration of journey via the following equation:

$$\text{Duration of journey} = \frac{\text{Two-way distance}}{\text{Vehicle speed}} \tag{C.2}$$

3. Determine the total driving time by multiplying the number of journeys by the duration of the journey. This will give us the number of hours a journey requires per day.
4. Determine the total loading and unloading time for a particular journey as follows:

$$\text{Total loading/unloading time} = \text{Loading/unloading time} \times \text{No. of journey} \tag{C.3}$$

5. The total delivery time for a journey is equal to:

$$\text{Total delivery time} = \text{Total driving time} + \text{Total loading/unloading time} \tag{C.4}$$

6. The number of vehicles is equal to:

$$\text{No. of vehicles} = \frac{\text{Total delivery time}}{\text{Vehicle availability per day}} \tag{C.5}$$

C.4.2 Operating Cost

The transportation operating cost includes:

1. Fuel cost which is a function of daily fuel usage and fuel price.

$$\text{Daily fuel usage} = \frac{\text{Two-way distance} \times \text{Demand per day}}{\text{Vehicle capacity} \times \text{Fuel efficiency}} \tag{C.6}$$

2. Labour cost which is a function of total delivery time and driver wage. The total delivery time is given in Equation C.4.

3. Maintenance cost which is a function of total daily distance driven and the cost per distance travelled.

$$\text{Total distance travelled} = \frac{\text{Two-way distance} \times \text{Demand per day}}{\text{Vehicle capacity}} \tag{C.7}$$

4. General costs which are a function of the total number of vehicles and the general expenses associated with the vehicles. The total number of vehicles is given by Equation C.5.

C.5 Hydrogen Dispensing Technologies

This section presents estimates of the daily cost of dispensing liquid hydrogen to customers via fuelling stations. The section will not focus on estimating the capital cost associated with establishing such stations because it will be assumed that current petrol stations will be used to dispense hydrogen. To perform the economic analysis, a fuelling station with a capacity of 5,000 kg/d is assumed, based on petrol fuelling stations that are currently available [81]. Also, the assigned capacity can be worked out by the following calculations:

$$\left[10\ \frac{\text{pumps}}{\text{garage}}\right]\left[12\ \frac{\text{hr}}{\text{d}}\right]\left[60\ \frac{\text{min}}{\text{hr}}\right]\left[\frac{1}{10}\ \frac{\text{filling}}{\text{min}}\right]\left[25\ \frac{\text{L}}{\text{filling}}\right]\left[\frac{1}{3.785}\ \frac{\text{US gal}}{\text{L}}\right]$$

$$= 4{,}756\ \frac{\text{US gal}}{\text{garage.d}}$$

Since the above parameters are subject to uncertainty, a fuelling station with a capacity of 5,000 kg/d is a reasonable assumption. Bear in mind that one kilogram of hydrogen has the same energy content of one US gallon of gasoline.

The examined fuelling station can support 15,620 fuel cell vehicles assuming an average utilisation rate of 90%. It consists of a buffer storage tank and a dispenser. The storage tank is assumed to hold 7 days' worth of stock of liquid hydrogen to accommodate for daily demand fluctuations. The data used to calculate the dispensing cost of liquid hydrogen is summarised in Table C.19.

Table C.19: Data used for LH_2-based fuelling station

Parameter	*Value*	*Remark*	*Source*
Fuelling station capacity	5,000 kg/d		[81]
Fuelling station availability	329 d/yr	90% utilisation rate	
Annual actual production	1,643 t/yr	Calculated from above	
Storage pressure	1–2 atm		[73]
Boil-off rate	0.20%/d		[76]
Storage period	7 days	Assumption	
Storage capacity	35,000 kg	Calculated from above	
LH_2 dispenser rate	5,000 kg/hr/dispenser		[73]
Number of dispensers required	1	Calculated from above	
Unit cost of LH_2 storage	\$37/kg	At 1 t/d H_2 basis	[73]
Size factor of LH_2 storage	70%		[73]
Unit cost of LH_2 dispenser	\$100,000/dispenser		[73]
Cost of LH_2 tank	\$806,034	Calculated from above	
Cost of LH_2 dispenser	\$100,000	Calculated from above	
Cost of site for fuelling	\$45,302	5% of total process unit cost	[126]
General facilities cost	\$90,603	10% of total process unit cost	[126]
Engineering permits & start-up	\$49,832	5% of direct cost excluding land	[126]
FCI	\$1,091,771		
Contingency	\$109,771	10% of FCI	[126]
Working capital	\$153,765	3 months payback period	
Total capital cost	\$1,354,713		
Unit capital cost	\$271/kg/d	Calculated from above	
Manpower (operating labour)	\$615,060/yr	Labour wage = \$26/hr Total personnel required = 12 Personnel availability = 2010 hr/yr	[109]
Maintenance & repairs	\$49,832/yr	5% of direct cost excluding land	[126]
Operating supplies	\$9,966/yr	1% of direct cost excluding land	[126]
Interest	\$60,047/yr	5% of FCI + contingency	[126]
Local taxes	\$36,028/yr	3% of FCI + contingency	[126]
Insurance	\$12,009/yr	1% of FCI + contingency	[126]
Total operating cost	\$782,944/yr		
Unit dispensing cost	\$0.48/kg	Calculated from above	

Appendix D

Availability of Primary Energy Sources

D.1 Introduction

This appendix presents the procedure used to estimate the availability of primary energy sources in the UK. Four types of primary energy sources will be examined namely natural gas, coal, biomass, and electrical energy. For each type of energy sources, the geographical location and the quantity will be estimated. Such a determination will be made based on statistical data obtained from disparate sources. The same data obtained for the UK will be applied in a Great Britain context. This is because of difficulty faced in finding data dedicated entirely for Great Britain.

Since this thesis addresses the design of steady-state and multi-period models, the availability of resources for each model will be slightly different. The following sections detail how these availabilities were calculated.

D.2 Natural Gas

D.2.1 Resource Availability

Steady-State Model

According to the BP statistical review [115], the proven reserve of natural gas at the end of 2003 was 0.59 trillion cubic meters. For simplicity and to obtain the maximum daily availability, it is assumed that this reserve will last for at least five years. Since the flow rate of materials in the entire thesis is expressed in terms of mass, the daily maximum availability of natural gas is equal to:

$$\left[\frac{0.59\times10^{12}}{5}\ \frac{\mathrm{m}^3}{\mathrm{yr}}\right]\left[0.68\ \frac{\mathrm{kg}}{\mathrm{m}^3}\right]\left[\frac{1}{365}\ \frac{\mathrm{yr}}{\mathrm{d}}\right]=220\times10^{6}\ \frac{\mathrm{kg}}{\mathrm{d}}$$

The division by five in the first term of the left-hand-side of the equation denotes the maximum consumption rate of natural gas, while the second term denotes the density of methane at standard temperature and pressure. The density of methane is used due to the fact that more than 95% of natural gas is composed of methane [129].

Multi-Period Model

The addition of a time element to Chapter 5 will slightly affect the procedure used to estimate the daily availability of natural gas. Since the daily flow rate of materials over a particular time period of the planning horizon is constant, the initial availability of natural gas must be sufficient for the entire time period. Taking this into consideration, the average maximum daily availability of natural gas is equal to:

$$\left[0.59\times10^{12}\ \mathrm{m}^3\right]\left[0.68\ \frac{\mathrm{kg}}{\mathrm{m}^3}\right]\left[\frac{1}{365}\ \frac{\mathrm{yr}}{\mathrm{d}}\right]\left[\frac{1}{6}\ \frac{1}{\mathrm{yr}}\right]=183\times10^{6}\ \frac{\mathrm{kg}}{\mathrm{d}}$$

where the fourth term of the left-hand-side of the equation represents the duration of each time period of the planning horizon. The estimated availability provides the initial condition for the multi-period model.

D.2.2 Resource Allocation

The majority of UK's natural gas resources are located offshore in the North Sea, with a small quantity available in the Irish Sea [130]. These resources supply the vast demand of the country via six main gas terminals situated at the coastline. The location of these terminals is shown in Table D.1.

Table D.1: Location of gas terminals in the UK [130]

Gas terminal no.	Terminal name	Location
1	St. Fergus	East of Scotland
2	Teesside	North East of England
3	Warrington	North of Wales
4	Easington	Yorkshire and the Humberside
5	Theddlethorpe	East Midlands
6	Bacton	East Anglia

In the context of our study, the previously mentioned gas terminals lie in the grids summarised in Table D.2.

Table D.2: Location of gas terminals with respect to grid number

Gas terminal no.	Grid, g
1	05
2	14
3	17
4	19
5	19
6	25

The quantity of natural gas in each grid is estimated based on the assumption that 50% of UK's total natural gas is available in grid 5, 10% is available in grid 17, and 40% is available in grids 14, 19, and 25. The latter percentage was divided equally between the three grids. As noted, grid 5, which is supplied by gas terminal 1, has the highest percentage due to the fact that most of UK's offshore associated and non-associated gas fields are located in the Northern region of the North Sea [130]. Also, grid 5 is connected to the UK-Norway gas interconnector which has an import capacity of 11 billion cubic meters [131]. Using these percentages, the daily amount of natural gas available in the above mentioned grids was calculated for the steady-state and the multi-period models. The corresponding results for both models are summarised in Tables D.3 and D.4 respectively.

Table D.3: Availability of natural gas for the steady-state model

Grid, g	Availability (million kg/d)
05	110
14	29
17	22
19	29
25	29
Total	220

Table D.4: Average availability of natural gas for the multi-period model

Grid, g	Availability (million kg/d)
05	92
14	24
17	18
19	24
25	24
Total	183

D.3 Coal

D.3.1 Resource Availability

Steady-State Model

BP stated in its 2004 annual statistical review that there exists 1500 million tonnes of proven coal reserves in the UK, which are estimated to last for 53 years at the current consumption rate [115]. Assuming that these reserves could be consumed in at least five years, the maximum daily availability of coal in kilograms is equal to:

$$\left[\frac{1500\times10^{6}}{5}\ \frac{\text{t}}{\text{yr}}\right]\left[1000\ \frac{\text{kg}}{\text{t}}\right]\left[\frac{1}{365}\ \frac{\text{yr}}{\text{d}}\right]=822\times10^{6}\ \frac{\text{kg}}{\text{d}}$$

Again, the division by five in the first term represents the consumption rate of coal.

Multi-Period Model

Taking into account the time effect, the average maximum daily availability of coal is calculated as follows:

$$\left[1500\times10^{6}\ \text{t}\right]\left[\frac{1}{365}\ \frac{\text{yr}}{\text{d}}\right]\left[1000\ \frac{\text{kg}}{\text{t}}\right]\left[\frac{1}{6}\ \frac{1}{\text{yr}}\right]=685\times10^{6}\ \frac{\text{kg}}{\text{d}}$$

Again, the last term of the left-hand-side represents the duration of each time period of the planning horizon, and the calculated availability provides the total amount of coal that is initially available.

D.3.2 Resource Allocation

The largest areas of the UK's on-land coal resources are in Yorkshire, Lancashire, and Warwickshire [132]. There are also small deposits of coal in North East, Central Scotland and South Wales [132]. The corresponding grids that these resources reside in are tabulated in D.5.

Table D.5: Location of coalfields with respect to grid number

Coalfield location	Grid, g
Yorkshire	18
Lancashire	17
Warwickshire	23
North East	11
Central Scotland	7, 9 & 10
South Wales	27

The percentage of coal available in each field was estimated by comparing the size of each field to the total size. For instance, grids 17, 18, and 23 were given 60% of the total coal share since they contain most of the UK's coal resources. The percentage given to the remaining grids and the quantities available are shown in Table D.6.

Table D.6: Availability of coal in each grid for the steady-state model

Grid, g	Percentage (%)	Availability (million kg/d)
07	7	55
09	7	55
10	7	55
11	10	82
17	20	164
18	20	164
23	20	164
27	10	82
Total	100	822

It is worth emphasising that the availability values given in Table D.6 are applicable only for the steady-state model. Also, it can be seen from the table that an even distribution of coal was assumed for grids 7, 9, and 10 as well as grids 17, 18, and 23.

For the multi-period model, the average availability of coal is listed in Table D.7.

Table D.7: Average availability of coal in each grid for the multi-period model

Grid, *g*	Availability (million kg/d)
07	46
09	46
10	46
11	68
17	137
18	137
23	137
27	68

D.4 Biomass

D.4.1 Resource Availability

Steady-State Model

The available biomass in the UK during 2000 was around 25 million dry tonnes [133]. This includes agriculture, forests, and industrial residues as well as regulated and non-regulated wastes. On a daily basis, the maximum daily amount of biomass available is equal to:

$$\left[25\times10^{6}\ \frac{\text{t}}{\text{yr}}\right]\left[\frac{1}{365}\ \frac{\text{yr}}{\text{d}}\right]\left[1000\ \frac{\text{kg}}{\text{t}}\right]=68.5\times10^{6}\ \frac{\text{kg}}{\text{d}}$$

Multi-Period Model

Since biomass is an inexhaustible resource, it can be obtained at any time period of the planning horizon. As a result, the initial average availability of biomass for the multi-period model is identical to one given for the steady-state model, i.e. 68.5×10^{6} kg/d.

D.4.2 Resource Allocation

Since the UK has approximately 6.5 million hectares of arable land [134], biomass was assumed to be available in all grids with an even distribution. However, this excludes grids that reside in metropolitan areas such as 14, 17, 18, 23, and 29, which will be given a lower distribution percentage. Grids that contain metropolitan areas make up about 15% of the total number of grids, however, only 5% of the total biomass is assumed to be available in these grids. Therefore, the daily biomass availability for both models in the metropolitan grids is:

$$\left[68.5\times10^{6}\ \frac{\text{kg}}{\text{d}}\right]\left[\frac{0.05}{5}\right]=685\times10^{3}\ \frac{\text{kg}}{\text{d}}$$

Similarly, the daily availability of biomass for both models in remaining grids is:

$$\left[68.5\times10^{6}\ \frac{\text{kg}}{\text{d}}\right]\left[\frac{0.95}{29}\right]=2\times10^{6}\ \frac{\text{kg}}{\text{d}}$$

In the above equations, the division by 5 and 29 denotes the total number of metropolitan and normal grids respectively.

D.5 Electricity

D.5.1 Resource Availability

Steady-State Model

Currently, the UK generates its electricity from a wide range of resources including natural gas, coal, oil, nuclear energy and hydropower. According to the Department of Trade and Industry (DTI) [135], the total electricity available in the UK during 2003 was 379 TWh. Assuming that this amount will be consumed in one year and only 10% of electricity could be used for electrolysis, the maximum daily amount is equal to:

$$[0.1]\left[379\times10^{9}\ \frac{\text{kWh}}{\text{yr}}\right]\left[\frac{1}{365}\ \frac{\text{yr}}{\text{d}}\right]=104\times10^{6}\ \frac{\text{kWh}}{\text{d}}$$

Multi-Period Model

Taking into account the time effect, the daily average amount of electricity is assumed to be identical to the one given above, i.e. 104×10^{6} kWh/d. This is due to the fact that electricity is produced on a daily basis; thus it can be harnessed at any time regardless of the time period's duration.

D.5.2 Resource Allocation

Due to the fact that electricity is available throughout the UK, we will assume an even distribution of electricity in all grids. Therefore, the amount of electricity available in each grid for both models is equal to the total availability divided by the total number of grids, i.e. 34 grids:

$$\left[\frac{104\times10^{6}\ \text{kWh}}{34\ \text{d}}\right]=3\times10^{6}\ \frac{\text{kWh}}{\text{d}}$$

Appendix E

Detailed Results

E.1 Introduction

This appendix contains auxiliary results concerning the five mathematical models derived throughout this thesis. The results for each model are given in a separate section for convenience and ease of reference. In each section, the value of some variables will be listed. The values of the remaining variables are not shown here since they can be worked out easily from the ones that are given.

E.2 Steady-State Model

Table E.1: Flow rate of liquid hydrogen by transport modes for the steady-state model

Configuration 1				Configuration 3			
Mode	From	To	Flow rate, $Q_{ilgg'}$ (kg/d)	Mode	From	To	Flow rate, $Q_{ilgg'}$ (kg/d)
TRK	G04	G01	102130	TRK	G04	G01	102130
TRK	G04	G02	80020	TRK	G04	G02	80020
TRK	G04	G03	157930	TRK	G04	G03	157930
TRK	G04	G05	41060	TRK	G04	G05	41060
TRK	G04	G06	129500	TRK	G04	G06	129500
TRK	G04	G07	172670	TRK	G04	G07	172670
TRK	G04	G08	7370	TRK	G04	G09	33380
TRK	G13	G09	13900	TRK	G11	G08	7370
TRK	G13	G10	301590	TRK	G11	G09	51900
TRK	G13	G12	9480	TRK	G11	G10	315940
TRK	G14	G11	34140	TRK	G11	G12	9480
TRK	G14	G15	23620	TRK	G11	G15	142920
TRK	G17	G16	24450	TRK	G11	G17	47580
TRK	G17	G18	36640	TRK	G13	G17	324970
TRK	G19	G15	119300	TRK	G14	G17	57760
TRK	G19	G20	40610	TRK	G19	G18	36640
TRK	G22	G21	63170	TRK	G19	G20	40610
TRK	G22	G23	87490	TRK	G19	G23	87490
TRK	G22	G26	62810	TRK	G19	G25	297830
TRK	G24	G25	53840	TRK	G22	G16	24450

Table E.1 (*Continued*)

Configuration 1				Configuration 3			
Mode	From	To	Flow rate, $Q_{ilgg'}$ (kg/d)	Mode	From	To	Flow rate, $Q_{ilgg'}$ (kg/d)
TRK	G24	G30	45130	TRK	G22	G17	58210
TRK	G27	G33	185030	TRK	G22	G21	63170
TRK	G28	G34	81460	TRK	G22	G26	62810
TRK	G29	G30	142830	TRK	G22	G27	127410
TRK	G29	G34	10600	TRK	G24	G25	58670
RTC	G04	G09	71380	TRK	G24	G30	40300
RTC	G17	G10	14350	TRK	G28	G34	81460
RTC	G17	G11	350670	TRK	G29	G30	147660
RTC	G19	G25	302660	TRK	G29	G34	5770
RTC	G22	G31	78710	TRK	G32	G27	266320
RTC	G22	G34	43870	TRK	G32	G31	207720
RTC	G27	G31	129010	TRK	G32	G33	185030
RTC	G27	G32	252230	TRK	G32	G34	48700

G: grid square; TRK: tanker truck; RTC: railway tank car

Table E.2: Flow rate of hydrogen gas via transport modes for the steady-state model

Configuration 2			
Mode	From	To	Flow rate, $Q_{ilgg'}$ (kg/d)
TUB	G04	G05	41060
TUB	G10	G09	85280
TUB	G10	G12	9480
TUB	G11	G08	7370
TUB	G14	G15	57760
TUB	G17	G16	24450
TUB	G22	G21	63170
TUB	G25	G20	40610
TUB	G28	G33	81460
TUB	G29	G30	153430
RTB	G04	G01	102130
RTB	G04	G02	80020
RTB	G04	G03	157930
RTB	G04	G06	129500
RTB	G04	G07	172670
RTB	G17	G18	36640
RTB	G19	G15	85160
RTB	G22	G23	87490
RTB	G22	G26	62810
RTB	G24	G30	34530
RTB	G24	G34	64440
RTB	G27	G33	103570
RTB	G27	G34	71490
RTB	G32	G31	207720

TUB: tube trailer; RTB: railway tube car

Table E.3: Summary of results of configurations 1 and 3 for the steady-state model

Configuration	1				3		
Variable	D_{ig}^{L} (kg/d)	D_{ig}^{I} (kg/d)	P_{ig}^{T} (kg/d)	S_{ig}^{T} (kg)*	D_{ig}^{L} (kg/d)	D_{ig}^{I} (kg/d)	P_{ig}^{T} (kg/d)
G01	–	102130	–	1021300	–	102130	–
G02	–	80020	–	800200	–	80020	–
G03	–	157930	–	1579300	–	157930	–
G04	197940	–	960000	1979400	197940	–	914630
G05	–	41060	–	410600	–	41060	–

Table E.3 (*Continued*)

Configuration	1				3		
Variable	D_{ig}^{L} (kg/d)	D_{ig}^{I} (kg/d)	P_{ig}^{T} (kg/d)	S_{ig}^{T} (kg)*	D_{ig}^{L} (kg/d)	D_{ig}^{I} (kg/d)	P_{ig}^{T} (kg/d)
G06	–	129500	–	1295000	–	129500	–
G07	–	172670	–	1726700	–	172670	–
G08	–	7370	–	73700	–	7370	–
G09	–	85280	–	852800	–	85280	–
G10	–	315940	–	3159400	–	315940	–
G11	–	384810	–	3848100	384810	–	960000
G12	–	9480	–	94800	–	9480	–
G13	635030	–	960000	6350300	635030	–	960000
G14	902240	–	960000	9022400	902240	–	960000
G15	–	142920	–	1429200	–	142920	–
G16	–	24450	–	244500	–	24450	–
G17	488520	–	914630	4885200	–	488520	–
G18	960000	36640	960000	9966400	960000	36640	960000
G19	497430	–	960000	4974300	497430	–	960000
G20	–	40610	–	406100	–	40610	–
G21	–	63170	–	631700	–	63170	–
G22	623950	–	960000	6239500	623950	–	960000
G23	960000	87490	960000	10474900	960000	87490	960000
G24	861030	–	960000	8610300	861030	–	960000
G25	–	356500	–	3565000	–	356500	–
G26	–	62810	–	628100	–	62810	–
G27	393730	–	960000	3937300	–	393730	–
G28	878540	–	960000	8785400	878540	–	960000
G29	2726570	–	2880000	27265700	2726570	–	2880000
G30	–	187960	–	1879600	–	187960	–
G31	–	207720	–	2077200	–	207720	–
G32	–	252230	–	2522300	252230	–	960000
G33	–	185030	–	1850300	–	185030	–
G34	–	135930	–	1359300	–	135930	–

* S_{ig}^{T} is only given for network configuration 1 since networks 2 and 3 have the same values. The same approach is adopted in the subsequent models.

Table E.4: Summary of results of configuration 2 for the steady-state model

Configuration	2		
Variable	D_{ig}^{L} (kg/d)	D_{ig}^{I} (kg/d)	P_{ig}^{T} (kg/d)
G01	–	102130	–
G02	–	80020	–
G03	–	157930	–
G04	197940	–	881250
G05	–	41060	–
G06	–	129500	–
G07	–	172670	–
G08	–	7370	–
G09	–	85280	–
G10	315940	–	410700
G11	384810	–	392180
G12	–	9480	–
G13	635030	–	635030
G14	902240	–	960000
G15	–	142920	–
G16	–	24450	–
G17	488520	–	549610

Table E.4 (*Continued*)

Configuration	2		
Variable	D_{ig}^{L} (kg/d)	D_{ig}^{I} (kg/d)	P_{ig}^{T} (kg/d)
G18	960000	36640	960000
G19	497430	–	582590
G20	–	40610	–
G21	–	63170	–
G22	623950	–	837420
G23	960000	87490	960000
G24	861030	–	960000
G25	356500	–	397110
G26	–	62810	–
G27	393730	–	568790
G28	878540	–	960000
G29	2726570	–	2880000
G30	–	187960	–
G31	–	207720	–
G32	252230	–	459950
G33	–	185030	–
G34	–	135930	–

E.3 Extended Model

Table E.5: Flow rate of liquid hydrogen via transport modes for the extended model

Configuration 1				Configuration 2			
Mode	From	To	Flow rate, $Q_{ilgg'}$ (kg/d)	Mode	From	To	Flow rate, $Q_{ilgg'}$ (kg/d)
TRK	G05	G01	102130	TRK	G05	G04	197940
TRK	G05	G02	80020	TRK	G05	G07	172670
TRK	G05	G03	157930	TRK	G14	G08	7370
TRK	G05	G04	197940	TRK	G14	G10	315940
TRK	G05	G06	129500	TRK	G14	G11	384810
TRK	G05	G07	172670	TRK	G14	G13	635030
TRK	G05	G09	33380	TRK	G14	G15	142920
TRK	G14	G08	7370	TRK	G14	G18	473138
TRK	G14	G09	51900	TRK	G17	G16	24450
TRK	G14	G10	315940	TRK	G17	G21	63170
TRK	G14	G11	384810	TRK	G17	G22	623950
TRK	G14	G12	9480	TRK	G19	G18	523502
TRK	G14	G13	635030	TRK	G19	G23	899068
TRK	G14	G15	142920	TRK	G25	G20	40610
TRK	G14	G18	430310	TRK	G25	G24	861030
TRK	G17	G16	24450	TRK	G25	G30	187960
TRK	G17	G18	566330	TRK	G29	G28	749642
TRK	G17	G21	63170	TRK	G29	G33	185030
TRK	G17	G22	623950	TRK	G29	G34	135930
TRK	G17	G23	111020	RTC	G05	G01	102130
TRK	G17	G26	62810	RTC	G05	G02	80020
TRK	G17	G27	393730	RTC	G05	G03	157930
TRK	G17	G28	86070	RTC	G05	G06	129500
TRK	G17	G31	207720	RTC	G05	G09	76208
TRK	G17	G32	252230	RTC	G14	G09	9072
TRK	G19	G23	936470	RTC	G14	G12	9480
TRK	G19	G24	486100	RTC	G17	G26	62810

Table E.5 (*Continued*)

Configuration 1				Configuration 2			
Mode	From	To	Flow rate, $Q_{ilgg'}$ (kg/d)	Mode	From	To	Flow rate, $Q_{ilgg'}$ (kg/d)
TRK	G25	G20	40610	RTC	G17	G27	393730
TRK	G25	G24	374930	RTC	G17	G31	11140
TRK	G25	G30	187960	RTC	G17	G32	252230
TRK	G29	G28	792470	RTC	G25	G23	148422
TRK	G29	G33	185030	RTC	G25	G28	128898
TRK	G29	G34	135930	RTC	G25	G31	196580

Table E.6: Surplus of natural gas in each grid for the extended model

Configuration 1		Configuration 2	
Grid, g	Surplus, SR_{eg} (t/d)	Grid, g	Surplus, SR_{eg} (t/d)
G05	107110	G05	106974
G14	19899	G14	19899
G17	12899	G17	15933
G19	22933	G19	22933
G25	13832	G25	10934

Table E.7: Summary of results for the extended model

Configuration	1				2		
Variable	D_{ig}^{L} (kg/d)	D_{ig}^{I} (kg/d)	P_{ig}^{T} (kg/d)	S_{ig}^{T} (kg)	D_{ig}^{L} (kg/d)	D_{ig}^{I} (kg/d)	P_{ig}^{T} (kg/d)
G01	–	102130	–	1021300	–	102130	–
G02	–	80020	–	800200	–	80020	–
G03	–	157930	–	1579300	–	157930	–
G04	–	197940	–	1979400	–	197940	–
G05	41060	–	914630	410600	41060	–	957458
G06	–	129500	–	1295000	–	129500	–
G07	–	172670	–	1726700	–	172670	–
G08	–	7370	–	73700	–	7370	–
G09	–	85280	–	852800	–	85280	–
G10	–	315940	–	3159400	–	315940	–
G11	–	384810	–	3848100	–	384810	–
G12	–	9480	–	94800	–	9480	–
G13	–	635030	–	6350300	–	635030	–
G14	902240	–	2880000	9022400	902240	–	2880000
G15	–	142920	–	1429200	–	142920	–
G16	–	24450	–	244500	–	24450	–
G17	488520	–	2880000	4885200	488520	–	1920000
G18	–	996640	–	9966400	–	996640	–
G19	497430	–	1920000	4974300	497430	–	1920000
G20	–	40610	–	406100	–	40610	–
G21	–	63170	–	631700	–	63170	–
G22	–	623950	–	6239500	–	623950	–
G23	–	1047490	–	10474900	–	1047490	–
G24	–	861030	–	8610300	–	861030	–
G25	356500	–	960000	3565000	356500	–	1920000
G26	–	62810	–	628100	–	62810	–
G27	–	393730	–	3937300	–	393730	–
G28	–	878540	–	8785400	–	878540	–
G29	2726570	–	3840000	27265700	2726570	–	3797172
G30	–	187960	–	1879600	–	187960	–
G31	–	207720	–	2077200	–	207720	–
G32	–	252230	–	2522300	–	252230	–
G33	–	185030	–	1850300	–	185030	–

Table E.7 (*Continued*)

Configuration	1				2		
Variable	D_{ig}^{L} (kg/d)	D_{ig}^{I} (kg/d)	P_{ig}^{T} (kg/d)	S_{ig}^{T} (kg)	D_{ig}^{L} (kg/d)	D_{ig}^{I} (kg/d)	P_{ig}^{T} (kg/d)
G34	–	135930	–	1359300	–	135930	–

E.4 Multi-Period Model

Table E.8: Flow rate of liquid hydrogen via transport modes during the first period

Configuration 1				Configuration 2			
Mode	From	To	Flow rate, $Q_{ilgg't}$ (kg/d)	Mode	From	To	Flow rate, $Q_{ilgg't}$ (kg/d)
TRK	G07	G01	5107	TRK	G07	G01	5107
TRK	G07	G03	7897	TRK	G07	G03	7897
TRK	G07	G04	9897	TRK	G07	G04	9897
TRK	G07	G06	6475	TRK	G07	G06	6475
TRK	G07	G09	4264	TRK	G07	G09	4264
TRK	G07	G10	15797	TRK	G07	G10	15797
TRK	G07	G11	19241	TRK	G07	G15	7146
TRK	G07	G13	31752	TRK	G17	G18	40760
TRK	G07	G14	45112	TRK	G17	G22	31198
TRK	G07	G15	7146	TRK	G17	G23	52375
TRK	G07	G18	49832	TRK	G29	G24	4082
TRK	G07	G19	4082	TRK	G29	G28	34744
TRK	G17	G19	10790	TRK	G29	G30	9398
TRK	G17	G22	31198	TRK	G29	G33	9252
TRK	G17	G23	52375	TRK	G29	G34	6797
TRK	G17	G24	43052	RTC	G07	G11	19241
TRK	G17	G27	9687	RTC	G07	G13	31752
TRK	G17	G28	5477	RTC	G07	G14	45112
TRK	G17	G31	10386	RTC	G07	G18	9072
TRK	G17	G32	12612	RTC	G07	G19	14872
TRK	G29	G25	17825	RTC	G07	G24	29595
TRK	G29	G28	38450	RTC	G07	G25	17825
TRK	G29	G30	9398	RTC	G17	G24	9375
TRK	G29	G33	9252	RTC	G17	G27	9687
TRK	G29	G34	6797	RTC	G17	G28	9184
				RTC	G17	G31	10386
				RTC	G17	G32	12612

Table E.9: Flow rate of liquid hydrogen via transport modes during the second period

Configuration 1				Configuration 2			
Mode	From	To	Flow rate, $Q_{ilgg't}$ (kg/d)	Mode	From	To	Flow rate, $Q_{ilgg't}$ (kg/d)
TRK	G07	G01	20426	TRK	G07	G03	31586
TRK	G07	G02	15704	TRK	G07	G04	39588
TRK	G07	G03	31586	TRK	G07	G05	7912
TRK	G07	G04	39588	TRK	G07	G06	25900
TRK	G07	G05	7912	TRK	G07	G09	17056
TRK	G07	G06	25900	TRK	G07	G10	63188
TRK	G07	G09	17056	TRK	G17	G16	4590
TRK	G07	G10	63188	TRK	G17	G18	199328
TRK	G07	G11	76962	TRK	G17	G21	12334
TRK	G07	G13	127006	TRK	G17	G22	124790
TRK	G07	G14	180448	TRK	G17	G23	209498

Table E.9 (*Continued*)

Configuration 1				Configuration 2			
Mode	From	To	Flow rate, $Q_{ilgg'i}$ (kg/d)	Mode	From	To	Flow rate, $Q_{ilgg'i}$ (kg/d)
TRK	G07	G15	28584	TRK	G29	G20	7822
TRK	G17	G16	4590	TRK	G29	G28	78236
TRK	G17	G21	12334	TRK	G29	G30	37592
TRK	G17	G22	124790	TRK	G29	G33	37006
TRK	G17	G26	12262	TRK	G29	G34	27186
TRK	G17	G27	68746	RTC	G07	G01	20426
TRK	G17	G31	41544	RTC	G07	G02	15704
TRK	G17	G32	50446	RTC	G07	G11	76962
TRK	G19	G18	199328	RTC	G07	G13	127006
TRK	G19	G20	7822	RTC	G07	G14	180448
TRK	G19	G23	209498	RTC	G07	G15	28584
TRK	G19	G24	172206	RTC	G07	G19	89186
TRK	G19	G25	71300	RTC	G07	G24	130620
TRK	G29	G28	175708	RTC	G07	G25	71300
TRK	G29	G30	37592	RTC	G17	G24	41586
TRK	G29	G33	37006	RTC	G17	G26	12262
TRK	G29	G34	27186	RTC	G17	G27	68746
				RTC	G17	G28	97472
				RTC	G17	G31	41544
				RTC	G17	G32	50446

Table E.10: Flow rate of liquid hydrogen via transport modes during the third period

Configuration 1				Configuration 2			
Mode	From	To	Flow rate, $Q_{ilgg'i}$ (kg/d)	Mode	From	To	Flow rate, $Q_{ilgg'i}$ (kg/d)
TRK	G05	G01	51065	TRK	G07	G03	78965
TRK	G05	G02	39710	TRK	G07	G04	98970
TRK	G05	G03	78965	TRK	G07	G05	20230
TRK	G05	G04	98970	TRK	G07	G06	64750
TRK	G05	G06	64750	TRK	G07	G09	42640
TRK	G05	G13	296507	TRK	G07	G10	157970
TRK	G05	G15	67378	TRK	G07	G11	4082
TRK	G07	G09	42640	TRK	G07	G12	4440
TRK	G07	G10	157970	TRK	G14	G11	188323
TRK	G07	G11	192405	TRK	G14	G15	71460
TRK	G07	G12	4440	TRK	G14	G18	249397
TRK	G07	G13	21008	TRK	G17	G16	11925
TRK	G07	G14	451120	TRK	G17	G21	31285
TRK	G07	G15	4082	TRK	G17	G22	311975
TRK	G17	G16	11925	TRK	G19	G13	6672
TRK	G17	G18	329750	TRK	G19	G18	248923
TRK	G17	G21	31285	TRK	G19	G20	20005
TRK	G17	G22	311975	TRK	G19	G24	430515
TRK	G17	G26	31105	TRK	G29	G30	93980
TRK	G19	G18	168570	TRK	G29	G34	67965
TRK	G19	G20	20005	RTC	G07	G01	51065
TRK	G19	G24	430515	RTC	G07	G02	39710
TRK	G19	G25	102195	RTC	G07	G13	310843
TRK	G23	G27	186865	RTC	G17	G26	31105
TRK	G23	G28	439270	RTC	G17	G27	186865
TRK	G23	G31	103860	RTC	G17	G31	103860
TRK	G23	G32	126115	RTC	G17	G32	39025
TRK	G29	G25	76055	RTC	G19	G25	178250
TRK	G29	G30	93980	RTC	G19	G28	439270
TRK	G29	G33	92515	RTC	G19	G32	87090

Table E.10 (*Continued*)

Configuration 1				Configuration 2			
Mode	From	To	Flow rate, $Q_{ilgg'i}$ (kg/d)	Mode	From	To	Flow rate, $Q_{ilgg'i}$ (kg/d)
TRK	G29	G34	67965	RTC	G19	G33	92515

Table E.11: Flow rate of liquid hydrogen via transport modes during the fourth period

Configuration 1				Configuration 2			
Mode	From	To	Flow rate, $Q_{ilgg'i}$ (kg/d)	Mode	From	To	Flow rate, $Q_{ilgg'i}$ (kg/d)
TRK	G05	G01	86811	TRK	G05	G04	168249
TRK	G05	G02	67717	TRK	G07	G06	110075
TRK	G05	G03	134241	TRK	G07	G08	5965
TRK	G05	G04	168249	TRK	G07	G09	72488
TRK	G05	G06	110075	TRK	G07	G10	268549
TRK	G05	G13	223623	TRK	G07	G12	7758
TRK	G07	G08	5965	TRK	G14	G13	50086
TRK	G07	G09	72488	TRK	G14	G15	121482
TRK	G07	G10	268549	TRK	G17	G16	20483
TRK	G07	G11	327089	TRK	G17	G21	53395
TRK	G07	G12	7758	TRK	G17	G22	471181
TRK	G07	G13	131383	TRK	G19	G20	34219
TRK	G14	G13	184770	TRK	G19	G24	731876
TRK	G14	G15	121482	TRK	G23	G28	70234
TRK	G14	G18	847144	TRK	G29	G30	159766
TRK	G17	G16	20483	TRK	G29	G33	128045
TRK	G17	G21	53395	TRK	G29	G34	115541
TRK	G17	G22	4082	RTC	G05	G01	86811
TRK	G17	G26	53089	RTC	G05	G02	67717
TRK	G17	G27	320589	RTC	G05	G03	134241
TRK	G17	G31	93422	RTC	G05	G13	468382
TRK	G19	G24	528742	RTC	G07	G11	327089
TRK	G19	G32	18443	RTC	G07	G13	21308
TRK	G23	G27	4082	RTC	G14	G22	59177
TRK	G23	G28	746759	RTC	G14	G26	53089
TRK	G23	G31	83140	RTC	G14	G27	324671
TRK	G23	G32	195953	RTC	G14	G28	153935
TRK	G25	G20	34219	RTC	G14	G31	176562
TRK	G25	G24	203134	RTC	G14	G32	214396
TRK	G25	G30	159766	RTC	G18	G28	113456
TRK	G29	G33	157276	RTC	G19	G25	303025
TRK	G29	G34	115541	RTC	G19	G28	409135
				RTC	G19	G33	29231

Table E.12: Flow rate of liquid hydrogen via transport modes during the fifth period

Configuration 1				Configuration 2			
Mode	From	To	Flow rate, $Q_{ilgg'i}$ (kg/d)	Mode	From	To	Flow rate, $Q_{ilgg'i}$ (kg/d)
TRK	G05	G01	102130	TRK	G05	G04	197940
TRK	G05	G02	79720	TRK	G07	G06	129500
TRK	G05	G03	157930	TRK	G07	G08	7070
TRK	G05	G04	197940	TRK	G07	G09	85280
TRK	G05	G06	129500	TRK	G07	G10	315940
TRK	G05	G11	14950	TRK	G14	G13	397960
TRK	G05	G13	237070	TRK	G14	G15	142920
TRK	G07	G08	7070	TRK	G17	G16	24150
TRK	G07	G09	85280	TRK	G17	G21	62870
TRK	G07	G10	315940	TRK	G18	G23	86890
TRK	G07	G11	369860	TRK	G19	G20	40310

Table E.12 (*Continued*)

Configuration 1				Configuration 2			
Mode	From	To	Flow rate, $Q_{ilgg't}$ (kg/d)	Mode	From	To	Flow rate, $Q_{ilgg't}$ (kg/d)
TRK	G07	G12	9180	TRK	G19	G24	861030
TRK	G14	G13	397960	TRK	G22	G27	336350
TRK	G14	G15	142920	TRK	G29	G30	18400
TRK	G14	G18	477480	TRK	G29	G34	135930
TRK	G17	G18	471780	RTC	G05	G01	102130
TRK	G19	G18	47380	RTC	G05	G02	79720
TRK	G19	G24	425190	RTC	G05	G03	157930
TRK	G22	G16	24150	RTC	G05	G11	144450
TRK	G22	G21	62870	RTC	G05	G13	237070
TRK	G22	G26	62510	RTC	G07	G11	240360
TRK	G22	G28	47640	RTC	G07	G12	9180
TRK	G22	G33	139180	RTC	G14	G27	47380
TRK	G23	G24	41910	RTC	G14	G28	292100
TRK	G23	G28	830900	RTC	G14	G32	137700
TRK	G25	G20	40310	RTC	G17	G26	62510
TRK	G25	G24	393930	RTC	G17	G31	207720
TRK	G25	G30	169560	RTC	G17	G32	114530
TRK	G27	G31	207720	RTC	G18	G28	586440
TRK	G27	G32	252230	RTC	G18	G33	185030
TRK	G27	G33	45850	RTC	G19	G25	356500
TRK	G29	G30	18400	RTC	G19	G30	169560
TRK	G29	G34	135930				

Table E.13: Flow rate of natural gas between grids during the first time period

Configuration 1			Configuration 2		
From	To	Flow rate, $QE_{egg't}$ (kg/d)	From	To	Flow rate, $QE_{egg't}$ (kg/d)
G05	G02	16931	G05	G02	16931
G05	G07	715935	G05	G07	773977
G05	G08	1481	G05	G08	1559
G05	G10	2111	G05	G10	2111
G05	G27	35158	G10	G12	2006
G10	G12	2006	G17	G16	5173
G17	G16	5173	G17	G21	27354
G17	G21	27354	G17	G22	35158
G19	G20	8592	G19	G20	8592
G21	G26	13289	G21	G26	13289
G25	G29	725845	G22	G27	33400
			G25	G29	667802

Table E.14: Flow rate of natural gas between grids during the second time period

Configuration 1			Configuration 2		
From	To	Flow rate, $QE_{egg't}$ (kg/d)	From	To	Flow rate, $QE_{egg't}$ (kg/d)
G05	G02	1269	G05	G02	1269
G05	G07	2233843	G05	G07	3193263
G05	G08	6237	G05	G08	6237
G05	G27	35158	G05	G10	8445
G07	G10	8445	G10	G12	8023
G10	G12	8023	G17	G16	947
G17	G16	947	G17	G21	2404
G17	G21	2404	G17	G22	33400
G19	G20	1269	G19	G20	1269
G21	G26	1269	G21	G26	1078
G25	G29	2737456	G22	G27	35158

Table E.14 (*Continued*)

Configuration 1			Configuration 2		
From	To	Flow rate, $QE_{egg't}$ (kg/d)	From	To	Flow rate, $QE_{egg't}$ (kg/d)
			G25	G29	2284157

Table E.15: Flow rate of natural gas between grids during the third time period

Configuration 1			Configuration 2		
From	To	Flow rate, $QE_{egg't}$ (kg/d)	From	To	Flow rate, $QE_{egg't}$ (kg/d)
G05	G02	1269	G05	G02	1269
G05	G07	3193263	G05	G07	3193449
G05	G08	15593	G05	G08	15593
G05	G10	177	G07	G10	177
G10	G12	705	G10	G12	705
G14	G23	4590105	G17	G16	1269
G14	G27	35158	G17	G21	2606
G17	G16	1206	G17	G27	35158
G17	G21	2606	G19	G20	1269
G19	G20	713	G19	G23	1742413
G21	G26	1269	G19	G29	1475808
G25	G29	5634928	G21	G26	1269
			G25	G29	3598403

Table E.16: Flow rate of natural gas between grids during the fourth time period

Configuration 1			Configuration 2		
From	To	Flow rate, $QE_{egg't}$ (kg/d)	From	To	Flow rate, $QE_{egg't}$ (kg/d)
G05	G02	1269	G05	G02	1269
G05	G07	3193263	G05	G07	3194670
G05	G08	1269	G05	G08	37
G05	G10	1206	G05	G18	69946
G10	G12	1206	G07	G10	1336
G14	G23	6387796	G10	G12	1269
G17	G16	1206	G14	G18	3125856
G17	G21	2606	G17	G16	1143
G17	G22	1750830	G17	G21	2606
G17	G27	35158	G17	G27	35158
G19	G20	1206	G19	G20	1269
G21	G26	1269	G19	G23	2976224
G25	G29	8617305	G21	G26	1269
			G25	G29	9051505

Table E.17: Flow rate of natural gas between grids during the fifth time period

Configuration 1			Configuration 2		
From	To	Flow rate, $QE_{egg't}$ (kg/d)	From	To	Flow rate, $QE_{egg't}$ (kg/d)
G05	G02	169	G05	G02	169
G05	G07	2566785	G05	G07	3543326
G05	G08	51	G05	G08	1206
G05	G10	1206	G07	G10	1076
G05	G27	155878	G07	G23	1026418
G10	G12	1206	G10	G12	1143
G14	G18	350852	G14	G18	5702526
G14	G27	499277	G17	G16	1206
G17	G16	1206	G17	G22	3034806
G17	G22	2947265	G17	G23	1982262
G17	G27	2182129	G17	G27	28126

Table E.17 (*Continued*)

Configuration 1			Configuration 2		
From	To	Flow rate, $QE_{egg't}$ (kg/d)	From	To	Flow rate, $QE_{egg't}$ (kg/d)
G18	G23	350852	G19	G20	586
G19	G20	1206	G21	G26	543
G19	G23	5168659	G25	G29	8398132
G19	G29	7181692			
G21	G26	351			
G25	G29	1036949			

Table E.18: Availability of primary energy source during the first time period

Configuration 1			Configuration 2		
Resource, e	Grid, g	Availability, A_{egt} (unit/d)	Resource, e	Grid, g	Availability, A_{egt} (unit/d)
NG	G02	847	NG	G02	847
NG	G05	91220131	NG	G05	91197169
NG	G07	35797	NG	G07	38699
NG	G10	106	NG	G08	78
NG	G12	100	NG	G10	106
NG	G14	24000000	NG	G12	100
EL	G14	2984253	NG	G14	24000000
NG	G16	259	NG	G16	259
NG	G17	17335473	NG	G17	17300315
NG	G19	23958008	NG	G19	23958008
NG	G20	430	NG	G20	430
NG	G21	1368	NG	G21	1368
NG	G25	23274155	NG	G22	1758
NG	G26	664	NG	G25	23332198
NG	G27	1758	NG	G26	664
NG	G29	36292	NG	G29	33390

NG: natural gas; EL: electricity

Table E.19: Availability of primary energy source during the second time period

Configuration 1			Configuration 2		
Resource, e	Grid, g	Availability, A_{egt} (kg/d)	Resource, e	Grid, g	Availability, A_{egt} (kg/d)
NG	G02	910	NG	G02	910
NG	G05	88942418	NG	G05	87986747
NG	G07	147489	NG	G07	198362
NG	G08	312	NG	G08	390
NG	G10	528	NG	G10	528
NG	G12	501	NG	G12	501
NG	G14	24000000	NG	G14	24000000
NG	G17	16028629	NG	G17	14228757
NG	G19	21554476	NG	G19	23922132
NG	G20	493	NG	G20	493
NG	G21	1297	NG	G21	1488
NG	G25	20536700	NG	G25	21048041
NG	G26	728	NG	G26	537
NG	G27	3516	NG	G27	1758
NG	G29	173165			

Table E.20: Availability of primary energy source during the third time period

Configuration 1			Configuration 2		
Resource, e	Grid, g	Availability, A_{egt} (kg/d)	Resource, e	Grid, g	Availability, A_{egt} (kg/d)
NG	G02	973	NG	G02	973
NG	G05	83463372	NG	G05	84775229
NG	G07	307152	NG	G07	358034
NG	G08	1092	NG	G08	1170
NG	G14	19374737	NG	G14	20965194
NG	G17	12990011	NG	G16	63
NG	G19	18486763	NG	G17	11154918
NG	G21	1427	NG	G19	15164406
NG	G23	229505	NG	G20	557
NG	G25	14901771	NG	G21	1618
NG	G26	791	NG	G23	87121
NG	G27	5274	NG	G25	17449638
NG	G29	454911	NG	G26	600
			NG	G27	3516
			NG	G29	253711

Table E.21: Availability of primary energy source during the fourth time period

Configuration 1			Configuration 2		
Resource, e	Grid, g	Availability, A_{egt} (kg/d)	Resource, e	Grid, g	Availability, A_{egt} (kg/d)
NG	G02	1037	NG	G02	1037
NG	G05	77657160	NG	G05	78474501
NG	G07	466815	NG	G07	517768
NG	G08	1155	NG	G10	67
NG	G14	6918535	NG	G12	63
NG	G17	8165405	NG	G14	11770932
NG	G19	15418557	NG	G17	8081206
NG	G21	1557	NG	G18	159790
NG	G22	87542	NG	G19	6085107
NG	G23	548895	NG	G20	620
NG	G25	4071755	NG	G21	1749
NG	G26	855	NG	G23	27333
NG	G27	7032	NG	G25	8398132
NG	G29	885777	NG	G26	664
			NG	G27	5274
			NG	G29	706286

Table E.22: Availability of primary energy source during the fifth time period

Configuration 1			Configuration 2		
Resource, e	Grid, g	Availability, A_{egt} (kg/d)	Resource, e	Grid, g	Availability, A_{egt} (kg/d)
NG	G05	71898265	NG	G05	71894995

Table E.23: Summary of results for the first time period

Configuration	1				2		
Variable	D_{igt}^{L} (kg/d)	D_{igt}^{I} (kg/d)	P_{igt}^{T} (kg/d)	S_{igt}^{T} (kg)	D_{igt}^{L} (kg/d)	D_{igt}^{I} (kg/d)	P_{igt}^{T} (kg/d)
G01	–	5107	–	51065	–	5107	–
G02	4001	–	4001	40010	4001	–	4001
G03	–	7897	–	78965	–	7897	–
G04	–	9897	–	98970	–	9897	–
G05	2053	–	2053	20530	2053	–	2053
G06	–	6475	–	64750	–	6475	–

Table E.23 (*Continued*)

Configuration	1				2		
Variable	D^L_{igt} (kg/d)	D^I_{igt} (kg/d)	P^T_{igt} (kg/d)	S^T_{igt} (kg)	D^L_{igt} (kg/d)	D^I_{igt} (kg/d)	P^T_{igt} (kg/d)
G07	8634	–	215234	86335	8634	–	232683
G08	369	–	369	3685	369	–	369
G09	–	4264	–	42640	–	4264	–
G10	–	15797	–	157970	–	15797	–
G11	–	19241	–	192405	–	19241	–
G12	474	–	474	4740	474	–	474
G13	–	31752	–	317515	–	31752	–
G14	–	45112	–	451120	–	45112	–
G15	–	7146	–	71460	–	7146	–
G16	1223	–	1223	12225	1223	–	1223
G17	24426	–	200000	244260	24426	–	200000
G18	–	49832	–	498320	–	49832	–
G19	10000	14872	10000	248715	10000	14872	10000
G20	2031	–	2031	20305	2031	–	2031
G21	3159	–	3159	31585	3159	–	3159
G22	–	31198	–	311975	–	31198	–
G23	–	52375	–	523745	–	52375	–
G24	–	43052	–	430515	–	43052	–
G25	–	17825	–	178250	–	17825	–
G26	3141	–	3141	31405	3141	–	3141
G27	10000	9687	10000	196865	10000	9687	10000
G28	–	43927	–	439270	–	43927	–
G29	136329	–	218050	1363285	136329	–	200600
G30	–	9398	–	93980	–	9398	–
G31	–	10386	–	103860	–	10386	–
G32	–	12612	–	126115	–	12612	–
G33	–	9252	–	92515	–	9252	–
G34	–	6797	–	67965	–	6797	–

Table E.24: Summary of results for the second period

Configuration	1				2		
Variable	D^L_{igt} (kg/d)	D^I_{igt} (kg/d)	P^T_{igt} (kg/d)	S^T_{igt} (kg)	D^L_{igt} (kg/d)	D^I_{igt} (kg/d)	P^T_{igt} (kg/d)
G01	–	20426	–	204260	–	20426	–
G02	300	15704	300	160040	300	15704	300
G03	–	31586	–	315860	–	31586	–
G04	–	39588	–	395880	–	39588	–
G05	300	7912	300	82120	300	7912	300
G06	–	25900	–	259000	–	25900	–
G07	34534	–	668894	345340	34534	–	960000
G08	1474	–	1474	14740	1474	–	1474
G09	–	17056	–	170560	–	17056	–
G10	–	63188	–	631880	–	63188	–
G11	–	76962	–	769620	–	76962	–
G12	1896	–	1896	18960	1896	–	1896
G13	–	127006	–	1270060	–	127006	–
G14	–	180448	–	1804480	–	180448	–
G15	–	28584	–	285840	–	28584	–
G16	300	4590	300	48900	300	4590	300
G17	97704	–	412416	977040	97704	–	960300
G18	–	199328	–	1993280	–	199328	–
G19	99486	–	759640	994860	10300	89186	10300
G20	300	7822	300	81220	300	7822	300
G21	300	12334	300	126340	300	12334	300

Table E.24 (*Continued*)

Configuration	1				2		
Variable	D_{igt}^{L} (kg/d)	D_{igt}^{I} (kg/d)	P_{igt}^{T} (kg/d)	S_{igt}^{T} (kg)	D_{igt}^{L} (kg/d)	D_{igt}^{I} (kg/d)	P_{igt}^{T} (kg/d)
G22	–	124790	–	1247900	–	124790	–
G23	–	209498	–	2094980	–	209498	–
G24	–	172206	–	1722060	–	172206	–
G25	–	71300	–	713000	–	71300	–
G26	300	12262	300	125620	300	12262	300
G27	10000	68746	10000	787460	10000	68746	10000
G28	–	175708	–	1757080	–	175708	–
G29	545314	–	822806	5453140	545314	–	733156
G30	–	37592	–	375920	–	37592	–
G31	–	41544	–	415440	–	41544	–
G32	–	50446	–	504460	–	50446	–
G33	–	37006	–	370060	–	37006	–
G34	–	27186	–	271860	–	27186	–

Table E.25: Summary of results for the third time period

Configuration	1				2		
Variable	D_{igt}^{L} (kg/d)	D_{igt}^{I} (kg/d)	P_{igt}^{T} (kg/d)	S_{igt}^{T} (kg)	D_{igt}^{L} (kg/d)	D_{igt}^{I} (kg/d)	P_{igt}^{T} (kg/d)
G01	–	51065	–	510650	–	51065	–
G02	300	39710	300	400100	300	39710	300
G03	–	78965	–	789650	–	78965	–
G04	–	98970	–	989700	–	98970	–
G05	20530	–	717875	205300	300	20230	300
G06	–	64750	–	647500	–	64750	–
G07	86335	–	960000	863350	86335	–	960000
G08	3685	–	3685	36850	3685	–	3685
G09	–	42640	–	426400	–	42640	–
G10	–	157970	–	1579700	–	157970	–
G11	–	192405	–	1924050	–	192405	–
G12	300	4440	300	47400	300	4440	300
G13	–	317515	–	3175150	–	317515	–
G14	–	451120	–	4511200	451120	–	960300
G15	–	71460	–	714600	–	71460	–
G16	300	11925	300	122250	300	11925	300
G17	244260	–	960300	2442600	244260	–	960300
G18	–	498320	–	4983200	–	498320	–
G19	248715	–	970000	2487150	248715	–	1751955
G20	300	20005	300	203050	300	20005	300
G21	300	31285	300	315850	300	31285	300
G22	–	311975	–	3119750	–	311975	–
G23	523745	–	1379855	5237450	523745	–	523745
G24	–	430515	–	4305150	–	430515	–
G25	–	178250	–	1782500	–	178250	–
G26	300	31105	300	314050	300	31105	300
G27	10000	186865	10000	1968650	10000	186865	10000
G28	–	439270	–	4392700	–	439270	–
G29	1363285	–	1693800	13632850	1363285	–	1525230
G30	–	93980	–	939800	–	93980	–
G31	–	103860	–	1038600	–	103860	–
G32	–	126115	–	1261150	–	126115	–
G33	–	92515	–	925150	–	92515	–
G34	–	67965	–	679650	–	67965	–

Table E.26: Summary of results for the fourth time period

Configuration	1				2		
Variable	D^L_{igt} (kg/d)	D^I_{igt} (kg/d)	P^T_{igt} (kg/d)	S^T_{igt} (kg)	D^L_{igt} (kg/d)	D^I_{igt} (kg/d)	P^T_{igt} (kg/d)
G01	–	86811	–	868105	–	86811	–
G02	300	67717	300	680170	300	67717	300
G03	–	134241	–	1342405	–	134241	–
G04	–	168249	–	1682490	–	168249	–
G05	34901	–	825616	349010	34901	–	960300
G06	–	110075	–	1100750	–	110075	–
G07	146770	–	960000	1467695	146770	–	960000
G08	300	5965	300	62645	300	5965	300
G09	–	72488	–	724880	–	72488	–
G10	–	268549	–	2685490	–	268549	–
G11	–	327089	–	3270885	–	327089	–
G12	300	7758	300	80580	300	7758	300
G13	–	539776	–	5397755	–	539776	–
G14	766904	–	1920300	7669040	766904	–	1920300
G15	–	121482	–	1214820	–	121482	–
G16	300	20483	300	207825	300	20483	300
G17	415242	–	960300	4152420	415242	–	960300
G18	–	847144	–	8471440	847144	–	960600
G19	422816	–	970000	4228155	422816	–	1930300
G20	300	34219	300	345185	300	34219	300
G21	300	53395	300	536945	300	53395	300
G22	526276	4082	526276	5303575	–	530358	–
G23	890367	–	1920300	8903665	890367	–	960600
G24	–	731876	–	7318755	–	731876	–
G25	303025	–	700144	3030250	–	303025	–
G26	300	53089	300	533885	300	53089	300
G27	10000	324671	10000	3346705	10000	324671	10000
G28	–	746759	–	7467590	–	746759	–
G29	2317585	–	2590401	23175845	2317585	–	2720936
G30	–	159766	–	1597660	–	159766	–
G31	–	176562	–	1765620	–	176562	–
G32	–	214396	–	2143955	–	214396	–
G33	–	157276	–	1572755	–	157276	–
G34	–	115541	–	1155405	–	115541	–

Table E.27: Summary of results for the fifth time period

Configuration	1				2		
Variable	D^L_{igt} (kg/d)	D^I_{igt} (kg/d)	P^T_{igt} (kg/d)	S^T_{igt} (kg)	D^L_{igt} (kg/d)	D^I_{igt} (kg/d)	P^T_{igt} (kg/d)
G01	–	102130	–	1021300	–	102130	–
G02	300	79720	300	800200	300	79720	300
G03	–	157930	–	1579300	–	157930	–
G04	–	197940	–	1979400	–	197940	–
G05	41060	–	960300	410600	41060	–	960300
G06	–	129500	–	1295000	–	129500	–
G07	172670	–	960000	1726700	172670	–	960000
G08	300	7070	300	73700	300	7070	300
G09	–	85280	–	852800	–	85280	–
G10	–	315940	–	3159400	–	315940	–
G11	–	384810	–	3848100	–	384810	–
G12	300	9180	300	94800	300	9180	300
G13	–	635030	–	6350300	–	635030	–
G14	902240	–	1920600	9022400	902240	–	1920300
G15	–	142920	–	1429200	–	142920	–

Table E.27 (*Continued*)

Configuration	1				2		
Variable	D^L_{igt} (kg/d)	D^I_{igt} (kg/d)	P^T_{igt} (kg/d)	S^T_{igt} (kg)	D^L_{igt} (kg/d)	D^I_{igt} (kg/d)	P^T_{igt} (kg/d)
G16	300	24150	300	244500	300	24150	300
G17	488520	–	960300	4885200	488520	–	960300
G18	–	996640	–	9966400	996640	–	1855000
G19	497430	–	970000	4974300	497430	–	1924830
G20	300	40310	300	406100	300	40310	300
G21	300	62870	300	631700	300	62870	300
G22	623950	–	960300	6239500	623950	–	960300
G23	1047490	–	1920300	10474900	960600	86890	960600
G24	–	861030	–	8610300	–	861030	–
G25	356500	–	960300	3565000	–	356500	–
G26	300	62510	300	628100	300	62510	300
G27	393730	–	899530	3937300	10000	383730	10000
G28	–	878540	–	8785400	–	878540	–
G29	2726570	–	2880900	27265700	2726570	–	2880900
G30	–	187960	–	1879600	–	187960	–
G31	–	207720	–	2077200	–	207720	–
G32	–	252230	–	2522300	–	252230	–
G33	–	185030	–	1850300	–	185030	–
G34	–	135930	–	1359300	–	135930	–

E.5 Multi-Echelon Model

The results concerning this model are similar to the multi-period model since it is an extension. However, the results obtained for the fuelling stations and secondary distribution are given in the discussion section of Chapter 6.

E.6 Stochastic Model

Table E.28: Flow rate of liquid hydrogen during time period 1 and scenario 1

Configuration 1				Configuration 2			
Mode	From	To	Flow rate, $Q_{ilgg'tk}$ (kg/d)	Mode	From	To	Flow rate, $Q_{ilgg'tk}$ (kg/d)
TRK	G07	G01	5107	TRK	G07	G01	5107
TRK	G07	G03	7897	TRK	G07	G03	7897
TRK	G07	G04	9897	TRK	G07	G04	9897
TRK	G07	G06	6475	TRK	G07	G06	6475
TRK	G07	G09	4264	TRK	G07	G09	4264
TRK	G07	G10	15797	TRK	G07	G10	15797
TRK	G07	G11	19241	TRK	G07	G15	7146
TRK	G07	G13	31752	TRK	G17	G18	49832
TRK	G07	G14	45112	TRK	G17	G22	31198
TRK	G07	G15	7146	TRK	G17	G23	52375
TRK	G07	G18	23809	TRK	G29	G25	4082
TRK	G07	G19	14872	TRK	G29	G28	34144

Table E.28 (*Continued*)

Configuration 1				Configuration 2			
Mode	From	To	Flow rate, $Q_{ilgg'tk}$ (kg/d)	Mode	From	To	Flow rate, $Q_{ilgg'tk}$ (kg/d)
TRK	G17	G18	26023	TRK	G29	G30	9398
TRK	G17	G22	31198	TRK	G29	G33	9252
TRK	G17	G23	52375	TRK	G29	G34	6797
TRK	G17	G24	33295	RTC	G07	G11	19241
TRK	G17	G27	9687	RTC	G07	G13	31752
TRK	G17	G31	10386	RTC	G07	G14	45112
TRK	G17	G32	12612	RTC	G07	G19	14872
TRK	G29	G24	9757	RTC	G07	G24	10066
TRK	G29	G25	17825	RTC	G07	G25	13743
TRK	G29	G28	43927	RTC	G17	G24	32986
TRK	G29	G30	9398	RTC	G17	G27	9687
TRK	G29	G33	9252	RTC	G17	G28	9784
TRK	G29	G34	6797	RTC	G17	G31	10386
				RTC	G17	G32	12612

Table E.29: Flow rate of liquid hydrogen during time period 2 and scenario 1

Configuration 1				Configuration 2			
Mode	From	To	Flow rate, $Q_{ilgg'tk}$ (kg/d)	Mode	From	To	Flow rate, $Q_{ilgg'tk}$ (kg/d)
TRK	G07	G01	15320	TRK	G07	G03	23690
TRK	G07	G02	11703	TRK	G07	G04	29691
TRK	G07	G03	23690	TRK	G07	G05	5859
TRK	G07	G04	29691	TRK	G07	G06	19425
TRK	G07	G05	5859	TRK	G07	G09	12792
TRK	G07	G06	19425	TRK	G07	G10	47391
TRK	G07	G09	12792	TRK	G17	G13	95255
TRK	G07	G10	47391	TRK	G17	G14	135336
TRK	G07	G11	57722	TRK	G17	G18	149496
TRK	G17	G13	95255	TRK	G17	G21	9176
TRK	G17	G14	135336	TRK	G17	G22	93593
TRK	G17	G15	21438	TRK	G17	G23	157124
TRK	G17	G18	149496	TRK	G29	G20	5792
TRK	G17	G19	64615	TRK	G29	G24	129155
TRK	G17	G21	9176	TRK	G29	G25	53475
TRK	G17	G22	93593	TRK	G29	G30	28194
TRK	G17	G23	157124	TRK	G29	G33	27755
TRK	G17	G26	9122	TRK	G29	G34	20390
TRK	G17	G27	49060	RTC	G07	G01	15320
TRK	G17	G31	31158	RTC	G07	G02	11703
TRK	G17	G32	37835	RTC	G07	G11	24204
TRK	G29	G20	5792	RTC	G17	G11	33518
TRK	G29	G24	129155	RTC	G17	G15	21438
TRK	G29	G25	53475	RTC	G17	G19	64615
TRK	G29	G28	131781	RTC	G17	G26	9122
TRK	G29	G30	28194	RTC	G17	G27	49060
TRK	G29	G33	27755	RTC	G17	G31	31158
TRK	G29	G34	20390	RTC	G17	G32	37835
				RTC	G29	G28	131781

Table E.30: Flow rate of liquid hydrogen during time period 2 and scenario 5

Configuration 1				Configuration 2			
Mode	From	To	Flow rate, $Q_{ilgg'tk}$ (kg/d)	Mode	From	To	Flow rate, $Q_{ilgg'tk}$ (kg/d)
TRK	G07	G01	20426	TRK	G07	G03	31586
TRK	G07	G02	15704	TRK	G07	G04	39588

Table E.30 (*Continued*)

Configuration 1				Configuration 2			
Mode	From	To	Flow rate, $Q_{ilgg'tk}$ (kg/d)	Mode	From	To	Flow rate, $Q_{ilgg'tk}$ (kg/d)
TRK	G07	G03	31586	TRK	G07	G05	7912
TRK	G07	G04	39588	TRK	G07	G06	25900
TRK	G07	G05	7912	TRK	G07	G09	17056
TRK	G07	G06	25900	TRK	G07	G10	63188
TRK	G07	G09	17056	TRK	G17	G16	4590
TRK	G07	G10	63188	TRK	G17	G18	199328
TRK	G07	G11	76962	TRK	G17	G19	24924
TRK	G07	G13	127006	TRK	G17	G21	12334
TRK	G07	G14	133548	TRK	G17	G22	124790
TRK	G17	G14	46900	TRK	G17	G23	209498
TRK	G17	G15	28584	TRK	G29	G20	7822
TRK	G17	G16	4590	TRK	G29	G24	172206
TRK	G17	G18	199328	TRK	G29	G25	71300
TRK	G17	G19	89486	TRK	G29	G28	61874
TRK	G17	G21	12334	TRK	G29	G30	37592
TRK	G17	G22	124790	TRK	G29	G33	37006
TRK	G17	G23	168314	TRK	G29	G34	27186
TRK	G17	G26	12262	RTC	G07	G01	20426
TRK	G17	G28	175708	RTC	G07	G02	15704
TRK	G29	G20	7822	RTC	G07	G11	76962
TRK	G29	G23	41184	RTC	G07	G13	127006
TRK	G29	G24	172206	RTC	G07	G14	180448
TRK	G29	G30	37592	RTC	G07	G15	28584
TRK	G29	G31	41544	RTC	G07	G19	64562
TRK	G29	G32	50446	RTC	G17	G26	12262
TRK	G29	G33	37006	RTC	G17	G27	68746
TRK	G29	G34	27186	RTC	G17	G28	113834
				RTC	G17	G31	41544
				RTC	G17	G32	50446

Table E.31: Flow rate of liquid hydrogen during time period 2 and scenario 9

Configuration 1				Configuration 2			
Mode	From	To	Flow rate, $Q_{ilgg'tk}$ (kg/d)	Mode	From	To	Flow rate, $Q_{ilgg'tk}$ (kg/d)
TRK	G07	G01	25533	TRK	G05	G04	49485
TRK	G07	G02	19705	TRK	G07	G06	32375
TRK	G07	G03	39483	TRK	G07	G09	21320
TRK	G07	G04	49485	TRK	G07	G10	78985
TRK	G07	G05	9965	TRK	G14	G11	4175
TRK	G07	G06	32375	TRK	G14	G13	158758
TRK	G07	G09	21320	TRK	G14	G15	35730
TRK	G14	G10	78985	TRK	G14	G18	249160
TRK	G14	G11	96203	TRK	G14	G19	114058
TRK	G14	G13	158758	TRK	G17	G16	5813
TRK	G14	G15	35730	TRK	G17	G21	15493
TRK	G14	G18	245078	TRK	G17	G22	155988
TRK	G14	G19	114358	TRK	G17	G23	261873
TRK	G17	G16	5813	TRK	G29	G24	52250
TRK	G17	G18	4082	TRK	G29	G25	89125
TRK	G17	G21	15493	TRK	G29	G28	39753
TRK	G17	G22	155988	TRK	G29	G30	46990
TRK	G17	G23	261873	TRK	G29	G33	46258
TRK	G17	G26	15403	TRK	G29	G34	33983
TRK	G17	G27	88433	RTC	G05	G01	25533
TRK	G17	G28	67908	RTC	G05	G02	19705

Table E.31 (*Continued*)

Configuration 1				Configuration 2			
Mode	From	To	Flow rate, $Q_{ilgg'tk}$ (kg/d)	Mode	From	To	Flow rate, $Q_{ilgg'tk}$ (kg/d)
TRK	G17	G31	51930	RTC	G05	G03	39483
TRK	G17	G32	63058	RTC	G05	G11	67875
TRK	G20	G24	215258	RTC	G07	G11	24153
TRK	G20	G25	89125	RTC	G14	G20	9853
TRK	G29	G28	151728	RTC	G14	G24	163008
TRK	G29	G30	46990	RTC	G17	G26	15403
TRK	G29	G33	46258	RTC	G17	G27	88433
TRK	G29	G34	33983	RTC	G17	G28	179883
				RTC	G17	G31	51930
				RTC	G17	G32	63058

Table E.32: Flow rate of liquid hydrogen during time period 3 and scenario 1

Configuration 1				Configuration 2			
Mode	From	To	Flow rate, $Q_{ilgg'tk}$ (kg/d)	Mode	From	To	Flow rate, $Q_{ilgg'tk}$ (kg/d)
TRK	G07	G01	30639	TRK	G07	G03	47379
TRK	G07	G02	23706	TRK	G07	G04	59382
TRK	G07	G03	47379	TRK	G07	G05	12018
TRK	G07	G04	59382	TRK	G07	G06	38850
TRK	G07	G05	12018	TRK	G07	G09	25584
TRK	G07	G06	38850	TRK	G07	G10	94782
TRK	G07	G09	25584	TRK	G17	G14	43641
TRK	G07	G10	94782	TRK	G17	G16	7035
TRK	G14	G11	115443	TRK	G17	G18	298992
TRK	G14	G13	190509	TRK	G17	G21	18651
TRK	G14	G15	42876	TRK	G17	G22	187185
TRK	G14	G18	74390	TRK	G17	G23	4698
TRK	G14	G20	11883	TRK	G20	G24	258309
TRK	G14	G24	254227	TRK	G20	G25	106950
TRK	G16	G21	18651	TRK	G29	G28	4082
TRK	G16	G22	187185	TRK	G29	G30	56388
TRK	G16	G26	18543	TRK	G29	G33	41680
TRK	G16	G27	108119	TRK	G29	G34	40779
TRK	G16	G28	54837	RTC	G07	G01	30639
TRK	G16	G31	62316	RTC	G07	G02	23706
TRK	G16	G32	75669	RTC	G07	G11	115443
TRK	G16	G33	55509	RTC	G07	G13	190509
TRK	G17	G18	224602	RTC	G07	G14	227031
TRK	G17	G23	314247	RTC	G07	G15	42876
TRK	G17	G24	4082	RTC	G17	G26	18543
TRK	G17	G25	61788	RTC	G17	G27	96714
TRK	G17	G28	208725	RTC	G17	G31	62316
TRK	G29	G25	45162	RTC	G17	G32	75669
TRK	G29	G30	56388	RTC	G20	G23	309549
TRK	G29	G34	40779	RTC	G20	G28	259480
				RTC	G20	G33	13829

Table E.33: Flow rate of liquid hydrogen during time period 3 and scenario 5

Configuration 1				Configuration 2			
Mode	From	To	Flow rate, $Q_{ilgg'tk}$ (kg/d)	Mode	From	To	Flow rate, $Q_{ilgg'tk}$ (kg/d)
TRK	G05	G01	41390	TRK	G07	G03	78965
TRK	G05	G02	39710	TRK	G07	G04	98970
TRK	G05	G04	98970	TRK	G07	G05	20230
TRK	G07	G01	9675	TRK	G07	G06	64750

Table E.33 (*Continued*)

Configuration 1				Configuration 2			
Mode	From	To	Flow rate, $Q_{ilgg'tk}$ (kg/d)	Mode	From	To	Flow rate, $Q_{ilgg'tk}$ (kg/d)
TRK	G07	G03	78965	TRK	G07	G09	42640
TRK	G07	G06	64750	TRK	G07	G10	157970
TRK	G07	G09	42640	TRK	G07	G12	4440
TRK	G07	G10	157970	TRK	G14	G11	192405
TRK	G07	G11	35850	TRK	G14	G15	71460
TRK	G07	G12	4440	TRK	G17	G18	305265
TRK	G14	G11	156555	TRK	G17	G23	410475
TRK	G14	G13	277083	TRK	G20	G19	238715
TRK	G14	G15	71460	TRK	G20	G24	430515
TRK	G14	G18	4082	TRK	G20	G25	178250
TRK	G17	G13	40432	TRK	G21	G16	11925
TRK	G17	G18	494238	TRK	G21	G22	311975
TRK	G17	G23	181070	TRK	G21	G26	31105
TRK	G19	G23	294852	TRK	G21	G27	186865
TRK	G19	G24	426433	TRK	G29	G28	303155
TRK	G21	G16	11925	TRK	G29	G30	93980
TRK	G21	G22	311975	TRK	G29	G33	92515
TRK	G21	G23	47823	TRK	G29	G34	67965
TRK	G21	G26	31105	RTC	G07	G01	51065
TRK	G21	G27	186865	RTC	G07	G02	39710
TRK	G21	G28	109047	RTC	G07	G13	265255
TRK	G21	G31	103860	RTC	G14	G13	52260
TRK	G21	G32	126115	RTC	G14	G18	193055
TRK	G25	G24	4082	RTC	G20	G23	92515
TRK	G25	G30	27668	RTC	G21	G23	20755
TRK	G29	G28	330223	RTC	G21	G28	136115
TRK	G29	G30	66312	RTC	G21	G31	103860
TRK	G29	G33	92515	RTC	G21	G32	126115
TRK	G29	G34	67965				

Table E.34: Flow rate of liquid hydrogen during time period 3 and scenario 9

Configuration 1				Configuration 2			
Mode	From	To	Flow rate, $Q_{ilgg'tk}$ (kg/d)	Mode	From	To	Flow rate, $Q_{ilgg'tk}$ (kg/d)
TRK	G07	G01	71491	TRK	G05	G04	138558
TRK	G07	G02	55714	TRK	G07	G06	90650
TRK	G07	G03	110551	TRK	G07	G08	4859
TRK	G07	G04	138558	TRK	G07	G09	59696
TRK	G07	G05	28442	TRK	G07	G10	221158
TRK	G07	G06	90650	TRK	G07	G12	6336
TRK	G07	G08	4859	TRK	G14	G15	100044
TRK	G07	G09	59696	TRK	G14	G19	228688
TRK	G07	G10	221158	TRK	G17	G23	559075
TRK	G07	G12	6336	TRK	G18	G19	98184
TRK	G07	G13	51676	TRK	G18	G23	174168
TRK	G14	G11	4082	TRK	G21	G22	436765
TRK	G14	G13	333850	TRK	G21	G26	43667
TRK	G15	G13	58995	TRK	G21	G27	265611
TRK	G15	G18	697648	TRK	G25	G20	28127
TRK	G15	G19	103313	TRK	G25	G24	592152
TRK	G17	G16	16815	TRK	G25	G30	90171
TRK	G17	G21	38080	TRK	G29	G30	41401
TRK	G17	G22	436765	RTC	G05	G01	71491
TRK	G17	G26	34467	RTC	G05	G02	55714
TRK	G17	G27	91909	RTC	G05	G03	110551

Table E.34 (*Continued*)

Configuration 1				Configuration 2			
Mode	From	To	Flow rate, $Q_{ilgg'tk}$ (kg/d)	Mode	From	To	Flow rate, $Q_{ilgg'tk}$ (kg/d)
TRK	G20	G19	94888	RTC	G05	G11	110723
TRK	G20	G24	602721	RTC	G05	G13	444521
TRK	G20	G28	110772	RTC	G07	G11	158644
TRK	G20	G32	123492	RTC	G07	G19	11029
TRK	G23	G27	33702	RTC	G16	G28	614978
TRK	G23	G28	4082	RTC	G16	G31	136332
TRK	G23	G31	145404	RTC	G16	G32	15595
TRK	G23	G32	53069	RTC	G16	G33	129521
TRK	G25	G28	500124	RTC	G16	G34	46759
TRK	G25	G29	4082	RTC	G17	G24	10569
TRK	G25	G30	131572	RTC	G17	G34	48392
TRK	G25	G33	129521	RTC	G21	G31	9072
TRK	G25	G34	95151	RTC	G21	G32	160966

Table E.35: Flow rate of primary energy source during time period 1 and scenario 1

Configuration 1				Configuration 2			
Resource, e	From	To	$QE_{egg'tk}$ (kg/d)	Resource, e	From	To	$QE_{egg'tk}$ (kg/d)
NG	G05	G02	16084	NG	G05	G02	16931
NG	G05	G07	632000	NG	G05	G07	632000
NG	G10	G12	2006	NG	G10	G12	1905
NG	G14	G08	1481	NG	G14	G08	1481
NG	G14	G10	2006	NG	G14	G10	1905
NG	G17	G16	5173	NG	G17	G16	4914
NG	G17	G21	25322	NG	G17	G21	25322
NG	G17	G22	33400	NG	G17	G22	33400
NG	G21	G26	12625	NG	G21	G26	12625
NG	G22	G27	33400	NG	G22	G27	33400
NG	G25	G20	8592	NG	G25	G20	8592
NG	G25	G29	737174	NG	G25	G29	632000

Table E.36: Flow rate of primary energy source during time period 2 and scenario 1

Configuration 1				Configuration 2			
Resource, e	From	To	$QE_{egg'tk}$ (kg/d)	Resource, e	From	To	$QE_{egg'tk}$ (kg/d)
NG	G05	G02	1206	NG	G05	G02	1269
NG	G05	G07	788395	NG	G05	G07	682478
NG	G10	G12	6017	NG	G10	G12	5716
NG	G14	G08	4678	NG	G14	G08	4444
NG	G14	G10	6334	NG	G14	G10	5716
NG	G17	G16	14485	NG	G17	G16	14743
NG	G17	G21	2606	NG	G17	G21	2412
NG	G17	G27	35158	NG	G17	G27	35158
NG	G21	G26	1269	NG	G21	G26	1206
NG	G25	G20	1269	NG	G25	G20	1269
NG	G25	G29	2545461	NG	G25	G29	2546235

Table E.37: Flow rate of primary energy source during time period 2 and scenario 5

Configuration 1				Configuration 2			
Resource, e	From	To	$QE_{egg'tk}$ (kg/d)	Resource, e	From	To	$QE_{egg'tk}$ (kg/d)
NG	G05	G02	1269	NG	G05	G02	1269
NG	G05	G07	1875176	NG	G05	G07	2317721
NG	G10	G12	8023	NG	G10	G12	8023

Table E.37 (*Continued*)

Configuration 1				Configuration 2			
Resource, e	From	To	$QE_{egg'tk}$ (kg/d)	Resource, e	From	To	$QE_{egg'tk}$ (kg/d)
NG	G14	G08	5925	NG	G14	G08	5925
NG	G14	G10	8023	NG	G14	G10	8023
NG	G17	G16	1269	NG	G17	G16	1206
NG	G17	G21	2606	NG	G17	G21	2412
NG	G17	G27	276854	NG	G17	G27	35158
NG	G21	G26	1269	NG	G21	G26	1206
NG	G25	G20	1269	NG	G25	G20	1269
NG	G25	G29	3034806	NG	G25	G29	3034806

Table E.38: Flow rate of primary energy source during time period 2 and scenario 9

Configuration 1				Configuration 2			
Resource, e	From	To	$QE_{egg'tk}$ (kg/d)	Resource, e	From	To	$QE_{egg'tk}$ (kg/d)
NG	G05	G02	1269	NG	G05	G02	1269
NG	G05	G07	761663	NG	G05	G07	632000
NG	G10	G12	9427	NG	G10	G12	9527
NG	G14	G08	7407	NG	G14	G08	7797
NG	G14	G10	9427	NG	G14	G10	9527
NG	G17	G16	947	NG	G17	G16	1206
NG	G17	G21	2412	NG	G17	G21	2539
NG	G17	G27	35158	NG	G17	G27	33400
NG	G21	G26	1206	NG	G21	G26	1206
NG	G25	G20	993759	NG	G25	G20	1269
NG	G25	G29	3036012	NG	G25	G29	3133800

Table E.39: Flow rate of primary energy source during time period 3 and scenario 1

Configuration 1				Configuration 2			
Resource, e	From	To	$QE_{egg'tk}$ (kg/d)	Resource, e	From	To	$QE_{egg'tk}$ (kg/d)
NG	G05	G02	1206	NG	G05	G02	296
NG	G05	G07	1213886	NG	G05	G07	3033600
NG	G10	G12	11032	NG	G10	G12	11433
NG	G14	G08	8654	NG	G14	G08	8888
NG	G14	G10	10715	NG	G14	G10	11433
NG	G17	G16	1858856	NG	G17	G16	1206
NG	G17	G21	2218	NG	G17	G21	2412
NG	G17	G27	31642	NG	G17	G27	69735
NG	G21	G26	1143	NG	G21	G26	1206
NG	G25	G20	713	NG	G25	G20	713
NG	G25	G29	3034806	NG	G25	G29	3037218
				CL	G23	G20	5116800

CL: coal

Table E.40: Flow rate of primary energy source during time period 3 and scenario 5

Configuration 1				Configuration 2			
Resource, e	From	To	$QE_{egg'tk}$ (kg/d)	Resource, e	From	To	$QE_{egg'tk}$ (kg/d)
NG	G05	G02	1143	NG	G05	G02	296
NG	G05	G07	1518775	NG	G05	G07	2876643
CL	G07	G05	1066000	NG	G10	G12	805
NG	G10	G12	705	NG	G14	G08	14814
NG	G14	G08	14814	NG	G14	G10	805
NG	G14	G10	705	NG	G17	G16	1206
NG	G17	G16	884	NG	G17	G21	3036012

Table E.40 (*Continued*)

Configuration 1				Configuration 2			
Resource, e	From	To	$QE_{egg'tk}$ (kg/d)	Resource, e	From	To	$QE_{egg'tk}$ (kg/d)
NG	G17	G21	3035818	NG	G17	G27	31642
NG	G17	G27	19557	NG	G21	G26	1206
NG	G21	G26	1143	NG	G25	G20	3034313
CL	G23	G24	1066000	NG	G25	G29	6068406
CL	G24	G25	1066000				
NG	G25	G20	67530				
NG	G25	G29	6068406				

Table E.41: Flow rate of primary energy source during time period 3 and scenario 9

Configuration 1				Configuration 2			
Resource, e	From	To	$QE_{egg'tk}$ (kg/d)	Resource, e	From	To	$QE_{egg'tk}$ (kg/d)
NG	G05	G02	1143	NG	G05	G02	296
NG	G05	G07	3033600	NG	G05	G07	2127442
NG	G10	G12	1206	NG	G10	G12	1206
NG	G14	G08	1206	NG	G14	G08	816
NG	G14	G10	1206	NG	G14	G10	1206
NG	G14	G11	838301	NG	G17	G16	3034806
NG	G14	G15	3033600	NG	G17	G18	3067000
NG	G17	G16	1206	NG	G17	G21	3035885
NG	G17	G21	62869	NG	G17	G27	33400
NG	G17	G27	499242	NG	G21	G26	1206
NG	G19	G23	3071790	NG	G25	G20	713
NG	G21	G26	38190	NG	G25	G29	6167400
NG	G25	G20	3034806				
NG	G25	G29	6019048				

Table E.42: Availability of primary energy source during time period 1 and scenario 1

Configuration 1			Configuration 2		
Resource, e	Grid, g	Availability, A_{egtk} (kg/d)	Resource, e	Grid, g	Availability, A_{egtk} (kg/d)
NG	G05	91343663	NG	G02	847
NG	G12	100	NG	G05	91342816
NG	G14	23996513	NG	G14	23996613
NG	G16	259	NG	G17	17199189
NG	G17	17304105	NG	G19	23966600
NG	G19	23966600	NG	G20	430
NG	G20	430	NG	G25	23359408
NG	G25	23254234			

Table E.43: Availability of primary energy source during time period 2 and scenario 1

Configuration 1			Configuration 2		
Resource, e	Grid, g	Availability, A_{egtk} (kg/d)	Resource, e	Grid, g	Availability, A_{egtk} (kg/d)
NG	G05	90552856	NG	G02	910
NG	G08	234	NG	G05	90657863
NG	G10	317	NG	G14	23986453
NG	G12	401	NG	G17	14113276
NG	G14	23985501	NG	G19	23933200
NG	G17	14324173	NG	G20	493
NG	G19	23933200	NG	G25	20811904
NG	G20	493	NG	G27	1758
NG	G21	130			

Table E.43 (*Continued*)

Configuration 1			Configuration 2		
Resource, e	Grid, g	Availability, A_{egtk} (kg/d)	Resource, e	Grid, g	Availability, A_{egtk} (kg/d)
NG	G25	20707503			
NG	G26	63			
NG	G27	1758			

Table E.44: Availability of primary energy source during time period 2 and scenario 5

Configuration 1			Configuration 2		
Resource, e	Grid, g	Availability, A_{egtk} (kg/d)	Resource, e	Grid, g	Availability, A_{egtk} (kg/d)
NG	G02	63	NG	G02	910
NG	G05	89466012	NG	G05	89022620
NG	G12	501	NG	G12	401
NG	G14	23982564	NG	G14	23982665
NG	G16	322	NG	G17	14126813
NG	G17	13989775	NG	G19	23933200
NG	G19	23933200	NG	G20	493
NG	G20	493	NG	G25	20323332
NG	G21	130	NG	G27	1758
NG	G25	19980016			
NG	G26	63			
NG	G27	13843			

Table E.45: Availability of primary energy source during time period 2 and scenario 9

Configuration 1			Configuration 2		
Resource, e	Grid, g	Availability, A_{egtk} (kg/d)	Resource, e	Grid, g	Availability, A_{egtk} (kg/d)
NG	G02	63	NG	G02	910
NG	G05	90579525	NG	G05	90038279
NG	G14	20962662	NG	G08	390
NG	G17	14572930	NG	G14	20944483
NG	G19	23933200	NG	G17	14128444
NG	G25	19224463	NG	G19	23931994
NG	G27	1758	NG	G20	493
			NG	G21	127
			NG	G25	20224338

Table E.46: Availability of primary energy source during time period 3 and scenario 1

Configuration 1			Configuration 2		
Resource, e	Grid, g	Availability, A_{egtk} (kg/d)	Resource, e	Grid, g	Availability, A_{egtk} (kg/d)
NG	G05	89336559	NG	G05	87622761
NG	G14	20932532	NG	G14	23966132
NG	G17	9397857	NG	G17	11006323
NG	G19	23434775	NG	G19	23434775
NG	G25	17671985	NG	G25	17773973

Table E.47: Availability of primary energy source during time period 3 and scenario 5

Configuration 1			Configuration 2		
Resource, e	Grid, g	Availability, A_{egtk} (kg/d)	Resource, e	Grid, g	Availability, A_{egtk} (kg/d)
NG	G05	87943682	NG	G05	86144475
CL	G07	44934000	NG	G14	20932240
NG	G14	20932240	NG	G17	8024353
NG	G17	7899916	NG	G19	23899800

Table E.47 (*Continued*)

Configuration 1			Configuration 2		
Resource, e	Grid, g	Availability, A_{egtk} (kg/d)	Resource, e	Grid, g	Availability, A_{egtk} (kg/d)
NG	G19	20866200	NG	G25	11220613
CL	G23	135934000			
NG	G25	13810680			

Table E.48: Availability of primary energy source during time period 3 and scenario 9

Configuration 1			Configuration 2		
Resource, e	Grid, g	Availability, A_{egtk} (kg/d)	Resource, e	Grid, g	Availability, A_{egtk} (kg/d)
NG	G05	87543576	NG	G05	84875735
NG	G14	14016560	NG	G14	17907655
NG	G17	10976013	NG	G17	1923753
NG	G19	20360410	NG	G19	23897388
NG	G25	6636009	NG	G25	11022625

Table E.49: Summary of results during time period 1 and scenario 1

Configuration	1				2		
Variable	D^L_{igtk} (kg/d)	D^I_{igtk} (kg/d)	P^T_{igtk} (kg/d)	S^T_{igtk} (kg)	D^L_{igtk} (kg/d)	D^I_{igtk} (kg/d)	P^T_{igtk} (kg/d)
G01	–	5107	–	51065	–	5107	–
G02	4001	–	4001	40010	4001	–	4001
G03	–	7897	–	78965	–	7897	–
G04	–	9897	–	98970	–	9897	–
G05	2053	–	2053	20530	2053	–	2053
G06	–	6475	–	64750	–	6475	–
G07	8634	–	200000	86335	8634	–	200000
G08	369	–	369	3685	369	–	369
G09	–	4264	–	42640	–	4264	–
G10	–	15797	–	157970	–	15797	–
G11	–	19241	–	192405	–	19241	–
G12	474	–	474	4740	474	–	474
G13	–	31752	–	317515	–	31752	–
G14	–	45112	–	451120	–	45112	–
G15	–	7146	–	71460	–	7146	–
G16	1223	–	1223	12225	1223	–	1223
G17	24426	–	200000	244260	24426	–	233283
G18	–	49832	–	498320	–	49832	–
G19	10000	14872	10000	248715	10000	14872	10000
G20	2031	–	2031	20305	2031	–	2031
G21	3159	–	3159	31585	3159	–	3159
G22	–	31198	–	311975	–	31198	–
G23	–	52375	–	523745	–	52375	–
G24	–	43052	–	430515	–	43052	–
G25	–	17825	–	178250	–	17825	–
G26	3141	–	3141	31405	3141	–	3141
G27	10000	9687	10000	196865	10000	9687	10000
G28	–	43927	–	439270	–	43927	–
G29	136329	–	233283	1363285	136329	–	200000
G30	–	9398	–	93980	–	9398	–
G31	–	10386	–	103860	–	10386	–
G32	–	12612	–	126115	–	12612	–
G33	–	9252	–	92515	–	9252	–
G34	–	6797	–	67965	–	6797	–

Table E.50: Summary of results during time period 2 and scenario 1

Configuration	1				2		
Variable	D^L_{igtk} (kg/d)	D^I_{igtk} (kg/d)	P^T_{igtk} (kg/d)	S^T_{igtk} (kg)	D^L_{igtk} (kg/d)	D^I_{igtk} (kg/d)	P^T_{igtk} (kg/d)
G01	–	15320	–	153195	–	15320	–
G02	300	11703	300	120030	300	11703	300
G03	–	23690	–	236895	–	23690	–
G04	–	29691	–	296910	–	29691	–
G05	300	5859	300	61590	300	5859	300
G06	–	19425	–	194250	–	19425	–
G07	25901	–	249492	259005	25901	–	215974
G08	1106	–	1106	11055	1106	–	1106
G09	–	12792	–	127920	–	12792	–
G10	–	47391	–	473910	–	47391	–
G11	–	57722	–	577215	–	57722	–
G12	1422	–	1422	14220	1422	–	1422
G13	–	95255	–	952545	–	95255	–
G14	–	135336	–	1353360	–	135336	–
G15	–	21438	–	214380	–	21438	–
G16	3668	–	3668	36675	3668	–	3668
G17	73278	–	926482	732780	73278	–	960000
G18	–	149496	–	1494960	–	149496	–
G19	10000	64615	10000	746145	10000	64615	10000
G20	300	5792	300	60915	300	5792	300
G21	300	9176	300	94755	300	9176	300
G22	–	93593	–	935925	–	93593	–
G23	–	157124	–	1571235	–	157124	–
G24	–	129155	–	1291545	–	129155	–
G25	–	53475	–	534750	–	53475	–
G26	300	9122	300	94215	300	9122	300
G27	10000	49060	10000	590595	10000	49060	10000
G28	–	131781	–	1317810	–	131781	–
G29	408986	–	805526	4089855	408986	–	805526
G30	–	28194	–	281940	–	28194	–
G31	–	31158	–	311580	–	31158	–
G32	–	37835	–	378345	–	37835	–
G33	–	27755	–	277545	–	27755	–
G34	–	20390	–	203895	–	20390	–

Table E.51: Summary of results during time period 2 and scenario 5

Configuration	1				2		
Variable	D^L_{igtk} (kg/d)	D^I_{igtk} (kg/d)	P^T_{igtk} (kg/d)	S^T_{igtk} (kg)	D^L_{igtk} (kg/d)	D^I_{igtk} (kg/d)	P^T_{igtk} (kg/d)
G01	–	20426	–	204260	–	20426	–
G02	300	15704	300	160040	300	15704	300
G03	–	31586	–	315860	–	31586	–
G04	–	39588	–	395880	–	39588	–
G05	300	7912	300	82120	300	7912	300
G06	–	25900	–	259000	–	25900	–
G07	34534	–	593410	345340	34534	–	733456
G08	1474	–	1474	14740	1474	–	1474
G09	–	17056	–	170560	–	17056	–
G10	–	63188	–	631880	–	63188	–
G11	–	76962	–	769620	–	76962	–
G12	1896	–	1896	18960	1896	–	1896
G13	–	127006	–	1270060	–	127006	–
G14	–	180448	–	1804480	–	180448	–
G15	–	28584	–	285840	–	28584	–

Table E.51 (*Continued*)

Configuration	1				2		
Variable	D^L_{igtk} (kg/d)	D^I_{igtk} (kg/d)	P^T_{igtk} (kg/d)	S^T_{igtk} (kg)	D^L_{igtk} (kg/d)	D^I_{igtk} (kg/d)	P^T_{igtk} (kg/d)
G16	300	4590	300	48900	300	4590	300
G17	97704	–	960000	977040	97704	–	960000
G18	–	199328	–	1993280	–	199328	–
G19	10000	89486	10000	994860	10000	89486	10000
G20	300	7822	300	81220	300	7822	300
G21	300	12334	300	126340	300	12334	300
G22	–	124790	–	1247900	–	124790	–
G23	–	209498	–	2094980	–	209498	–
G24	–	172206	–	1722060	–	172206	–
G25	71300	–	71300	713000	–	71300	–
G26	300	12262	300	125620	300	12262	300
G27	78746	–	78746	787460	10000	68746	10000
G28	–	175708	–	1757080	–	175708	–
G29	545314	–	960300	5453140	545314	–	960300
G30	–	37592	–	375920	–	37592	–
G31	–	41544	–	415440	–	41544	–
G32	–	50446	–	504460	–	50446	–
G33	–	37006	–	370060	–	37006	–
G34	–	27186	–	271860	–	27186	–

Table E.52: Summary of results during time period 2 and scenario 9

Configuration	1				2		
Variable	D^L_{igtk} (kg/d)	D^I_{igtk} (kg/d)	P^T_{igtk} (kg/d)	S^T_{igtk} (kg)	D^L_{igtk} (kg/d)	D^I_{igtk} (kg/d)	P^T_{igtk} (kg/d)
G01	–	25533	–	255325	–	25533	–
G02	300	19705	300	200050	300	19705	300
G03	–	39483	–	394825	–	39483	–
G04	–	49485	–	494850	–	49485	–
G05	300	9965	300	102650	10265	–	212345
G06	–	32375	–	323750	–	32375	–
G07	43168	–	241033	431675	43168	–	200000
G08	1843	–	1843	18425	1843	–	1843
G09	–	21320	–	213200	–	21320	–
G10	–	78985	–	789850	–	78985	–
G11	–	96203	–	962025	–	96203	–
G12	2370	–	2370	23700	2370	–	2370
G13	–	158758	–	1587575	–	158758	–
G14	225560	–	954671	2255600	225560	–	960300
G15	–	35730	–	357300	–	35730	–
G16	300	5813	300	61125	300	5813	300
G17	122130	–	852107	1221300	122130	–	960000
G18	–	249160	–	2491600	–	249160	–
G19	10000	114358	10000	1243575	10300	114058	10300
G20	10153	–	314535	101525	300	9853	300
G21	300	15493	300	157925	300	15493	300
G22	–	155988	–	1559875	–	155988	–
G23	–	261873	–	2618725	–	261873	–
G24	–	215258	–	2152575	–	215258	–
G25	–	89125	–	891250	–	89125	–
G26	300	15403	300	157025	300	15403	300
G27	10000	88433	10000	984325	10000	88433	10000
G28	–	219635	–	2196350	–	219635	–
G29	681643	–	960600	6816425	681643	–	990000
G30	–	46990	–	469900	–	46990	–

Table E.52 (*Continued*)

Configuration	1				2		
Variable	D^L_{igtk} (kg/d)	D^I_{igtk} (kg/d)	P^T_{igtk} (kg/d)	S^T_{igtk} (kg)	D^L_{igtk} (kg/d)	D^I_{igtk} (kg/d)	P^T_{igtk} (kg/d)
G31	–	51930	–	519300	–	51930	–
G32	–	63058	–	630575	–	63058	–
G33	–	46258	–	462575	–	46258	–
G34	–	33983	–	339825	–	33983	–

Table E.53: Summary of results during time period 3 and scenario 1

Configuration	1				2		
Variable	D^L_{igtk} (kg/d)	D^I_{igtk} (kg/d)	P^T_{igtk} (kg/d)	S^T_{igtk} (kg)	D^L_{igtk} (kg/d)	D^I_{igtk} (kg/d)	P^T_{igtk} (kg/d)
G01	–	30639	–	306390	–	30639	–
G02	300	23706	300	240060	300	23706	300
G03	–	47379	–	473790	–	47379	–
G04	–	59382	–	593820	–	59382	–
G05	300	12018	300	123180	300	12018	300
G06	–	38850	–	388500	–	38850	–
G07	51801	–	384141	518010	51801	–	960000
G08	2211	–	2211	22110	2211	–	2211
G09	–	25584	–	255840	–	25584	–
G10	–	94782	–	947820	–	94782	–
G11	–	115443	–	1154430	–	115443	–
G12	2844	–	2844	28440	2844	–	2844
G13	–	190509	–	1905090	–	190509	–
G14	270672	–	960000	2706720	–	270672	–
G15	–	42876	–	428760	–	42876	–
G16	7335	–	588164	73350	300	7035	300
G17	146556	–	960000	1465560	146556	–	960000
G18	–	298992	–	2989920	–	298992	–
G19	149229	–	149229	1492290	149229	–	149229
G20	300	11883	300	121830	12183	–	960300
G21	300	18651	300	189510	300	18651	300
G22	–	187185	–	1871850	–	187185	–
G23	–	314247	–	3142470	–	314247	–
G24	–	258309	–	2583090	–	258309	–
G25	–	106950	–	1069500	–	106950	–
G26	300	18543	300	188430	300	18543	300
G27	10000	108119	10000	1181190	21405	96714	21405
G28	–	263562	–	2635620	–	263562	–
G29	817971	–	960300	8179710	817971	–	960900
G30	–	56388	–	563880	–	56388	–
G31	–	62316	–	623160	–	62316	–
G32	–	75669	–	756690	–	75669	–
G33	–	55509	–	555090	–	55509	–
G34	–	40779	–	407790	–	40779	–

Table E.54: Summary of results during time period 3 and scenario 5

Configuration	1				2		
Variable	D^L_{igtk} (kg/d)	D^I_{igtk} (kg/d)	P^T_{igtk} (kg/d)	S^T_{igtk} (kg)	D^L_{igtk} (kg/d)	D^I_{igtk} (kg/d)	P^T_{igtk} (kg/d)
G01	–	51065	–	510650	–	51065	–
G02	300	39710	300	400100	300	39710	300
G03	–	78965	–	789650	–	78965	–
G04	–	98970	–	989700	–	98970	–

Table E.54 (*Continued*)

Configuration	1				2		
Variable	D^L_{igtk} (kg/d)	D^I_{igtk} (kg/d)	P^T_{igtk} (kg/d)	S^T_{igtk} (kg)	D^L_{igtk} (kg/d)	D^I_{igtk} (kg/d)	P^T_{igtk} (kg/d)
G05	20530	–	200600	205300	300	20230	300
G06	–	64750	–	647500	–	64750	–
G07	86335	–	480625	863350	86335	–	910330
G08	3685	–	3685	36850	3685	–	3685
G09	–	42640	–	426400	–	42640	–
G10	–	157970	–	1579700	–	157970	–
G11	–	192405	–	1924050	–	192405	–
G12	300	4440	300	47400	300	4440	300
G13	–	317515	–	3175150	–	317515	–
G14	451120	–	960300	4511200	451120	–	960300
G15	–	71460	–	714600	–	71460	–
G16	300	11925	300	122250	300	11925	300
G17	244260	–	960000	2442600	244260	–	960000
G18	–	498320	–	4983200	–	498320	–
G19	248715	–	970000	2487150	10000	238715	10000
G20	20305	–	20305	203050	20305	–	960300
G21	31585	–	960300	315850	31585	–	960300
G22	–	311975	–	3119750	–	311975	–
G23	–	523745	–	5237450	–	523745	–
G24	–	430515	–	4305150	–	430515	–
G25	178250	–	210000	1782500	–	178250	–
G26	300	31105	300	314050	300	31105	300
G27	10000	186865	10000	1968650	10000	186865	10000
G28	–	439270	–	4392700	–	439270	–
G29	1363285	–	1920300	13632850	1363285		1920900
G30	–	93980	–	939800	–	93980	–
G31	–	103860	–	1038600	–	103860	–
G32	–	126115	–	1261150	–	126115	–
G33	–	92515	–	925150	–	92515	–
G34	–	67965	–	679650	–	67965	–

Table E.55: Summary of results during time period 3 and scenario 9

Configuration	1				2		
Variable	D^L_{igtk} (kg/d)	D^I_{igtk} (kg/d)	P^T_{igtk} (kg/d)	S^T_{igtk} (kg)	D^L_{igtk} (kg/d)	D^I_{igtk} (kg/d)	P^T_{igtk} (kg/d)
G01	–	71491	–	714910	–	71491	–
G02	300	55714	300	560140	300	55714	300
G03	–	110551	–	1105510	–	110551	–
G04	–	138558	–	1385580	–	138558	–
G05	300	28442	300	287420	28742	–	960300
G06	–	90650	–	906500	–	90650	–
G07	120869	–	960000	1208690	120869	–	673241
G08	300	4859	300	51590	300	4859	300
G09	–	59696	–	596960	–	59696	–
G10	–	221158	–	2211580	–	221158	–
G11	265285	4082	265285	2693670	–	269367	–
G12	300	6336	300	66360	300	6336	300
G13	–	444521	–	4445210	–	444521	–
G14	631568	–	969500	6315680	631568	–	960300
G15	100044	–	960000	1000440	–	100044	–
G16	300	16815	300	171150	17115	–	960300
G17	341964	–	960000	3419640	341964	–	960000
G18	–	697648	–	6976480	697648	–	970000
G19	150000	198201	150000	3482010	10300	337901	10300

Table E.55 (*Continued*)

Configuration	1				2		
Variable	D^{L}_{igtk} (kg/d)	D^{I}_{igtk} (kg/d)	P^{T}_{igtk} (kg/d)	S^{T}_{igtk} (kg)	D^{L}_{igtk} (kg/d)	D^{I}_{igtk} (kg/d)	P^{T}_{igtk} (kg/d)
G20	28427	–	960300	284270	300	28127	300
G21	6139	38080	6139	442190	44219	–	960300
G22	–	436765	–	4367650	–	436765	–
G23	733243	–	969500	7332430	–	733243	–
G24	–	602721	–	6027210	–	602721	–
G25	249550	–	1110000	2495500	249550	–	960000
G26	9500	34467	9500	439670	300	43667	300
G27	150000	125611	150000	2756110	10000	265611	10000
G28	–	614978	–	6149780	–	614978	–
G29	1904517	4082	1904517	19085990	1908599	–	1950000
G30	–	131572	–	1315720	–	131572	–
G31	–	145404	–	1454040	–	145404	–
G32	–	176561	–	1765610	–	176561	–
G33	–	129521	–	1295210	–	129521	–
G34	–	95151	–	951510	–	95151	–

The results of the third network configuration are not given here since they are similar to the results obtained for configurations 1 and 2. However, the results concerning the fuelling stations and secondary distribution are given in the discussion section of Chapter 7.